LONG NONCODING RNA DYSREGULATION ALTERS ETHANOL DRINKING BEHAVIOR AND ETHANOL-RELATED PHENOTYPES

by

Sonja Lorean Plasil

B.S., University of California, Santa Cruz, 2017

Submitted to the Graduate Faculty of the

School of Medicine in partial fulfillment

of the requirements for the degree of

Doctor of Philosophy

University of Pittsburgh

2023

UNIVERSITY OF PITTSBURGH

SCHOOL OF MEDICINE

This dissertation was presented

by

Sonja Lorean Plasil

It was defended on

April 13, 2023

and approved by

Michael J. Palladino, PhD
Committee Chair
Professor, Department of Pharmacology and Chemical Biology

Mary Torregrossa, PhD
Associate Professor, Department of Psychiatry

Shirley Y. Hill, PhD
Professor, Department of Psychiatry

Colleen A. McClung, PhD
Professor, Department of Psychiatry

Gregg E. Homanics, PhD
Major Advisor
Professor, Department of Anesthesiology and Perioperative Medicine

LONG NONCODING RNA DYSREGULATION ALTERS ETHANOL DRINKING BEHAVIOR AND ETHANOL-RELATED PHENOTYPES

Sonja Lorean Plasil, PhD

University of Pittsburgh, 2023

Alcohol use disorder (AUD) is a chronic, relapsing brain disease associated with a myriad of debilitating consequences. Unfortunately, current therapies are limited, and the etiology is incomplete. Chronic alcohol use impacts molecular processes, one of great importance being gene expression. Transcriptomic changes are thought to underly the transition from recreational drinking to AUD, and persistent transcriptional change is a hypothesized mechanism for AUD withdrawal and relapse. Long noncoding RNAs (lncRNAs) have emerged as key regulators of the transcriptome and hold great therapeutic potential. LncRNA dysregulation has been linked to AUD, drug addiction, psychiatric disorders, and immune responses. However, out of thousands of lncRNAs known to exist, only a small percentage have been functionally characterized. Further, the impact of chronic alcohol misuse on lncRNA regulation and function is largely unknown. For important AUD-regulating lncRNAs to be identified and characterized, ethanol-responsive lncRNAs must be screened for AUD-linked behavior. Based on RNA-sequencing and microarray data from brain tissue of chronically exposed subjects, the ethanol-responsive lncRNAs *Tx2*, *Pitt1*, *Pitt2*, *Pitt3*, *Pitt4*, and *Gas5* were selected for functional interrogation. Cutting-edge CRISPR/Cas9 mutagenesis techniques were applied to generate mutant mouse cohorts of all six genes. The overall goal was to elucidate the involvement of six ethanol-responsive lncRNAs in ethanol action to test **the central hypothesis that individual lncRNAs act as determinants of ethanol consumption and ethanol-related behaviors**. Each mutant line was functionally investigated using a variety of behavioral and molecular methods. All six mutant lncRNA lines demonstrated significant sex-specific alterations in ethanol drinking behavior when compared to controls. Ethanol consumption was significantly altered in mutant *Tx2* males and mutant *Pitt1*, *Pitt3*, and *Pitt4* females. Ethanol preference was significantly altered in mutant *Tx2*, *Pitt1*, and *Pitt2* males, and mutant *Gas5* females. These findings add to the literature implicating noncoding RNAs in addiction and suggest that lncRNAs play an important regulatory role in AUD. The dissertation

presented herein advances our understanding of the molecular impacts of ethanol-responsive lncRNAs and how they relate to addictive behaviors. This project provided substantial training opportunities, a strong research foundation, and a collaborative environment with other researchers in the field.

TABLE OF CONTENTS

LIST OF FREQUENTLY USED ABBREVIATIONS

ABBREVIATION	FULL TERMINOLOGY
AUD	Alcohol Use Disorder
SUD	Substance Use Disorder
ncRNA	Noncoding RNA
lncRNA	Long noncoding RN
miRNA	Micro RNA
circRNA	Circular RNA
ceRNA	Competing Endogenous RNA
CRISPR	Clustered Regulatory Interspaced Short Palindromic Repeats
crRNA	CRISPR RNA
tracrRNA	Trans-activating CRISPR RNA
gRNA	Guide RNA
sgRNA	Single Guide RNA
bp	Base Pair
nt	Nucleotide
indel	Insertion/Deletion
AAV	Adeno-Associated Virus
mPFC	Medial Prefrontal Cortex
NAc	Nucleus Accumbens
BLA	Basolateral Amygdala
KO	Knockout
TAKO	Turbo Accelerated Knockout
CIEV	Chronic Intermittent Ethanol Vapor
DID	Drinking in the Dark
BEC	Blood Ethanol Concentration
EOD-2BC	Every-Other-Day, Two Bottle-Choice
AFT	Acute Functional Tolerance
LORR	Los of Righting Response
EPM	Elevated Plus Maze
RT-PCR	Reverse Transcriptase Polymerase Chain Reaction
RT-qPCR	Reverse Transcriptase Quantitative Polymerase Chain Reaction

LIST OF TABLES

LIST OF FIGURES

PREFACE

I dedicate this dissertation to my brother, I. Kazrak Plasil (1971 – 2019). He was my childhood hero, my motivation for researching addiction, my big brother, and I miss him every day.

Working towards a PhD has been the most demanding, intensive, and exhausting thing I have ever done. However, after 5 years of many ups and downs, I would not change my experience for the world. I have grown so much, learned new skills and techniques, and successfully completed three long-term research projects. I am proud of all the knowledge I have gained, and so excited to move on to the next level of my preclinical pharmacology research training.

I first want to tremendously thank my mentor, Dr. Gregg Homanics. Not only is this dissertation the culmination of over 5 years of constant communication and collaboration, but he has molded me into an inquisitive, critical, and independent scientific researcher. His patience, understanding, and kindness have been traits I can always rely on, which I believe allowed for me to flourish. I am so grateful for everything he has helped me accomplish, and I know we will remain peers in the future.

I would also like to thank Dr. Sean Farris. Although not required, he has taken on a strong mentoring role with me from the first day of beginning his professorship at the University of Pittsburgh. He has provided support for grant applications, manuscript writing, publishing, and helped me solidify my next career steps. He was also heavily involved in all my projects from start to finish, helping me improve and preparing for the future, and I would not be where I am now without his guidance.

I would also like to thank our wonderful laboratory manager Carolyn Ferguson. I would not be here without her constant encouragement and assistance throughout the years. She is not only running the show, but she is the glue that holds us all together. I truly do not know what I would have done without her kindness and friendship.

I must also acknowledge the current students of the Homanics/Farris laboratories, Annalisa Baratta, Rachel Rice, Adam Brandner, and Daniela Gil. We have all grown to be such good friends over the years and I will miss them all so much. We were all involved with each other's projects, check in on each other, and support each other through the ups and downs of graduate school.

Every day we had fun and help each other out whenever needed, which makes the inevitable research failures easier to bare and our successes more triumphant.

Of course, I cannot forget my absolutely amazing parents Lorean Canon and Ivan Plasil, step-mother Sinikka Plasil, brother Kaz Plasil, and my close friends and family who have supported me constantly throughout my training. It has been a very tough road and I could not have done it without their constant reassurance, encouragement and perspective over the years.

I want to also thank my dissertation committee, Drs. Michael Palladino, Mary Torregrossa, Colleen McClung, and Shirley Hill for their insight throughout the years to help ensure my research is as stringent and rigorous as possible. And lastly, I want to thank the MPGP program, Drs. Tija Jacobs, Patrick Pagano, and Jonathan Beckel as well as administrator Shannon Granahan. They have provided me with so much support, knowledge, advice, and collaboration over the years. What I have learned during my time at the University of Pittsburgh is truly invaluable; the skills I have learned, and people I have met, I will carry on with me for the rest of my career.

.

1.0 INTRODUCTION

The research completed herein to form this dissertation addresses a gap in knowledge surrounding Alcohol Use Disorder etiology. Ethanol, as a pharmacological agent, is known to dramatically alter the transcriptome (*e.g.*, expression changes and alternative splicing events). How does this dysregulation shift the propensity to consume ethanol or alter behavior in response to ethanol? Can individual ethanol-responsive RNA molecules exert these effects? Can consistent RNA dysregulation lead to addictive behavior over time? These questions led to a more specific one: does long noncoding RNA expression and function have direct impacts on ethanol consumption and ethanol-related behaviors?

1.1 ALCOHOL USE DISORDER (AUD)

1.1.1 AUD Background

Alcohol (ethanol) has been produced and consumed by humans for close to 10,000 years[1-4]. It is a socially accepted psychoactive drug with relaxant and euphoric effects, often associated with celebration and socializing[1,4,5]. Small or low doses of ethanol can be associated with health benefits[6-8], whereas moderate doses are at higher risk for adverse outcomes (dose-dependently)[9-11]. High doses act as a depressant, associated with a plethora of detrimental health outcomes[12-16]. When ethanol is consumed, blood alcohol concentration (BAC) increases. BACs ranging from 0.0% to 0.1% (0 – 100 mg/dL) produce a stimulative effect, resulting in disinhibition and relaxation. Once high doses are achieved (BAC > 0.1%; > 100 mg/dL) sedation sets in. As the dose of alcohol increases beyond 0.1%, there are progressive impaired sensory and motor function, slowed cognition, unconsciousness (0.3 - 0.4% BAC; 300 – 400 mg/dL), and the potential for death (0.4 - 0.5% BAC; 400 – 500 mg/dL)[17-21].

Alcohol misuse is the seventh leading risk factor for premature death and disability worldwide[22] and contributes to over 200 different diseases and injury-related health conditions

ranging from suicide, road injuries, and violence, to cancers, liver diseases, and cardiovascular diseases[23]. Alcohol misuse commonly has comorbid conditions (*e.g.,* alcohol-associated liver disease, heart disease, stroke, unspecified liver cirrhosis, various cancers, and hypertension)[24]. Due to these factors, alcohol-related deaths are the third leading preventable cause of death in the United States (tobacco is first, and poor diet and physical inactivity is second)[25,26]. Unfortunately, alcohol misuse is the first leading preventable cause of death in the age group of 15 – 49[22].

Alcohol Use Disorder (AUD) moves beyond general alcohol consumption. AUD is classified as a mental disorder, and defined as 'continued alcohol use despite negative psychological, biological, behavioral, and social consequences' by the Diagnostic and Statistical Manual of Mental Disorders (DSM-V)[27] and the International Classification of Disease[28]. AUD is among the most prevalent mental disorders worldwide impacting both biological sexes (although AUD prevalence is ~5x higher in males than females[29]). AUD is largely characterized by heavy compulsive alcohol use, loss of control of alcohol intake, and continued use despite negative consequences[29]. AUD is associated with a high burden of disease; it can cause disability and has a high risk of mortality[29-31]. Individuals suffering from AUD often exhibit escalating alcohol intake despite detrimental impact on relationships and health[29]. Nearly 15 million adults and 500,000 adolescents in the United States suffer from AUD[32], and 95 million globally[33]. AUD can range from mild to severe[27], but recovery is possible, regardless of severity[34-36].

AUD seriously impacts both physical and mental health[31,37-40]. Adverse physical effects of alcohol misuse include: vasodilation[41,42], increased levels of cholesterol-carrying high-density lipoproteins[43,44], allergic-like reactions[45-50], liver damage[51-56], brain damage[57-61], increased cancer risk[62-67], gastrointestinal effects[68-73], cardiovascular disease[74-76], birth defects if pregnant[77-79], and cognitive[60,80], motor[81-84], memory[85-88], and sensory[89-91] impairment. The co-occurrence of AUD with mental health disorders is also incredibly pervasive[92,93]. The most common co-occurrences, either simultaneously with AUD or sequentially, are depressive disorders[94-98], anxiety disorders[99-102], stress disorders[103-105], sleep disorders[106-109], and substance use disorders (SUDs)[39,40,110]. Despite considerable progress in our understanding of ethanol action, the etiology and pathogenesis of AUD remain unclear. It is largely accepted, however, that the development of dependance to alcohol result from long-term alterations to brain function and structure[111].

1.1.2 AUD Symptoms

Diagnosing AUD requires close analysis of an individual's symptomology. The DSM-V defines AUD as mild, moderate, and severe subclassifications[112]. Another symptom of continued alcohol misuse is the development of tolerance[88,113,114] (*i.e.*, a diminished effect of ethanol with the same amount as previously consumed). With tolerance, increased amounts of ethanol are needed to achieve the desired level of intoxication. Following the cessation of alcohol consumption, withdrawal events can set in[115-117]. Alcohol Withdrawal Syndrome is largely a result of neuroadaptations to long-term ethanol consumption[118,119]. Withdrawal effects can be defined in three main categories[120,121]: mild[122], moderate[123], and delirium tremens[124]. Delirium tremens is the most severe, and includes anxiety, insomnia, tremor, headache, palpitations, gastrointestinal disturbances, diaphoresis, increased systolic blood pressure, confusion, mild hypothermia as well as disorientation, impaired attention, visual hallucinations, auditory hallucinations, and seizures[120]. If the symptoms are too great, often alcohol or a related substance (*e.g.*, benzodiazepine[125,126]) are taken to relieve or avoid the symptoms[118,119]. Withdrawal symptoms often leads to relapse behavior, the resumption of alcohol drinking following an extended period of abstinence[119,127].

In humans, BACs of 150 – 300 mg/dL generally cause mental confusion, and disturbances of balance, sensation, perception, and coordination[128]. Fatal intoxications generally occur at BAC concentrations over 400 – 500 mg/dL[128,129]. However, for those with low tolerance, concentrations as low as 260 mg/dL have been fatal[128]. Tolerance to ethanol, conversely, can allow for much higher concentrations followed by a quick recovery. For example, two patients with BACs of 650[130] and 780[131] mg/dL respectively, were hospitalized for less than a day, and one man made a full recovery after a recorded BAC of 1127 mg/dL[132]. Consistently, many individuals have appeared "sober" (*i.e.*, ambulatory, oriented, neurological normality) but presented BACs spanning from 120 to 540 mg/dL[133].

1.1.3 Treatment Options

Ethanol is rather chemically inert under physiological conditions. The high alcohol concentrations needed for physiological effects, combined with the difficulties identifying targets

that respond to relevant inebriating ethanol concentrations, has led to the view that ethanol has a significant number of targets, and that intoxicating actions of ethanol are simply due to a summation of effects on numerous molecular targets[134].

Pharmacologic treatment of alcohol misuse and withdrawal are limited and under-prescribed. It often involves substituting alcohol for a long-acting agent, then gradually reducing dosage over time. There are currently three FDA-approved pharmacologic treatments for AUD, Acamprosate, Naltrexone, and Disulfiram, however none of them target the underlying disease progression and largely only work when the patient has a strong desire to quit[135]. Despite the widespread consequences of alcohol misuse, AUD has a very low treatment prevalence[29,136]. It has been shown that only 7.3% of adults suffering from AUD receive treatment[137], and less than 4% were prescribed FDA-approved AUD medications[138]. This could be due to the fact that current treatment options are only modestly effective, or that there is a lack of system-wide standardization of prescribing AUD pharmacotherapies[139].

Acamprosate was designed as an 'anti-craving' compound to ease withdrawal symptoms such as insomnia, anxiety, and restlessness (*i.e.,* negative reinforcement), thereby dampening the desire to relapse[140,141]. Acamprosate is formed as a dimer of acetyl-homotaurine, linked by calcium salt, and is a derivative of the amino acid taurine[142] with no addictive potential[140]. Acamprosate enhances GABA transmission, interferes with glutamate action, can act on calcium channels, and is thought to stabilize chemical signaling in the brain that is disrupted by alcohol misuse[142].

Placebo-controlled clinical studies in humans have reported increased abstinence rates in patients[143-156], however, Acamprosate is not an effective therapy for all individuals. Some clinical trials have found no success[157-160], and others have shown it works best in combination with psychosocial therapy or strong motivation to quit drinking[161-163] in order to facilitate a reduction in alcohol consumption and extended abstinence. The current view of Acamprosate is that its mechanism involves interfering with receptor and neurotransmitter systems to counteract the alteration of the system spurred by chronic alcohol exposure.

Naltrexone removes the pleasure associated with drinking by acting as a long-term competitive mμ-opioid receptor antagonist, blocking opioids from binding to their receptor, with no addictive potential[136,164]. Naltrexone blocks alcohol-induced dopamine release and reduces the associated "high" normally felt under opiate release (*i.e.,* positive reinforcing effects)[136,165,166].

In clinical trials Naltrexone has shown success at reducing alcohol consumption and relapse rates[150,152,154,156-158,167,168]. Like Acamprosate, Naltrexone has also proved to be ineffective in some cases[169,170]. If prescribed, it should be done so in conjunction with psychosocial therapy[164,167,171-174].

Disulfiram inhibits acetaldehyde dehydrogenase, which prevents acetate metabolism and results in a buildup of acetaldehyde, a toxic metabolite of ethanol[175,176]. The medication is used to treat AUD by producing a sensitivity to alcohol, and results in immediate non-specific withdrawal-like symptoms upon alcohol consumption[136,176,177]. This is designed to cause the patient to avoid alcohol when on the medication.

In clinical studies Disulfiram has been shown to have superiority for maintaining abstinence and increased days between relapse events than Acamprosate and Naltrexone, but mainly in conjunction with strong familial support[175,178-185]. However, Disulfiram did not show success at aiding severe AUD patients[186]. Disulfiram can cause serious adverse effects when alcohol is consumed including hospitalization if abstinence is not maintained[177,187,188], so proper adherence and commitment is critical of the patient[136]. Unfortunately, Disulfiram has also been shown to induce neuropathy[189-193], so thoughtful prescribing and close monitoring when taking Disulfiram is crucial.

There are also several potential therapeutics for AUD that are under experimentation or are a repurposed medication. These options do not have FDA approval for the treatment of AUD but hold potential. Metronidazole was marketed as an antibacterial agent that has been studied in conjunction with AUD since the 1960's[194-196]. It was originally a proven trichomonacide with its first reports on its usefulness in AUD treatment showing mixed results[196-199]. Imidazobenzodiazepine Ro15-4513 is a $GABA_A$ receptor ($GABA_AR$) ligand that has been reported as an antagonist to ethanol-induced behavioral intoxication[200-203]. Unfortunately, it is not useful in humans due to its half-life of 3 minutes[204], and insufficient efficacy for clinical development[203]. Dihydromyricetin (DHM) is a flavonoid component of herbal medicines that can counteract acute ethanol intoxication and withdrawal symptoms (*e.g.,* tolerance, anxiety, and seizure susceptibility)[205-207]. DHM was able to antagonize ethanol-induced potentiation and plasticity of $GABA_ARs$[205,206]. DHM's bioactivity showed great promise and is currently being marketed as hangover relief by More Labs in their drinkable Morning Recovery product. Unfortunately, DHM's pharmacokinetic properties are not optimal; DHM's poor oral bioavailability and

absorption, short half-life, and rapid clearance limit its clinical utility to treat AUD[207]. Gabapentin was originally marketed as an anticonvulsant and nerve pain medication[208]. Gabapentin has shown success at reducing the symptoms of alcohol withdrawal, alcohol dependance, and craving[208-212]. Unfortunately, its misuse, toxicity, and use in suicide attempts have been used to underscore the healthcare burden associated with clinical gabapentin utilization[213]. Lastly, Benzodiazepines and anticonvulsants have been shown to prevent alcohol withdrawal seizures and delirium tremens for decades[126,214]. These medications can reduce psychomotor agitation and prevent the progression of withdrawal symptoms[120,126]. Benzodiazepines target GABA to curb excitability in the brain during withdrawal, allowing time for the brain to restore its homeostasis. Unfortunately, these drugs also come with their own set of limitations, such as misuse liability, blunted cognition, and the potential for alcohol and opioid interactions[208].

Existing treatments for AUD are only moderately effective and minimally prescribed. This leaves behind a need for therapeutics where an understanding of the underlying pharmacokinetics of ethanol action is required. While there is no definitive mechanism for AUD, receptors and channels are still actively being researched. It is clear that receptors and neurotransmitter systems have been targeted for AUD treatment, however they have been met with limited success. There is a lack of knowledge surrounding how alcohol can dysregulate cellular systems, which leads to drug design that is subpar and drugs that target side effects and not the underlying cause. I aim to diverge from proteins and neurotransmitters for the study and treatment of AUD and produce a foundation on which the idea of noncoding RNAs for drug design and targeting can be built.

1.2 PHARMACOKINETICS AND PHARMACODYNAMICS OF ETHANOL

Ethanol has hydrophilic and hydrophobic properties, allowing it to interact with proteins and lipid molecules involved in signal transduction[215]. Ethanol crosses biological membranes easily through passive diffusion down its concentration gradient[216,217], and has been linked to blood-brain-barrier impairment[218-220]. There is also no single ethanol receptor, instead ethanol can interact either directly or indirectly with multiple molecular targets and interfere with cellular communication[215,221,222]. Ethanol can be absorbed in several different ways: orally, inhalation, rectally, and injection. It is distributed rapidly throughout the body, but mostly to tissues with the

greatest blood supply, primarily the brain, liver, and kidneys[216,217]. Approximately 90 - 95% of alcohol metabolism occurs in the liver via the enzyme alcohol dehydrogenase[216,217,223]. This converts ethanol to acetaldehyde; acetaldehyde is then metabolized by the enzyme aldehyde dehydrogenase into acetate[216,217]. At low-to-moderate physiological concentrations, ethanol completely saturates alcohol dehydrogenase[216]. Therefore, ethanol metabolism follows Michalis-Menten zero-order kinetics at typical physiological concentrations[216,224-226]. Ethanol does not have an elimination half-life at these concentrations (*i.e.,* it is not metabolized at an exponential rate) and instead is eliminated from the circulation at a constant rate[227]. Lastly, ethanol is eliminated via metabolism into carbon dioxide and water[227]. Roughly 5 – 10% of ethanol is also eliminated, unchanged, in urine, sweat, and breath[227].

Despite decades of extensive research, the pharmacodynamics of ethanol are not solidified. This is due in part to the very low molecular weight of ethanol (46.07 g/mol; CH_3CH_2OH)[228] and that it acts as a nonspecific drug[229]. It is only able to interact with other molecules via hydrogen bonds and weak hydrophobic interactions[229]. This is compounded with the fact that ethanol only produces potent effects at high concentrations[229]. No exact mechanism of action for ethanol is known, which makes identifying pharmacological targets very challenging. Traditional biochemical assays to assess ethanol binding are not yet possible, so functional studies are used to determine molecular actions. What is known, is that ethanol can modulate ligand-gated ion channels, receptors, and neurotransmitter systems to facilitate molecular adaptations in the CNS. Examples include: $GABA_AR$[230,231], GABA[232] and GABAergic neurons[233], ionotropic glutamate AMPA receptor[234,235], glutamate and glutamatergic neurons[236], NMDA receptor[234,235,237,238], glycine receptor[239], nicotinic acetylcholine receptors[240], serotonin 5-HT_3 receptor[241], voltage-gated calcium channels[242], dopamine[243,244] and dopaminergic neurons[245], and the endocannabinoid system[246,247].

Ethanol also impacts neuronal firing. For example, it can stimulate dopamine release[244,248,249] and can differentially alter GABAergic transmission[250-252]. Ethanol's effects on excitability are brain region[229,253,254] and cell-type[229,255,256] specific. Ethanol is also known to act as a GABA-memetic[257,258] and have synergism with GABAergic drugs (*e.g.*, barbiturates, benzodiazepines, and general anesthetics)[228,259-262], as they both act on $GABA_A$Rs. This has led to one of the main hypotheses for ethanol action. It is widely accepted that, at least in part, ethanol

function involves interactions with inhibitory neurotransmitter GABA and the GABAergic system[263-266].

The pharmacodynamics of ethanol in the brain involve the reward pathway, connecting the ventral tegmental area (VTA) to the nucleus accumbens (NAc)[232,233]. For example, the dopamine reward pathway transverses the prefrontal cortex (PFC), NAc, and VTA[267]. Alcohol's pleasurable effects result from increased levels of dopamine and endogenous opioids in the brains reward pathways[268,269], which may impact consumption when dysregulated in response to ethanol[270-273]. The reinforcing effects of alcohol are partially mediated by acetaldehyde, which plays a role on the activation of the mesolimbic dopamine system[274,275]. Reinforcement is also mediated by neurochemical systems, such as dopamine, serotonin, and GABA[276-279].

1.3 AUD AND THE CENTRAL NERVOUS SYSTEM (CNS)

1.3.1 AUD and Behavior

Ethanol impacts neurological systems, some of which are related to reward, stress, habit formation, decision making, and addictive reinforcement[280]. Further, alcohol misuse causes neuroadaptations in brain circuitry linked to AUD behaviors such as escalated alcohol use over time, tolerance, dependance, and propensity to relapse[281]. In order of increasing dose, alcohol can be anxiolytic and mood-enhancing, then lead to sedation and slowed reactivity, resulting in motor incoordination and impaired judgement (see: **Chapter 1.1.1**). To improve behavioral intervention outcomes, the underlying mechanisms that change such behaviors must be understood for effective therapeutics to be designed. Therefore, preclinical cognitive neuroscience research is required to continue providing insight into the pathophysiological processes that lead to and maintain AUD.

One way to research ethanol's molecular effects is through reverse-genetics approaches, also known as the bottom-up approach. This method builds from the identification of ethanol-responsive or ethanol-sensitive molecules, followed by determination and characterization of its roles in ethanol physiology and behavior[229]. Genetic alteration of the target gene (*e.g.*, knockout (KO) and knockin (KI) animal models[282]) allows for the precise detailing of ethanol's impact on

the system being tested. The reverse-genetics approach allows for analysis of the behavioral consequences of ethanol's effects on specific and individual targets.

In the alcohol addiction field, there are a plethora of employable paradigms that underly specific behavioral responses of interest. Some are used as a voluntary measure of drinking, such as binge-like drinking behavior (drinking in the dark[283,284]), chronic consumption (two-bottle choice[285]), or chronic intermittent consumption (every other day, two-bottle choice; escalation of drinking behavior that mimics human addiction[286,287]). Involuntary ethanol consumption paradigms to elicit addictive behaviors allow for a set quantity of ethanol to be absorbed, such as chronic intermittent ethanol vapor (CIEV) exposure[288]. CIEV can also been paired with voluntary consumption models to elicit dependence[289]. Selectivity of behavioral models is critical and dependent on the hypothesis being tested, as gene expression will differ based on the paradigm being employed[290].

Other experiments are used to measure behavioral responses to a set dose of ethanol, such as responses to a sedative/hypnotic dose (3.5 – 3.8g/kg; loss of righting response[291]) or doses that elicit altered motor incoordination (2.0g/kg; rotarod[292]) and sensitivity (1.5 - 2.0g/kg; acute functional tolerance[293] or chronic tolerance[230]) to ethanol. Related behaviors can also be of interest, such as anxiety-like behavior (elevated plus maze[294] and light/dark box[295,296]), depressive-like behavior (Porsolt forced swim test[297]), and altered activity (open field[298]). Taken together, a battery of behavioral experiments can be conducted in animal models of addiction to understand different facets of ethanol action.

1.3.2 AUD and the Brain

The brain, like the majority of organs, is vulnerable to alcohol-induced injury[299]. Susceptibility to AUD-related brain damage can be associated with biological sex, age, drinking history, family history, nutrition, as well as the vulnerability of specific brain regions[299]. In humans, the alcohol-addicted brain shows extensive gray and white matter loss when compared to controls[300]. AUD patients also showed an increased rate of gray and white matter volume loss than controls over time[301-303]. There is a significant negative association between global cortical

thickness and alcohol intake[304]; even light-to-moderate alcohol consumption has been negatively associated with brain macro and microstructure, dose-dependently[305,306].

Ethanol affects many signaling systems in the brain[215] and does not exert its influence identically across all brain regions. Not only do male AUD patients display global reductions in brain efficiency, but when multiple brain regions were analyzed for brain network efficiency and functional connectivity, eight regions were differentially disrupted[307]. Brain imaging analysis also revealed three regions involved in error-monitoring as being implicated in relapse behavior [bilateral orbitofrontal cortex (OFC), right medial PFC, and right anterior cingulate cortex], showing pronounced atrophy in these regions[308]. Morphological alterations of brain regions in response to alcohol intake have been observed as early as adolescence in humans, with the PFC and hippocampus showing heightened sensitivity[309]. Further, large-scale alterations in brain structure and networks have been identified from AUD patients[310], demonstrating the widespread impacts of chronic ethanol exposure.

It should be noted that humans may have pre-existing conditions or alternative regulation that results in differential susceptibility to SUDs (*i.e.,* cause versus consequence; high-risk versus low-risk for SUD development)[311-313]. Differences in brain morphology potentially originating prior to substance misuse should be considered as a factor when using data derived from human samples. There are brain region-specific susceptibilities, sensitivities, and molecular adaptations in response to chronic alcohol exposure in the brain, which then have distinct physiological impacts on behavior[314-316].

Individuals with AUD show variation from normal healthy controls in many brain regions[299-302]. Gray matter loss has been reported in both cortical and subcortical regions[317,318], and adults with AUD have additionally shown volumetric reductions of the OFC and amygdala compared to healthy controls[319,320]. While this may indicate that these regions are susceptible to alcohol misuse, abnormalities in these regions may occur prior to developing AUD or SUD. In a longitudinal investigation, OFC volume in relation to amygdala volume was predictive of SUD outcome[313], suggesting that atypical structure and function of these regions may be one biological mechanism that confers risk for SUDs. These observations underscore the limitations associated with analysis of human brain samples. Samples from individuals with AUD therefore include characteristics may precede development of AUD as well as the consequences of multiple years

of alcohol misuse. Nevertheless, they are a first step in human analysis of genetic variation that may point to important medication development.

1.3.3 AUD and the Prefrontal Cortex (PFC)

Humans who suffer from AUD often show frontal lobe morphological abnormalities[321] and share behaviors characteristic of frontal lobe disfunction (*i.e.*, impaired judgement, poor insight, and reduced motivation)[322]. Consistently, one key feature of humans suffering from AUD is their continued use of alcohol despite their knowledge of physiological and psychological damage in response to their behavior[322]. These behaviors are indicative of AUD-linked executive function dysregulation within the frontal lobe.

The frontal lobes of the cerebral cortex are especially sensitive to the effects of alcohol[61,316]; it has been consistently documented than the frontal lobes are more vulnerable to alcohol-related damage than other cerebral regions[323,324]. The PFC performs decision making and regulates craving[37], as well as controlling executive function, which includes abstract thinking, motivation, planning, attention, and impulsivity control[325]. The PFC is a key player of addictive behaviors and the propagation of addiction[316,323,326]. Impaired function of the PFC is linked to relapse drivers such as alcohol craving and preoccupation with alcohol[326]. PFC disruption in addiction underlies compulsive drug taking as well as detrimental behaviors and "the erosion of free will[326]."

Humans suffering from AUD experience gradual PFC dysfunction as a function of both time and alcohol consumption[37]. Neuropathological changes have been consistently observed, and neuroradiological studies demonstrate abnormalities consistent with cerebral atrophy[321]. Heavy drinking and corresponding high BACs induce neurodegeneration and PFC dysfunction that occurs over time[325]. Human brain imaging studies have demonstrated alterations in PFC function and composition, such as the reduction of gray matter[327] and decreased dopamine transmission in the medial PFC (mPFC)[328], in patients addicted to alcohol.

The mPFC is a subregion of the PFC with high importance to addiction[329,330]. Alcohol-paired cues have been shown to induce mPFC activity[331,332] and it has high interconnectivity to the BLA[333,334] and NAc[335-337], both also involved in ethanol action[334,335]. Neuronal circuitry between the mPFC-NAc and mPFC-BLA has been linked to drug misuse[338]. mPFC neurons projecting to

the NAc blocked cue-induced reinstatement of alcohol seeking[335], and the mPFC-BLA pathway was found to be a target of chronic ethanol-associated plasticity[334]. Distinct populations of neurons within these three brain regions have been shown to encode features of alcohol-seeking behavior[339,340]. Targeting such neurons involved in these mPFC pathways offers the potential for multiple ethanol-responsive circuits to be dysregulated and reveal further mechanisms to be explored (See: **Chapter 4**).

1.3.4 AUD and the Hippocampus

It has been posited that the hippocampus is involved in both the development and maintenance of addiction[341]. The hippocampus mediates a cognitive/spatial form of memory[342] and is important in learning and for the formation and storage of memories[341]. There is significant overlap between the neurobiology of learning and memory and the neurobiology of addiction[343]. Further, addictive behavior has been posited as a drug-associated pathological memory[344]. Both short- and long-term memory processes (*i.e.*, long-term potentiation[345]) and those involving synaptic plasticity are needed for drug-associated learning and memory[346].

Chronic ethanol exposure impairs the hippocampus on multiple levels: anatomy, plasticity, cell signaling[343]. Animal models for ethanol misuse have shown impairment in hippocampus-dependent learning and memory[343], hippocampus-dependent contextual cued fear conditioning[343], and reinforcement of alcohol misuse through learning and memory[342]. Ethanol exposure resulted in hippocampus-dependent spatial learning deficits[343], necrotic cell death and neurodegeneration[343], and dramatic and persistent decrease in hippocampal proliferation and neurogenesis[347,348]. Extensive hippocampal gene expression changes have been reported in response to cocaine[346], alcohol[346], and opioids[344], suggestive of common addictive neuronal adaptations within the hippocampus. The hippocampus has its own set of insults in response to ethanol, and while not part of the reward pathway, it is clear that hippocampal learning and memory is critical for the development of addiction.

1.3.5 AUD and the Neuroimmune System

Alcohol and other drugs of abuse strongly impact the neuroimmune system[280,349-351]. Neuroimmune signaling acts together with neurotransmitter and neuropeptide systems to mediate neuroinflammation and modulate normal brain function, and conversely, brain dysfunction[280]. Genetic and behavioral evidence supports a neuroimmune hypothesis of alcohol addiction: alcohol misuse activates innate immune signaling in the brain and drives further misuse[352]. Alcohol has been shown to interact with the neuroimmune system by altering gene expression and signaling, which can cascade into various aspects of addiction[280,349]. External stimuli (*i.e.,* alcohol) causes neuroimmune cells such as microglia to release neuroimmune factors that can exert either neuroprotective or neurotoxic effects within the brain[280]. Immune molecules interact with neurotransmitter systems to modulate synaptic function[280]. In turn, neuroimmune signaling can regulate alcohol consumption, and excessive alcohol consumption then alters neuroimmune signaling, creating a positive feedback loop increasing consumption, craving, and dependance over time[350]. Alcohol action on neuroimmune function has been suggested as key for the development of dependence, consumption escalation, craving, tolerance, and withdrawal[350].

Cytokines are very important within the neuroimmune system. They are multifunctional proteins involved in cell-to-cell communication and immune responses[353]. Such cytokines include interleukins (IL) and similar proteins like Oncostatin M (OSM), which transduces its signals via the OSM Receptor (OSMR)[354,355]. OSMR is a member of the IL-6 receptor family, and its signals can lead to activated monocytes, macrophages, T cells, dendritic cells, neutrophils, and Schwann cell precursors[356]. The OSM-OSMR signaling pathway has already been the target for therapeutic intervention[357] and linked to traumatic brain injury[358], several cancer types[359-364] and other disease states[357,365-368]. Of specific interest is the fact that OSMR has been linked to methamphetamine-induced astrogliosis within the striatum[369] and was identified as significantly dysregulated between human's who suffered from AUD and control in a whole genome-transcriptomic organization analysis of the PFC[370]. Further, OSMR was characterized as a central hub within a set network involved in respiratory and infectious disease implicated in AUD[370].

Another member of the IL family is Myeloid Differentiation 88 (MyD88). MyD88 has been suggested as a signal transduction IL-1 and Toll-like receptor (TLR) adaptor involved in innate immune responses such as inflammatory and apoptotic signaling pathways[371-374]. *MyD88*

mutation has been linked to cancers[375-377] and AUD[378-380]. Like OSMR, MyD88 has also been a suggested therapeutic target for disease[381,382].

Glucocorticoids and the glucocorticoid receptor (GR) are another example of important players within the neuroimmune system. Glucocorticoids ensure proper function of inflammatory events[383-385]. Glucocorticoid action occurs via binding to the GR, transcriptionally activating anti-inflammatory, immunosuppressive, and regulatory proteins[383-385]. Glucocorticoids and GR signaling have been strongly linked to AUD[386-391]. Studies emphasize the importance of GR signaling in ethanol-drinking and addictive behaviors[386-392]. Epigenome-wide association studies revealed a network of differentially methylated regions in glucocorticoid signaling and inflammation-related genes associated with alcohol use behaviors[393]. Further, glucocorticoids are synthesized and released in response to ethanol exposure and withdrawal[386,390,392], GR mRNA expression is reduced in the mPFC of ethanol-dependent animals, and pharmacological treatment with GR antagonist blocks escalated ethanol consumption[386,389,391]. The GR can also be regulated by noncoding RNA (ncRNA). *Growth arrest-specific 5 (Gas5)* is a ncRNA that can bind within the GR DNA-binding domain to act as a repressive decoy, inhibiting GR function and regulating GR signaling[394]. *Gas5* is strongly implicated in regulating transcriptional activity of the GR, and has multiple documented functions related to the immune system[393,395].

While receptor signaling pathways are critical for normal cellular communication, their dysregulation can lead to diseases like addiction. A better understanding of cellular regulation, how these systems become and maintain dysregulation, and potential targets to inhibit such sustained alterations, is crucial for understanding the mechanism of ethanol action.

1.4 AUD AND RNA

The transcriptome is widely dysregulated in AUD[111,396-399]. Many AUD research targets have been identified through RNA sequencing (RNA-Seq) and microarray strategies because of their substantial dysregulation[396,400-403]. Standard RNA-Seq techniques enrich for poly-adenylated (poly-A) RNA, which skews the results to largely be highly expressed coding messenger RNA (mRNA) transcripts[404,405]. AUD-linked mRNAs and their respective proteins have been researched

extensively[378,406-410], but there are many other RNA subtypes besides mRNA that are also responsive to ethanol[398,411] and have vast functions beyond protein production.

1.4.1 Noncoding RNA (ncRNA) Epigenetics

The human transcriptome can be divided into two subgroups: coding and noncoding. Only ~2% of the mammalian genome encodes protein-coding genes (*i.e.*, mRNA), and ~80-90% of the transcriptome are ncRNA [*e.g.,* micro-RNA (miRNA), long noncoding RNA (lncRNA), circular RNA (circRNA), transfer RNA, ribosomal RNA, *etc*.][412-416]. The noncoding transcriptome is known for its wide breadth of regulatory function[334,417-420]. ncRNAs can act as potent and multifunctional epigenetic modulators to alter gene expression without altering the genetic information, acting as 'puppet masters' (*e.g.,* scaffolds, decoys, sponges, enhancers, repressors, transcription factors)[334,417-420]. ncRNA have been largely overlooked for decades as 'junk' but have emerged as instrumental in the maintenance of homeostasis and the regulation of cellular functions[418,421-424]. ncRNAs generally function in specific networks with other ncRNAs to fulfill their role [competing endogenous RNA (ceRNA) networks], so disruption of coordinated co-expression can cascade into disruption of the entire ceRNA network (**Figure 1**)[396,425,426].

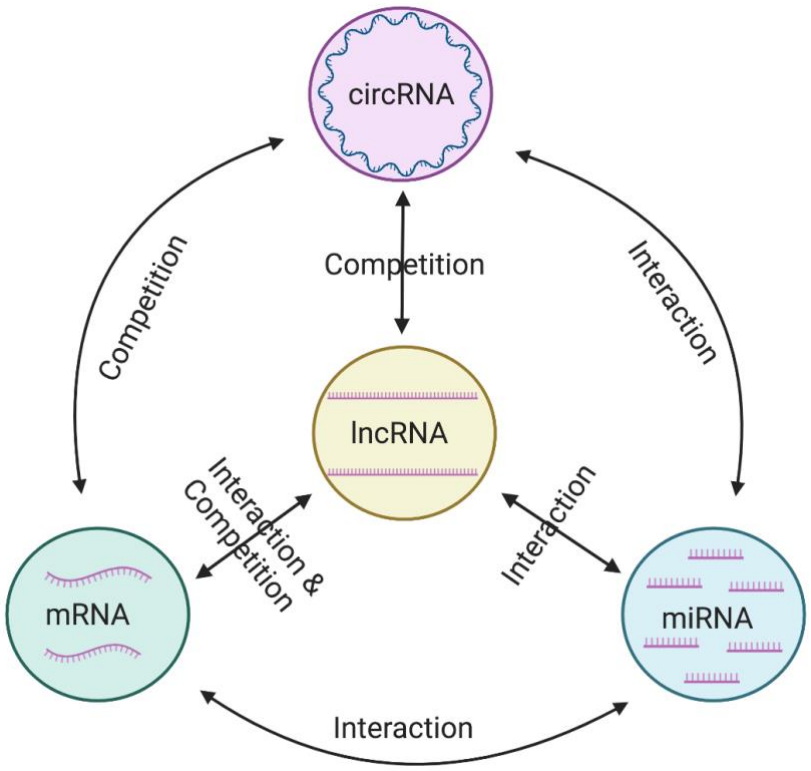

Figure 1: Schematic overview of ceRNA network connectivity. Micro RNA (miRNA) interacts with circular RNA (circRNA), messenger RNA (mRNA) and long noncoding RNA (lncRNA). CircRNA is in competition with mRNA and lncRNA. mRNA and lncRNA can both interact and compete. Figure adapted from Nei *et al*. 2017[420].

1.4.2 Competing Endogenous RNA (ceRNA)

Expression of ncRNAs are often correlated with each other, working in concert to fulfill cellular functions in response to stimuli (*e.g.*, alcohol, hormones, heat, pH, cell signaling events; **Figure 1**)[427]. They offer the potential to interact with other ncRNAs, DNA, and proteins[418]. Integrated networks of related ncRNAs, that influence, interact, or compete with each other are referred to as ceRNA networks[416,418,428]. This interplay among diverse RNA species allows for crosstalk, and RNAs can communicate via competition for, or interaction with, shared pools of binding partners[397,429,430]. A ceRNA (such as a lncRNA[431-437]) has the potential to act as a central 'hub' RNA. It is linked too and can impact its entire network of related RNAs, which can manifest as a significant cellular change[416,420,428].

1.4.3 Micro RNA (miRNA)

miRNAs are a subclass of ncRNAs that are small ~21 – 23 nucleotides (nts) long and can regulate gene expression and post-transcriptional processing[413,416,420]. miRNAs suppress gene expression by binding to their target RNA in a sequence-specific manner[413,416]. They do this via binding to 3' or 5' untranslated regions of mRNAs thereby targeting the mRNA for degradation or inhibiting ribosome binding and subsequent protein translation, respectively[438]. miRNA regulatory roles are far-reaching, including apoptosis, differentiation, proliferation, and cell cycle[420,438].

miRNA-orchestrated translational dysregulation has been linked to the transition of ethanol consumption to dependence[439]. For example, mPFC-expressed miRNA-30a-5p has been shown to control the transition from moderate to excessive alcohol consumption via the brain-derived neurotrophic factor (BDNF) pathway[440]. Further, ethanol-responsive miRNAs have been linked to neuroinflammatory TLR4 signaling responses in the murine cerebrum[441]. In humans, alcohol-responsive miRNA-mRNA interaction networks have been identified in various brain regions, with hundreds of miRNAs noted for future AUD research[397,430].

1.4.4 Circular RNA (circRNA)

CircRNAs are ncRNAs that form closed-loop structures and can alter gene expression through miRNA sequestration[413,417,420]. CircRNAs primarily arise from pre-mRNA backsplicing events, in which 5' and 3' ends of introns or alternatively spliced exons are covalently linked, creating a back-splice junction[413,417]. Due to their loop structure, they are resistant to exonuclease-mediated degradation and are more stable than linear ncRNAs[420]. Of the circRNAs characterized, a large percentage function as miRNA sponges, acting as ceRNAs[417,420]. miRNA sequestration via circRNA binding decreases miRNA-mRNA interactions, thereby regulating protein expression and correlating their expression[413,417].

CircRNA research is a relatively new area of study, so the links to AUD are just beginning to be explored. However, it has been shown that circRNA networks were significantly dysregulated in the NAc of postmortem AUD patients compared to control[417]. The circRNA

analysis was then combined with mRNA and miRNA to identify specific circRNAs hypothesized to be ceRNA hubs (*e.g.*, circRNA-406742)[417]. Beyond AUD specifically, neuronal circRNAs have been implicated in addition to methamphetamine[442], and both morphine and cocaine use induced widespread circRNA dysregulation in the NAc[443] and striatum[444], respectively. This highlights circRNA dysregulation within addiction.

1.4.5 Long Noncoding RNA (lncRNA)

LncRNAs are the largest subclass of ncRNAs, but like other RNA subtypes, they are understudied and underdefined[413]. LncRNAs are versatile molecules that can interact with DNA, RNA, and proteins to modulate expression patterns and molecular functions at multiple levels within the cell[412,413,415,416,427,445]. LncRNAs are non-protein coding transcripts that are at least 200 nts[412,413,415,416,427]. Like mRNA, some lncRNAs can be poly-adenylated, capped, and have multiple exons and splice variants[412,416,427,445]. The majority of characterized lncRNAs are developmentally, temporally, cellularly, and subcellularly regulated[412-414,427,446]. LncRNA-mediated regulation can occur in *cis* or *trans* fashion and can localize within the nucleus and/or the cytoplasm[413,446]. LncRNAs can be classified in several different ways depending on their genomic location: long intergenic noncoding RNAs, natural antisense transcripts, and intronic lncRNAs[412,413].

Functionally, lncRNAs act as master regulators within the cell to maintain homeostasis (**Figure 2**). LncRNA functions include imprinting genomic loci, managing chromosomal conformation, and regulation of enzymatic activity, cell state, and differentiation[415,427,445]. They can act as molecular decoys, scaffolds, transcription factors, and can both interact and compete with other regulatory ncRNAs (**Figure 1**)[427,445]. Their roles fall within both pre- and post-transcriptional regulation of diverse cellular processes[446]. They can positively or negatively regulate gene expression, for example, through recruiting transcription factors or sequestering miRNAs[446].

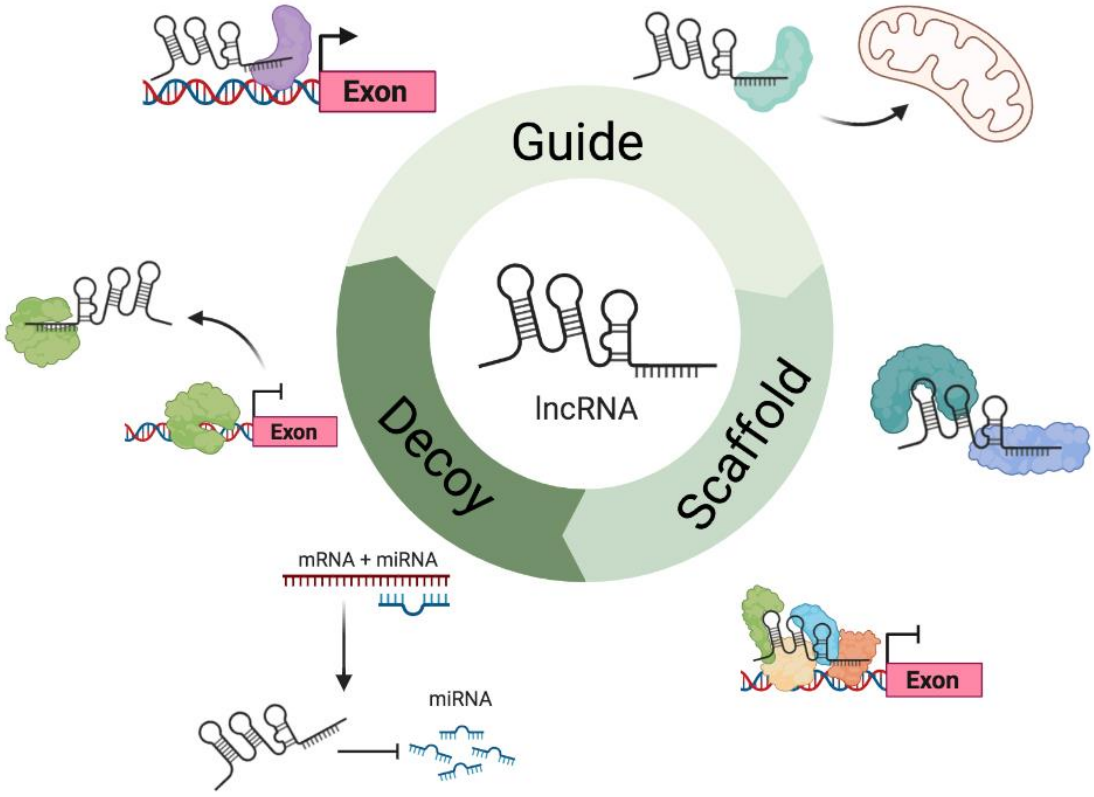

Figure 2: Schematic of lncRNA physiology. LncRNAs can act as guides, scaffolds, and decoys within the cell. Figure adapted from Dong *et al*. 2018[447].

There are over 55,000 lncRNA genes and 125,000 known lncRNA transcripts[413,415,445,448-452], however the majority of lncRNAs still have unknown functions[415,427]. Many are expressed at very low levels[413,427,445], but they are more highly expressed in the brain when compared to other organs[420,445]. LncRNAs are tightly regulated, underscoring the essential role lncRNAs have at determining cellular status[427]. There are distinct mechanisms for lncRNA transcription, processing, turnover, and export and import, all of which are linked to their respective function[445].

Taken together there is a lot known broadly about lncRNAs but deciphering individual specifics still remains a challenge. It is clear that their endogenous expression is very important, but what happens if they become dysregulated in response to disease? How do they respond to ethanol? Can their genetic mutation lead to cells that have altered susceptibility to ethanol action? The lncRNA subtype is of particular interest to research because of their sheer number, their

potential to be hub ceRNAs, the vastness of potential mechanisms they're involved in, the benefits for drug design, and their overwhelming implication in disease pathogenesis.

1.4.5.1 lncRNAs and Disease

lncRNAs are strongly implicated in disease states and disease progression[413,420,427,445,453-455]. Examples include cancers[456-461], neurological diseases[462,463], psychotic disorders[464], psychiatric disorders[465], and addiction[454,466-470]. The cancer field is farther along in lncRNA characterization than the addiction field, but as research progresses, many cancer-related lncRNAs have also been linked to psychiatric disorders, including drug addiction (*e.g.*, lncRNA *Gas5* has been implicated in various cancers[471,472], cocaine misuse[466], and AUD[393]).

A handful of literature has already begun to study lncRNAs in relation to the neurobiology of AUD[314,401,454,473-476], however to-date very few individual lncRNAs have been reported on for their specific roles in ethanol action. The biological functions of novel ethanol-linked lncRNAs have so far been associated with altered gene networks and RNA co-expression[314], alternative splicing[401], and neural function[475]. 19 lncRNA modules and 86 lncRNA hubs within those modules were identified from human post-mortem NAc via weighted gene co-expression and Pearson correlations analysis and were linked to neuronal and immune-related processes[314]. Analysis of spicing events in human post-mortem superior frontal cortex, NAc, BLA, and central nucleus of the amygdala revealed alternative transcriptome expression and widespread alternative splicing in AUD subjects when compared to control, linked to altered expression of splicing factors and splicing-related lncRNAs[401]. LncRNAs have also been suggested as biomarkers for disease. Analysis of patient samples for hepatocellular carcinoma (HCC) revealed lncRNAs linked to both HCC and HCC risk factors (*i.e.,* alcohol consumption), with ethanol-responsive *lnc-CFP-1:1* and *lnc-CD164L2-1:1* showing significant dysregulation in HCC patients and correlation with patient survival[474].

One example of a specific AUD-linked lncRNA is *Brain Derived Neurotrophic Factor-antisense* (*BDNF-AS*). *BDNF-AS* has been described as a regulator of *BDNF* expression and epigenetic reprogramming events in the amygdala of humans with AUD, with expression being differentially regulated between early onset and late onset AUD[473]. In early onset AUD samples, *BDNF-AS* expression was linked to decreased N6-methyladenosine on *BDNF-AS*, and *BDNF-AS* upregulation was associated with reduced *BDNF* expression (suggested as occurring via the

observed increase in EZH2 recruitment, which is known to deposit repressive trimethylations at regulatory regions of the *BDNF* gene)[473]. Another example comes from the lncRNA named *long non-coding RNA for alcohol preference* (*Lrap*). *Lrap* was identified as a hub gene from a gene co-expression module associated with alcohol consumption, and whose mutation increased ethanol consumption and preference in Wister rats compared to controls[476]. *Lrap* mutation also altered the expression and splicing of over 700 additional transcripts, putting it forward as a hub regulator within the brain[476]. While the field is growing, there are still thousands of individual lncRNAs that remain uncharacterized for their relevance to AUD and other human disorders but hold the potential to regulate cellular mechanisms and alter behaviors.

1.4.5.2 lncRNAs as Therapeutic Targets

LncRNA research has generated a novel therapeutic field and diagnostic methods[413,445,477,478]. They can act as specific drug targets[453,477,479,480] as well as potential biomarkers for disease (lncRNAs are easily detectable in saliva, plasma, urine, and tissues)[413,430,434,453,481,482]. They have already been proposed as both therapeutic targets and therapeutics themselves (for reviews, see: [483-487]). The high level of specificity and tight regulation that lncRNAs are under offer them up as superior targets when compared to proteins for disease pharmacology[431,445,482]. Since lncRNAs generally regulate specific networks of related genes, they offer reduced off-target effects as well[453].

LncRNAs may make better therapeutic targets than miRNAs or circRNAs too because of their size. LncRNAs are flexible and complex, forming large tertiary structures that function within set networks within discrete spatial and temporal patterns. RNA therapeutics are relatively simple and cost effective to manufacture, and can target pathways that were previously believed to be "undruggable[488]." It is also much more manageable to produce different RNA constructs, allowing for personalized therapeutics to become more widely available[488]. Single-stranded RNAs can be targeted by highly specific small molecules that can bind to the target RNA thereby impacting its function [*e.g.*, antisense oligonucleotides (ASO), small interfering RNAs (siRNA), short hairpin RNAs (shRNA)][479]. They offer potentially more options for drug design and on-target specificity simply due to more locations for siRNA or shRNA binding.

LncRNA biology is fascinating, complex, and incredibly important. Understanding the functions of specific lncRNAs offers the potential to discover novel players in disease, and easily

targetable molecules for research and pharmacological purposes. While there is a lot of generalizing within the field on mechanisms, it is important to characterize individual lncRNAs for their molecular roles. Does your lncRNA of interest function in the nucleus to regulate neighboring gene expression? Does it function cytoplasmically as a sponge or guide? Is its role structural, acting as a scaffold? And, most importantly, does individual lncRNA genetic mutation confer altered behavior?

1.5 NONCODING RNA MECHANISMS IN AUD

Ethanol exposure clearly alters gene expression[290,396,397,401,411,476,489-491], and conversely ncRNAs play an important role in alcohol addiction[37,314,396,401,411,473,476,492] (**Figure 3**). Thousands of genes, both coding and noncoding, their interactions with each other, and adaptations to consistent cellular alterations contribute toward the etiology of AUD[397]. For example, ncRNAs have been shown to alter synaptic plasticity[37] and miRNAs associated with cell death, cell proliferation, and cell-cycle pathways were significantly dysregulated in response to AUD[492]. Further, ethanol-induced miRNA alterations in animal models have been linked to cellular tolerance to ethanol[493], regulation of ethanol consumption and preference[494,495], binge-like drinking episodes[496,497], and dependence[495,498]. Chronic alcohol intake can cause both reversable and irreversible changes to the expression of the brain transcriptome, altering gene networks and crosstalk between gene networks[37,370,396,399,499]. Further, alcohol-induced transcriptional reprogramming within distinct brain regions can influence the risk of alcohol addiction progression[290,370,396,397,411,490,500].

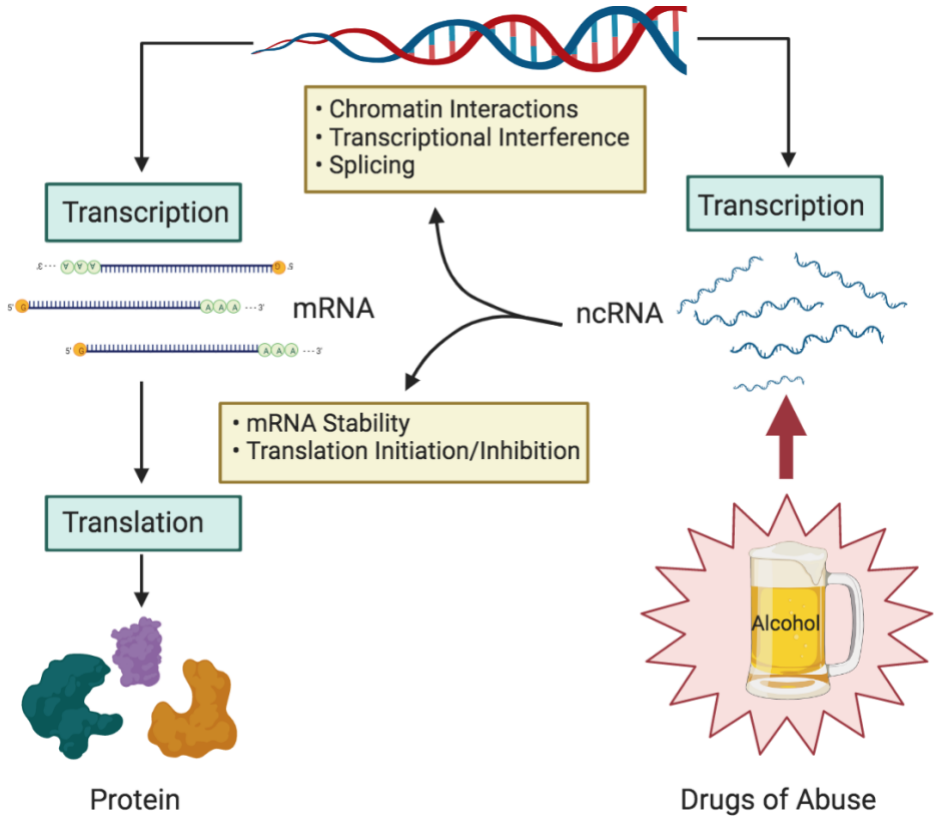

Figure 3: Schematic overview of alcohol-mediated ncRNA dysregulation. Schematic of alcohol-mediated regulation of ncRNAs. Green boxes represent the central dogma of gene expression. Yellow boxes represent ncRNA regulatory roles in gene expression. Drugs of abuse, including alcohol, impact the transcriptome which then alters ncRNA molecular functions. Figure adapted from Mayfield *et al.* 2017[411].

Human postmortem AUD PFC and NAc has a widely disrupted transcriptional landscape when compared to control[396,397,489,500] and AUD can cause global changes in RNA splicing throughout the brain[401]. The various roles of ncRNA implies a vast network of regulation and coordination of cellular pathways[397]. For example, 204 different lncRNAs and ncRNA networks have been identified from human AUD NAc samples as being significantly associated with alcohol dependence when compared to control[314]. The underlying mechanisms are not completely known and more lncRNAs need to be researched for their roles in AUD to continue pushing the field forward. Taken together, ncRNAs hold the potential to not only act as biomarkers for AUD progression, but also as predictors of therapeutic responses and as specific therapeutic targets for AUD themselves[37,454].

1.6 SEXUAL DIMORPHISM

Many areas of basic neuroscience are fundamentally different in males and females. This ranges from differential gene expression, reward pathways, cell signaling, and structural plasticity to complex decision making and behavioral manifestations[501-508]. Further, ncRNAs are known to differentially affect the sexes[465,509-514] (*e.g.,* depression[465,515]). Under normal physiological conditions, sex-specific and brain-specific differential expression of ncRNA fragments have been observed within the frontal cortex, hippocampus, and cerebellum[516], and cholinergic-targeting ncRNAs temporally modulated sex-specific acetylcholine signaling[517]. Some lncRNAs are also sex chromosome-specific, such as *Xist*, which is expressed in females and used for X chromosome inactivation[518]. Several unannotated lncRNA genes have also been identified on the Y chromosome and expressed only in males, while other genes expressed in both males and females showed imbalanced gene expression across sex during neurodevelopment[519]. Differential transcriptional programming has also been noted between males and females within the nervous system. Sexually dimorphic transcriptional reprogramming was observed in peripheral nerve regeneration[520] and following traumatic nerve injury within the dorsal root ganglia[511]. Sex differences are so pronounced that they have also been suggested in near-all phases of drug addiction (reinforcement, occasional to compulsive use transition, withdrawal-associated negative affective states, drug craving, and relapse propensity)[521,522] and are differentially dysregulated in response to drugs of abuse[523], including alcohol.

Direct comparison of alcohol-addicted men and women showed different brain morphological deficits[524], and sex-specific expression of key neural regulatory proteins can influence ethanol drinking behavior[525]. Ethanol exposure too can produce dimorphic differences in expression[526] and behavior (*e.g.,* ethanol consumption)[527-531]. Behavioral neurobiology quantifies select physical activity to infer cognitive states; if not considered as a variable, sex-dependent behaviors may be missed and experimental outcome interpretation may be misconstrued[501]. This is important to consider when researching addiction, because alcohol is not the only molecule that has a disparity between research conducted on male versus female subjects (*i.e.,* the sex-bias)[501,532-534].

1.7 CRISPR/CAS9 AND ASSOCIATED TECHNIQUES

1.7.1 The CRISPR System

Clustered Regulatory Interspaced Short Palindromic Repeats (CRISPR) is part of a bacterial immune system that protects bacteria from infection. This mechanism functions by using CRISPR RNA (crRNA) and invariant trans-activating CRISPR RNA (tracrRNA) to guide the silencing of foreign nucleic acids[535,536]. This system was quickly exploited for research purposes, and allows for site-specific DNA mutagenesis[535,537].

Many different CRISPR systems have now been identified, however the most commonly used version employs the *Streptococcus pyogenes* nuclease, CRISPR associated protein 9 (spCas9)[535]. Specifically designed guide RNA (gRNA; crRNA + tracrRNA) when combined with the spCas9 nuclease allow for highly accurate mutagenesis with limited off-target effects. Commercial guide RNAs are typically a single, short RNA (~85 – 125 nt) referred to as a single-guide RNA (sgRNA)[535,537]. This sgRNA has two functions: bind to its specific target DNA sequence and bind to the Cas9 protein. Recruitment of the Cas9 protein occurs via an invariant RNA scaffold region[535,537]. Alternatively, gRNAs can be generated by annealing a site-specific crRNA to the invariant tracrRNA[536]. Together the complex forms the gRNA, which is biologically identical to the sgRNA. The gRNA and Cas9 protein form a ribonucleoprotein (RNP) complex and search the genome until the complementary DNA sequence is found to the ~20 nt crRNA of the gRNA[535,536]. For functionality of the system, the crRNA must bind immediately upstream to a protospacer adjacent motif (PAM), which is specific to the subtype of Cas9 being employed[535-537]. The spCas9 PAM sequence is NGG, where N is any base and G is guanosine[535,536]. The spCas9 enzyme then cleaves the DNA with a double-strand break ~3 bp upstream of the PAM sequence[535,537]. Repair of the double-strand break occurs most frequently by non-homologous end joining, which is prone to errors, and often results in an insertion or deletion (indel) of bps[535]. The vast majority of on-target activity results in indels of less than 20 bps[538]. Alternatively, if multiple gRNAs are used large indels can be engineered into the genome[379].

1.7.2 CRISPR/Cas9 Specificity

Major concerns are frequently raised about Cas9 off-target binding and cleavage[539]. Off-target effects can lead to adverse impacts or effects that are not due to on-target mutagenesis. It's suggested that the RNA-guided, DNA-targeting Cas9 does result in some off-target DNA cleavage activity (the system allows 3 – 5 mismatches in the PAM distal region of the crRNA guide sequence)[540]. While off-target activity does happen, it has been shown largely *in vitro*[540-543]. However, when analyzed *in vivo* only a small percentage of the predicted off-target sites were substantially mutated[544-552]. Chromatin immunoprecipitation coupled with RNA-Seq (ChIP-Seq) was used to analyze off-target Cas9 sites genome-wide[540,553]. The off-target binding sites were found to be dependent on the gRNA used; site numbers ranged from only tens to the upper thousands[540]. However, it should be noted that off-target indel rates were significantly lower than on-target indels[540]. Further, despite a large number of off-target binding sites, the majority did not even harbor indels and those that were detected were at a very low frequency[553].

Other techniques to mitigate the possibility of off-target effects have been developed, such as delivery of CRPSPR/Cas9 RNPs as opposed to CRISPR/Cas9 DNA or RNA, modified Cas9 enzymes, and specific and improved delivery techniques[538] (for reviews, see: [554,555]). For example, high-fidelity Cas9 (HiFi Cas9) variants designed to reduce non-specific DNA interactions have significantly reduced off-target binding compared to the unaltered variant (*e.g.*, p.R691A mutation[556])[557,558], with another showing no detectable off-targets genome wide (altered hydrogen bonding contacts)[559]. gRNAs must also be highly specific, designed with avoidance of similar sequences in other regions within the genome[539,560]. For example, comparison of several different sgRNAs demonstrated a 5,000-fold decrease in off-target activity when nucleotide binding specificity was increased and when mismatched sequences were reduced[539]. If CRISPR/Cas9 reagents are selected and designed with careful thought and knowledge of the system, then the potential for off-target impacts can be greatly minimized.

1.7.3 Therapeutic Potential for CRISPR/Cas9

The development of CRISPR genome editing opens new possibilities in precision medicine. CRISPR/Cas9 gene therapy is in its infancy, however current clinical trials are ongoing for both *ex vivo* and *in vivo* utilization[561-563]. The most recent CRISPR/Cas9 clinical trials from 2022 fall within specific treatment areas in which CRISPR/Cas9 can be utilized (cancers, blood disorders, diabetes, eye disease, infectious disease, and protein-folding disorders)[561]. Current clinical use of CRISPR/Cas9 is limited by delivery modalities, which influence the safety and therapeutic efficacy. The CRISPR toolkit can be packaged and encoded as plasmid DNA, or packaged as Cas9 mRNA and gRNA, or delivered as an RNP complex[562]. These components can then be delivered *in vivo* or *ex vivo* through vehicles (*e.g.*, viral vectors, microinjection, electroporation).

1.7.4 CRISPR Techniques and Adeno-Associated Virus (AAV)

Genetically engineered animals are powerful *in vivo* tools that offer reverse genetics-based insights into gene function[535,537,564]. Gene-targeted animals (*e.g.*, KO and KI models) are the gold-standard for probing behavioral and molecular functions of novel genes of interest[535-537]. As science has improved this technique has been exploited for scientific gain. A variety of derivative CRISPR/Cas9 techniques have emerged to fulfil specific scientific niches. One example includes the development of an enzymatically dead version of Cas9 (dCas9) which can be fused to enhancer (*e.g.*, synergistic activation mediator; dCas9-SAM[565,566]) or repressor (*e.g.*, Krüppel-associated box; dCas9-KRAB[557,567-569]) elements. dCas9 does not mutate the genome but can alter expression profiles, and is referred to as CRISPR activation or inhibition, respectively. Other techniques, such as CRISPRainbow[570] and dCas9-SunTag[571] have been used as fluorescent markers in live cell imaging. CRISPR methods can be further specified to be functional only in designated cell or tissue types (*e.g.*, Cre lines, viral expression, Cas9-expressing animal lines). There are many options to select from in the genome editing toolbox; selection is dependent on the hypothesis being tested.

Global; non-specific: It has been extensively shown that Cas9 protein/gRNA RNP complex can be electroporated into single-cell pronuclear zygotes to generate global mouse mutants[379,537,572-575]. This method causes the desired mutation in every cell of the animal beginning at gestation but holds the potential for cellular compensation.

There are many ways to generate a global gene-targeted mutant animal line using CRISPR/Cas9. Promoters, exons, and introns are targetable by any number of gRNAs as well as targeted by different versions of Cas9 (*e.g.*, spCas9 and saCas9). While the Cas9 proteins function similarly, they differ in PAM sequence and protein size which further expands the genome editing and viral packaging options.

Regional, temporal, cellular; specific: CRISPR/Cas9 mutagenesis can be applied under very stringent conditions. One method for doing so is viral infection (*e.g.*, AAV[576,577] and lentivirus[578]). Genetically encoding CRISPR/Cas9 components into viral vectors offers the ability to introduce sequence-specific mutations into the genome via systemic or local injection[579-582]. AAVs specifically are attractive vectors that can be exploited for gene therapy[583] and are less inflammatory than other viral vectors[584]. When the AAV encounters a host cell, it is phagocytosed into the cell, escapes the endosome via a phospholipase domain, and gets transported into the nucleus via nuclear localization sequence where the viral DNA can be incorporated into the host genome[583]. By hijacking the hosts cellular machinery, the AAV genome is converted into a double-strand DNA, then integrated[583]. It has also been shown that AAVs can remain as episomal DNA within the host cell nucleus and not integrate into the host genome, however this is dependent on the host cell and does not impact viral expression[585]. AAVs for biomedical research offer long-term gene expression, cell-autonomous replication, and transduction of both dividing and nondividing cells[583]. One limitation, however, is the cargo capacity of AAV for CRISPR/Cas9-mediated mutagenesis (~4.7 kb). The spCas9 protein is too large to allow for packaging of more than the protein itself (4.2 kb) and necessary regulatory regions, so the options are to either apply the more compact saCas9 (~3.2 kb) that can fit with its sgRNA within a single virus[586,587], inject two viruses one with spCas9 and one with sgRNAs[588-590], or to inject only sgRNA into spCas9-expressing mice[579,581] (for reviews, see: [591,592]).

AAV stereotypes offer tropism for specific tissue and/or cell types[583,584,593]. AAV tropism is dictated by the AAV capsid proteins[584]. The utilization of different capsids impacts transduction efficiency, diffusion, and cell-type specificity[583,584]. AAV transduction occurs via the interaction

of the capsid proteins with cell surface proteins; different capsid proteins interact differently with cell-types that express different cell surface receptors[584]. Many different tropisms, however, have overlapping characteristics (*e.g.*, neuronal transduction: AAV1, AAV2, AAV5)[584] and can be combined as chimeric hybrids for heightened specificity (*e.g.*, AAV1/2)[594]. AAV1/2 combines the advantages of the AAV1 and AAV2 stereotypes to better target neurons and with reduced neuroinflammation[595,596]. AAVs can be delivered systemically[584,597,598] or can be delivered site-specifically via injection into a particular organ (*e.g.*, stereotaxic injection into the brain)[582,593,599-601]. The AAV system allows for temporal, regional, and cell-type specificity of CRISPR/Cas9 component expression[579,600,601]. This technique circumvents potential developmental adaptations that could arise from global gene mutation[579].

This is a golden age for genome editing; individual genes are rapidly being annotated and characterized, by increasingly novel techniques. While it is clear that the scientific understanding is expanding, increasingly specified questions are also being asked. Learning, adapting, and developing novel scientific techniques seems intimidating, however it is necessary for the continuation of preclinical molecular research. Herein, three different CRISPR/Cas9 techniques were employed to study ethanol-responsive lncRNA neurobiology from three different perspectives. (1) In-depth molecular, behavioral, and electrophysiological characterization of a single novel lncRNA, (2) rapid behavioral screening of multiple lncRNAs to identify novel targets worth perusing in-depth, and (3) viral-mediated lncRNA promoter mutation within a select brain region and select cell type for behavioral characterization. Six lncRNAs will be discussed in the following chapters, each exploring the molecular and behavioral underpinnings of AUD in different, but connected, methods.

1.8 Hypothesis and Specific Aims

I hypothesize that ethanol-responsive lncRNAs are critical hubs of molecular networks that act as determinants of ethanol consumption and ethanol-related behaviors.

Aim 1: *I hypothesize that ethanol-responsive lncRNA* Tx2 *contributes towards ethanol drinking and behavioral responses to ethanol.* Tx2 *Characterization*. *Tx2* expression will be

characterized via RT-PCR, RT-qPCR, and RNAscope HiPlex *in situ* hybridization. This will provide insight into *Tx2*'s molecular signature as well as cellular and subcellular localization.

Aim 2: *I hypothesize that mutation of ethanol-responsive lncRNAs identified from hippocampal ceRNA network analyses are sufficient to decrease (>20%) ethanol drinking and ethanol-related behaviors.* The top four candidate lncRNAs of interest will be identified for functional interrogation from microarray analysis and ceRNA networks of hippocampi from chronic intermittent ethanol vapor (CIEV)-exposed male mice. These genes will be inactivated using the Turbo Accelerated KnockOut (TAKO) method and subsequently screened against controls for alterations in DID and EOD-2BC drinking assays.

Aim 3: *I hypothesize that CRISPR/Cas9 mutation of the* Gas5 *promoter in the mPFC during adulthood in ethanol-naïve mice will increase (>20%) ethanol drinking and ethanol-related behaviors*. CRISPR/Cas9 mutation of the *Gas5* promoter in the mPFC will decrease gene expression as observed following various stages of withdrawal from CIEV exposure. A neuron-specific AAV expressing two *Gas5* promoter-targeting gRNAs will be stereotaxically injected bilaterally into the mPFC of ethanol-naïve Cas9-expressing mice to selectively disrupt *Gas5* expression. These animals will be compared to controls using the DID and EOD-2BC drinking paradigms, as well as EPM, AFT, and LORR. The acute temporal, regional, and cellular parameters selected for this aim support a very focused hypothesis, limiting the possibility of cellular compensation and global impacts. RT-qPCR will be used to quantify *Gas5* expression in response to CRISPR/Cas9-mediated mutagenesis of the *Gas5* promoter as well as in response to ethanol exposure.

2.0 AIM 1: MUTATION OF NOVEL ETHANOL-RESPONSIVE lncRNA *Gm41261* IMPACTS ETHANOL-RELATED BEHAVIORAL RESPONSES IN MICE

It should be made clear that this project was a collaborative effort from the Integrated Neuroscience Initiative on Alcoholism – Neuroimmune (INIA-N) Consortium. Gene identification was completed by Dr. Dayne Mayfield's group and Dr. Sean Farris. Gene-targeted mutagenesis was completed by Dr. Gregg Homanics' group prior to my involvement. Behavioral paradigms were completed by Dr. Yuri Blednov's group. Electrophysiology was completed by Dr. Regina Mangieri's group. I completed the molecular analysis. I combined and analyzed the independent data, wrote the complete manuscript, and hypothesized a potential mechanism for *Tx2*.

Methods and results presented in this chapter that were completed by a collaborative laboratory (*i.e.,* research that I did not complete myself) has been clearly labeled as such within each sub-heading. Sub-sections that are unlabeled represent research I completed myself while in the Molecular Pharmacology Graduate Program at the University of Pittsburgh.

2.1 INTRODUCTION

The functions of noncoding RNA (ncRNA) transcripts and their regulation is an emerging area of brain and alcohol research[370,396,411,602]. Chronic alcohol use is known to modulate molecular processes and cause global transcriptome dysregulation, disrupting the delicate balance of cellular homeostasis[370,396,411,602]. As alcohol modulates transcriptome regulation, associated downstream molecular networks are perturbed. A key question is how such ethanol-induced dysregulation contributes to the larger picture of alcohol action. These alcohol-induced transcriptomic changes are postulated to underly the transition from recreational drinking to uncontrolled drinking[396], and persistent transcriptomic changes may contribute to alcohol misuse, dependence, and relapse.

As the ncRNA transcriptome gains attention as an important layer of molecular regulation, long noncoding RNAs (lncRNAs) are being recognized for their vast impact on regulation of the transcriptome, proteome, and epigenome[411,415,427,603-606]. LncRNAs are commonly defined as

transcripts exceeding 200 nucleotides that lack an open reading frame[411,415,427]. Specific lncRNAs have been identified as critical for normal brain development and synaptic plasticity[607], with the majority of lncRNAs showing brain-specific expression[414]. The expression of lncRNAs is also tissue and cell-type specific and shows spatial and temporal variation in response to stimuli (*e.g.*, alcohol)[411,427,603,608,609]. LncRNAs have been implicated in a plethora of cellular pathways, including those involved in oncogenesis[457-459,461,610,611] and disease pathology[413,464,473,612,613]; but their roles in substance use disorders are just beginning to be uncovered[466,473,614].

The human genome encompasses at least 55,000 lncRNA genes that produce over 125,000 distinct transcripts[452]. This gene number is more than double that of known protein-coding genes. Despite the prevalence of lncRNAs, only a small number have been functionally characterized. Those that have been studied largely function by regulating gene expression through a variety of *cis*- and *trans*-mechanisms[615] (for reviews, see: [413,427,604,616]). Although several ncRNA subtypes (including lncRNAs) have been implicated in alcohol action[411,473,617,618], the molecular functions of lncRNAs in alcohol use disorder (AUD) are largely unknown. With only a small percentage of lncRNAs being characterized, combined with the fact that lncRNA sequences are not strongly conserved between species[603], predicting lncRNA function is challenging. Nevertheless, illuminating and characterizing the function and regulation of the ethanol-responsive long noncoding transcriptome should greatly increase our understanding of the vulnerability to ethanol and the development of AUD.

Here we report on a novel human lncRNA (*LINC01265*) that was differentially expressed in AUD versus control brain. We identified the predicted murine homolog (*Gm41261*) and used CRISPR/Cas9 genome editing to investigate this lncRNA's role in regulating ethanol drinking and other behavioral responses to ethanol. The results demonstrate that mutation of *Gm41261* (herein referred to as *Tx2*) resulted in a reduced development of tolerance after repeated ethanol exposure, and reduced sedative/hypnotic effects of ethanol and GABAergic drugs gaboxadol and zolpidem. Additionally, *Tx2* mutant animals demonstrated a male-specific reduction in ethanol intake and preference. Electrophysiologic findings were consistent with altered GABA release and $GABA_AR$ subunit composition in the NAc shell (NAcSh) of *Tx2* mutant mice.

2.2 METHODS AND MATERIALS

2.2.1 Case Selection and Postmortem Tissue Collection. Completed by the laboratories of collaborators Drs. Mayfield and Farris

Human samples were selected for inclusion based on AUD criteria previously reported[619,620]. Human autopsy brain tissue was acquired from the New South Wales Brain Tissue Resource Center at the University of Sydney (Sydney, Australia). Briefly, diagnosis of AUD was based on DSM-IV/DSM-5 and was confirmed by physician interviews, review of hospital medical records, questionnaires to next-of-kin, and from pathology, radiology, and neuropsychology reports. Tissue samples were matched as closely as possible according to age, sex, postmortem interval, pH of tissue, disease classification, and cause of death. To be included as part of the alcohol-dependent cohort, subjects had to meet the following criteria: greater than 18 years of age, no head injury at the time of death, lack of developmental disorder, no recent cerebral stroke, no history of other psychiatric or neurological disorders, no history of polysubstance use, negative screen for human immunodeficiency virus and hepatitis B and C, and postmortem interval not exceeding 48 hours. Fresh-frozen samples of the dorsolateral prefrontal cortex (dlPFC), NAc, and BLA were collected from each sample. All brain tissues were sectioned at 3-mm intervals in the coronal plane. There were no differences in the sectioning approach between the control and AUD groups.

2.2.2 Sample Preparation and Read Counting. Completed by the laboratories of collaborators Drs. Mayfield and Farris

Sample preparation, RNA-Seq, and analysis were conducted as previously reported[396]. Briefly, RNA was extracted from the brain tissues using the Qiagen RNeasy kit (Qiagen, #74104). RNA samples were DNase-treated with DNA-free kit (Invitrogen, #AM1906), and ribosomal RNA was depleted using RiboZero Eukaryote kit (Life Technologies, discontinued). One hundred and eighty samples (30 AUD and 30 controls for each brain region) were processed using the TruSeq RNA Library Prep Kit v.2 (Illumina, RS-122-2001) and sequenced on the Illumina HiSeq 2000 at the Genome Sequencing and Analysis Facility at The University of Texas at Austin. Paired-end

libraries with an average insert size of 180 bps were obtained. Sequence read archives have submitted for all brain regions, and their accession numbers are as follows: PRJNA530758 (dlPFC), PRJNA551775 (NAc), and PRJNA551909 (BLA).

2.2.3 Bioinformatic Analysis. Completed by the laboratory of collaborator Dr. Farris

Informatics analysis was performed as previously reported in Farris *et al.* 2015, Transcriptome Organization for Chronic Alcohol Abuse in Human Brain[396].

2.2.4 Animals

All experiments were approved by the Institutional Animal Care and Use Committees of the University of Pittsburgh and The University of Texas at Austin and were conducted in accordance with the National Institutes of Health Guidelines for the Care and Use of Laboratory Animals.

Mice used for behavior and molecular studies were housed under 12-hour light/dark cycles with lights on at 7 AM for all experiments except for the limited-access drinking procedure when mice were housed under a reversed light cycle. Mice had *ad libitum* access to food [irradiated 5P76 ProLab IsoProRMH3000, (LabDiet, St. Louis, MO)] and water, and the humidity and temperature of the rooms were kept constant. The *Tx2* mutant strain was maintained by heterozygous breeding. Wild-type (WT) littermates were used as controls for experiments and compared with *Tx2* mutants. Mice were initially group-housed 4 to 5 per cage. Behavioral testing began when the mice were at least 2 months old in isolated testing rooms in the Animal Resources Center at the University of Texas at Austin. Mice were moved to testing rooms 1 – 2 weeks before beginning experiments. Mice were weighed once a week and housed individually for each behavioral study. Separate groups of mice were used for each behavioral test except for the chronic tolerance study where the same groups of mice were used to measure loss of righting response twice, before and after chronic saline or ethanol treatments.

Mice used for electrophysiology were group housed in clear, polycarbonate cages (19 x 31 x 13 cm) with Sani-Chips wood bedding (PJ Murphy Forest Products, Montville, NJ) and a cotton fiber nestlet (Ancare, Bellmore, NY), in a temperature-controlled room (~21°C) with a reverse 12-

hour light/dark cycle (lights off at 9:30 AM). Mice had *ad libitum* access to standard chow (LabDiet® 5LL2 Prolab RMH 1800) and water. Brain slices were prepared for electrophysiology experiments from adult (approximately 14 – 26 weeks old) male mice between 6:00 AM and 9:40 AM. Tail snips for genotype confirmation were collected at the time of brain slice preparation.

2.2.5 CRISPR/Cas9 Mutagenesis and sgRNA Design. Completed by the laboratory of Dr. Homanics

Two tru-sgRNAs[621] designed to each uniquely bind within *Tx2* Exon 1 were selected using Benchling (benchling.com) (**Figure 4C**). A sgRNA-specific forward primer and a common overlapping reverse PCR primer (**Table 1**) were used to generate T7 promoter-containing sgRNA templates as described[622]. These DNA templates were transcribed *in vitro* using a MEGAshortscript Kit (Ambion, #AM1354). Cas9 coding sequence was *in vitro* transcribed and polyA-tailed using a mMessage mMachine T7 Ultra Kit (Ambion, #AM1345) as described[623]. Following synthesis, the sgRNAs and Cas9 mRNA were purified using a MEGAclear Kit (Ambion, #AM1908), ethanol precipitated, and resuspended in DEPC-treated water (Invitrogen, #AM9906). 50 ng/µL of *Tx2* sgRNA1, 50 ng/µL of *Tx2* sgRNA2, and 75 ng/µL Cas9 mRNA in embryo injection buffer [10mM Tris (Fisher Scientific, #BP1521; pH 7.4) and 0.1mM EDTA (Thermo Fisher, #AM9260G)] were microinjected into the cytoplasm of C57BL6/J embryos as previously described[624]. Injected embryos were surgically transferred into the oviducts of day 0.5 postcoitum pseudopregnant CD-1 females. The selected founder was mated to female C57BL/6J mice. The founder mouse was screened for the top off-target mutation sites that were predicted using Benchling software (benchling.com). Each off-target (n = 14 for sgRNA1 and n = 10 for sgRNA2) was amplified by PCR (See: **Appendix Table 1 and 2**, respectively) and amplicons were analyzed by Sanger sequencing. None were mutated.

Table 1 PCR primers and DNA repair templates for Chapter 2. All sequences are written in the 5' to 3' direction. Underlined sequences mark gRNA sites. Sequences in bold are T7 promoter.

Primer	Sequence
Tx2 sgRNA1F	**GAAATTAATACGACTCACTATAGG**ATTTGCAATTCTCTTCCA GTTTTAGAGCTAGAAATAGC
Tx2 sgRNA2F	**GAAATTAATACGACTCACTATAGG**AATAAACAGGTGTGACGG GTTTTAGAGCTAGAAATAGC
sgRNA common reverse	AAAAGCACCGACTCGGTGCCACTTTTTCAAGTTGATAACGGAC TAGCCTTATTTTAACTTGCTATTTCTAGCTCTAAAAC
Cas9 Forward	**TATTACGACTCACTATAGG**GAGAATGGACTATAAGGACCACGAC
Cas9 Reverse	GCGAGCTCTAGGAATTCTTAC
Tx2 F1	CTCACCAAAATTCAACCTGGAG
Tx2 R1	GCTTCAGAGCTCACTGGTGT
Tx2 F2	GCCAGCCTTTCTGCACATTT
Tx2 R2	CTCTGGTTCTGGCATTCCGT
Osmr F1	AGGAGATGCAGTGCAACCAA
Osmr R1	GGGACTCTGGCTGAAGGTTT
β-Actin F1	GACCTCTATGCCAACACAGT
β-Actin R1	AGTACTTGCGCTCAGGAGGA

2.2.6 Genotyping *Tx2* Mutants

DNA was isolated from tail snips using Quick Extract (Lucigen, #QE09050). Mice were genotyped by PCR and Sanger sequencing using primers F1 and R1 (**Table 1**). Genotypes of mice produced at UT Austin were genotyped by Transnetyx (Cordova, TN).

2.2.7 Drugs. Completed by the laboratory of collaborator Dr. Blednov

Injectable ethanol solutions (Decon Labs Inc., #2701; 15 and 20%, v/v) were prepared in 0.9% saline. Gaboxadol (55 mg/kg; Sigma-Aldrich, #T101) and ketamine (175 mg/kg; Sigma-Aldrich, #K2753) were dissolved in 0.9% saline and injected at 0.1 mL/10 g of body weight. Zolpidem (60 mg/kg; Tocris Bioscience, #0655) was freshly prepared as a suspension in saline

with 3 – 4 drops of Tween-80 (Sigma-Aldrich, #P1754) and administered daily in a volume of 0.1 mL/10 g of body weight. All drugs were administered interperitoneally (i.p.).

2.2.8 Loss of Righting Response (LORR). Completed by the laboratory of collaborator Dr. Blednov

Sensitivity to the sedative/hypnotic effects of ethanol (3.6 and 3.8g/kg), ketamine (175 mg/kg), gaboxadol (55 mg/kg), and zolpidem (60 mg/kg) was determined using the LORR assay in mice. When mice became ataxic following injection, they were placed in the supine position in V-shaped plastic troughs until they were able to right themselves three times within 30 seconds. LORR duration was measured as the time from being placed in the supine position until they regained their righting response.

2.2.9 Chronic Tolerance to Ethanol-Induced LORR. Completed by the laboratory of collaborator Dr. Blednov

For development of chronic tolerance to ethanol-induced LORR, mice received an initial sedative/hypnotic dose of ethanol (1st dose; 3.8g/kg) on day 1 and the duration of LORR was recorded as described above. After the first recovery, mice were divided into two groups. During the following period of time one group of mice received 5 daily saline injections (day 3, day 5, day 7, day 9 and day 11) whereas the other group of mice received 5 daily injections of ethanol (3.5g/kg) on the same days. On day 13 all mice were then given a second hypnotic dose of ethanol (2nd dose; 3.8g/kg) and the duration of the second LORR period was recorded. The difference between duration of the 1st and 2nd LORR was considered as the index of development of chronic tolerance to ethanol.

2.2.10 Every- Other-Day Two-Bottle Choice (EOD-2BC) Drinking. Completed by the laboratory of collaborator Dr. Blednov

Intermittent access to ethanol escalates voluntary drinking in mouse models[625,626]. Mice were given every-other-day access to ethanol (15 or 20% v/v) and water for 24-hour sessions, and water only was offered on off days. Ethanol solutions were prepared fresh daily in water, and

sipper bottles were weighed before placement and after removal from the experimental cages. The side placement of the ethanol bottles was alternated with each drinking session to avoid positional side biases. The quantity of ethanol consumed was calculated as g/kg body weight/24 hours.

2.2.11 Slice Preparation and Recording Conditions. Completed by the laboratory of collaborator Dr. Mangieri

Sagittal brain slices were prepared for acute brain slice electrophysiology from male control (n = 4) and *Tx2* mutant (n = 5) mice. Mice were anesthetized lightly with isoflurane (Animal Health International, #21138528), decapitated, and their brains were rapidly removed and placed in ice-cold high-sucrose artificial cerebrospinal fluid (ACSF) containing the following: 210 mM sucrose (Fisher Scientific, #S5-3), 26.2 mM $NaHCO_3$ (Fisher Scientific, #BP328-500), 1 mM NaH_2PO_4 (Fisher Scientific, #S369-500), 2.5 mM KCl (Fisher Scientific, #BP366-500), 11 mM dextrose (Fisher Scientific, #D16-1), 6mM $MgSO_4$ (Fisher Scientific, #M65-500), 2.5 mM $CaCl_2$ (Fisher Scientific, #C79-500), then bubbled with 95% O_2/5% CO_2. Sagittal slices (240 µm thick) containing the NAc were sectioned in ice-cold, high-sucrose ACSF using a Leica VT1000S vibrating microtome and then transferred to a recovery chamber containing ACSF [124 mM NaCl (Fisher Scientific, #BP358-212), 26 mM $NaHCO_3$, 1 mM NaH_2PO_4, 4.4 mM KCl, 10 mM dextrose, 2.4 mM $MgSO_4$, 1.8 mM $CaCl_2$] and bubbled with 95% O_2/5% CO_2, where they were maintained at approximately 33°C for at least one hour prior to transfer to the recording chamber. Recordings were conducted at 29.9 – 33.9 °C in ACSF (124 mM NaCl, 26 mM $NaHCO_3$, 1 mM NaH_2PO_4, 4.4 mM KCl, 10 mM dextrose, 1.2 mM $MgSO_4$, 2 mM $CaCl_2$), bubbled with 95% O_2/5% CO_2, and pumped into the recording chamber at ~2.0 mL/minute. Recording ACSF also contained 20 µM DNQX (Tocris Bioscience, #2312), 50 µM APV (Tocris Bioscience, #3693), and 1 µM CGP52432 (Tocris Bioscience, #1246) to pharmacologically isolate $GABA_AR$-mediated inhibitory postsynaptic currents (IPSCs). The voltage-gated sodium channel blocker tetrodotoxin citrate (TTX; Alomone Labs, #T-550) was added to the ACSF (final concentration of 1 µM) for miniature (action potential-independent) IPSC recordings (mIPSCs). Recording electrodes (4” thin-wall glass, 1.5 OD/1.12 ID; World Precision Instruments) were made using a P-97 Flaming/Brown micropipette puller (Sutter Instruments) to yield resistances of approximately 3.3 - 5.8 MΩ and contained: 145 mM KCl, 5 mM EGTA (Sigma-Aldrich, #E4378), 10 mM HEPES

(Sigma-Aldrich, #H4034), 5 mM $MgCl_2$ (Sigma-Aldrich, #M8266), 2 mM Na-ATP (Sigma-Aldrich, #A2383), 0.2 mM Na-GTP [(Sigma-Aldrich, #G8877); ~315 mOsm; pH adjusted to ~7.35 with KOH (Fisher Scientific, #P250-500)].

2.2.12 Electrophysiology Data Acquisition. Completed by the laboratory of collaborator Dr. Mangieri

Recordings were acquired on three electrophysiology recording stations: two utilized CV203BU headstages with Axopatch 200B amplifiers and one utilized a CV-7B headstage and MultiClamp 700B amplifier software (Molecular Devices). Neurons in the NAcSh were visually identified using MRK200 Modular Imaging systems (Siskiyou Corporation) mounted on vibration isolation tables. A series of hyperpolarizing and depolarizing intracellular current injections (300 msec duration steps from -400 pA to +500 pA in 50 pA increments) was delivered in current-clamp mode, just after obtaining whole-cell configuration. A short, small step (100 msec, -50 pA) was delivered 100 msec prior to each 300 msec step in the series and was used to determine input resistance. The recording configuration was then changed to voltage-clamp mode and postsynaptic currents were recorded for at least 15 minutes (command voltage set at -60 mV). All recordings were filtered at 2 kHz and digitized at either 5 kHz (membrane voltage responses) or 10 kHz (synaptic currents) via Digidata 1440A interface board using Clampex 10.3 (Molecular Devices). Access resistance was monitored throughout the recording using the Membrane Test feature of Clampex.

2.2.13 Electrophysiology Data Analysis. Completed by the laboratory of collaborator Dr. Mangieri

All raw data analysis was performed blind to genotype. IPSC frequency and average amplitude were determined over a 5-minute recording period (usually beginning at least 10 minutes after obtaining whole-cell access) using the Template Search feature of Clampfit 10.3. IPSCs for kinetics analysis were also identified using the Template Search feature, but were manually accepted for analysis, with a minimum of 50 non-overlapping events analyzed for each neuron. Access resistance >30 MΩ or depolarized resting membrane potential (> ~-55 mV) were criteria for exclusion of the data.

Membrane properties (resting membrane potential, membrane resistance, inward rectification, and – in the case of spontaneous IPSC-recorded cells – action potential properties) were used to categorize cells as either putative medium spiny neurons or interneurons, (*e.g.*, relatively depolarized resting membrane potential or high membrane resistance indicative of putative interneuron), with a default toward medium spiny neurons (MSNs) when ambiguous[627-630].

2.2.14 RNA Precipitation and Reverse Transcription PCR (RT-PCR)

Mice [8 WT control (n = 5 male, n = 3 female) and 10 *Tx2* mutant (n = 5 male, n = 5 female)] were 8-weeks old when sacrificed for tissue harvest. Total RNA was isolated using TRIzol reagent (Invitrogen, #15596018) according to the manufacturer's protocol, contaminating DNA was removed with a DNase-free kit (Qiagen, #AM1907), and 1µg of total RNA was synthesized into cDNA using Superscript™ III First-Strand Synthesis System (Invitrogen, #18080051) with random hexamer primers. A no-RT reaction was used as a negative control for each sample. RT-PCR primers are found in **Table 1**.

2.2.15 Reverse Transcription quantitative PCR (RT-qPCR)

cDNA and RT-qPCR primers were combined with SYBR green fluorescent master mix (Bio-Rad, #1708882; according to manufacturer's protocol) and data collected using a Bio-Rad iCycler. All primers were optimized for 90% to 110% efficiency at the following conditions: 3 minutes at 95°C (initial denaturation) followed by 40 cycles of 15 seconds at 95°C (denaturation), 30 seconds at 60°C (annealing), and 30 seconds at 72°C (extension), then followed lastly from 55 - 95°C in 0.5°C increments every 30 seconds. Primer sequences for *β-actin*, *Osmr*, and *Tx2* are shown in **Table 1**. N = 4 biological replicates were used. Reactions were carried out in technical triplicate for each gene tested. Threshold cycle (Ct) values were calculated for each well and triplicate values averaged. The difference between specific genes and *β-Actin* (ΔCt) was calculated for each animal and normalized to the average of control littermates (ΔΔCt). Fold change over controls was calculated for each animal using the following formula: $2^{-\Delta\Delta Ct}$.

2.2.16 *In Situ* Hybridization (ISH) and Immunohistochemistry (IHC)

C57BL/6J control adult male mice were anesthetized by i.p. injection of ketamine (Covetrus, #010177; 100 mg/kg) and xylazine (Covetrus, #033197; 100 mg/kg). Once anesthetized, the mice were immobilized and transcardially perfused with 0.9% phosphate-buffered saline (PBS; Gibco, #10010023; pH = 7.4) followed by 4% paraformaldehyde (PFA; Sigma-Aldrich, 158127; pH = 7.4). Brains were harvested and post-fixed in 4% PFA for 18 – 24 hours at 4°C. After post-fixation brains were equilibrated in 30% sucrose (Fisher Scientific, #BP220212) for 2 days at 4°C. Brains were cut into 14 – 20μm thick coronal sections on a cryostat (Leica Biosystems, Germany) and mounted on slides (Fisher Scientific, #12-550-15). Sections were stored at -80°C until RNAscope ISH. RNAscope v2 [Advanced Cell Diagnostics (ACD Bio), Newark, CA] was used for ISH using a *Tx2*-specific probe. RNAscope was conducted following the manufacturers protocol with slight modifications: 3x washes for 2 minutes, slides incubated in blocking buffer for 60 minutes. IHC was also conducted following the manufacturers protocol using IBA1 (Fugifilm, #019-19741) and GFAP (Millipore, #AB5804) antibodies. 2 biological replicates and 2 – 4 technical replicates were used.

2.2.17 RNAscope HiPlex ISH

Brain sections were prepared as above. All reagents for RNAscope HiPlex v2 were procured from ACD Bio. RNAscope HiPlex v2 was used for ISH using a *Tx2*-specific probe, as well as *Olig2* and *Rbfox3* probes to identify oligodendrocytes and neurons, respectively. DAPI was used to stain cell nuclei. RNAscope was conducted following the manufacturer's protocol, imaged on a confocal microscope, and aligned using the RNAscope HiPlex v2 alignment software. Blank images were taken with DAPI only and used to remove background fluorescence. 2 – 4 biological replicates were used.

2.2.18 Statistical Analysis

Statistical analyses were run using GraphPad Prism software (La Jolla, CA) and used to perform Student's t-tests, one-way or two-way ANOVAs (repeated measures when appropriate), and Bonferroni or Dunnett's *post-hoc* analyses. Statistical significance was defined by a p-value $\leq$ 0.05. All data are presented as mean ± S.E.M.

2.3 RESULTS

2.3.1 Gene Identification. Completed by the laboratories of collaborators Drs. Mayfield and Farris

To identify and prioritize novel lncRNAs for additional investigation in mice, differential gene expression analysis of human postmortem brain tissue from the dorsolateral prefrontal cortex (dlPFC), basolateral amygdala (BLA), and nucleus accumbens (NAc) was initially conducted. Differentially expressed human lncRNAs were further scrutinized for syntenic conservation in mice, genomic sequence conservation between mice and humans, and feasibility for creating a novel mutant C57BL/6J mouse line. RNA-Seq from human AUD versus control brain revealed widespread transcriptional dysregulation. Expression of the human lncRNA *LINC01265* was significantly increased in the dlPFC and BLA, regions controlling executive function and emotional responses, respectively, in humans with AUD (**Figure 4A**). A significant decrease in *LINC01265* transcript levels was found in AUD NAc relative to healthy NAc, a region involved in the brain reward system (**Figure 4A**). *LINC01265* is located on chromosome 5 (p13.1), showing evidence of synthetic conservation with mouse chromosome 15 (qA1); which includes neighboring protein-coding genes such as the *Oncostatin M Receptor* (*Osmr*). The human *LINC01265* demonstrates 48.5% sequence conservation with the annotated murine lncRNA *Gm41261* [*i.e.*, *Tx2*; NCBI genomic database (release 105)], suggesting a homologous relationship between *LINC01265* and *Tx2.*

LINC01265 and *Tx2* are both the natural antisense transcript to *OSMR* Intron 1 (**Figure 4B**), increasing the interest of this gene for functional interrogation. OSMR is a 'hub' receptor

involved in a vast regulatory network of the neuroimmune system, a system largely impacted by alcohol misuse[619].

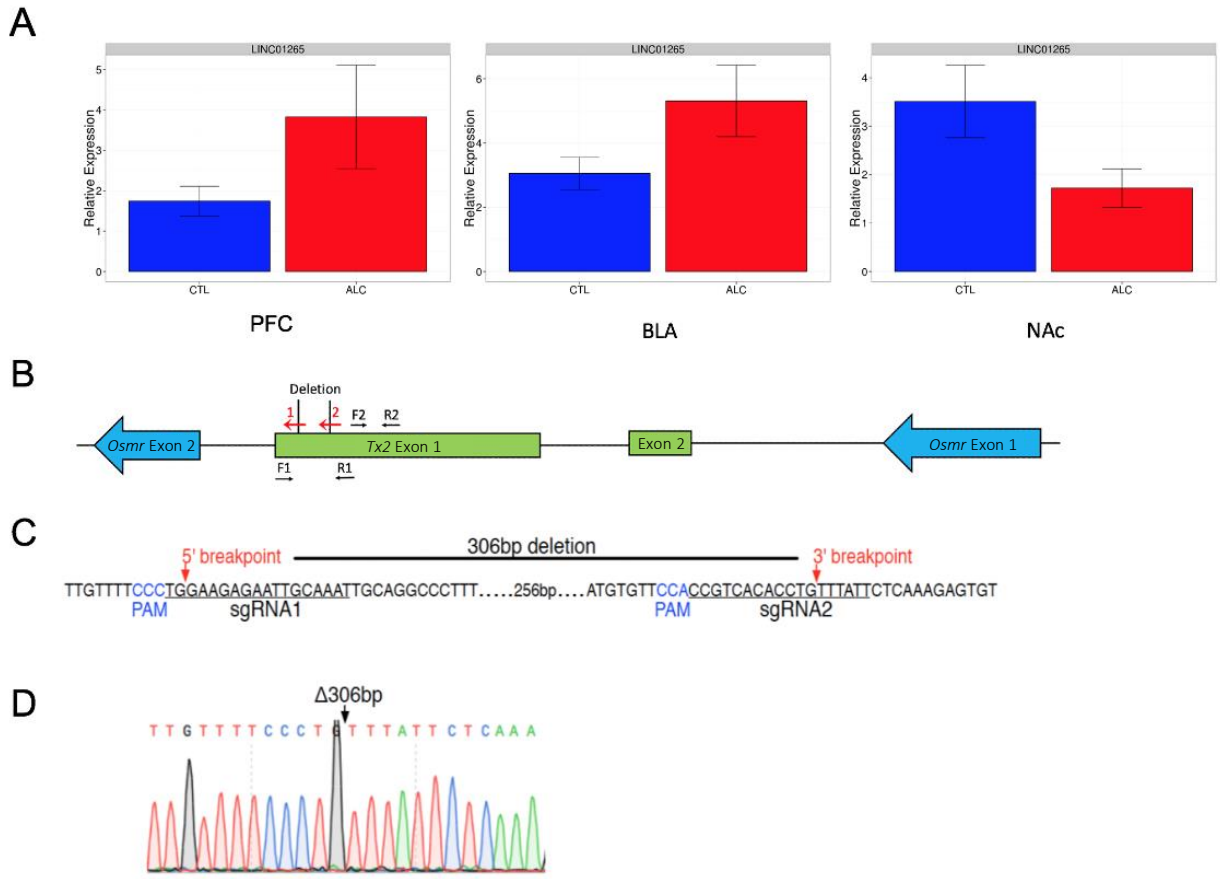

Figure 4 Gene identification and targeting strategy for Chapter 2. (**A**) Human brain RNA-sequencing results from the dorsolateral prefrontal cortex (dlPFC; left; 2.19-fold change; p = 0.013), basolateral amygdala (BLA; middle; 1.74-fold change; p = 0.022), and nucleus accumbens (NAc; right; 0.49-fold-change; p = 0.034) showing the relative expression of human *LINC01265*. Blue bars represent relative expression in healthy controls, red bars represent relative expression in AUD patients. (**B**) Overview of murine homolog *Gm41261*, a.k.a. *Tx2* locus showing *Tx2* exons (green boxes), *Osmr* Exons 1 and 2 (blue arrows), the location of the CRISPR-induced deletion site, sgRNA binding sites (red arrows), and PCR primer locations (black arrows). (**C**) Partial *Tx2* genomic DNA sequence with sgRNA locations underlined, protospacer adjacent motifs (PAM) in blue, and breakpoints present in the founder and the knockout line derived from this mouse. (**D**) DNA sequence chromatogram from the founder showing the sequence that results from deletion of 306 bp.

2.3.2 Validation of *Tx2* Mutation

We sought to validate that the deletion was harbored in the mutants at both the DNA (**Figure 5A**) and RNA (**Figure 5B**) level. Both primer sets were utilized, and *Tx2* was shown to contain the 306 bp deletion. *β-Actin* was used as a control to confirm successful cDNA synthesis and RT-PCR reaction.

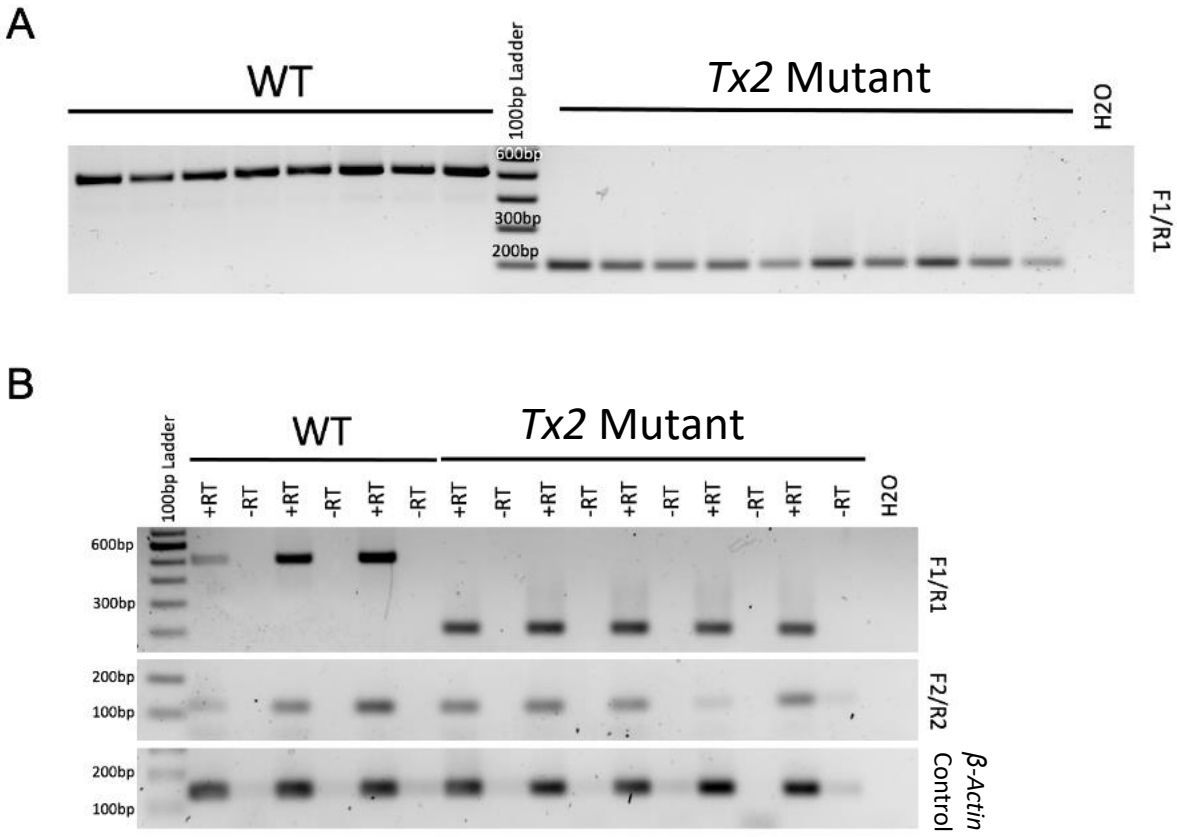

Figure 5 Validation of *Tx2* gene mutation at the DNA and RNA level. (**A**) PCR of WT control and *Tx2* mutant mice showing deletion in DNA in mutant mice. (**B**) RT-PCR of WT control and *Tx2* mutant mice with *Tx2* F1/R1 primers which span the deletion site demonstrating that the mutation is present in the expressed lncRNA. RT-PCR with *Tx2* F2/R2 primers which bind 3' to the deletion demonstrate that downstream sequences are expressed and are not changed in size. *β-Actin* was used as an internal control.

2.3.3 Molecular Characterization

As *Tx2* was a novel gene identified through RNA-Seq of human AUD brain (**Figure 4A**), its annotation and characterization were unknown. Therefore, basic molecular analysis with WT animals was necessary to characterize the *Tx2* transcript. In the process of experimentation, the NCBI annotation was found to be incorrect. *Tx2* was found to have two splice variants in cortex. Exon 1 is the primary transcript produced and is at least 2 kb in length (**Figure 4B**). We have been unable to identify the transcriptional start site to date. The second transcript variant includes Exons 1 and 2 and is expressed at greatly reduced levels compared with the primary transcript (unpublished observations).

Steady state *Tx2* RNA levels were low, as indicated by high Ct values, and expression was equal between males and females in cortex (**Figure 6A**). *Tx2* was not differentially expressed in the brain regions tested when compared to cortical *Tx2* expression (**Figure 6B**).

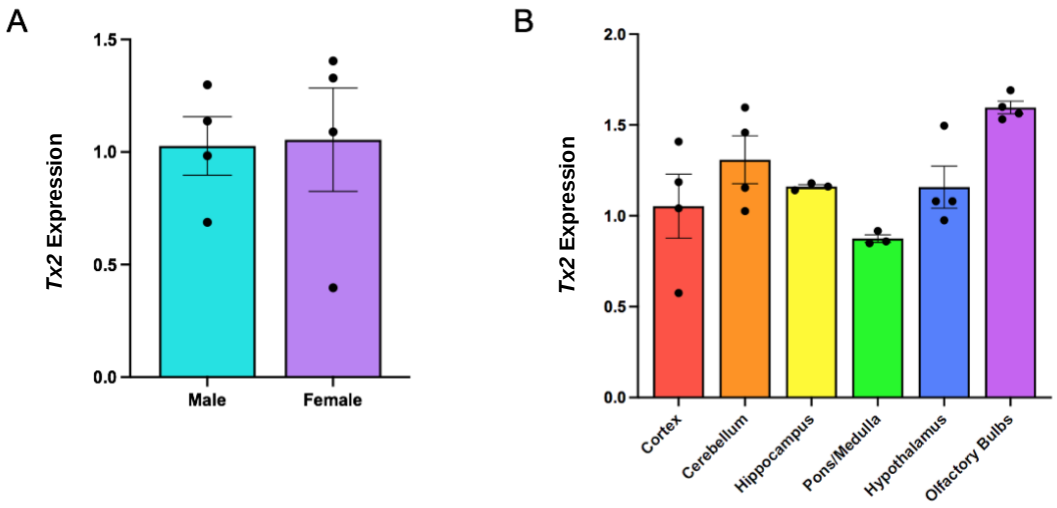

Figure 6 RT-qPCR characterization of *Tx2* lncRNA in WT mice. (**A**) No difference was observed in *Tx2* expression in cortex of males versus females. (**B**) Compared to the level of *Tx2* RNA present in the cortex, no differences were observed in several brain regions. N = 4 biological replicates, n = 3 technical replicates. *Tx2* expression was internally normalized to β-actin. Values represent Mean ± SEM. Unpaired t-test and one-way ANOVA were used for statistical analysis in A and B, respectively.

2.3.4 Cellular and Subcellular Localization

RNAscope Multiplex combined with IHC or RNAscope HiPlex alone were used to identify cellular and subcellular localization of the WT *Tx2* transcript (**Figure 7**). Large *Tx2* puncta were observed in IBA1-positive microglia (**Figure 7A-D**) and *Rbfox3*-positive neurons (**Figure 7I-L**), but not in GFAP-positive astrocytes (**Figure 7E-H**) or *Olig2*-positive oligodendrocytes (**Figure 7M-P**). *Tx2* was present in 96.5% of counted IBA1+ microglia (409 of 424) and 95.5% of *Rbfox3+* neurons (169 of 177). *Tx2* was only observed in 9% of GFAP+ astrocytes (20 of 223) and 0% of *Olig2+* oligodendrocytes (0 of 32). Additionally, *Tx2* expression did not overlap with DAPI-stained nuclei (0%), suggesting that *Tx2* is localized to the cytoplasm (*e.g.*, **Figure 7L**).

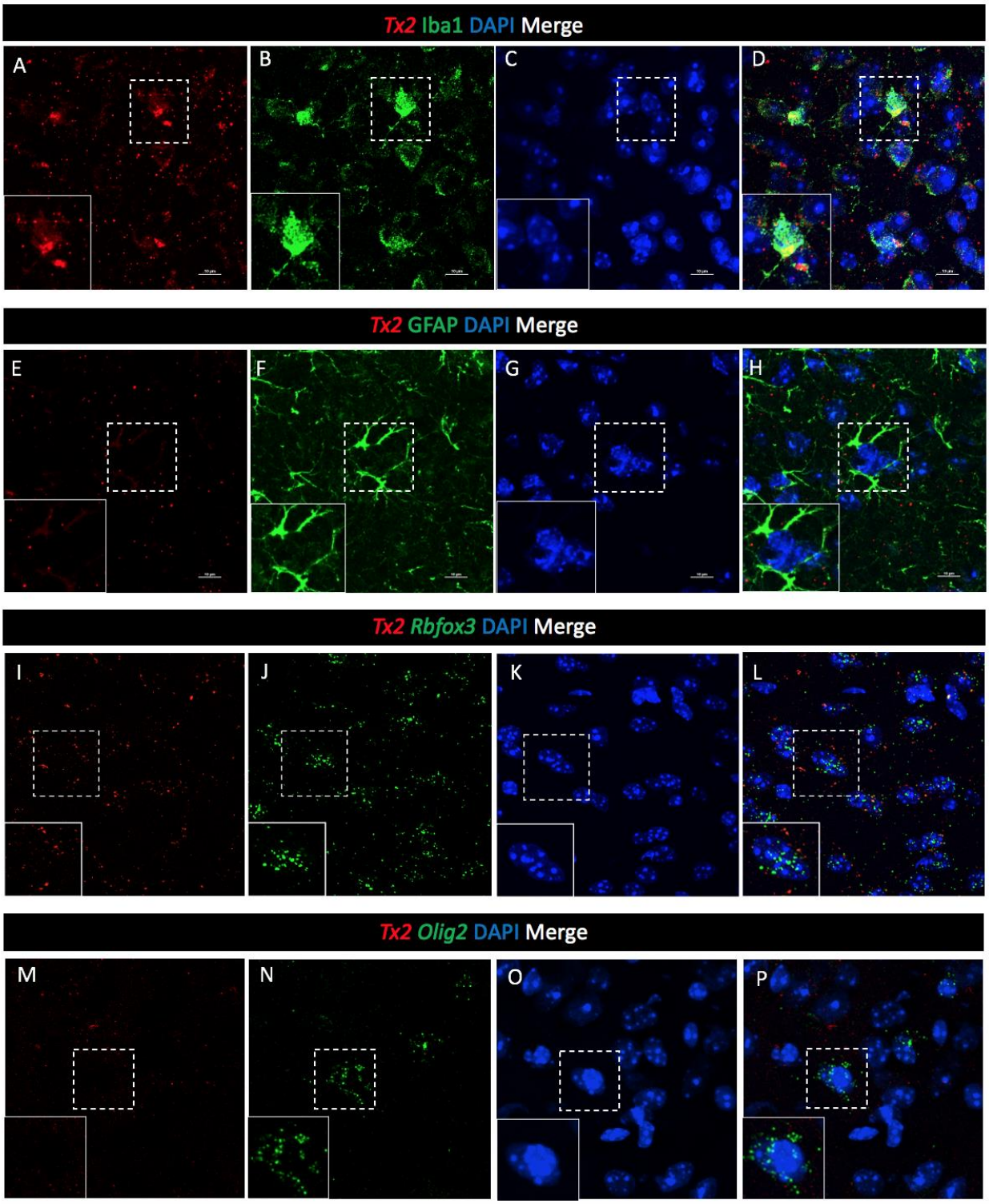

Figure 7 Cellular and subcellular *Tx2* localization visualized via RNAscope ISH and IHC in cortical cells. (**A, E, I, M**) Cells were hybridized with a *Tx2*-specific probe (red). Clear puncta are observed. (**B, F, J, N**) Cells stained with either (B) Iba1 for microglia, (F) GFAP for astrocytes, (J) *Rbfox3* for neurons, or (N) *Olig2* for oligodendrocytes (green). (**C, G, K, O**) Slides were mounted using DAPI to stain cell nuclei (blue). (**D, H, L, P**)

Representative images merged to show staining overlay, respectively. 20μm coronal sections for A – H (ISH followed by IHC); 14μm coronal sections for I – P (ISH).

2.3.5 CRISPR/Cas9-Mediated Mutagenesis. Completed by the laboratory of Dr. Homanics

We initially endeavored to create a mouse line in which a portion of the putative promoter and start of the Exon 1 of *Tx2* were deleted using CRISPR mutagenesis. Our strategy was based on the genomic structure of the *Tx2* locus that was reported in the NCBI genomic database (release 105) at the time the project was initiated and prior to the molecular characterization detailed above. Thus, our CRISPR strategy utilized two sgRNAs that both had target sites in what we now deem to be Exon 1 (**Figure 4B**). These sgRNAs along with Cas9 mRNA were used to create a *Tx2* mutant mouse line on the inbred C57BL/6J genetic background using standard embryo microinjection techniques[631]. The line described here harbors a 306 bp deletion in Exon 1 (**Figure 4C and D**).

2.3.6 Molecular Characterization of *Tx2* Mutant

The deletion was confirmed at the RNA level using RT-PCR from cortical RNA (**Figure 5B**). Mutant animals express a *Tx2* lncRNA that is 306 bp smaller than the WT *Tx2* lncRNA. Abundance of *Tx2* lncRNA in cortex of mutants was unchanged compared with WT controls (**Figure 8A**). Thus, CRISPR mutagenesis deleted 306 bp from the putative Exon 1 of *Tx2* but did not reduce abundance in cortex.

As *Tx2* is a natural antisense transcript to *Osmr* Intron 1, it was of interest to determine if *Osmr* RNA expression was altered by *Tx2* mutation. Abundance of *Osmr* in the cortex was unaltered in *Tx2* mutant mice compared with littermate controls (**Figure 8B**). This suggests that the deleted region of *Tx2* is not acting as a transcriptional regulator of *Osmr* in the nucleus via *cis*-mediated mechanisms.

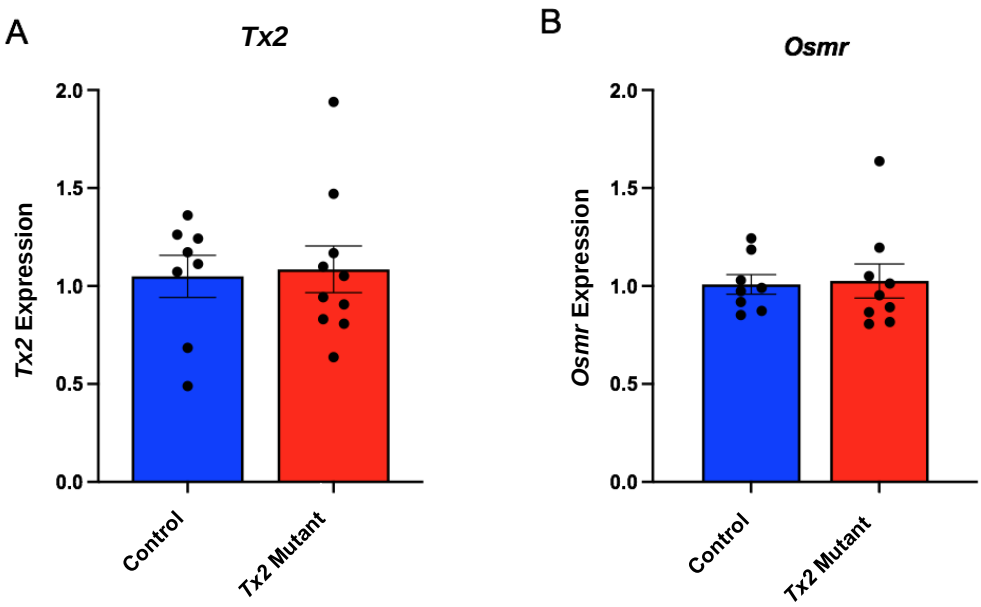

Figure 8 RT-qPCR quantification of *Tx2* lncRNA expression in cortex. (**A**) *Tx2* expression in control and *Tx2* mutant mice. No difference was observed between genotypes. (**B**) *Osmr* expression in control and *Tx2* mutant mice. No difference was observed between genotypes. Raw data were normalized to β-Actin. N = 8 – 10 per group. Values represent Mean ± SEM. Unpaired t-test was used for statistical analysis.

2.3.7 Loss of Righting Response (LORR). Completed by the laboratory of collaborator Dr. Blednov

For both males and females, there was a significant effect of genotype [F (1, 24) = 171.2, $p < 0.0001$; F (1, 24) = 176.4, $p < 0.0001$, respectively], dose [F (1, 24) = 202.6, $p < 0.0001$; F (1, 24) = 269.0, $p < 0.0001$, respectively], and genotype x dose interaction [F (1, 24) = 7.4, $p < 0.05$; F (1, 24) = 9.18, $p < 0.01$, respectively] on the duration of LORR induced by ethanol (**Figure 9A and E**, respectively). Mutation of *Tx2* in males and females reduced the duration of LORR induced by gaboxadol (t = 11.8, $p < 0.0001$; t = 25.3, $p < 0.0001$, respectively) and zolpidem (t = 12.2, $p < 0.0001$; t = 12.6, $p < 0.0001$, respectively) (**Figure 9C, G, D, and H**, respectively). No difference in duration of LORR after administration of ketamine was found in either sex between WT and *Tx2* mutant mice (**Figure 9B and F**).

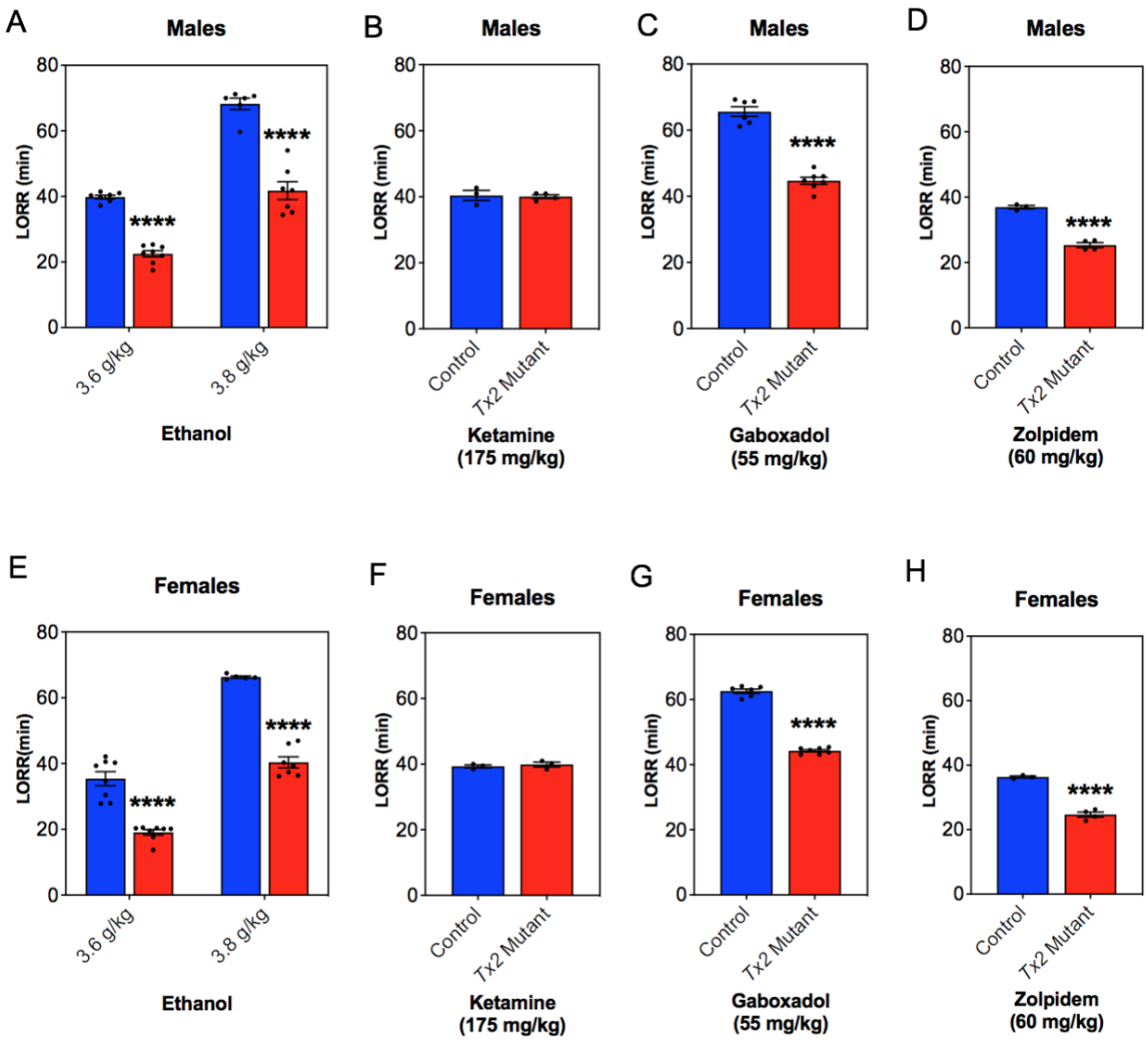

Figure 9 LORR behavioral assay in WT and *Tx2* mutants. (**A and E**) LORR (min) was reduced by *Tx2* mutation in response to ethanol (3.6 and 3.8g/kg) in both males (A) and females (E). (**B and F**) LORR (min) was not altered in *Tx2* mutant mice compared to controls in response to ketamine (175mg/kg) in either males (B) or females (F). (**C and G**) LORR (min) was reduced by *Tx2* mutation in response to gaboxadol (55mg/kg) in both males (C) and females (G). (**D and H**) LORR (min) was reduced in *Tx2* mutant mice in response to zolpidem (60mg/kg) in both males (D) and females (H). N = 3 – 8 per group. Values represent Mean ± SEM. Two-way ANOVA used for statistical analysis for ethanol-induced LORR, and students t-test was used for ketamine-, gaboxadol-, and zolpidem-induced LORR. ****p-value < 0.0001.

2.3.8 Chronic Tolerance to Ethanol-Induced LORR. Completed by the laboratory of collaborator Dr. Blednov

Development of tolerance is one of the criteria for diagnosing alcohol dependence in humans. Because changes in expression of *Tx2* were observed in brain of humans with AUD, we compared the development of chronic tolerance to ethanol in *Tx2* mutant mice and their WT littermates. An initial test injection of ethanol was given on day 1 (3.5 g/kg; i.p.), and a second test injection on day 13 (3.8 g/kg; i.p.). In mice that received five chronic injections of saline between the two test injections, the LORR duration was mildly reduced at the second test injection compared with the first in males [$F(1, 8) = 39.05$, $p < 0.001$, dependence on chronic treatment; $F(1, 8) = 63.03$, $p < 0.0001$, dependence on genotype] and females [$F(1, 10) = 6.56$; $p < 0.05$, dependence on chronic treatment; $F(1, 10) = 39.33$, $p < 0.0001$, dependence on genotype] (**Figure 10A and D**, respectively) of both genotypes. In contrast, in mice that received five repeated injections of ethanol between the two test injections, the LORR duration was markedly reduced in both males [$F(1, 8) = 143.6$, $p < 0.0001$, dependence on chronic treatment; $F(1, 8) = 8.28$, $p < 0.05$, dependence on genotype; $F(1, 8) = 38.54$, $p < 0.001$, genotype x chronic treatment] and females [$F(1, 10) = 10.44$, $p < 0.01$, dependence on chronic treatment; $F(1, 10) = 37.19$, $p < 0.001$, dependence on genotype; $F(1, 10) = 33.16$, $p < 0.001$, genotype x chronic treatment] (**Figure 10B and E**, respectively) of both genotypes. *Post-hoc* analysis showed significant reduction in control male and female mice ($p < 0.0001$ and $p < 0.001$, respectively). *Post-hoc* analysis of *Tx2* mutant mice revealed smaller changes in *Tx2* mutant male mice compared with WT males ($p < 0.01$) and no changes in duration of LORR were found in mutant females. We also defined a tolerance index of LORR as the duration of the LORR following the 2nd injection minus the 1st injection. Repeated administration of ethanol reduced the tolerance index in WT but not in *Tx2* mutant males [$F(1, 16) = 7.84$, $p < 0.05$, dependence on chronic treatment; $F(1, 16) = 9.53$, $p < 0.01$, dependence on genotype; $F(1, 16) = 23.12$, $p < 0.001$, genotype x chronic treatment] (**Figure 10C**) and females [$F(1, 20) = 74.43$, $p < 0.0001$, dependence on chronic treatment; $F(1, 20) = 13.6$, $p < 0.01$, dependence on genotype; $F(1, 20) = 24.99$, $p < 0.0001$, genotype x chronic treatment] (**Figure 10F**). *Post-hoc* analysis revealed a significant reduction in WT male and female mice ($p < 0.001$ and $p < 0.0001$, respectively) whereas in *Tx2* mutant mice, no difference in index of tolerance were found.

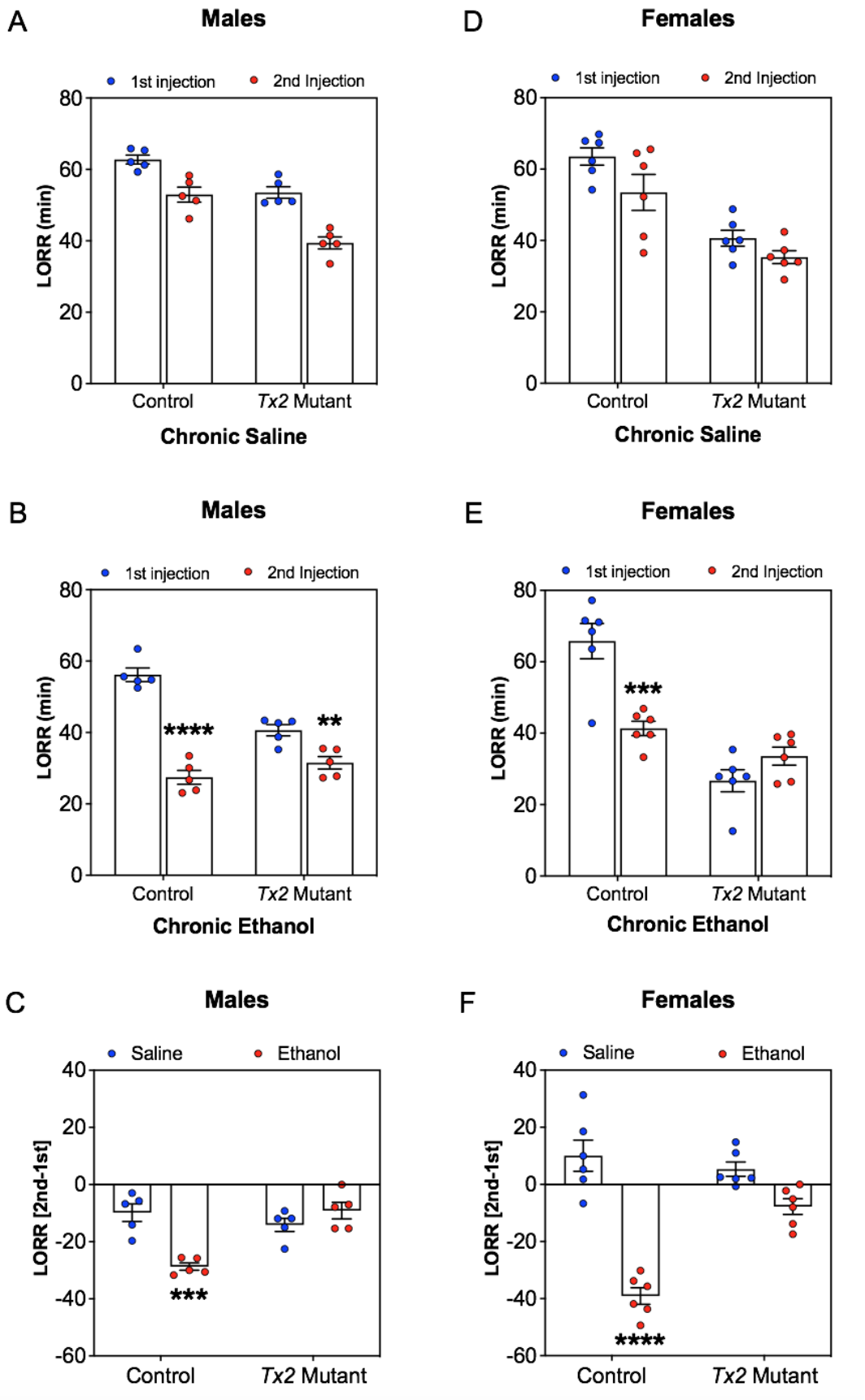
A
Males
1st injection
2nd Injection
LORR (min)
80
60
40
20
0
Control
Tx2 Mutant
Chronic Saline
D
Females
1st injection
2nd Injection
LORR (min)
Control
Tx2 Mutant
Chronic Saline
B
Males
1st injection
2nd Injection
LORR (min)
****
**
Control
Tx2 Mutant
Chronic Ethanol
E
Females
1st injection
2nd Injection
LORR (min)
***
Control
Tx2 Mutant
Chronic Ethanol
C
Males
Saline
Ethanol
LORR [2nd-1st]
40
20
0
-20
-40
-60
***
Control
Tx2 Mutant
F
Females
Saline
Ethanol
LORR [2nd-1st]
****
Control
Tx2 Mutant

Figure 10 Chronic ethanol tolerance on LORR behavioral assay in control and *Tx2* mutant mice. Controls are on the left and *Tx2* mutants are on the right. (**A and D**) 1st injection (3.5g/kg; i.p.; day 1) and 2nd injection (3.8g/kg; i.p.; day 13) are shown in blue and red, respectively. Male (A) and female (D) LORR (min) in response to 1st and 2nd injections of a sedative/hypnotic ethanol dose with chronic saline injections given on day's 3, 5, 7, 9, and 11. A main effect of treatment and genotype, but no treatment x genotype interaction was found in both sexes. (**B and E**) 1st injection (3.5g/kg; i.p.; day 1) and 2nd injection (3.8g/kg; i.p.; day 13) are shown in blue and red, respectively. Male (B) and female (E) LORR (min) in response to 1st and 2nd injections of a sedative/hypnotic ethanol dose with chronic ethanol injections (3.5g/kg; i.p.) given on day's 3, 5, 7, 9, and 11. A main effect of treatment, genotype, and treatment x genotype interaction was found in both sexes. *Post-hoc* analysis revealed that chronic ethanol injections significantly reduced duration of LORR in *Tx2* mutant and WT male mice as well as in WT female, but not *Tx2* mutant female, mice. (**C and F**) The LORR duration change (min) between the 1st and 2nd injection for saline (blue) and ethanol (red) in males (C) and females (F). The duration of LORR following the 2nd injection minus the 1st injection is defined as the tolerance index. Control mice of both sexes displayed a main effect of treatment, genotype, and treatment x genotype. *Post-hoc* analysis revealed significant changes in tolerance for controls of both sexes but not for *Tx2* mutant mice. N = 5 – 6 per group. Values represent Mean ± SEM. Unpaired t-test and two-way ANOVA used for statistical analysis. **p < 0.01, ***p < 0.001, ****p <0.0001.

2.3.9 Every-Other-Day Two-Bottle Choice (EOD-2BC) Drinking. Completed by the laboratory of collaborator Dr. Blednov

Mice were tested for ethanol drinking, preference, and total fluid intake using an intermittent EOD-2BC free choice consumption procedure. During the first 14 days they received 15% v/v ethanol, and during the second 14 days, 20% v/v ethanol. *Tx2* mutant male mice drank less 15% v/v ethanol than WT littermates with a significant main effect of genotype [$F(1, 30) = 7.630$, $p < 0.01$], but no effect of day or day x genotype (**Figure 11A**). *Tx2* mutant male mice showed a significant reduction in ethanol preference at 15% ethanol too, with significant main effect of genotype [$F(1, 30) = 10.24$, $p < 0.01$], but no effect of day or day x genotype (**Figure 11B**). In contrast, female *Tx2* female mice only showed an effect of day for ethanol intake [$F(6, 168) = 3.995$, $p < 0.001$] and ethanol preference [$F(6, 168) = 2.414$, $p < 0.05$].

During the second two weeks, *Tx2* mutant and WT males consumed similar amounts of 20% v/v ethanol, with only an effect of day for both ethanol intake [$F(6, 180) = 5.245$, $p < 0.0001$] and preference [$F(6, 180) = 2.230$, $p < 0.05$] (**Figure 11A and B**, respectively). The same was true for *Tx2* female mutant and WT mice, which showed similar 20% v/v ethanol intake and

preference, with only an observed effect of day on ethanol preference [$F(6, 168) = 3.059$, $p < 0.01$] (**Figure 11D and E**, respectively).

No change in total fluid intake was observed at either 15% or 20% v/v ethanol in either males or females for genotype or day x genotype (**Figure 11C and F**, respectively). There was a significant effect of day, however, at 15 and 20% v/v ethanol, for both males [$F(6, 180) = 4.454$, $p < 0.001$; $F(6, 180) = 2.268$, $p < 0.05$, respectively] and females [$F(6, 168) = 6.811$, $p < 0.0001$; $F(6, 168) = 3.425$, $p < 0.01$, respectively].

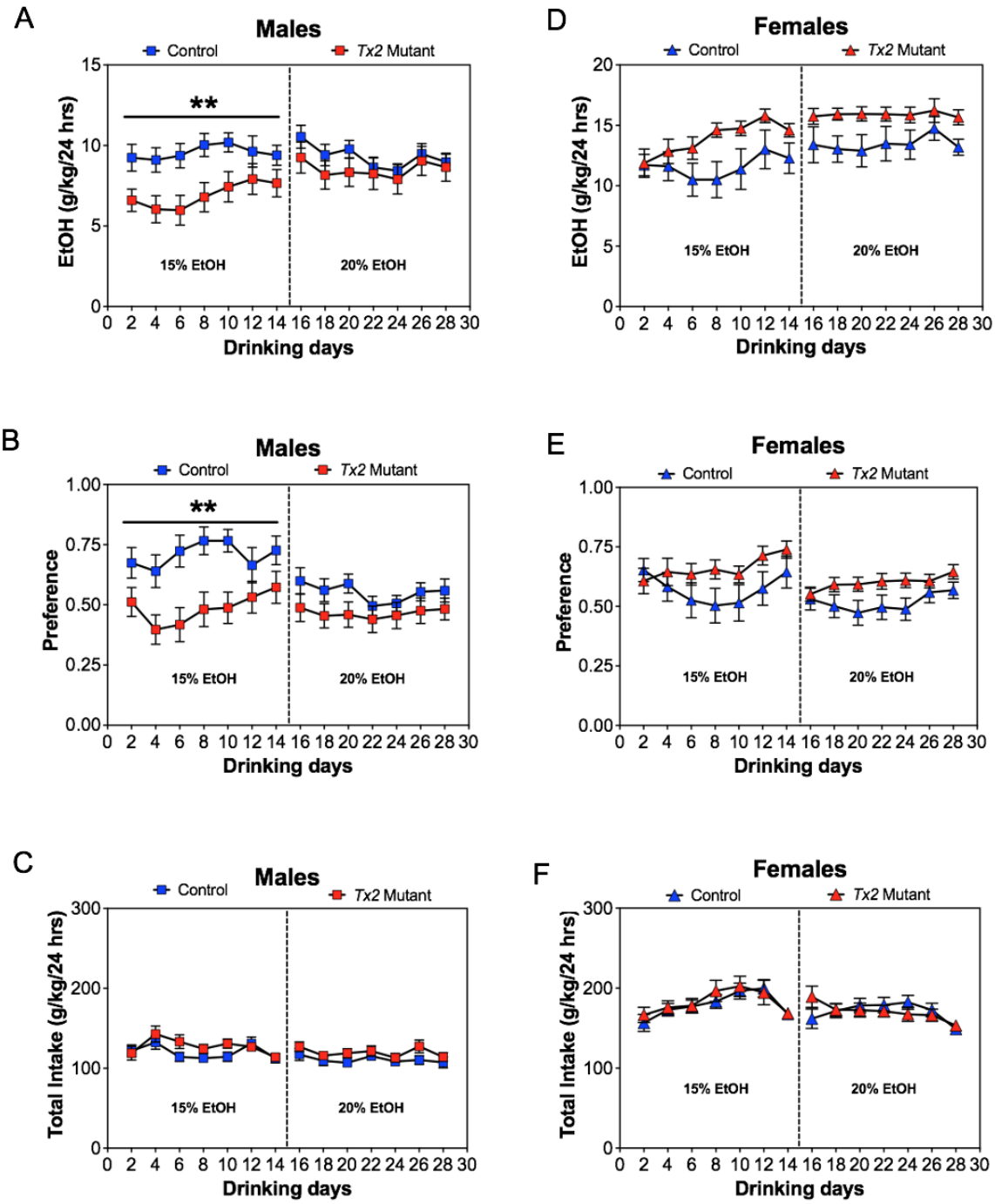

Figure 11 EOD-2BC drinking behavior of control and *Tx2* mutant mice. Experimentation was conducted for two weeks with 15% v/v ethanol, stopped for two days, then repeated for another two weeks with 20% v/v ethanol. (**A and D**) Ethanol intake (g/kg/24 hrs) in males (A) and females (D). Male *Tx2* mutant mice had a significant main effect of genotype and displayed a consistent reduction in ethanol intake specifically at 15% ethanol. No change observed at 20% ethanol or in females for either concentration. (**B and E**) Ethanol preference in males (B) and females (E). Male *Tx2* mutant mice displayed a reduction in ethanol preference specifically at 15% ethanol. No change observed at 20% or in females for either concentration. (**C and F**) Total fluid intake (g/kg/24 hrs) in males (C) and

females (F). No change observed in either concentration for either sex. N = 7 per group. Values represent Mean ± SEM. Two-way ANOVA used for statistical analysis. **p <0.001.

2.3.10 Electrophysiology. Completed by the laboratory of collaborator Dr. Mangieri

To assess whether GABA-mediated transmission was altered in *Tx2* mutant mice, we performed *ex vivo* patch clamp recordings of $GABA_A$ receptor-mediated inhibitory postsynaptic synaptic currents (IPSCs) in the NAcSh, a region rich in GABAergic circuitry. The NAc is comprised of several types of interneurons, which together make up approximately 10% of all neurons in the NAc, and projection neurons (MSNs), which make up the other 90%. Because we had no *a priori* reason to suspect specific effects of *Tx2* mutation on interneurons versus MSNs, we recorded from any neuron with a resting membrane potential of -55 mV or less, and later categorized neurons on the basis of cell membrane parameters indicative of interneurons versus MSNs.

When analyzed for all neurons regardless of putative cell type, spontaneous IPSCs (sIPSCs) were similar in amplitude and frequency between the two genotypes (**Table 2**). There were also no differences between genotypes in sIPSC amplitude or frequency when putative interneurons were excluded from the dataset (**Table 2**). Miniature IPSCs (mIPSCs) were recorded in the presence of TTX, which prevents action potential-dependent neurotransmitter release. The average amplitude of mIPSCs also did not differ between genotypes (**Figure 12A and C**). There was, however, a significant difference in mIPSC frequency ($t_{49} = 2.30$, $p < 0.05$), with *Tx2* mutants exhibiting a higher frequency of events (**Figure 12B and C**). This pattern of results was preserved when putative interneurons were excluded from the data set; specifically, there was no difference in amplitude but there was an elevated frequency ($t_{42} = 2.03$, $p < 0.05$) in *Tx2* mutants (**Figure 12A and B**). These results suggest that *Tx2* mutants have an increase in presynaptic GABA release probability in the NAcSh that was revealed when network activity was blocked by TTX.

Table 2 sIPSC properties of WT and *Tx2* neurons. Values reported as mean ± SEM.

	All neurons		**Putative interneurons excluded**	
	WT	*Tx2* Mutant	WT	*Tx2* Mutant
N (cells, mice)	20, 4	25, 5	17, 4	22, 5
Amplitude (pA)	-31.9 ± 3.3	-28.8 ± 2.0	-30.2 ± 3.5	-27.5 ± 2.1
Frequency (Hz)	1.8 ± 0.2	1.8 ± 0.2	2.0 ± 0.2	1.9 ± 0.2
Rise time (ms)	0.92 ± 0.05	0.86 ± 0.05	0.90 ± 0.05	0.85 ± 0.06
Decay time (ms)	19.8 ± 0.9	17.8 ± 0.8	20.2 ± 0.9	18.2 ± 0.8

Differences in behavioral responses to $GABA_AR$ modulators, such as zolpidem, can result from differences in receptor subtype composition[632], which may be evident at the cellular level as altered IPSC event kinetics. We therefore determined the average rise time (10% – 90% of peak) and average decay time (90% – 10% of peak) for individual IPSC events. We found no genotype differences in the average rise time for sIPSCs, evaluated for all neurons or when putative interneurons were excluded (**Table 2**). This was also true for mIPSC rise time (**Figure 12D**). We did, however, observe genotype differences in average IPSC decay time for both spontaneous and miniature IPSCs. In regard to sIPSCs, the difference in average decay times for all neurons was not statistically significant, but the distributions of average decay times were different between WT and *Tx2* mutant mice (Kolmogorov-Smirnov $D = 0.41$, $p < 0.05$; **Table 2**). Results were similar when putative interneurons were excluded ($t_{37} = 1.6$, $p = 0.11$; $D = 0.43$, $p = 0.054$). Genotype differences in decay times were more pronounced for mIPSCs (**Figure 12E – G**). Group means ($t_{49} = 2.72$, $p < 0.01$) and distributions ($D = 0.41$, $p < 0.05$) of average decay time per neuron were different in *Tx2* mutant mice, relative to WT, and exclusion of putative interneurons did not affect these results ($t_{42} = 2.69$, $p < 0.01$; $D = 0.42$, $p < 0.05$; **Figure 12E**). We further investigated genotype differences in mIPSC decay times by constructing histograms of mIPSC decay times (number of events per 2 msec bin, expressed as a percentage of the total number of events) for each neuron, and then averaging the histograms for each genotype (**Figure 12F**). Comparison of these histograms of decay times indicate that neurons from *Tx2* mutant mice had a greater proportion of fast-decaying mIPSCs and a smaller proportion of slow-decaying mIPSCs, relative to control mice (**Figure 12F**).

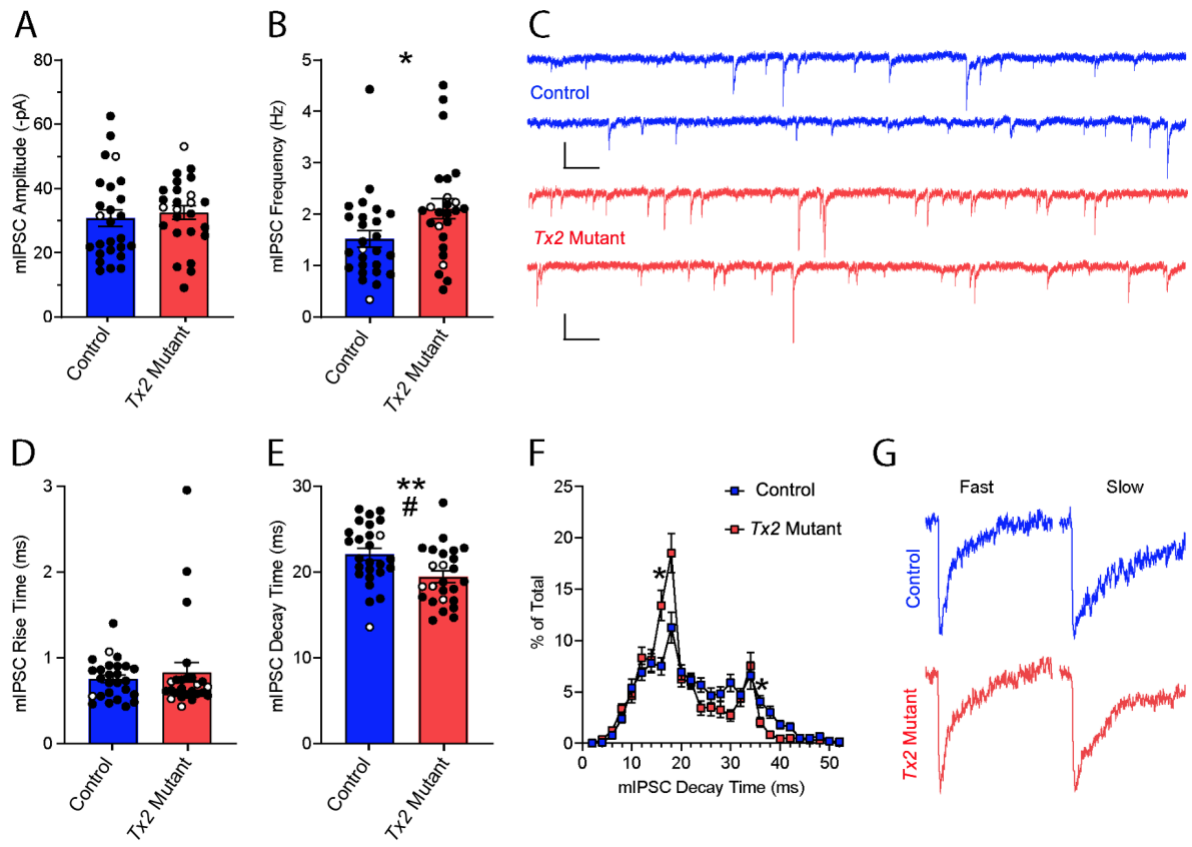

Figure 12 Electrophysiology of sagittal brain slices prepared from WT control and *Tx2* mutant male mice. $GABA_AR$-mediated IPSCs were recorded *ex vivo* from neurons in the NAcSh. (**A**) mIPSC amplitude did not differ between genotypes. (**B**) mIPSC frequency was increased in *Tx2* mutants compared to controls. (**C**) Representative current traces from WT and *Tx2* mutant mice. Scale indicates 500 msec duration and 40 pA amplitude. (**D**) Average mIPSC rise time was not different between genotypes. (**E**) Average mIPSC decay time was reduced in *Tx2* mutants compared to controls. (**F**) mIPSC decay times shown in 2 msec bins (expressed as a percentage of the total number of mIPSC events) revealed a significant bin x genotype interaction ($F [25,1225] = 4.6$, $p < 0.0001$), indicating *Tx2* mutant mice had a greater proportion of fast-decaying mIPSCs and a smaller proportion of slow-decaying mIPSCs compared to controls. (**G**) Scaled traces (to normalize amplitudes) showing examples of fast- and slow-decaying mIPSCs for each genotype. Panels A, B, D, and E show data for individual neurons (white circles, putative interneurons; black circles, putative MSNs) overlaid on group averages (of all neurons) ± SEM. Panel F symbols show group averages (of all neurons) ± SEM for each bin. N = 26 neurons from 4 mice (control) and 25 neurons from 5 mice (*Tx2* mutant). *$p < 0.05$, **$p < 0.01$, unpaired t-test or Sidak's multiple comparisons test. #$p < 0.05$, Kolmogorov-Smirnov comparison of distributions.

2.4 DISCUSSION

The present study was motivated by RNA-Seq results of postmortem human tissue that revealed the lncRNA *LINC01265* to be significantly dysregulated when compared with matched non-AUD controls in the dlPFC, BLA, and NAc (**Figure 4A**). *LINC01265* was upregulated in the PFC, a region involved in higher-order executive function[633] and regulation of the limbic reward system[634], and the BLA, a region involved in the reward pathway and emotions[635]. *LINC01265* was downregulated in the NAc of individuals with AUD compared with non-AUD controls, a region that integrates the cortical and limbic systems to mediate goal-directed behaviors and also functions to process and analyze rewarding and reinforcing stimuli[636]. All these regions are highly sensitive to chronic alcohol misuse[299,637,638].

Starting with *LINC01265*, sequence homology and synteny were used to identify the murine lncRNA homologue, *Gm41261* (referred to as *Tx2*). In both species, the gene was located in the first Intron, in an antisense orientation, of the *Osmr* gene. RT-qPCR of WT *Tx2* RNA from mouse cortex revealed low levels of *Tx2* expression that was similar between males and females. We also observed that compared with the cortex, other mouse brain regions showed similar levels of expression. RNAscope analysis (coupled with IHC for microglia and astrocytes) revealed that this lncRNA was present primarily in the cytoplasm of > 95% of IBA1-positive microglia and *Rbfox3*-positive neurons, in ~9% of GFAP-positive astrocytes, but not in *Olig2*-positive oligodendrocytes.

To test the hypothesis that the ethanol-responsive lncRNA *Tx2* contributes to behavioral responses to ethanol and ethanol drinking, we used CRISPR/Cas9 gene editing to create a *Tx2* mutant mouse line that was subsequently phenotypically characterized at the molecular, cellular, and behavioral levels. The gene targeting strategy used was designed to delete the putative promoter of *Tx2* and was based on the gene structure annotated in the NCBI genomic database (Version 105). Molecular characterization of the *Tx2* locus revealed that the 306 bp deletion that was created with CRISPR/Cas9 in the *Tx2* mutant mice removed sequences present in Exon 1, and not the actual promoter sequence (**Figure 4**; **Figure 5A**). Because the promoter was not disrupted, abundance of *Tx2* in brain of control and *Tx2* mutant mice did not differ (**Figure 8B**), although the size of the transcript was 306 nucleotides smaller in mutants compared with controls (**Figure 5B**).

Because tolerance is a diagnostic criteria for AUD[639] and because tolerance influences the amount of ethanol consumed to achieve the same response over time[640], *Tx2* mutants were tested for tolerance using an ethanol-induced LORR following repeated ethanol injections compared with repeated saline injections (**Figure 10**). *Tx2* mutants displayed reduced LORR time following both the 1st and 2nd sedative/hypnotic doses of ethanol compared with WT for both chronic saline and chronic ethanol experiments. Most strikingly, a substantial difference between genotypes was observed on the tolerance index (**Figure 10C and F**). While control and *Tx2* mutant mice developed a similar, low level of tolerance in response to the 1st and 2nd sedative/hypnotic ethanol doses following chronic saline injections, control mice developed strong ethanol tolerance following chronic ethanol-induced LORR. *Tx2* mutants on the other hand, presented a near unchanged ethanol-induced LORR time from the 1st injection of ethanol to the 2nd in the chronic ethanol experiment (**Figure 10B and E**), which was roughly the same tolerance gained due to chronic saline injections. This suggests an insensitivity to repeated ethanol exposure on the sedative/hypnotic response and is indicative of either heightened innate tolerance (as suggested by the reduced LORR duration) or lack of tolerance induction, following repeated ethanol injections in both male and female *Tx2* mutant mice

A male-specific decrease in ethanol drinking and preference was observed on the EOD-2BC assay specifically with 15% v/v ethanol (**Figure 11**). The decreased ethanol consumption observed at 15% in males was not observed in females, and no change in ethanol consumption or preference was observed in either sex at 20% v/v ethanol. Tolerance to ethanol's rewarding effects encourages more drinking to achieve a desired level of intoxication, while tolerance to ethanol's aversive properties reduces a disincentive to drink[641]. Therefore, it was expected that reduction of tolerance observed in *Tx2* mutant mice (**Figure 10C and F**) should be accompanied by increased ethanol consumption, but this was not the case (**Figure 11A and D**). In contrast, we saw reduction of ethanol consumption in male *Tx2* mutant mice and no change in *Tx2* mutant females. It should be noted, however, that tolerance to LORR is not necessarily reflective of aversive or rewarding properties of ethanol.

Several observations suggest that mutation of *Tx2* culminates in GABAergic dysfunction in the mutant animals. Both male and female *Tx2* mutants displayed a reduction in LORR duration in response to sedative/hypnotic injections of zolpidem, gaboxadol, and ethanol, but not to ketamine (**Figure 9**). Zolpidem is an imidazopyridine allosteric $GABA_AR$ agonist that functions

by potentiating the effects of GABA[632,642] and requires the α1 $GABA_AR$ subunit for LORR[643]. Gaboxadol is a direct acting $GABA_AR$ agonist that acts as a GABA mimetic[644] that induces LORR primarily through α4βδ subunit-containing $GABA_ARs$[645,646]. Similarly, GABAergic inhibitory neurotransmission is involved in both the acute and chronic effects of ethanol on brain and behavior (for reviews, see: [647,648]). In contrast, sedative/hypnotic responses induced by a high dose of ketamine are thought to be mediated via non-GABAergic targets that include excitatory glutamate receptors[649,650], cyclic nucleotide gated potassium channels[651,652], and possibly acetylcholine receptors[653]. Together, these behavioral studies point to alterations in GABAergic inhibition in the *Tx2* mutant animals.

Further supportive evidence comes from *ex vivo* electrophysiological studies of the NAcSh. Alterations were found in GABA transmission in the form of increased frequency of mIPSCs, as well as a reduction in the average decay time of these events that resulted from a larger proportion of fast-decaying events and smaller proportion of slow-decaying events (**Figure 12B, E, and F**). The increase in mIPSC frequency suggests *Tx2* mutants have an increase in presynaptic GABA release probability in the NAcSh that was unmasked when network activity was blocked by the neurotoxin TTX. Alternatively, increased event frequency may also reflect an increased number of synapses[654]. Activity of α4βδ subunit-containing $GABA_ARs$ (*i.e.,* those targeted by gaboxadol) negatively regulates IPSC frequency in NAc MSNs[655]. Therefore, reduction in α4βδ-containing $GABA_ARs$ would be consistent with both the increased mIPSC frequency (**Figure 12B**) and the reduced sedative effect of gaboxadol observed (**Figure 9C and G**) in *Tx2* mutants. $GABA_AR$ α1 and α2 subunits have been reported to underly the fast decaying component of IPSCs while the slow component is determined by the α3 subunit[656]. Thus, the reduced proportion of slow-decaying events in *Tx2* mutants is suggestive of relatively fewer α3-containing receptors. Because zolpidem binds at a much higher affinity to the α1 $GABA_AR$ subtype than α2 or α3 and requires the α1 $GABA_AR$ subunit for LORR[643,657], the behavioral finding of decreased sensitivity to zolpidem (**Figure 9D and H**) points to fewer α1-containing $GABA_ARs$ in *Tx2* mutants. However, fewer α1-containing $GABA_ARs$ would predict longer IPSC decay times for *Tx2* mutants, as α2 subunit inclusion slows the deactivation rate of the $GABA_AR$ relative to α1[658]. Thus, the interpretation of the kinetics results alongside the behavioral findings were not convergent, perhaps because the electrophysiology represents only NAcSh whereas the behavioral

results represent responses to global *Tx2* mutation. In summary, although further studies are needed, the data suggest that *Tx2* mutation altered GABAergic neurotransmission, leading to altered behavioral response to GABAergic drugs.

There are several notable limitations to the present study. First, the molecular mechanism of action of *Tx2* is currently unknown. Many diverse mechanisms of lncRNAs action have been reported in the literature (for reviews, see: [413,427,604]). Some lncRNAs are antisense transcripts that regulate abundance of their sense counterpart[473,659]. *Tx2* is a natural antisense transcript of *Osmr* Intron 1, a type 1 cytokine receptor involved in neuroinflammation that is linked to AUD[489]. It was therefore of interest to test if *Tx2* functions as a *cis*-mediated epigenetic regulator of *Osmr*. We found that *Osmr* RNA abundance was unaltered in response to *Tx2* mutation (**Figure 8B**) and that WT *Tx2* localizes to the cytoplasm (**Figure 7**), indicating that the *Tx2* mutation made, or WT *Tx2*, does not regulate expression of this neuroimmune-related receptor[355,367].

Second, the 306 bp deletion present in the mutated locus did not eliminate *Tx2* expression. Instead, *Tx2* lncRNA was expressed at a normal level, but harbored an internal 306 nt deletion (**Figure 5B**). As nothing is known about the functional domains of this novel lncRNA, we can only speculate that a critical functional region necessary to fulfill specific molecular and/or cellular roles was deleted. How deletion of such a putative functional domain alters GABAergic inhibition and ultimately ethanol drinking and other behavioral responses to ethanol awaits future investigation.

2.4.1 Conclusions

Here we show that expression of the human lncRNA *LINC01265* was dysregulated in several brain regions of humans with AUD when compared with controls. Production of a CRISPR/Cas9 engineered mouse line (C57BL/6J background strain) with a small (306 bp) deletion in *Tx2*, the mouse homologue of *LINC01265* (a.k.a. *Gm41261*), revealed that *Tx2* modulates ethanol drinking and sedative/hypnotic effects of ethanol. These behavioral changes are possibly mediated by alterations in the GABAergic system following mutation of *Tx2*. This study adds to a small but growing list of lncRNAs that are implicated in mediating ethanol's effects on the brain, ethanol-related behavioral responses, and AUD[473,660,661]. As individual RNAs are rapidly emerging as highly selective and efficacious therapeutic targets for small molecule drugs (for reviews, see:

[662,663]), we propose that the ethanol-responsive lncRNA transcriptome is an expansive, untapped resource for future development of novel AUD therapeutics.

3.0 AIM 2: IMPACT OF HIPPOCAMPAL lncRNA TAKOs ON ETHANOL DRINKING BEHAVIOR

Homogeneous cohorts of gene-targeted animals take considerable time, effort, animals, and money to generate. Global mutant animal cohorts require three generations and a minimum of 9 months of careful work before behavioral testing can begin on a single gene, and the resulting cohort still hold the potential to not demonstrate any significant changes from control.

To circumvent this issue, a method was needed in which newly identified genes of interest from large AUD datasets can be rapidly screened for behaviors of interest prior to in-depth analysis. This would allow for reduced workload and cost per gene-targeted cohort and would also vastly speed up the rate at which genes could be analyzed.

To fill in this gap, the CRISPR/Cas9 Turbo Accelerated KnockOut (CRISPy TAKO) method was conceptualized. This technique allows for the creation of a gene-targeted cohort in a single generation. By utilizing multiple gRNAs tiled across a small region of DNA (50 – 200 nts apart), variable mutations and indels can be produced within individual electroporated embryos. While each embryo could harbor a different mutation, each would still have the same relative genomic location mutated and were therefore hypothesized to manifest the same behavioral alterations from control. Specificity can be further enhanced by only selecting experimental mice that harbor a large DNA deletion in the desired location.

If successful, this method can be employed to study genes of interest 3 – 4 times faster at 1/3 – 1/4th the cost. Rapid behavioral batteries could then identify a significant change in ethanol drinking behavior. If one is identified, the gene can be deemed suitable for a true-breeding line and further characterization, or if no change is observed, then the gene can be removed from the list of top AUD candidates to research and no more resources need to be expended.

In order for this technique and Aim to be successful, the approach must first be validated with a previously characterized ethanol-responsive gene to determine its experimental value. If successful, then the second step is to use approach to complete Aim 2, Chapter 3.2.

3.1 CRISPR TURBO ACCELERATED KNOCK OUT (CRISPy TAKO) FOR RAPID *IN VIVO* SCREENING OF GENE FUNCTION

Adapted from: **Plasil SL,** Seth A, & Homanics GE. 2020. CRISPR Turbo Accelerated Knock Out (CRISPy TAKO) for Rapid *in vivo* Screening of Gene Function. *Frontiers in Genome Editing*. 2. PMID: 33604589.

3.1.1 Introduction

Clustered regulatory interspaced short palindromic repeats (CRISPR) paired with CRISPR associated protein 9 (Cas9) is currently the dominant and preferred gene editing tool in scientific research. CRISPR-based screens of gene function *in vitro* have been tremendously useful for identifying genes involved in tumor suppression[664], mitochondrial function[665], and dendritic development [666]. High throughput CRISPR loss-of-function reverse-genetic screens allow for the rapid identification of genes involved in phenotypes of interest. However, *in vitro* screens are limited by phenotypes that can be readily assayed in cell culture (*e.g.*, cellular proliferation, drug sensitivity, and cell survival). Further, the acquisition of transcriptome data has greatly outpaced our capacity to functionally study genes of interest. For many biological questions, particularly those that pertain to dysfunction of the CNS where behavioral abnormalities are the primary phenotype of interest, *in vivo* tests of behavior must be employed. Because behavior is the phenotype of interest, *in vitro* screens are unsatisfactory. In this study, we sought to develop a method with moderately high throughput that could be used *in vivo* to screen genes for effects on behavior.

Global gene knockout (KO) animal models are a gold standard approach that have been widely used to study and delineate the effects of individual molecules in whole organisms. The recent application and widespread adoption of CRISPR/Cas9 technology dramatically facilitated KO animal generation. However, the standard method of creating CRISPR KO animals, a.k.a., CRISPy Critters[535], typically requires three generations to produce experimental animals that can be phenotypically evaluated and therefore is unsuitable for moderate-high throughput *in vivo* screens (**Figure 13A**). Briefly, in a typical CRISPR KO animal study, CRISPR reagents are

introduced to one-cell embryos that develop into founder (F0) animals that are screened for the desired mutation. F0 animals are typically an eclectic mix of wild-type (WT) and mutant animals. The mutants may be heterozygotes, homozygotes, or compound heterozygotes, and most mutant alleles differ in the individual mutations they harbor in the target gene of interest. A founder animal that harbors a desirable mutation (typically a frameshift or a large deletion) is then mated to WT mice to produce heterozygous F1 offspring. Subsequently, heterozygotes are interbred to produce homozygous F2 mutant KO offspring. These F2 mutant animals have both alleles of the gene of interest inactivated, they all harbor the same mutation in the gene of interest, and they can be compared to WT littermate controls for relevant phenotypic changes. Although this CRISPR approach to creating gene KO animals represents a dramatic savings in time, effort, and expense compared to traditional embryonic stem cell-based gene targeting approaches, the CRISPR approach still requires considerable time and expense. Three generations of animal production is time consuming and results in substantial animal care and housing expenses. This process also requires a considerable amount of personnel time for colony maintenance and genotyping.

We endeavored to establish a one generation CRISPR KO approach in which F0 animals could be directly used to test for the behavioral consequences of gene inactivation. We reasoned that a very high efficiency CRISPR mutagenesis approach could be used to efficiently create F0 animals in which both alleles of the gene of interest are mutated and are functionally inactivated (*i.e.,* gene KOs) (**Figure 13B**). Although each F0 animal may have different mutations, they would all be functionally and phenotypically equivalent if a critical part of the gene were sufficiently mutated.

Our long-term goal is to employ this accelerated technique to vastly speed up the screening process of testing novel ethanol-responsive genes for involvement in ethanol-related behavioral phenotypes, including ethanol consumption. Therefore, we initially piloted this approach *in vitro* on two novel ethanol-responsive long noncoding RNA (lncRNA) genes (*4930425L21Rik* and *Gm41261*). We subsequently sought to validate this method *in vivo* by mutating a gene previously shown to alter behavioral responses to ethanol when inactivated using traditional global KO technology. *Myd88* was chosen as a well-characterized ethanol-responsive gene for proof-of-concept as prior studies have evaluated the effects of *Myd88* global KO on ethanol-related behaviors, including ethanol drinking[378] and response to ethanol's acute sedative/hypnotic and motor ataxic effects[380,667]. Single generation F0 *Myd88* KO animals were hypothesized to exhibit

decreased ethanol-induced sedative/hypnotic effects, decreased sensitivity to ethanol-induced motor ataxia, and a male-specific increase in ethanol consumption relative to controls.

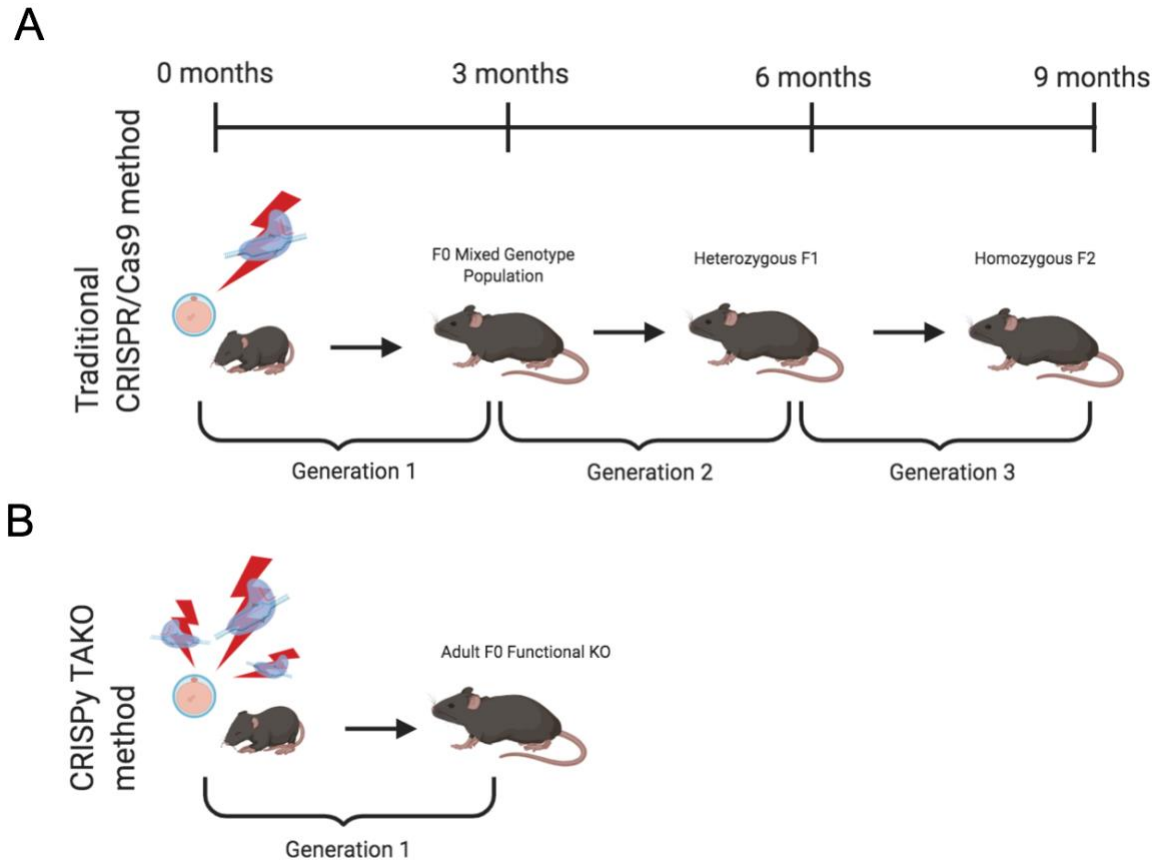

Figure 13: Comparison of the timeline required to produce KO and TAKO mice. (**A**) Traditional CRISPR/Cas9-mediated method to create a stable KO line. Founder (F0) animals are an eclectic mix of WT, heterozygous, and homozygous KOs. A founder with an inactivating mutation is selected for breeding to establish a KO line of mice. First generation offspring (F1) are heterozygous and must be interbred to produce an F2 generation. A subset (~25%) of the F2 generation are homozygous KO mice and can be compared for behavioral phenotypes with WT littermates. (**B**) CRISPy TAKO method for creating functional KO mice. By using multiple gRNAs that target a small but functionally critical part of the gene of interest, most F0 mice harbor biallelic mutations that functionally inactivate the gene of interest and are suitable for behavioral phenotyping.

To further streamline this accelerated KO mouse protocol, we reasoned that for first pass screening of genes for behavioral phenotypes, isogenic animals purchased directly from a vendor could be used as a control group for comparison to KOs. However, one concern is that the CRISPR

and/or electroporation procedures, irrespective of the gene being mutated, could hypothetically exert uncharacterized deleterious effects. Therefore, we also created in-house Mock treatment controls that were produced under an identical protocol to the KOs except that the Mock-treated animals were created with procedures that lacked crRNAs. This Mock-treated control group was directly compared to isogenic C57BL/6J WT mice (Jax controls) purchased from the Jackson Laboratory (JAX). We hypothesized that these two control groups would not differ on behavioral endpoints of interest.

In this report, we describe implementation and validation of a novel technique for the accelerated production of CRISPR/Cas9 KO mice in one generation. Animals produced via this protocol are herein affectionately referred to as CRISPR Turbo Accelerated Knock Outs (*i.e.*, CRISPy TAKOs). We report that our CRISPR protocol can reliably produce a large number of F0 KO animals and that the ethanol phenotype of *Myd88* CRISPy TAKOs largely recapitulates results previously reported for traditional *Myd88* global KOs. Furthermore, for the behaviors tested in this study, vendor purchased mice and Mock treatment controls did not differ substantially. Together, these results establish the CRISPy TAKO method for screening gene function *in vivo*. This method has moderately high throughput and will be especially useful for phenotypes, such as behavioral responses, that cannot be assayed *in vitro*.

3.1.2 Materials and Methods

3.1.2.1 Animals

All experiments were approved by the Institutional Animal Care and Use Committee of the University of Pittsburgh and conducted in accordance with the National Institutes of Health Guidelines for the Care and Use of Laboratory Animals. C57BL/6J male and female mice used to generate embryos for electroporation and the purchased control group were procured from The Jackson Laboratory (Bar Harbor, ME). CD-1 recipient females and vasectomized males were procured from Charles River Laboratories, Inc. (Wilmington, MA). Mice were housed under 12 – hour light/dark cycles, with lights on at 7 AM and had *ad libitum* access to food (irradiated 5P76 ProLab IsoProRMH3000; LabDiet, St. Louis, MO) and water.

3.1.2.2 Guide RNA Design

Guide RNAs (gRNAs) were generated using a commercially available two-piece system termed ALT-R™ CRISPR/Cas9 Genome Editing System (IDT DNA, Coralville, IA). This system combines a custom CRISPR RNA (crRNA) for genomic specificity with an invariant trans-activating crRNA (tracrRNA) to produce gRNAs[535]. crRNAs were designed using the computational program CCTop/CRISPRator[668,669], which gauges candidate gRNAs for efficiency and specificity.

Four crRNAs were used to target the ethanol-responsive lncRNA gene *4930425L21Rik* (see **Table 3** for all gRNA target sequences). These four crRNAs bind within a 366 bp region that includes the putative promoter and first Exon (**Figure 14A**). Similarly, four crRNAs were used to target the lncRNA gene *Gm41261*. These four crRNAs bind with a 316 bp region that includes the putative promoter and first Exon (**Figure 14C**). Four crRNAs were also selected for *Myd88* that bind within a 209 bp region that includes *Myd88* Exon 3 and flanking DNA (**Figure 15A**). For each project, the four crRNAs were annealed separately with tracrRNA in a 1:2 molar ratio then combined into a single solution.

Table 3: gRNA target sites and PCR primer sequences for Chapter 3.1.

Name	Sequence
4930425L21Rik #1 gRNA	AGACACTAATATTGCAGACG AGG
4930425L21Rik #2 gRNA	TTATTTTTCTGCAAGGGGTT GGG
4930425L21Rik #3 gRNA	ACACTATCGACCTAATAGCT AGG
4930425L21Rik #4 gRNA	ATTTTAAACCCTCTGTTACT TGG
Gm41261 #1 gRNA	CAATTTGCAATTCTCTTCCA GGG
Gm41261 #2 gRNA	AGAATAAACAGGTGTGACGG TGG
Gm41261 #3 gRNA	CTTATCAGGTCTTTGATCAG AGG
Gm41261 #4 gRNA	GGTCTTTTACTTTTCTCTTT AGG
Myd88 T3 gRNA	CCTTTTCTCAATTAGCTCGC TGG
Myd88 T5 gRNA	GCACAAACTCGATATCGTTG GGG
Myd88 T15 gRNA	AGGTTGGTTAAACATCTAAG AGG
Myd88 T30 gRNA	GGCGTTTGTCCTGAGGACAG GGG
4930425L21Rik F5 PCR primer	GTGTCCAGCATTGTGCCAAG
4930425L21Rik R5 PCR primer	TCTAAAAGGGGCCCTCCAGT
Gm41261 F10 PCR primer	CTCACCAAAATTCAACCTGGAG
Gm41261 R10 PCR primer	GCTTCAGAGCTCACTGGTGT
Myd88 F1 PCR primer	CCGGGATTTCATCTGGGAGG
Myd88 R1 PCR primer	ACTGCGGTGACTTCCTTCAG
Myd88 F2 PCR primer	GGTGGCCAGAGTGGAAAGCAGTGTCCC
Myd88 R2 PCR primer	GAAACAACCACCACCATGCGGCGACA

3.1.2.3 CRISPR/Cas9 Mutagenesis

Female C57BL/6J mice were superovulated with 0.1mL of CARD HyperOva (CosmoBio, #KYD-010) between 10 AM and 11 AM, followed by 100 IU of human chorionic gonadotropin

(Sigma, #CG10) 46 – 48 hours later. Donor females were caged overnight with C57BL/6J males starting 4 – 6 hours post-gonadotropin injection and allowed to mate. Embryos were harvested from oviducts between 9 AM and 10 AM the following morning, cumulus cells were removed using hyaluronidase, and embryos were cultured under 5% CO_2 in KSOM medium (Cytospring, #K0101) for 1 – 2 hours. Embryos were electroporated in 5µL total volume of Opti-MEM medium (ThermoFisher, #31985088) containing 100ng/µL of each sgRNA and 100 or 200ng/µL Alt-R® S.p. HiFi Cas9 Nuclease V3 protein (IDT, #1081060) with a Bio-Rad Gene-Pulser Xcell in a 1mm-gap slide electrode (Protech International, #501P1-10) using square-wave pulses (five repeats of 3msec 25V pulses with 100msec interpulse intervals). Two different concentrations of Cas9 protein were used to assess which produced greater mutagenesis in embryos targeting genes *4930425L21Rik* and *Gm41261*; only the 200ng/µL concentration was used for *Myd88*-targeted embryos. Electroporated embryos were placed back into culture under 5% CO_2 in KSOM. For *4930425L21Rik* and *Gm41261*, embryos were cultured for 3 days until the morulea/blastocyst stage and subsequently analyzed for mutations. For *Myd88*, one- or two-cell embryos were implanted into the oviducts of plug-positive CD-1 recipient (20 – 40 embryos per recipient) that had been mated to a vasectomized male the previous night. Mock-treated controls were manipulated in parallel as described above, except that the electroporation mix lacked the *Myd88*-specific crRNAs (*i.e.*, only tracrRNA and Cas9 protein were used).

3.1.2.4 Genotyping

For *4930425L21Rik* and *Gm41261*, DNA was amplified from individual embryos using a Qiagen Repli-G kit (Qiagen, #150025) and subject to PCR genotyping under the following settings: 95°C for 5 minutes (1x); 95°C for 30 seconds, 60°C for 30 seconds, 72°C for 1 minute (40x); 72°C for 10 minutes (1x). Primers for PCR amplification of *4930425L21Rik* and *Gm41261* are listed in **Table 3**. PCR amplicons (WT = 613 and 506 bp, respectively) were analyzed by agarose gel electrophoresis and Sanger sequencing (Genewiz; South Plainfield, NJ).

For *Myd88*, DNA was isolated from tail snips of *Myd88* CRISPy TAKO and Mock-treated control offspring using Quick Extract (Lucigen, #QE09050). Primers for *Myd88* genotyping are listed in **Table 3**. PCR amplicons (WT = 494 bp) were analyzed by agarose gel electrophoresis and Sanger sequencing.

3.1.2.5 Subcloning

Samples that did not produce clear chromatograms were subcloned to identify allelic variants. The TOPO™ TA cloning kit (ThermoFisher Scientific, #K457501) was used according to manufacturer's instructions, with slight modifications. Briefly, sample PCR product was incubated at room temperature for 15 minutes with TOPO reagents, then the TOPO vector mixture was incubated with chemically competent DH5α (ThermoFisher Scientific, #18265017) cells on ice for 30 minutes. Cells were then heat-shocked for 45 seconds in a 42°C water bath then immediately placed back on ice for 2 minutes. S.O.C. medium (ThermoFisher Scientific, #15544034) was added and cells were incubated in a bacterial shaker at 37°C for 90 minutes at 225 RPM. Cells were plated on kanamycin-resistant LB plates and incubated at 37°C for 16 – 18 hours. Single colonies (n = 10 per sample) were collected, and their DNA was used for PCR. Colonies that produced a single PCR band were then Sanger sequenced.

3.1.2.6 RNA Precipitation

Brain cerebellar tissue from one Mock treatment control (n = 1 male), one Jax control (n = 1 male), and 6 *Myd88* mutants (n = 3 male, n = 3 female) were used for RT-PCR analysis. All mice were 11 – 12 weeks of age at time of sacrifice. Total RNA was isolated using TRIzol (Invitrogen, #15596018) according to the manufacturer's protocol, and purified with a TURBO DNA-*free*™ Kit (Invitrogen, #AM1907). Total RNA was analyzed for purity and concentration using a Nanodrop Spectrophotometer (Thermo Scientific, Waltham, MA). 1μL of purified RNA was converted into cDNA using Superscript™ III First-Strand Synthesis System (Invitrogen, #18080051) with random hexamer primers. RT-PCR primers were used that span from Exon 2 to Exon 4 (**Table 3**) of *Myd88*. A reaction that lacked reverse transcriptase was used as a negative control for each sample tested. RT-PCR amplicon size is 280 bp for WT, and 99 bp when Exon 3 is lacking.

3.1.2.7 Behavioral Testing

All mice were moved into a reverse light-cycle housing/testing room (lights off at 10 AM) at 5 weeks of age and allowed to acclimate for 2 – 3 weeks before the start of

experimentation. Experiments were performed in the housing room (ethanol drinking) or an adjoining room (LORR, rotarod). Mice were group-housed 4 to 5 per cage based on genotype and sex. The same mice were sequentially tested on the rotarod, LORR, and drinking assays, with 4 – 7 days between assays.

3.1.2.8 Drugs

Injectable ethanol solutions (Decon Laboratories, Inc.) were prepared fresh daily in 0.9% saline. Ethanol was injected intraperitoneally (i.p.) at 0.02mL/g of body weight.

3.1.2.9 Rotarod

In order to assess ethanol-induced motor ataxia, mice were trained on a fixed speed rotarod (Ugo Basile, Gemonio, Province of Varese, Italy) at 11 RPM. Training was considered complete when mice were able to remain on the rotarod for 60 seconds. Following training, mice were injected with ethanol (2.0g/kg, i.p.) and every 15 minutes mice were placed back on the rotarod and latency to fall was measured until mice were able to remain on the rotarod for 60 seconds.

3.1.2.10 Loss of Righting Response (LORR)

Sensitivity to the sedative/hypnotic effects of ethanol was determined using the LORR assay. Mice were injected with ethanol (3.5g/kg, i.p.) and when mice became ataxic, they were placed in the supine position in V-shaped plastic troughs until they were able to right themselves 3 times within 30 seconds. LORR was defined as the time from being placed in the supine position until they regained their righting response. Body temperatures were maintained using a heat lamp throughout the assay.

3.1.2.11 Every-Other-Day Two-Bottle Choice (EOD-2BC) Drinking

Mice were given access to ethanol (15%, v/v) and water for 24-hour sessions every other day for 12 days starting at 12 PM. Water alone was offered on off days. Purchased drinking bottles were 15mL with 3.5-inch sipper tubes (Amuza, San Diego). The side placement of the ethanol bottles was switched with each drinking session to avoid side preference. Ethanol solutions were

prepared fresh daily. Bottles were weighed before placement and after removal from the experimental cages. Empty cages with sipper bottles were used to control for leakage, and leakage amount was subtracted from amount consumed by the mice. The quantity of ethanol consumed, and total fluid intake, was calculated as g/kg body weight per 24 hours. Preference was calculated as amount ethanol consumed divided by total fluid consumed per 24 hours.

3.1.2.12 Statistical Analysis

Statistical analysis was performed with GraphPad Prism (GraphPad Software, Inc., La Jolla, CA) for two-tailed Mann-Whitney test and two-way ANOVA (with mixed-effects analysis (*i.e.,* when technical failures were present), multiple comparisons, and repeated measures when appropriate). Significant main effects were subsequently analyzed with Benjamini, Krieger, and Yekutieli two-stage linear step up procedure *post-hoc* analysis[670]. Technical failures were appropriately removed from analysis.

The two control groups were first compared to one another; if no difference was found between control groups, these groups were pooled and tested against the *Myd88* TAKO group. Graphs show control groups plotted separately for completeness even though they were analyzed together, unless noted otherwise. Because of well-known sex differences on the behaviors of interest, and because male and female mice were tested on separate days, each sex was analyzed separately. Statistical significance was defined as $p \leq 0.05$ and $q \leq 0.05$. All data are presented as mean ± S.E.M.

3.1.3 Results

3.1.3.1 CRISPR/Cas9-Mediated Mutagenesis

Preliminary testing of the CRISPy TAKO method occurred *in vitro* using embryos electroporated at the one-cell stage, cultured until the blastocyst stage, then genotyped (**Figure 14**). To enhance CRISPR mutagenesis frequency, each gene was targeted simultaneously with four gRNAs that were tiled across a small section of the gene. In addition, we tested two concentrations of Cas9 protein (100 and 200ng/μL) that were higher than the minimum amount we typically use (*i.e.,* 50ng/μL).

The first gene targeted was an unannotated ethanol-responsive gene, *4930425L21Rik*, using 4 gRNAs that span 366 bp of the putative promoter and first Exon (**Figure 14A**). Agarose gel electrophoresis of PCR amplicons that span the targeted locus indicated that 3 of 5 embryos tested at 100ng/µL Cas9 had obvious indels whereas 2 embryos (#'s 1.2 and 1.3; **Figure 14A and B**) had amplicons that were grossly indistinguishable from the 613 bp WT control amplicon (**Figure 14B**). Sanger sequencing revealed #1.2 as heterozygous for WT and a 21 bp deletion (**Figure 14A**). At 200ng/µL Cas9 protein, all seven embryos assessed were found to harbor deletions of varying sizes (**Figure 14A and B**). Thus, none of the embryos electroporated with 200ng/µL Cas9 harbored WT amplicons that were visible on the agarose gel or detectable by amplicon bulk sequencing.

The second gene targeted was another ethanol-responsive gene, *Gm41261* (a.k.a. *Tx2*). Four gRNAs spanning 316 bp within the putative first Exon were used (**Figure 14C**). Agarose gel electrophoresis of PCR amplicons that span the targeted locus indicated that 1 of 5 embryos tested at 100ng/µL Cas9 had an obvious indel (#5.6; **Figure 14C and D**), whereas the other 4 of 5 embryos had amplicons that were indistinguishable from the 506 bp WT control amplicon (**Figure 14D**). Sanger sequencing revealed only one embryo (#5.3; **Figure 14C and D**) was homozygous WT, whereas the other four embryos harbored various small deletions (**Figure 14C**). At 200ng/µL Cas9, all six embryos assessed were found to harbor deletions of varying sizes (**Figure 14C and D**). Although one embryo (#7.5) had a PCR product approximately the size of the WT amplicon (506 bp), Sanger sequencing revealed a 14 bp deletion. Sanger sequencing also revealed a sequence inversion in #8.1, along with a 16 bp insertion directly following the inverted sequence (**Figure 14C**). Thus, 5 of 6 embryos electroporated at 200ng/µL Cas9 protein did not harbor detectable WT amplicons by agarose gel or amplicon bulk sequencing. Because the higher 200ng/µL Cas9 concentration showed greater mutagenic activity in both *4930425L21Rik* and *Gm41261*, this concentration was utilized in targeting *Myd88*.

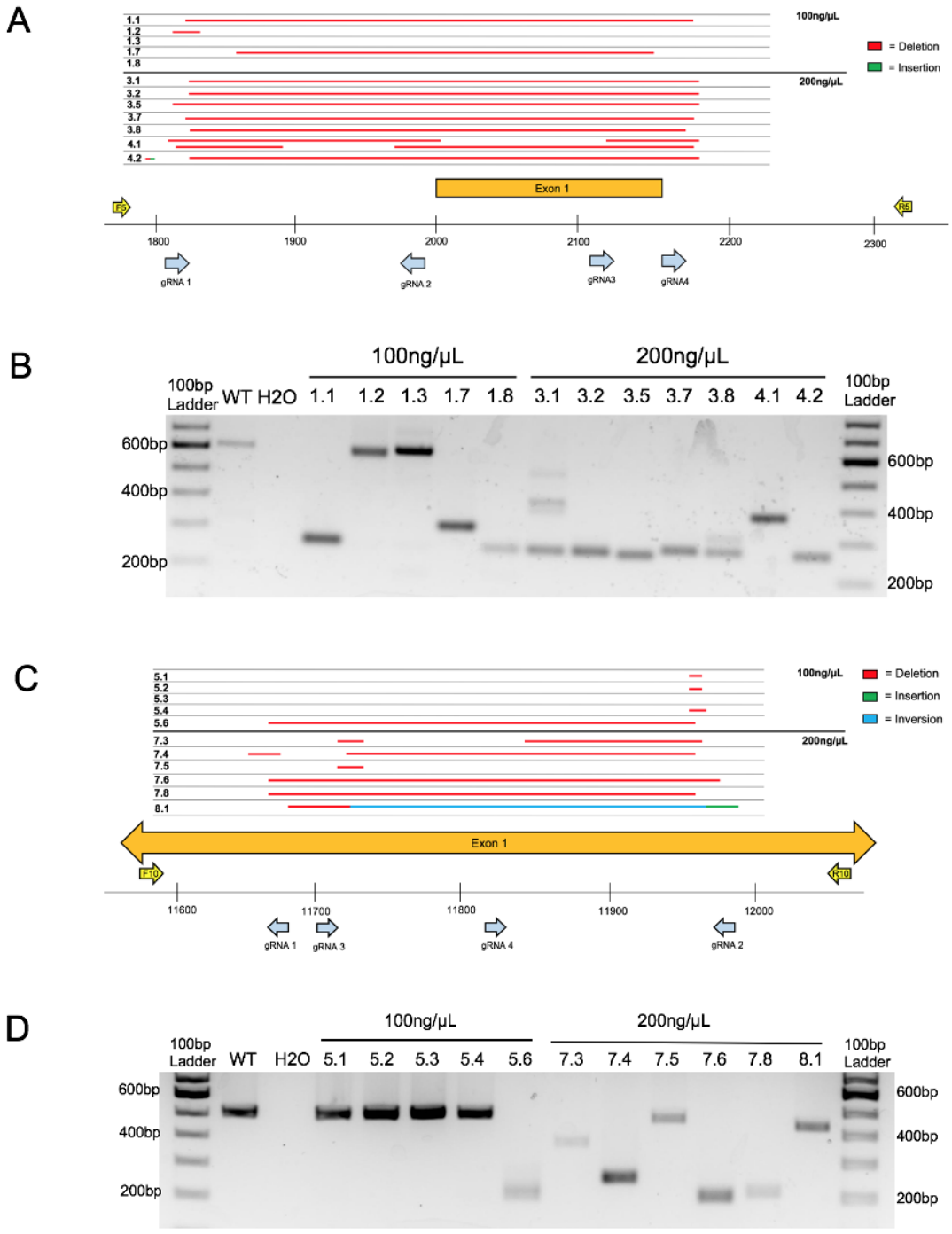

Figure 14: Embryo CRISPy TAKO genotypes for *4930425L21Rik* and *Gm41261*. (**A**) Sequence results for the major product(s) of TAKO embryos targeting gene *4930425L21Rik* electroporated with 100ng/µL and 200ng/µL Cas9 protein. Full deletions are shown in red. Sequence insertions are shown in green. Individual animal tag numbers are presented on the left. The gRNAs and PCR primers used are shown as blue and yellow arrows, respectively. (**B**)

Agarose gel electrophoresis of PCR amplicons for *4930425L21Rik* in embryos. Samples 1.1 through 1.8 were electroporated with 100ng/µL Cas9 protein while samples 3.1 through 4.2 were electroporated with 200ng/µL Cas9 protein. (**C**) Sequence results from TAKO embryos targeting gene *Gm41261* with 100ng/µL and 200ng/µL Cas9. Sequence inversions are shown in blue. (**D**) Agarose gel electrophoresis of PCR amplicons for *Gm41261* in embryos. Samples 5.1 through 5.6 were embryos electroporated with 100ng/µL Cas9 while samples 7.3 through 8.1 were electroporated with 200ng/µL Cas9 protein.

As proof-of-concept and to validate our method *in vivo*, we created *Myd88* CRISPy TAKO mice. The four gRNAs were tiled across a 209 bp region of *Myd88* that included Exon 3 (**Figure 15A**). Exon 3 was targeted because prior traditional global *Myd88* KO studies demonstrated that deletion of this Exon inactivates Myd88[671] and imparts an alcohol behavioral phenotype[378,380,667].

Implantation of embryos electroporated on six different days with *Myd88* gRNAs yielded 54 offspring (n = 26 females, n = 28 males). Thirty-one offspring (n = 16 females, n = 15 males) were derived from electroporation of Mock-treated control embryos that were handled identically except that the crRNAs were omitted from the electroporation solution (see: **Chapter 3.1.2**). All mice born from electroporated embryos were genotyped for gross indels at *Myd88* Exon 3 using endpoint PCR (data not shown). The 494 bp WT PCR amplicon was invariant and readily detectable in Jax and Mock-treated control samples as expected (**Figure 15B**; unpublished results). In stark contrast, 52 of 54 *Myd88* TAKO mice displayed gross indels encompassing *Myd88* Exon 3 that were readily apparent following gel electrophoresis of PCR products (unpublished results). Out of the 54 *Myd88* mutant mice created, a subset were selected for behavioral phenotyping based on indel size (n = 30), and PCR results are shown in **Figure 15B**. The indels varied from animal to animal and most appeared to be deletions, as evidenced by the PCR products being approximately 50 – 300bp smaller than the 494 bp WT amplicon. To more accurately characterize the mutations present, we sequenced the PCR products of the mutated mice selected for behavior (**Figure 15A**). As illustrated in **Figure 15A and B**, the mice used for phenotyping presented variable deletions mainly ranging from 200 – 300bp. All deletions broadly encompassed Exon 3, therefore all mice were expected to manifest the same behavioral phenotypes. It is important to note that 100% of all crRNA-electroporated pups contained a *Myd88* indel. Based on the genotyping results, a subset of *Myd88* CRISPy TAKOs (n = 15/sex) containing Myd88-inactivating mutations were selected for ethanol-related behavioral interrogation.

Cerebellar tissue from a random subset of *Myd88* CRISPy TAKOs and controls were used for RT-PCR analysis using PCR primers that bind to Exons 2 and 4 to examine *Myd88* mRNA. This analysis revealed the expected 280 bp fragment in both WT control samples (**Figure 15C**). In contrast, none of the six *Myd88* CRISPy TAKO mice examined produced a fragment of this size. Five of the six samples produced a predominant band of ~99 bp as would be expected for *Myd88* mRNA that lacked Exon 3. One sample produced a major band of ~210 bp and may represent a splicing defect. Thus, *Myd88* CRISPy TAKO mice are likely to be functional KOs.

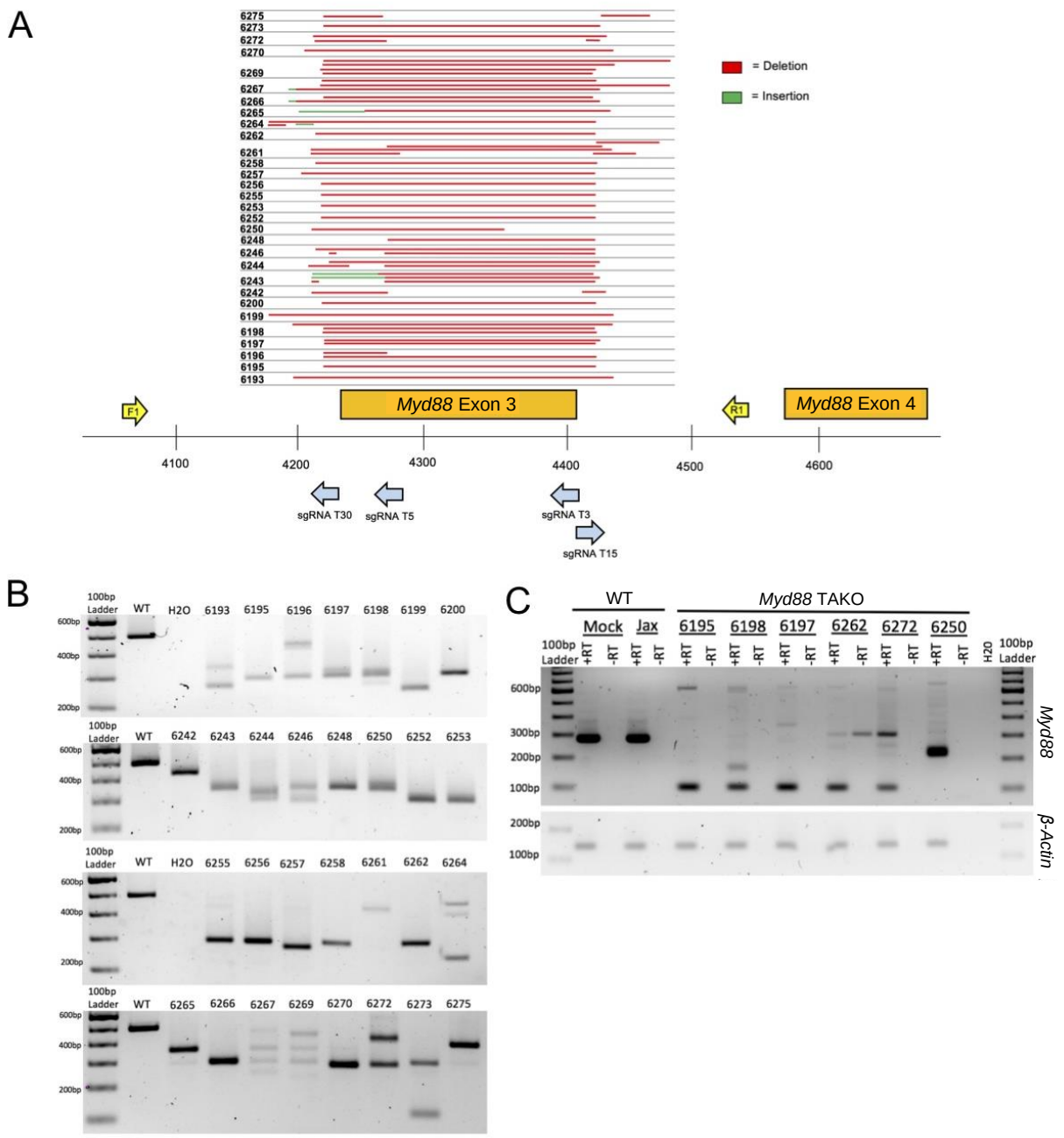

Figure 15: *In vivo Myd88* CRISPy TAKO genotypes. (**A**) Sequencing results from mice selected for behavioral experimentation. CRISPR/Cas9 mutagenesis of *Myd88* Exon 3 was performed and animals used for experimentation were sequenced to confirm successful deletion. Full deletions are shown in red. Sequence insertions are shown in green. Individual animal tag numbers are presented on the left. The gRNAs and PCR primers used are shown as blue and yellow arrows, respectively. (**B**) PCR results from DNA of *Myd88* CRISPy TAKO mice used for experimentation. Jax mouse used as control. (**C**) Random sample subset RT-PCR results from cerebellar brain tissue showing abnormal *Myd88* RNA transcripts in TAKOs. *β-Actin* RT-PCR was used as a control.

3.1.3.2 Ethanol-Induced Loss of Righting Response (LORR)

No difference in ethanol-induced LORR (3.5g/kg, i.p.) was found between the Mock and Jax control groups for males or females (**Figure 16**). Therefore, Mock controls and Jax controls were combined and compared to *Myd88* KOs (for completeness, control results are plotted separately). Male *Myd88* TAKOs exhibited a significant reduction in ethanol-induced LORR duration when compared to controls ($p < 0.01$; **Figure 16A**). No difference was observed in females for ethanol-induced LORR (**Figure 16B**).

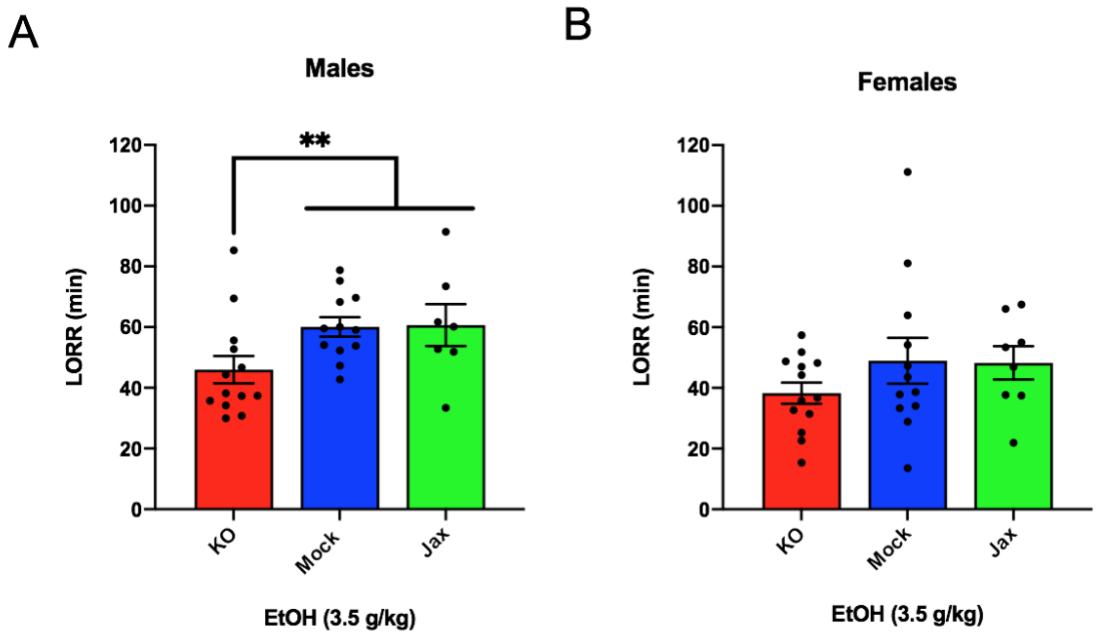

Figure 16: Duration of ethanol-induced LORR in *Myd88* KO and control mice. *Myd88* KOs, Mock controls and Jax controls. 3.5g/kg ethanol, i.p. injection. For both males (**A**) and females (**B**), mock controls and Jax controls did not differ and therefore were pooled and compared to same sex *Myd88* KOs (data are plotted separately for completeness). KO males had reduced duration of LORR compared to the combined control group (**$p < 0.01$). For females, no difference was observed between *Myd88* KOs and the combined control group. Control (Jax C57BL/6J, n = 7 – 8; Mock-treatment control, n = 13 – 14) versus mutant mice (n = 13 – 14 *Myd88* KO). Values represent Mean ± SEM. Data were analyzed using a two-tailed Mann-Whitney test.

3.1.3.3 Ethanol-Induced Motor Incoordination

The ataxic effects of an acute ethanol injection (2.0g/kg, i.p.) were measured using a constant speed (11 RPM) rotarod test. For male mice, comparison of Mock and Jax controls

showed a significant effect of time [F (2.281, 41.05) = 36.41, $p < 0.0001$], and time x genotype [F (9, 162) = 3.209, $p < 0.01$], but no effect of genotype (**Figure 17A**). Because of the time x genotype interaction, control groups were not combined for this analysis. Repeated measures two-way ANOVA of all three groups revealed a significant effect of time [F (2.474, 71.73) = 59.01, $p < 0.0001$], and an effect of time x genotype [F (18, 261) = 1.964, $p < 0.05$] but no effect of genotype (**Figure 17A**). *Post-hoc* comparisons revealed that male Mock control mice recovered more quickly than Jax controls at the 15-minute timepoint ($q < 0.01$).

For females, comparison of Mock and Jax controls revealed a significant effect of time [F (2.775, 55.51) = 89.05, $p < 0.0001$], but no effect of genotype or time x genotype (**Figure 17B**). Therefore, the two control groups were combined (data plotted separately for completeness) and compared to *Myd88* TAKOs. There was a significant effect of time [F (2.664, 87.90) = 148.3, $p < 0.0001$], and genotype [F (1, 33) = 4.721, $p < 0.05$], but no effect of the time x genotype interaction (**Figure 17B**). *Post-hoc* analysis did not reveal any significant differences.

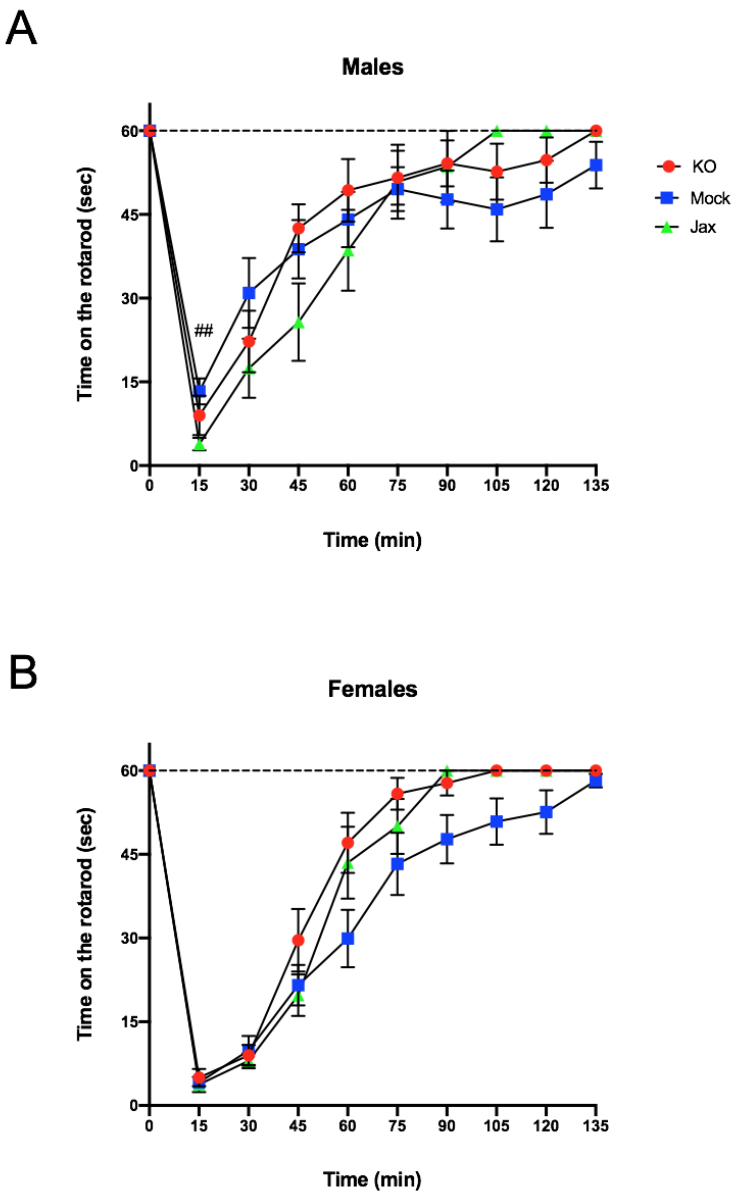

Figure 17: Recovery from ethanol-induced motor incoordination in *Myd88* KO and control mice. (**A**) A significant time x genotype interaction was observed for male mock controls and Jax controls. Therefore. control groups were not combined. Jax controls recovered more slowly compared to Mock controls at the 30 min timepoint ($^{\#\#}q < 0.01$). (**B**) Female mock controls and Jax controls did not differ and were combined for comparison to *Myd88* KOs (data are plotted separately for completeness). *Post-hoc* analysis did not reveal any significant differences between groups at any time points. Data represent time in seconds on the rotarod after injection of ethanol (2 g/kg, i.p.). Control (Jax C57BL/6J, n = 8; Mock-treatment control, n = 13 – 14) versus mutant mice (n = 13 – 14 *Myd88* KO). Values represent Mean ± SEM. Data were analyzed by repeated-measures Two-way ANOVA with multiple comparisons followed by Benjamini, Krieger, and Yekutieli *post-hoc* test.

3.1.3.4 Every-Other-Day Two-Bottle Choice (EOD-2BC) Drinking

Mice were tested for ethanol drinking using an intermittent EOD-2BC free choice consumption assay over a period of 12 days. Mock and Jax control groups were first compared against each other; two-way ANOVA mixed-effects analysis was used for all EOD-2BC statistical analyses. For males, there was a significant effect of time for ethanol intake [$F (3.333, 62.00) = 5.740$, $p < 0.01$], ethanol preference [$F (2.702, 50.27) = 10.85$, $p < 0.0001$], and total fluid intake [$F (3.392, 63.09) = 17.98$, $p < 0.0001$], but there was no effect of genotype or time x genotype interaction for any of these parameters (**Figure 18A, B, and C,** respectively). Therefore, both Mock and Jax control groups were combined (data plotted separately for completeness) and compared to *Myd88* TAKOs. Analysis of ethanol intake in males between the combined control group and *Myd88* TAKOs revealed a main effect of time [$F (4.123, 129.5) = 10.67$, $p < 0.0001$] and genotype [$F (1, 32) = 4.850$; $p < 0.05$], but no interaction between the two (**Figure 18A**). *Post-hoc* analysis revealed that *Myd88* TAKO males had significantly greater intake on day 10 ($q < 0.05$) compared to controls. For preference in males, there was an effect of time [$F (3.365, 105.7) = 24.02$, $p < 0.0001$] but no effect of genotype or time x genotype (**Figure 18B**). For total fluid intake in males, there was a main effect of time [$F (3.915, 122.9) = 36.79$, $p < 0.0001$] and genotype [$F (1, 32) = 8.897$, $p < 0.01$], but no time x genotype interaction between *Myd88* TAKO and controls (**Figure 18C**). *Post-hoc* analysis revealed significantly increased total fluid consumption in *Myd88* TAKOs versus controls on days 4, 6, 8 ($q < 0.05$), and day 10 ($q < 0.001$) (**Figure 18C**).

In females, Mock and Jax control groups were first compared. There was a significant effect of time on ethanol intake [$F (2.412, 47.27) = 8.979$, $p < 0.001$] and ethanol preference [$F (2.626, 51.47) = 22.58$, $p < 0.0001$], but no effect of genotype or time x genotype interaction on either parameter (**Figure 18D and E,** respectively). Therefore, both control groups were combined (data plotted separately for completeness) and compared to *Myd88* TAKOs. For ethanol intake, females showed a main effect of time [$F (2.632, 86.85) = 12.50$, $p < 0.0001$] but not genotype or time x genotype (**Figure 18D**). Similarly, for ethanol preference a significant effect of time [$F (3.317, 109.5) = 29.10$, $p < 0.0001$] but not genotype and time x genotype interaction was observed (**Figure 18E**). Thus, ethanol intake and preference did not differ between female *Myd88* TAKOs and the combined control group.

Comparing total fluid intake in female Mock and Jax controls revealed significant main effects of time [$F (2.818, 55.22) = 9.800$, $p < 0.0001$] and genotype [$F (1, 20) = 10.41$, $p < 0.01$],

but no time x genotype interaction (**Figure 18F**). Therefore, for female total fluid intake, control groups were not combined, and each genotype was considered separately. This analysis revealed a significant effect of time [$F (2.650, 84.79) = 11.20$, $p < 0.0001$] and genotype [$F (2, 33) = 4.221$, $p < 0.05$] (**Figure 18F**), but no time x genotype interaction. *Post-hoc* analysis did not reveal any significant differences.

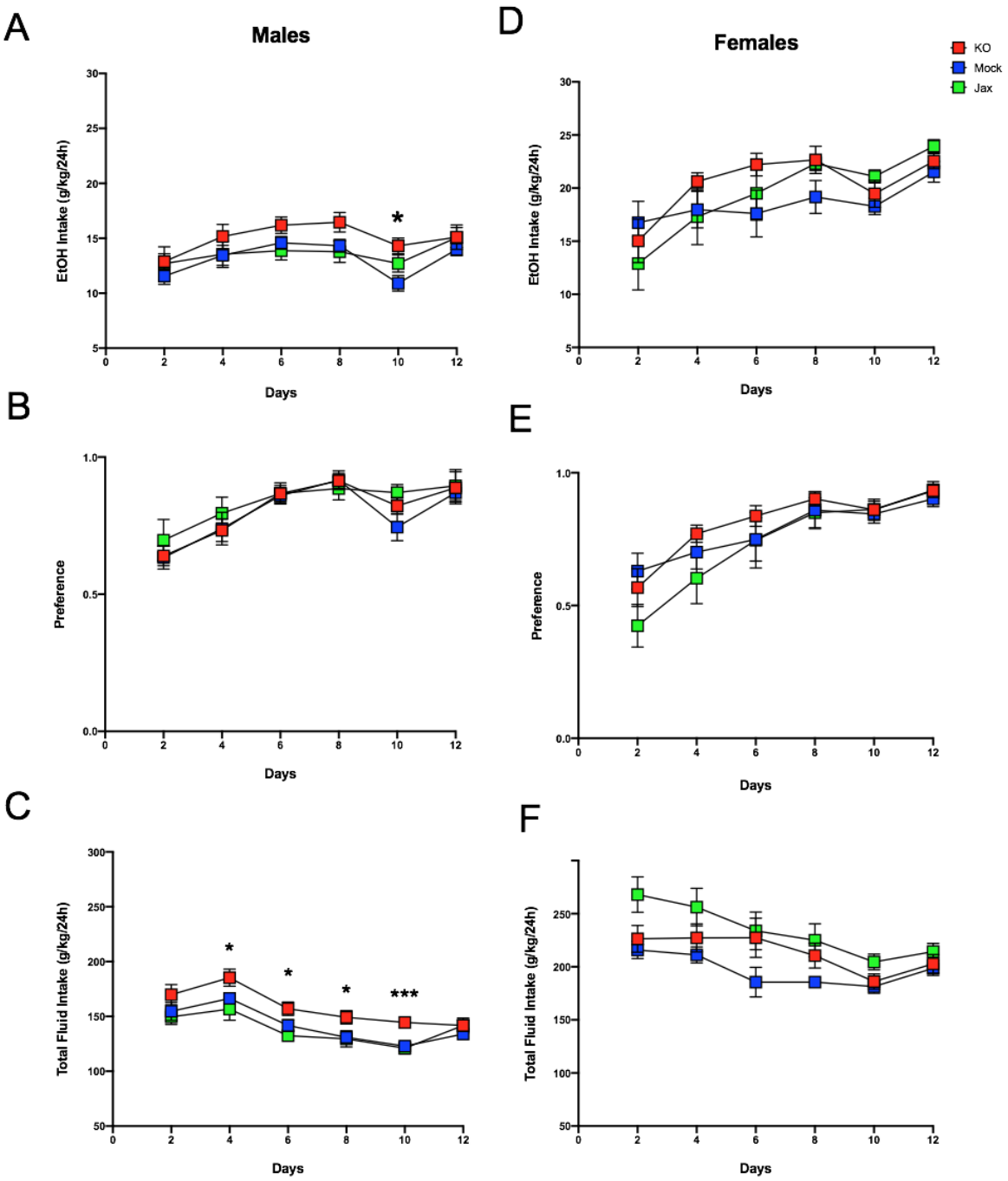

Figure 18: EOD-2BC in *Myd88* KO, Mock control and Jax control mice. Left, males; right, females. (**A and D**) Ethanol (EtOH) intake (g/kg/24 h), (**B and E**) Ethanol preference. (**C and F**) Total fluid intake (g/kg/24 h) in control (Jax C57BL/6J, n = 8; Mock-treatment control, n = 13 – 14) versus mutant mice (n = 13 – 14 *Myd88* KO). Values represent Mean ± SEM. Data were analyzed by repeated-measures two-way ANOVA (mixed-effects analysis where appropriate) with multiple comparisons followed by Benjamini, Krieger, and Yekutieli *post-hoc* tests (*p < 0.05 and ***p < 0.001 between *Myd88* KO and combined controls).

3.1.4 Discussion

The current study reports on a CRISPR/Cas9-mediated mutagenesis protocol that is suitable for rapid screening for the phenotypic effects of gene KO *in vivo*. Traditional CRISPR mouse KO procedures require three generations of animal breeding and genotyping, which is time consuming and expensive. In contrast, with the CRISPy TAKO protocol described here, first generation gene-targeted F0 mice can be rapidly produced and screened for phenotypic effects. Although individual F0 mice harbor a variety of mutant alleles for the gene of interest, careful project design ensures that each F0 animal is functionally equivalent (*i.e.*, a gene KO). F0 animals can be directly screened for phenotypes of interest. If no phenotype is detected, the gene is rapidly eliminated from further consideration. If an interesting phenotype is observed, a F0 animal can be bred as in traditional approaches to establish a true breeding line that can first be tested to confirm the phenotype. This will ensure rigor and reproducibility in the experimental pipeline. Subsequently, the line can be maintained long-term and more detailed, rigorous mechanistic studies can be conducted. The CRISPy TAKO approach can save valuable time and minimize animal numbers and financial resources.

There are several keys to the success of this approach. First, we use embryo electroporation to facilitate genetic modification of a large number of animals with minimal effort. Large numbers of embryos (n = 30 – 50) can be simultaneously transfected with CRISPR reagents at a very high efficiency[537,572-574,672]. This avoids the limiting bottleneck of directly injecting each individual embryo. Second, achieving a very high level of indel formation that ablates function of the gene of interest in each animal is critical. We observed that 52 of 54 of animals harbored inactivating indels, while the other two harbored smaller mutations that may or may not have been inactivating (mice were deemed unsuitable for experimentation and therefore the mutations were not sequenced). To achieve this high KO efficiency, we simultaneously utilized four gRNAs that targeted a small, functionally important portion of the gene of interest. In other experiments, we have observed that the mutagenesis efficiency of a single gRNA is highly variable. Simultaneous use of two gRNAs tends to increase mutagenesis efficiency. We reasoned that an even higher number of gRNAs tiled across a small but functionally important part of a gene would result in even higher efficiency. We are unsure if four is the optimal number of gRNAs, but this should be rigorously explored in future studies. For *in vivo* proof-of-concept, we focused on a small, single

Exon of the *Myd88* gene that results in a null allele when disrupted[378,380,667,671]. This approach should also work by targeting the promoter or any region that is critical for function of the gene and/or gene product. It should also be noted that we observed that 200ng/µL Cas9 protein in the electroporation mix produced a much higher rate of indel formation compared to 100ng/µL. While 200 ng/µL is 4x the minimum amount we typically use in our laboratory for most CRISPR embryo electroporation experiments, this amount is less than that reported in the literature[537,573].

Unbeknownst to us at the time we conducted these experiments, a similar multi-gRNA CRISPR strategy termed C-CRISPR had been previously reported[673]. Although the primary application of the C-CRISPR method was to create KO mice and nonhuman primates with reduced levels of mosaicism, the authors also recognized the usefulness of such an approach for phenotypic screens in F0 animals. Together, the current study and that of Zuo *et al.* 2017[673] demonstrate that multi-gRNA approaches are remarkably robust across laboratories and target loci. Despite the similarities, CRISPy TAKO and C-CRISPR differ in a few subtle, but possibly important ways. To introduce CRISPR reagents into embryos, we used electroporation whereas C-CRISPR used microinjection of individual embryos. With electroporation, large numbers of embryos can be transfected with minimal time and effort, and electroporation does not require expensive embryo microinjection equipment and embryo micromanipulation skills. Secondly, we used high fidelity Cas9 protein whereas C-CRISPR used Cas9 mRNA. Lastly, as described below, we also tested and validated the use of animals procured directly from a vendor as a control group for comparison to F0 KO animals in phenotypic screens. These subtle differences provide the CRISPy TAKO approach with significant savings of time and financial resources.

The CRISPy TAKO approach could be further streamlined and throughput increased if control animals for comparison could be procured directly from a vendor. However, it is conceivable that the *in vitro* embryo manipulation/CRISPR electroporation procedure could introduce some unknown variable that could impact the phenotype of interest regardless of the gene targeted for modification. Therefore, we compared phenotypes of control animals procured directly from JAX with isogenic controls that were produced in-house, in parallel to the *Myd88* TAKOs. This in-house control group was created using procedures that were identical to those used to create *Myd88* TAKOs except that crRNAs were omitted from the electroporation reactions. We observed near complete concordance between these Mock controls and Jax control animals for the behavioral phenotypes of interest. We only observed a subtle female-specific difference in

total fluid consumption in the EOD-2BC assay (**Figure 18F**) and a male-specific genotype x time interaction on the rotarod (**Figure 17A**). We conclude that mice purchased directly from a vendor can be used as a control group for screening CRISPy TAKO mice for behavioral alterations provided the controls are the same genetic background as those animals that served as embryo donors. Using a single vendor-derived control group will substantially increase throughput and reduce expenses.

As proof-of-concept of the CRISPy TAKO approach, we focused on *Myd88* as a candidate gene. We sought to functionally validate our approach by comparing behavioral phenotypes observed with those previously reported for global *Myd88* KO mice produced using traditional gene targeting technology, which displayed robust alterations in ethanol-induced behavioral responses and ethanol drinking behavior[378,380,667]. Overall, similar behavioral results were observed between traditional *Myd88* KOs and *Myd88* CRISPy TAKOs (**Table 4**). Consistent with previous findings, the *Myd88* TAKO females show faster recovery time from ethanol's incoordination effects (**Figure 17B**), but contrary to those studies, no difference between male *Myd88* TAKOs and controls is reported here (**Figure 17A**). Also consistent with previous reports, albeit with a milder effect size[378], *Myd88* TAKO males had greater consumption of ethanol than controls (**Figure 18A**). However, TAKO males in the present study did not have a difference in preference when compared to controls (**Figure 18B**) but had significantly increased total fluid intake compared to controls (**Figure 18C**), suggesting these male mice drink more fluid in general, and it is not specific to ethanol. Altered total fluid intake in *Myd88* TAKO females compared to controls (**Figure 18F**) is consistent with the published literature[378].

Table 4: Comparison of *Myd88* TAKO cohort results with previous findings.

	CRISPy TAKO		**Previous Reports**	
	Males	Females	Males	Females
Rotarod	No change	Faster recovery	Faster recovery [380,667]	Faster recovery [380]
Ethanol-Induced LORR	Reduced duration	No change	Reduced duration [380,667]	Reduced duration[380]
2BC-EOD (15% v/v)	Increased ethanol drinking	Reduced total fluid intake	Increased ethanol drinking and preference. Reduced total fluid intake [378]	Reduced total fluid intake [378]

It is unclear if the results presented here show a milder phenotype than those previously reported[380,667], or if these differences are simply due to experimental variation that is common in behavioral studies between laboratories, facilities, and universities[674,675]. Although all studies were conducted using C57BL/6J mice, the current study utilized mice sourced directly from JAX, whereas Blednov *et al*., 2017[378,380] used mice sourced from JAX that were bred in-house for an unspecified number of generations. It is also possible that the CRISPy TAKO approach is slightly less sensitive than the traditional KO approach for detecting phenotypic changes. The most-likely explanation for such a possibility is that F0 CRISPR mice are often mosaic and it is conceivable that tail DNA genotyping is not reflective of the genetic changes that occur in the brain of the mutant animals. It is possible that some WT *Myd88* is expressed in the brain of some F0 animals, however this is unlikely because RT-PCR analysis from the cerebellum of a subset of *Myd88* TAKO mice did not have WT bands (**Figure 15C**). The approach described here should be very useful for a first pass screening method to identify genes with a large effect on a phenotype of interest. The usefulness of this approach for detecting subtle genotypic differences requires further evaluation.

One limitation of the approach as outlined is the potential for off-target effects of CRISPR mutagenesis. This approach uses multiple gRNAs simultaneously along with a relatively high concentration of Cas9, both of which could lead to off-target effects. Although off-target effects were not examined in this study, they are unlikely to explain the phenotypic changes we observed. The main behavioral phenotypes observed in the *Myd88* CRISPy TAKO mice are the same as those observed in *Myd88* global KOs that were produced using traditional, non-CRISPR gene targeting techniques. Furthermore, several studies have reported that off-target effects in CRISPR/Cas9 animals is minimal with careful selection of gRNAs as done in the present study[549,676,677]. We also used a high fidelity Cas9 variant to minimize the potential for off-target effects. Lastly, an extensive analysis of gene KO mice and nonhuman primates that were produced by CRISPR mutagenesis with multiple gRNAs found no significant off-target effects[673].

In summary, we propose using the CRISPy TAKO approach for rapidly screening large numbers of genes *in vivo* to identify those that have large effects on a phenotype of interest. Once such a gene is identified, an individual animal that harbors a confirmed KO allele should be mated to establish a true breeding mutant KO line. A true breeding line will be useful for future studies to (1) confirm the phenotype of interest, (2) to test for and rule out the potential impact of off-

target mutations, (3) to enable the rigorous testing of control and KO littermates derived from heterozygous mating's, and (4) to provide an unlimited source of uniform animals for further, in-depth analyses and long-term line maintenance.

We conclude that the CRISPy TAKO method can be used for efficient, moderate throughput, *in vivo* screens to identify genes that impact whole animal responses when ablated. This method avoids the extensive animal breeding, time, and resources required with traditional CRISPR animal KO approaches. This method should find widespread use in studies where moderate to large numbers of genes must be rapidly screened for effects that cannot be interrogated *in vitro*, such as whole animal behavioral responses.

3.2 HIPPOCAMPAL ceRNA NETWORKS FROM CHRONIC ETHANOL VAPOR-EXPOSED MALE MICE AND FUNCTIONAL ANALYSIS OF TOP-RANKED lncRNA GENES FOR ETHANOL DRINKING PHENOTYPES

Adapted from: **Plasil SL**, Collins VJ, Baratta AM, Farris SP, and Homanics GE. 2022. Hippocampal ceRNA Networks from Chronic Ethanol Vapor - Exposed Male Mice and Functional Analysis of Top-Ranked lncRNA Genes for Ethanol Drinking Phenotypes. *Advances in Drug and Alcohol Research*. 10. PMID: 36908580.

3.2.1 Introduction

Alcohol use disorder (AUD) is a chronic and debilitating neurological disorder that has extensive global, social, and economic burdens. In the United States AUD is one of the leading risk factors for premature death and disability[678] and has an annual estimated socioeconomic cost of ~$250 billion[679]. Many consequences of chronic alcohol misuse are attributed to alcohols effect on the brain[322,401], and alcohol acts in part by altering neural gene expression[111,396,401,411,499]. Deciphering alcohol's impact on gene expression within discrete brain regions and subsequent downstream effects offers an opportunity to identify novel pharmacological targets that could prevent sustained alcohol-induced alterations from occurring in humans.

The hippocampus is an important ethanol-sensitive brain region involved in the transition of AUD[680-682]. The hippocampus is susceptible to the detrimental impacts of excessive alcohol exposure[683-685], and binge-like ethanol consumption has been shown to significantly impact neuroimmune functions within the hippocampus in mice[686]. Neuroimmune, transcriptional, and epigenetic cell signaling changes are shown to underly loss of hippocampal neurogenesis[343,686-689] and plasticity[343,680,690] following both exposure to ethanol and other drugs of abuse[343,344,687,691]. This supports the concept that hippocampal neuroadaptations are critical targets to understand ethanol withdrawal and consumption.

The ncRNA transcriptome acts as epigenetic regulators controlling cellular homeostasis[418]. Evidence supports important roles for noncoding RNA (ncRNA) in the progression of AUD[396,411,489,692,693]. Functional studies targeting specific RNAs in animal models for AUD have shown that the ethanol-responsive RNA transcriptome is involved in ethanol consumption,

withdrawal, and the progression of addiction. Transcriptome data gathered from both human and animals chronically exposed to ethanol has revealed mass dysregulation of multiple RNA subtypes in the brain[396,411], such as mRNAs and their coded proteins[282,408,409,694-697], miRNAs[397,411,492,618,698-700], circular RNAs (circRNA)[417], and long noncoding RNAs (lncRNAs)[401,473,476,701]. LncRNAs are an abundant and diverse subclass of ncRNAs defined as transcripts exceeding 200 nts that do not encode protein[411,427]. There are over 125,000 different lncRNA transcripts[448-452], with many showing brain-specific expression[702]. LncRNAs are known for their roles in epigenetic regulation[413,415,427,604,702], such as impacting chromatin modifications, RNA processing events, modulation of miRNAs, gene silencing, regulation of neighboring genes, synaptic plasticity[427] and molecular networks by acting and interacting as central hubs[396,445]. Those that have been studied largely function by regulating gene expression through *cis*- and *trans*-mechanisms[615,616]. LncRNA expression can be developmentally regulated, can show tissue- and cell-type specific expression, and can be involved in numerous cellular pathways critical to normal development and physiology[413,415,603-605,607,702]. The dysregulation of lncRNAs has been linked to the pathophysiology of several disease states[396,411,413,427,461,462,464,473,609,617,703,704] including AUD[473,705,706], drug addiction[467,614,703,707], psychiatric disorders[708,709], and stress responses[575,710]. Identifying and directly testing lncRNAs that regulate ethanol consumption and related behaviors is important to fully understand the initiation and progression of AUD. Here, we hypothesize that specific ethanol-responsive lncRNAs are critical hubs of molecular networks that act as determinants of ethanol consumption. Targeting individual ethanol-responsive lncRNAs for genetic modulation that have strong correlations to other ethanol-responsive RNAs may help discern transcriptomic network alterations that can impact ethanol drinking phenotypes.

To shed light on how ncRNAs interact with each other *in vivo*, competing endogenous RNA (ceRNA) networks can be bioinformatically generated from transcriptome data sets[711-716]. LncRNA, circRNA, and miRNA are all known as ncRNA epigenetic regulators, which work in concert to coordinate mRNA expression, protein levels, and homeostasis via such functions as transcription factors, molecular sponges, scaffolds, decoys, and guides (for reviews, see: [411,413,418,427,445,604,703]). These networks provide insight into discrete clusters of RNAs that interact and/or compete with each other to maintain the network's function[711-716]. These correlated RNAs can then be intertwined and linked together computationally to either increase or decrease the rank of hub genes based on their relative interconnectivity with other genes. Generating ethanol-

responsive ceRNA networks from four prominent RNA subtypes, lncRNA, mRNA, miRNA, and circRNA, allowed for novel networks and hub genes to be identified in the present study. A list of top-ranked putative hub ethanol-responsive lncRNAs was generated and genes were prioritized for functional interrogation via CRISPR/Cas9 mutagenesis.

The acquisition of transcriptome data has greatly outpaced our capacity to functionally study genes *in vivo* that are hypothesized to contribute to AUD[717]. To circumvent this bottleneck, we developed an accelerated CRISPR/Cas9 approach to create a cohort of functional knockout (KO) animals in a single generation[379]. Here we applied this CRISPR Turbo Accelerated KO (CRISPy TAKO) methodology to test the hypothesis that mutation of neuroimmune-linked, ethanol-responsive, lncRNAs identified from hippocampal ceRNA network analyses impact ethanol drinking behavior (based on the neuroimmune hypothesis of addiction[352,718]). We tested the top four lncRNAs that were identified as potential hubs for ethanol-responsive networks via ceRNA analysis. We generated four CRISPy TAKO mouse lines targeting the top four lncRNA candidates identified: *Gm42575, 4930413E15Rik, Gm15767,* and *Gm33447,* hereafter referred to as *Pitt1, Pitt2, Pitt3,* and *Pitt4,* respectively. All gene-targeted cohorts were tested for binge-like drinking behavior and intermittent ethanol consumption and preference.

3.2.2 Materials and Methods

3.2.2.1 Animals

All experiments were approved by the Institutional Animal Care and Use Committee of the University of Pittsburgh and conducted in accordance with the National Institutes of Health Guidelines for the Care and Use of Laboratory Animals. C57BL/6J male and female mice used for chronic intermittent ethanol vapor (CIEV) exposure, generation of embryos for electroporation, and purchased control groups were procured from The Jackson Laboratory (Bar Harbor, ME). CD-1 recipient females and vasectomized males were procured from Charles River Laboratories, Inc. (Wilmington, MA). Mice were housed in individually ventilated caging under specific pathogen-free conditions with 12-hour light/dark cycles (lights on at 7 AM) and had *ad libitum* access to food (irradiated 5P76 ProLab IsoProRMH3000; LabDiet, St. Louis, MO) and water.

3.2.2.2 Chronic Intermittent Ethanol Vapor (CIEV) Exposure

Male mice were exposed to a 16-hour CIEV or room-air paradigm as previously reported[719] (n = 5 – 6/treatment). Briefly, mice were given a priming intraperitoneal injection of either 1.5g/kg ethanol (Decon Labs, Inc., #2716GEA) and 68mg/kg pyrazole (Sigma-Aldrich, P56607-5G) or saline and 68mg/kg pyrazole, then immediately subjected to vaporized ethanol or room air (respectively) for 16 hours/day, 4 days/week, for 7 weeks. Hippocampal tissue was harvested 24 hours following the final vapor exposure.

3.2.2.3 Total RNA Isolation and Microarray Profiling

Left hippocampi were homogenized in 1mL TRIzol reagent (Invitrogen, #15596018) and sent to Arraystar Inc. (Rockville, MD) for transcriptome analysis. For circRNA analysis, Arraystar Inc. isolated total RNA, digested with RNase R (Epicentre, Inc.), fluorescently labeled (Arraystar Super RNA Labeling Kit), and subsequently hybridized to Arraystar Mouse circRNA Array V2 (8x15K). For lncRNA and mRNA analysis, Arraystar Inc. isolated ribosomal RNA-depleted RNA (mRNA-ONLY™ Eukaryotic mRNA Isolation Kit, Epicentre) from total RNA. Ribosomal RNA-depleted RNA was amplified, fluorescently labeled (Arraystar Flash RNA Labeling Kit), and hybridized to Agilent Arrays (Mouse LncRNA Array v3.0, 8 x 60K). An Agilent Scanner G2505C was used to scan the arrays. The University of Pittsburgh Genomics Sequencing Core used Applied Biosystems GeneChip miRNA 4.0 Arrays to measure changes in abundance of miRNAs from the total RNA samples isolated from hippocampal tissue. The median intensity expression values were $\log_2$ transformed and quantile normalized across samples. Differential expression were determined using linear models for microarray data (limma)[720] with nominal p-value less than or equal to 0.05 as statistically significant. Weighted gene co-expression network (WGCNA) was used to determine all pairwise correlation among RNAs (*i.e.*, lncRNA, mRNA, miRNA, circRNA) across samples. An unsigned network was constructed using minimum module size of 100, a cut height of 0.99, and a power of 6 to approximate a scale-free topology. The expression of unassigned RNAs were labeled as gray. The total connectivity of individual probes was determined from the pairwise adjacency matrix for an unsigned network.

3.2.2.4 Guide RNA Design

Guide RNAs (gRNAs) were generated using a commercially available two-piece system termed ALT-R™ CRISPR/Cas9 Genome Editing System (IDT DNA, Coralville, IA). This system combines a custom CRISPR RNA (crRNA) for genomic specificity with an invariant trans-activating RNA (tracrRNA) to produce gRNAs[535]. crRNAs were designed using the computational program CCTop/CRISPRator[668,669], which gauges candidate gRNAs for efficiency and specificity. Each crRNA was annealed separately with tracrRNA in a 1:2 molar ratio then combined into a single solution for each gene.

Four gRNAs were used to target each of the ethanol-responsive lncRNA genes *Pitt1*, *Pitt3*, and *Pitt4* and six gRNAs for *Pitt2* (see: **Table 5** for gRNA target sequences). These specifically designed gRNAs bind within a 598, 796, 341, or 372 bp target region that includes the putative promoter and first exon of *Pitt1 – Pitt4*, respectively. We followed the annotations available at the time on the Ensembl Genome Browser (GRCm38/mm10).

Table 5: gRNA target sites, and PCR and RT-PCR primer sequences for Chapter 3.2. All sequences are written in a 5' to 3' orientation. Note: underlined sequence in each gRNA target site is the protospacer adjacent motif.

Name	Sequence
Pitt1 #1 gRNA	CACAACTGGAAGCAAAGACG AGG
Pitt1 #2 gRNA	AGATGAGACTCGAGACATCT GGG
Pitt1 #3 gRNA	GAACTGTAAACCATTAAACT GGG
Pitt1 #4 gRNA	CTTGGAACCAACTCAGTGAG AGG
Pitt2 #1 gRNA	AGTAGGCCATGAGGTCACAG AGG
Pitt2 #2 gRNA	TGTGATAGGCCAGGGTATCA GGG
Pitt2 #3 gRNA	TTGAGAATAGGCTTCCACAG AGG
Pitt2 #4 gRNA	GTCCCTAACAAGAAAAACCA AGG
Pitt2 #5 gRNA	CCCCTCCACAGGGGGCATGG AGG
Pitt2 #6 gRNA	GTAGTCATCATGGAAATATG AGG
Pitt3 #1 gRNA	CTGAGCCAATCACTGTGGCT GGG
Pitt3 #2 gRNA	GATGACAGAGCGATCTTACG AGG
Pitt3 #3 gRNA	TGTGTCCACATCATCGAGTG GGG
Pitt3 #4 gRNA	GCAGTTGGTGATTGCTGTGG AGG
Pitt4 #1 gRNA	GAACTTCAGTGAAACGTGAG AGG
Pitt4 #2 gRNA	GTTGGGTTTTAATTGCGCCA GGG
Pitt4 #3 gRNA	ACTTTATGGACAGTATGGGG TGG
Pitt4 #4 gRNA	GATCAGCACATGTGTCCGTG TGG
Pitt1 F1 PCR primer	AGCCCATGGAATGCTTGACA
Pitt1 R1 PCR primer	TGAGTAATGCTGGCCTT
Pitt1 F2 RT-PCR primer	CTGGCTGCTGGTGAAAGAGA
Pitt1 R2 RT-PCR primer	GGGAAACTCCAAAGCTTCCG
Pitt1 F3 RT-PCR primer	CCAGGTCCTAGATGTTTTGGGG
Pitt1 R3 RT-PCR primer	AGAGCAAAATACCATTAGAATAGCAC

Pitt2 F1 PCR primer	CATGTGACTGGTGAAGGCCT
Pitt2 R1 PCR primer	AATGAGTCCCAGGAAGTGCG
Pitt3 F1 PCR primer	CCATGCACTTCTCAAAGTCAGA
Pitt3 R1 PCR primer	TCAATGAGCTCCCCCTTTCC
Pitt3 F2 RT-PCR primer	AGATCGCTCTGTCATCCCCT
Pitt3 R2 RT-PCR primer	GGCTGCTTTTCTTCATGGCT
Pitt3 F3 RT-PCR primer	TGAAGCTCTCCATGACAGGGA
Pitt3 R3 RT-PCR primer	ATGAGGTACGTGCAATGCCA
Pitt4 F1 PCR primer	AGAGAGGCTGAGACGTGGAT
Pitt4 R1 PCR primer	CAACCCTTCCCTGGCATCTT
Pitt4 F2 RT-PCR primer	TCCGGAAGTAAGGCCTCTCA
Pitt4 R2 RT-PCR primer	TGGCCCAGTGGTTTAAAGCA
Pitt4 F3 RT-PCR primer	GCCTCTCACCTTGTTGGCAA
Pitt4 R3 RT-PCR primer	GAAAGAAACCGGCACCTCCT
Myd88 F1 RT-PCR primer	GGTGGCCAGAGTGGAAAGCAGTGTCCC
Myd88 R1 RT-PCR primer	GAAACAACCACCACCATGCGGCGACA

3.2.2.5 CRISPR/Cas9-Mediated Mutagenesis

Female C57BL/6J mice were superovulated with 0.1mL of CARD HyperOva (CosmoBio, #KYD-010) between 10 AM and 11 AM, followed by 100 IU of human chorionic gonadotropin (Sigma, #CG10) 46 – 48 hours later. Donor females were caged overnight with C57BL/6J males starting 4 – 6 hours post-gonadotropin injection and allowed to mate. Embryos were harvested from oviducts between 9 AM and 10 AM the following morning, cumulus cells were removed using hyaluronidase, and embryos were cultured under 5% CO_2 in KSOM medium (Cytospring, #K0101) for 1 – 2 hours. Embryos were electroporated in 5µL total volume of Opti-MEM medium (ThermoFisher, #31985088) containing 100ng/µL of each gRNA cocktail and 200ng/µL Alt-R® S.p. HiFi Cas9 Nuclease V3 protein (IDT, #1081060) with a Bio-Rad Gene-Pulser Xcell in a 1mm-

gap slide electrode (Protech International, #501P1-10) using square-wave pulses (five repeats of 3msec 25V pulses with 100msec interpulse intervals). Electroporated embryos were placed back into culture under 5% CO_2 in KSOM. For *in vitro* validation of *Pitt1 – Pitt4* gRNAs, embryos were cultured for 3 days until the morulea/blastocyst stage and subsequently analyzed for mutations. For *in vivo* cohort generation, one- or two-cell embryos were surgically implanted into the oviducts of plug-positive CD-1 recipient (20 – 40 embryos per recipient) that had been mated to a vasectomized male the previous night.

3.2.2.6 Genotyping

DNA was amplified from individual *Pitt1 – Pitt4* gRNA-electroporated embryos using a Qiagen Repli-G kit (Qiagen, #150025). DNA was isolated from ear snips of *Pitt1 – Pitt4* TAKO offspring using Quick Extract (Lucigen, #QE09050). DNAs were genotyped by PCR under the following settings: 95°C for 5 minuntes (1x); 95°C for 30 seconds, 60°C for 30 seconds, 72°C for 1 minute (40x); 72°C for 10 minutes (1x). Primers for PCR amplification of *Pitt1 – Pitt4* are listed in **Table 5**. PCR amplicons of *Pitt1 – Pitt4* [Wild-type (WT): 929, 963, 581 and 583 bp, respectively] were analyzed by agarose gel electrophoresis.

3.2.2.7 RNA Precipitation

Hippocampal brain tissue from *Pitt1 – Pitt4* mice was used for RT-PCR analysis. All mice were 16 – 20 weeks of age at time of euthanasia. Total RNA was isolated using TRIzol (Invitrogen, #15596018) according to the manufacturer's protocol, and DNA contamination was removed with a TURBO DNA-*free*™ Kit (Invitrogen, #AM1907). Total RNA was analyzed for purity and concentration using a Nanodrop Spectrophotometer (Thermo Scientific, Waltham, MA). 1µL of purified RNA was converted into cDNA using Superscript™ III First-Strand Synthesis System (Invitrogen, #18080051) with random hexamer primers. RT-PCR primers were used that span both the mutation site as well as the downstream probe-binding exonic region for *Pitt1 – Pitt4* (**Table 5**). A reaction that lacked reverse transcriptase was used as a negative control for each sample tested.

3.2.2.8 Behavioral Testing

All mice were moved into a reverse light-cycle housing/testing room (lights off at 10 AM) at 5 weeks of age and allowed to acclimate for 2 – 3 weeks before the start of experiments. Mice were weighed weekly during behavioral experimentation. Ethanol-drinking experiments were performed in the housing room. Mice were singly-housed for all behavioral studies. Mice were sequentially tested on DID and EOD-2BC, with a minimum of seven days between assays.

Pitt1 and *Pitt2* were studied together with a purchased control group (controlled for age, sex, and strain) previously shown to be comparable to mock-treatment controls[379]. Similarly, *Pitt3* and *Pitt4* were studied together with a separate purchased control group.

3.2.2.9 Drinking in the Dark (DID)

Mice were given access to ethanol (20% v/v) in 15mL drinking bottles with 3.5-inch sipper tubes (Amuza, San Diego) for two hours into the dark-cycle for two days. Fresh ethanol solution was prepared daily. The first day training session lasted for 2 hours. The second day the experimental session lasted 4 hours. The amount of ethanol consumed by each mouse was recorded. Empty cages with sipper bottles only were used to control for sipper tube leakage, and leakage amount was subtracted from amount of ethanol consumed by the mice. Immediately following the experimental session, blood samples were collected from tail nicks and the plasma isolated. An Analox analyzer was used to measure the blood ethanol concentrations (BECs) of each mouse (mg/dL; 5μL).

The *Pitt1*/*Pitt2*/control cohorts were assayed based on genotype and not sex (*i.e.*, the *Pitt1* TAKOs were assayed separately from the *Pitt2* TAKOs). The *Pitt3*/*Pitt4*/control cohorts were assayed based on sex and not genotype (*i.e.*, the male *Pitt3* and *Pitt4* TAKOs were assayed separately from the female *Pitt3* and *Pitt4* TAKOs).

3.2.2.10 Every-Other-Day Two-Bottle Choice (EOD-2BC) Drinking

Mice were given access to ethanol (v/v; ramping every-other-day from 3%, 6%, 9%, 12% until 15% was reached then maintained for a total of 12 days at 15%) and water for 24-hour sessions every other day. If a 20% difference from controls in ethanol consumption was not observed at 15% ethanol, then the concentration was increased to 20% v/v and the experiment

extended an additional 12 days. Water alone was offered on off days. The side placement of the ethanol bottles was switched with each drinking session to avoid side preference. Bottles were weighed before placement and after removal from the experimental cages. Empty cages with sipper bottles only were used to control for fluid leakage, and leakage amount was subtracted from the amount consumed by the mice. The quantity of ethanol consumed, and total fluid intake was calculated as g/kg body weight per 24 hours. Preference was calculated as amount ethanol consumed divided by total fluid consumed per 24 hours. Ethanol drinking results were transformed to reflect the percent change in ethanol consumption compared to control. Ethanol solutions were prepared fresh daily.

3.2.2.11 Preference for Non-Ethanol Tastants

When a significant difference in ethanol consumption was observed between genotypes, mice were subsequently tested for saccharin (sweet tastant; Sigma-Aldrich, 240931) and quinine (bitter tastant; Sigma-Aldrich, 145912) preference using a 24-hour Two-Bottle Choice (2BC) paradigm. One sipper bottle contained the tastant solution and the other contained water. Mice were offered two concentrations of saccharin (0.03% and 0.06%) and quinine (0.03mM and 0.06mM) for two days at each concentration. For each tastant, the lower concentration was presented first followed by the higher concentration. Each concentration was presented for two days (four days total) with at least 7 days of water-only between tastants. Empty cages with sipper bottles only were used to control for leakage, and leakage amount was subtracted from the amount consumed by the mice. Fresh tastant solution was prepared daily.

3.2.2.12 Statistical Analysis

Statistical analysis was performed using GraphPad Prism (GraphPad Software, Inc., La Jolla, CA). Two-way ANOVA with multiple comparisons was used for *Pitt1*, *Pitt2*, and control DID and BEC data, and one-way ANOVA with multiple comparisons was used for *Pitt3*, *Pitt4*, and control DID and BEC data. Two-way mixed-effects ANOVA with multiple comparisons and repeated measures was used for *Pitt1*, *Pitt2*, and control weight over time, and two-way ANOVA with multiple comparisons and repeated measures was used for EOD-2BC data and *Pitt3*, *Pitt4*, and control weight over time. Significant main effects were subsequently analyzed with

Benjamini, Krieger, and Yekutieli two-stage linear step up procedure *post-hoc* analysis[670]. Technical failures were appropriately removed from analysis.

Because of well-known sex differences of C57BL/6J on ethanol consumption in the DID and EOD-2BC assays[528,721-723], male and female mice were tested on separate days (except for *Pitt1*/*Pitt2*/control DID and BEC), and each sex was analyzed separately. Statistical significance was defined as $p \leq 0.05$ and $q \leq 0.05$. All data are presented as mean ± S.E.M.

3.2.3 Results

3.2.3.1 Perturbation of the transcriptome following CIEV Exposure

Hippocampi were dissected from male mice chronically exposed to ethanol vapor (chronic intermittent ethanol vapor; CIEV) or room air control (CTL) for 16 hours/day, 4 days/week, for 7 weeks 24 hours after the final vapor exposure. The first 24 hours of withdrawal from alcohol is a critical window of time associated with relapse, which can be highly detrimental to the long-term goal of reduced drinking[724]. This hippocampal tissue originated from the sires previously described in Rathod RS, Ferguson C, Seth A, Baratta AM, **Plasil SL**, and Homanics GE, 2020[719] wherein males maintained BECs ranging from 100 to 250mg/dL throughout the experiment. Total RNA was isolated from hippocampi for transcriptome analysis to identify biological systems affected by chronic ethanol exposure (**Figure 19**). Our analysis examined statistically significant changes in expression for mRNA, lncRNA, circRNA, and miRNA ($p < 0.05$). Among these four classes of RNAs we found that lncRNAs showed the largest number of changes in expression due to chronic ethanol exposure (n = 1923 up-regulated, n = 2694 down-regulated). This was followed by mRNA (n = 1948 up-regulated, n = 2121 down-regulated), circRNA (n = 750 up-regulated, n = 729 down-regulated), and miRNA (n = 481 up-regulated, n = 723 down-regulated) (**Figure 20**). This data may suggest that lncRNAs within the hippocampus are susceptible to chronic ethanol exposure; however, lncRNAs do not exist in isolation and work in concert with other RNA biotypes for homeostatic function of cellular systems.

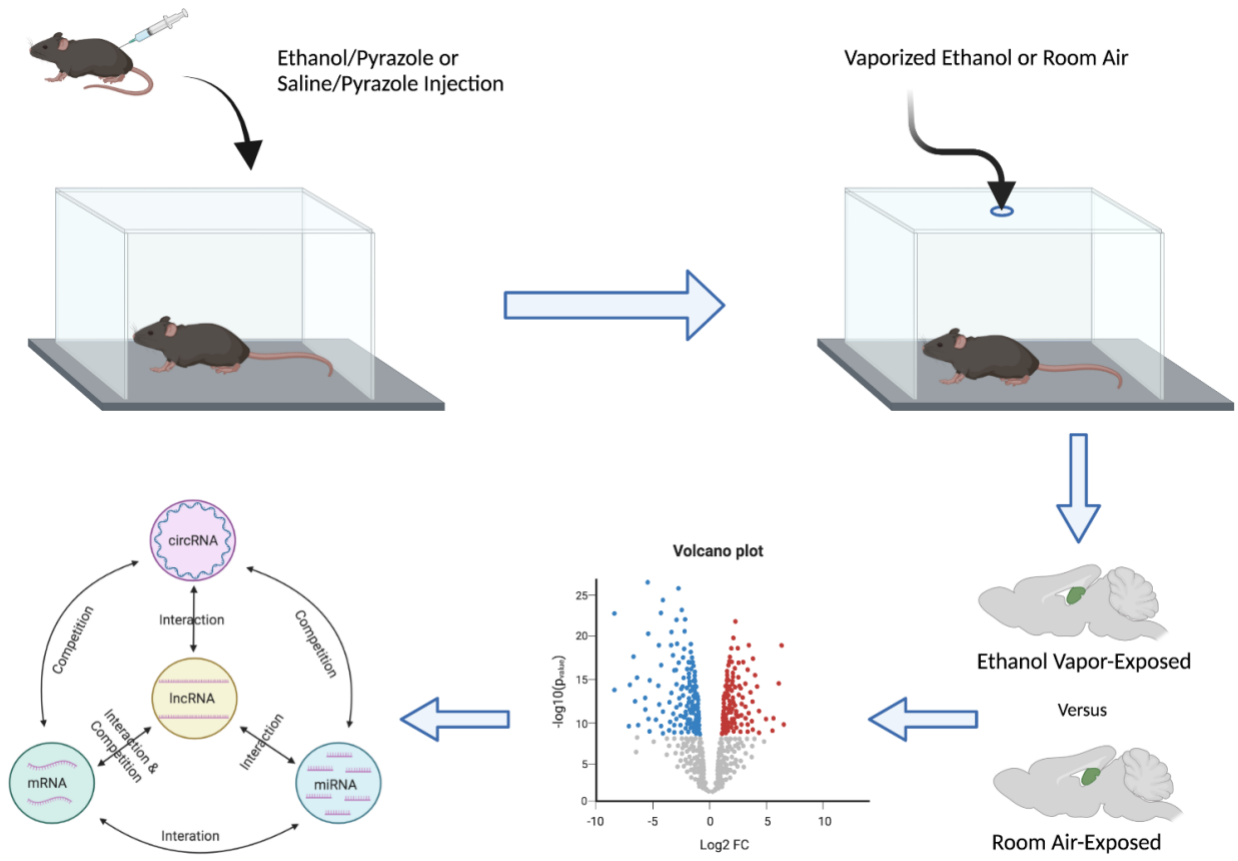

Figure 19: Schematic diagram of the experimental pipeline utilized to generate the list of top novel ethanol-responsive hub lncRNA candidates to target for ethanol-related functional interrogation in Chapter 3.2. Male mice were given a priming injection of either ethanol and pyrazole or saline and pyrazole and placed in either an ethanol- or room-air vapor champers for 16 hours/day, 4 days/week, for 7 weeks, respectively. Hippocampi were dissected 24 hours after the final vapor exposure and then subject to mRNA, lncRNA, circRNA, and miRNA microarray analysis. These data sets were then used to generate ceRNA networks of ethanol-responsive RNA genes.

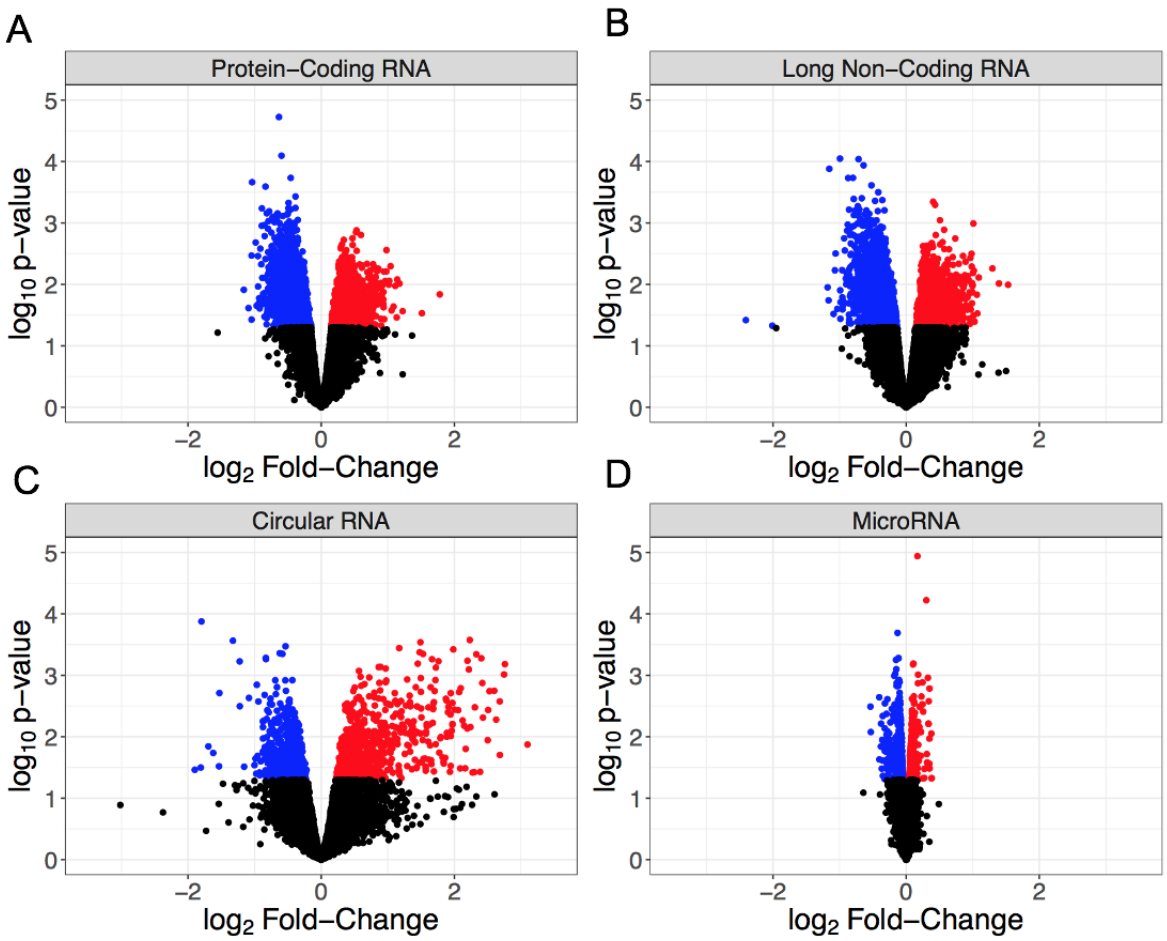

Figure 20: Volcano plots showing differential RNA expression in the hippocampi of male mice exposed to CIEV. Based on log2 fold-change in expression (x-axis) and log10 p-value (y-axis) for (**A**) protein-coding RNA (mRNA), (**B**) long non-coding RNA (lncRNA), (**C**) circular RNA (circRNA), and (**D**) microRNA (miRNA). Each point indicates an individual non-duplicated probe on the microarray with blue = significantly down-regulated, red = significantly up-regulated, and black = non-significant. Significance is defined by $p < 0.05$.

The expression of different RNA subtypes creates tightly coordinated ceRNA networks to mediate the biological function of molecular circuits[711-716] (**Figure 19**). We used weighted gene co-expression network (WGCNA) to determine the pairwise correlation of RNA expression across samples and assess the total connectivity of lncRNA, mRNA, circRNA, and miRNA. Due to the known biological roles in the regulation of gene expression and their perturbation by chronic ethanol exposure, our analysis focused on identifying ethanol-responsive lncRNAs for *in vivo* characterization. Our analysis focused on previously annotated genes that are present in the

GRCm38/mm10 mouse genome assembly but have yet to be biologically characterized. To determine suitable lncRNAs for follow-up *in vivo* KO studies, we used a summed rank of lncRNAs based on their statistical significance ($p < 0.05$), fold-change in up-regulation of expression, overall level of expression to focus on the most abundant lncRNAs, and lncRNAs with the highest total connectivity within the correlation networks to concentrate on hubs of coordinately regulated RNA expression. Of those, genes with the strongest overall correlation to dysregulated neuroimmune genes (genes with a recognized role in the immune system; based on the neuroimmune hypothesis of excessive ethanol consumption[280,350,352,718]) were then selected for functional studies. Additionally, lncRNAs were screened for the capacity to easily create CRISPy TAKO animal models. Based on this selection criteria the top 4 candidate lncRNA selected for testing were *Gm42575*, *4930413E15Rik*, *Gm15767*, and *Gm33447* (**Table 6**).

Table 6: Bioinformatic data of the top-ranked lncRNA genes identified from ceRNA networks for Chapter 3.2. Given name, probe, gene symbol, chromosome, strand, gene start, gene end, log fold-change, mean expression, p-value, and immune gene correlation number are presented.

Name	***Pitt1***	***Pitt2***	***Pitt3***	***Pitt4***
Probe	ASMM10P031898	ASMM10P032341	ASMM10P034032	ASMM10P010493
Gene Symbol	*Gm42575*	*4930413E15Rik*	*Gm15767*	*Gm33447*
Chromosome	chr5	chr5	chr6	chr13
Strand	+	+	-	+
Start	74754373	118961191	147242527	97380367
End	74754432	118961250	147242586	97380426
Log Fold-Change	0.35	0.28	0.27	0.35
Mean Expression	9.71	8.82	9.27	8.25
p-value	0.03	0.02	0.03	0.02
Immune Gene Correlations	384	441	443	400

3.2.3.2 CRISPy TAKOs – *Pitt1* and *Pitt2*

3.2.3.2.1 CRISPR/Cas9-Mediated Mutagenesis

To enhance CRISPR mutagenesis frequency as previously described[379], all lncRNA genes were targeted simultaneously with 4 – 6 gRNAs tiled 50 – 200 bp apart from each other, spanning the putative promoter and first exon of each gene. Four gRNAs were designed to span a 598 bp range within the *Pitt1* gene (**Figure 22A**). Six gRNAs were designed to span a 796 bp range within the *Pitt2* gene (**Figure 22D**).

Pitt1 and *Pitt2* gRNAs were validated for efficient mutagenesis by analyzing *in vitro* cultured embryos following electroporation. Agarose gel electrophoresis of PCR amplicons that span the targeted locus of *Pitt1* and *Pitt2* indicated that 100% of embryos harbored indels of various sizes (**Figure 21A and B**, respectively).

A cohort of 35 *Pitt1* offspring and 42 *Pitt2* offspring, all on the C57BL/6J genetic background, were generated using the CRISPy TAKO approach. All mice born from electroporated embryos were genotyped for gross indels using PCR. The *Pitt1* 929 bp WT PCR amplicon was readily apparent in control WT DNA but only 2 out of 35 *Pitt1* animals (data not shown). The remaining 33 displayed gross indels encompassing the targeted region of interest. PCR bands from a random representative subset of *Pitt1* mice selected for behavioral experimentation is shown in **Figure 22B**. The *Pitt2* 963 bp WT PCR amplicon was readily apparent in the WT control and 2 out of 42 *Pitt2* animals (data not shown). The remaining 40 displayed gross indels encompassing the targeted region of interest. PCR bands from a random representative subset of *Pitt2* mice selected for behavioral experimentation is shown in **Figure 22E**.

The indels varied from animal to animal and most appeared to be deletions, as evidenced by the PCR products being ~50 – 400 bp smaller than the 929 bp WT amplicons for *Pitt1*, and ~50 – 600 bp smaller than the 963 bp WT amplicons for *Pitt2* (**Figure 22B and E**, respectively). Out of the 35 *Pitt1* mice and 42 *Pitt2* mice, only a subset (n = 11M/14F *Pitt1*; 16M/12F *Pitt2*) harboring a large mutation(s) spanning the putative promoter and exon 1 of *Pitt1* or *Pitt2* were selected for behavioral phenotyping. It should be noted that the mice used for phenotyping presented variable deletions mainly ranging in 230 – 730 bp (**Figure 22B and E**, respectively). Despite all *Pitt1* and *Pitt2* mice showing variability in mutation site and size, all mice within a genotype were expected

to manifest the same effect on gene expression and behavioral phenotypes (as previously shown (see: **Chapter 3.1**).

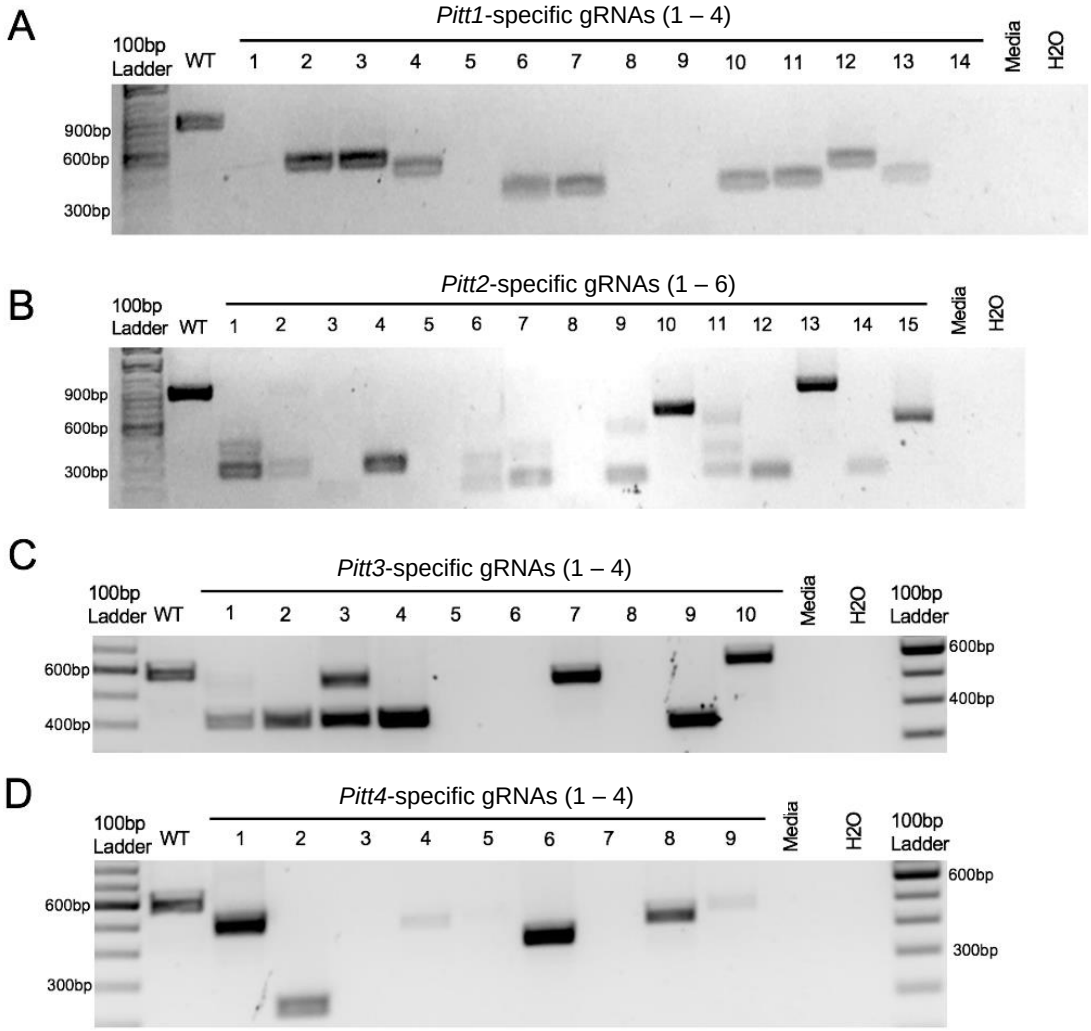

Figure 21: Embryo CRISPy TAKO genotypes for *Pitt1*, *Pitt2*, *Pitt3*, and *Pitt4*. Agarose gel electrophoresis of PCR amplicons of DNA in embryos electroporated with (**A**) *Pitt1*, (**B**) *Pitt2*, (**C**) *Pitt3*, and (**D**) *Pitt4* gRNAs, respectively. Individual embryo numbers are presented above the gel.

We have previously demonstrated that control C57BL/6J mice purchased from Jackson Laboratories are not significantly different from in-house generated Mock-treatment control mice (see: **Chapter 3.1**). Therefore, *Pitt1* and *Pitt2* TAKO mice were compared to age and sex-matched C57BL/6J controls. Mice were weighed once per week during behavioral experimentation. Both TAKO cohorts for both sexes had significantly increased weight compared to controls. Males and

females had an effect of genotype (F (1.715, 7.717) = 87.22; $p < 0.0001$] and [F (1.626, 9.758) = 89.44; $p < 0.0001$], respectively (**Figure 23**). *Post-hoc* analysis revealed an effect of genotype for both *Pitt1* and *Pitt2* males ($q < 0.001$), and *Pitt1* and *Pitt2* females ($q < 0.0001$). These results are consistent with previously observed differences in our laboratory in purchased versus in-house produced offspring (data not shown).

A *Pitt1 – Gm42575*

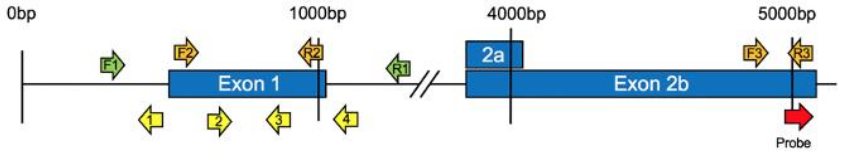

B

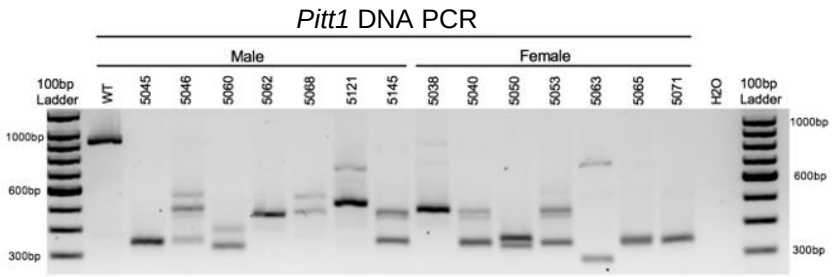

C

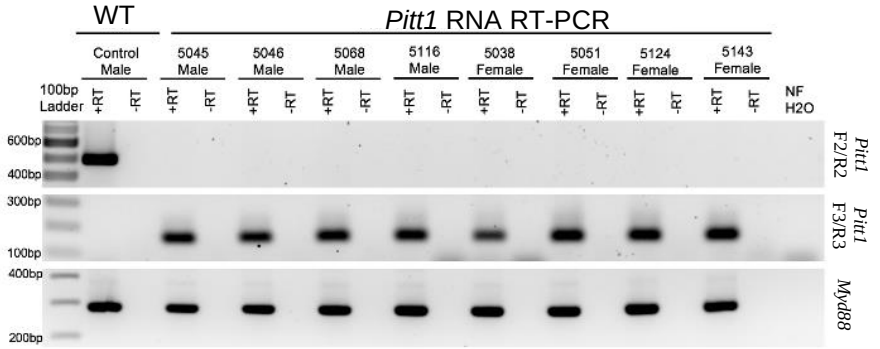

D *Pitt2 – 4930413E15Rik*

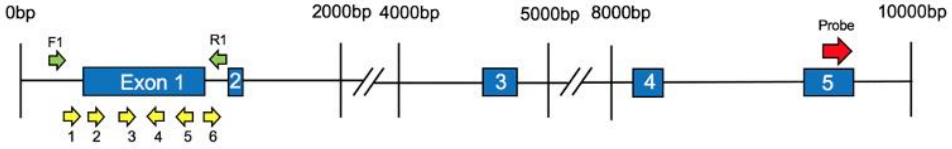

E

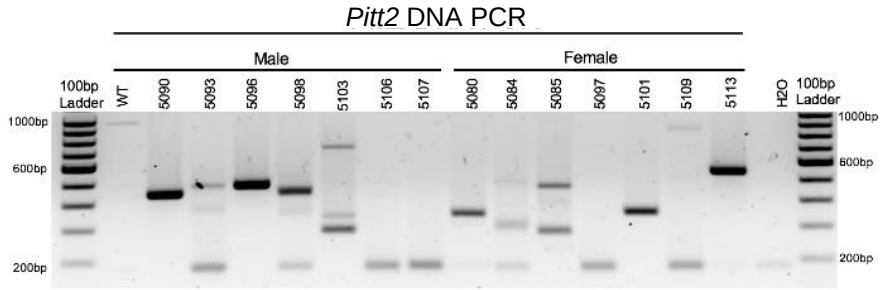

Figure 22: CRISPy TAKO schematics and genotypes for *Pitt1* and *Pitt2*. (**A**) *Pitt1* gene symbol and structure. The gRNAs, PCR primers, RT-PCR primers, and probe binding site are shown as yellow, green, orange, and red arrows, respectively. (**B**) Agarose gel electrophoresis of PCR amplicons of *Pitt1* DNA in a random representative subset of *Pitt1* TAKOs demonstrating abnormal amplicons in TAKO mice compared to WT control. Individual mouse numbers are presented above the gel. (**C**) Random representative subset RT-PCR results from *Pitt1* hippocampal brain tissue showing abnormal RNA transcripts. (Top) RT-PCR of *Pitt1* exon 1 amplicons using the F2/R2 primers demonstrating abnormal RNA transcripts in TAKO mice compared to WT control. (Middle) RT-PCR amplicons using the F3/R3 primers spanning downstream *Pitt1* exons, demonstrating abnormal RNA products in *Pitt1* mutant TAKOs that are not present in WT. (Bottom) RT-PCR of *Myd88* amplicons used as an internal control. (**D**) *Pitt2* gene symbol and structure. The gRNAs, PCR primers, and probe binding site are shown as yellow, green, and red arrows, respectively. (**E**) Agarose gel electrophoresis of PCR amplicons of *Pitt2* DNA in a random representative subset of *Pitt2* TAKOs demonstrating abnormal amplicons in TAKO mice compared to WT control. Individual mouse numbers are presented above the gel.

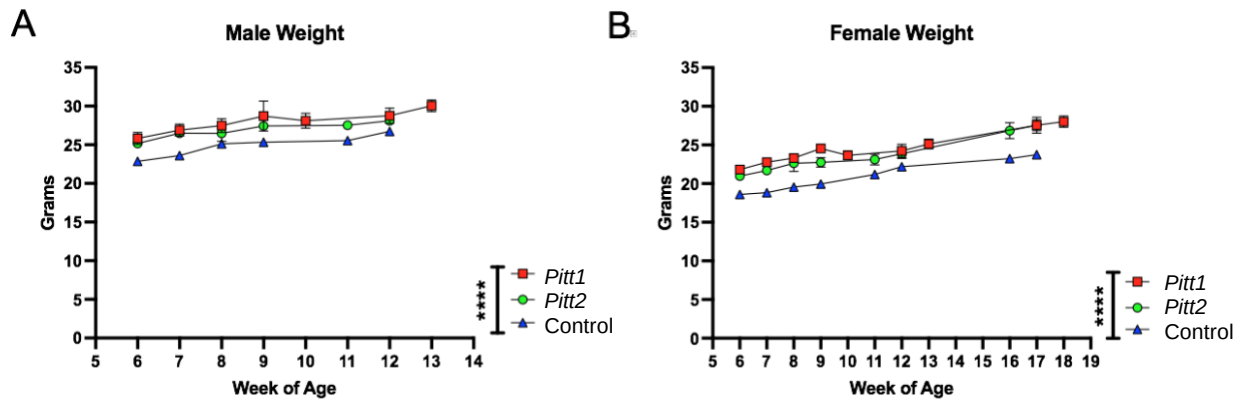

Figure 23: *Pitt1*, *Pitt2*, and control mouse weights over time. (**A**) Males, (**B**) females. N = 11 – 16/sex/genotype. Values represent Mean ± SEM. Data points missing due to no behavioral testing that week (*i.e.*, Males not weighed at 10 – 11 weeks of age, and females not weighed at 13 – 16 weeks of age).

3.2.3.2.2 RNA Analysis

Hippocampal RNA from a subset of mutant mice was analyzed by RT-PCR to validate that the DNA mutations surrounding the putative promoter and first exon of *Pitt1* and *Pitt2* disrupted expression of the targeted genes. Two RT-PCR primer sets were used for each genotype to characterize the RNA transcript in TAKO versus WT hippocampal RNA. F2/R2 RT-PCR primers were used to validate KO of RNA at the mutation site. F3/R3 RT-PCR primers were used to

characterize the downstream exon containing the microarray probe-binding site to investigate expression of downstream lncRNA sequences (**Figure 22A and D**, respectively).

Pitt1 – The top panel of **Figure 22C** demonstrates that the targeted exon 1 region is not transcribed in *Pitt1* TAKOs. The middle panel highlights that the mutation(s) modulate the downstream lncRNA transcript, resulting in expression of a novel transcript that is not observed in the WT control. The bottom panel targeting *Myd88* was used as an internal control.

Pitt2 – Despite extensive efforts to produce reliable RT-PCR amplicons for the *Pitt2* RNA transcript(s), it was not achievable. RT-PCR amplicons for both the mutation site and probe-binding site of the *Pitt2* transcript were inconsistent and variable even in WT control samples (data not shown).

3.2.3.2.3 Drinking in the Dark (DID)

Pitt1 and *Pitt2* DID data were analyzed separately based on genotype (*i.e.*, *Pitt1* males and females were analyzed together with half of the controls, and *Pitt2* males and females were analyzed together with the other half of the controls). No statistically significant difference was observed between *Pitt1* versus control or *Pitt2* versus control for either the 2-hour training day (data not shown) or the 4-hour experimental day (**Figure 24A and B**, respectively). Consistently, there was no significant difference between the BECs of *Pitt1* and control or *Pitt2* and control following the 4-hour experimental day for both males and females (**Figure 24C and D**, respectively). We observed a significant main effect of sex for *Pitt1* DID [$F(1, 39) = 8.300$; $p < 0.01$] where females consumed more ethanol than males. Interestingly, a significant main effect of sex was also observed in *Pitt2* DID [$F(1, 37) = 5.545$; $p < 0.05$], however females unexpectedly consumed less ethanol than the males.

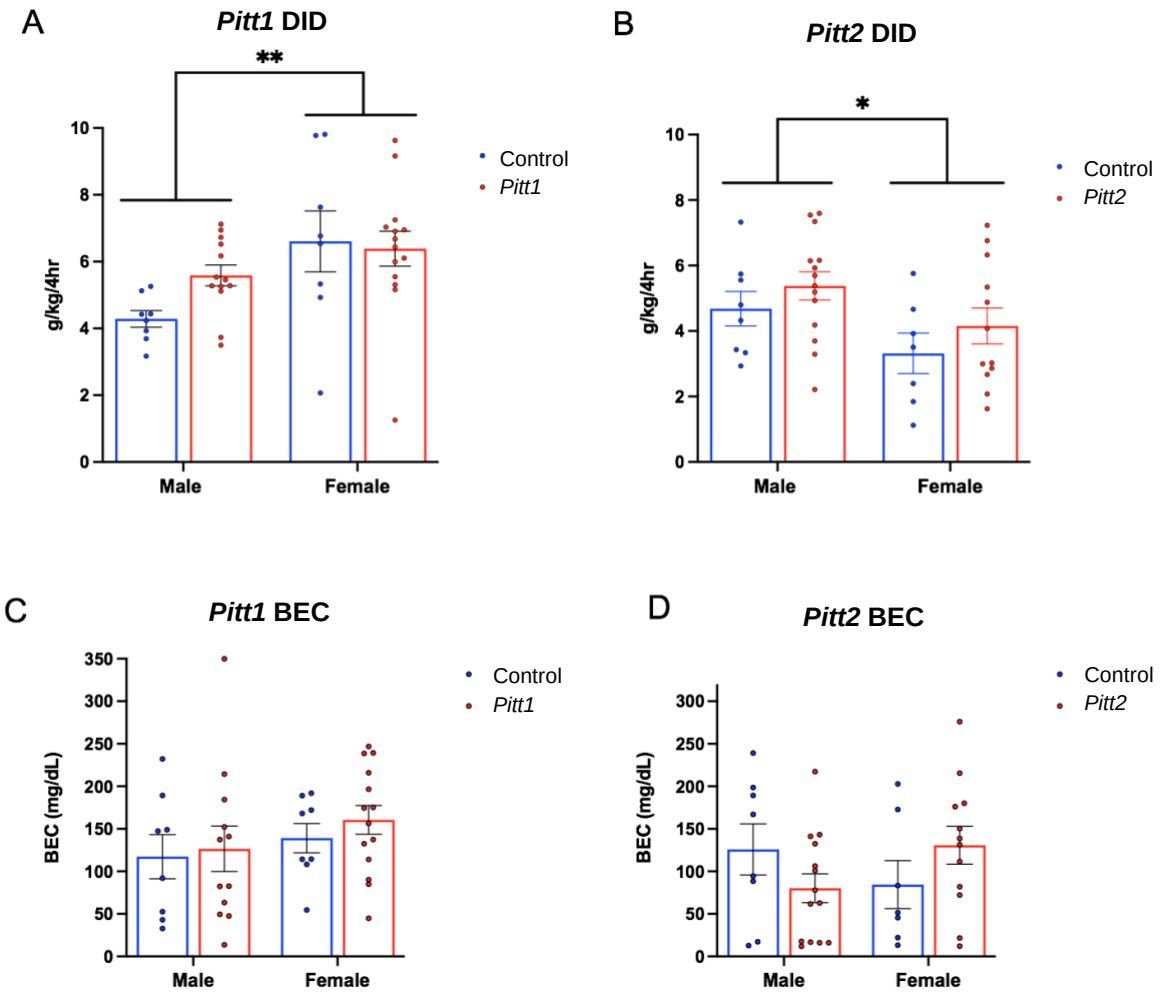

Figure 24: Effect of *Pitt1* and *Pitt2* mutation on the DID assay. (**A**) Total ethanol consumption of *Pitt1* and control mice over a 4-hour experimental period (g/kg/4hr). N = 13 – 14 *Pitt1* TAKOs; n = 8 controls. (**B**) Total ethanol consumption of *Pitt2* and control mice over a 4-hour experimental period (g/kg/4hr). N = 12 – 14 *Pitt2* TAKOs; n = 7 – 8 controls. (**C**) Blood Ethanol Concentrations (mg/dL; 5µL) from plasma collected from all *Pitt1* mice immediately removal of ethanol-filled bottles. N = 12 – 14 *Pitt1* TAKOs; n = 8 controls. (**D**) Blood Ethanol Concentrations (mg/dL; 5µL) from plasma collected from all *Pitt2* mice immediately following removal of ethanol-filled bottles. N = 12 – 14 *Pitt2* TAKOs; n = 7 – 8 controls. Values represent Mean ± SEM.

3.2.3.2.4 Every-Other-Day Two-Bottle Choice (EOD-2BC) Drinking

Pitt1, *Pitt2*, and control mice were tested for ethanol drinking using an EOD-2BC ethanol consumption assay over a period of 20 days. *Pitt1*, *Pitt2* and control male analysis of ethanol intake revealed a main effect of day [$F(5.103, 199.0) = 159.5$; $p < 0.0001$], but no effect of genotype or

day x genotype (**Figure 25A**). Analysis of ethanol preference in males revealed a main effect of day [$F(4.715, 183.9) = 15.83$; $p < 0.0001$] and genotype [$F(2, 39) = 3.755$; $p < 0.05$], but no significant day x genotype interaction (**Figure 25C**). *Post-hoc* analysis revealed that on day 14 *Pitt1* males had significantly higher ethanol preference than control males ($q < 0.05$). *Pitt1* male ethanol preference at 15% v/v ranged from 0% to 9% increase, while *Pitt2* male ethanol preference ranged from an increase of 6% to a decrease of 17% (**Figure 26C**). For total fluid intake, there was a main effect of day [$F(3.508, 136.8) = 4.612$; $p < 0.01$] but no effect of genotype or day x genotype interaction for the males (**Figure 25E**). Due to a record-keeping error, data from day 16, at 15% v/v ethanol, was lost.

Analysis of *Pitt1*, *Pitt2*, and control female cohorts on total ethanol intake revealed a day x genotype interaction [$F(16, 304) = 2.679$; $p < 0.001$] and main effect of day [$F(4.409, 167.5) = 286.3$; $p < 0.0001$], but no effect of genotype (**Figure 25B**). *Post-hoc* analysis revealed that on days 14, 16, and 20 *Pitt1* females consumed significantly less ethanol than control ($q < 0.01$), and *Pitt2* females consumed significantly more ethanol than control on day 4 ($q < 0.05$), and significantly less on day 14 ($q < 0.05$). *Pitt1* females consistently consumed 10 – 20% less ethanol at 15% v/v. *Pitt2* females only consumed up to 10% less ethanol at 15% v/v (**Figure 26B**). Analysis of ethanol preference in females revealed a main effect of day [$F(3.743, 142.2) = 13.60$; $p < 0.0001$], but no effect of genotype or day x genotype (**Figure 25D**). For total fluid intake, there was a day x genotype [$F(16, 304) = 1.938$; $p < 0.01$] and main effect of day [$F(2.272, 86.32) = 31.91$; $p < 0.0001$], but no effect of genotype (**Figure 25F**). *Post-hoc* analysis revealed that on days 14, 18, and 20 *Pitt1* females consumed significantly less total fluid than control females ($q < 0.0001$, $q < 0.05$, and $q < 0.01$, respectively) and that on days 14 and 18 *Pitt2* females consumed less total fluid than control females ($q < 0.0001$ and $q < 0.05$, respectively). The change in ethanol intake coincided with a reduction in total fluid for *Pitt1* females at 15% v/v ethanol ranging from a reduction of 8.5% to 20.5%, and *Pitt2* females ranging from a reduction of 5% to 18% (**Figure 26F**). Due to a record-keeping error, data from day 8, at 12% v/v ethanol, was lost. Since the decrease in female ethanol intake could be linked to a reduction in overall fluid intake, and the male data was not highly compelling, the experiment was terminated following the completion of 15% v/v EOD-2BC.

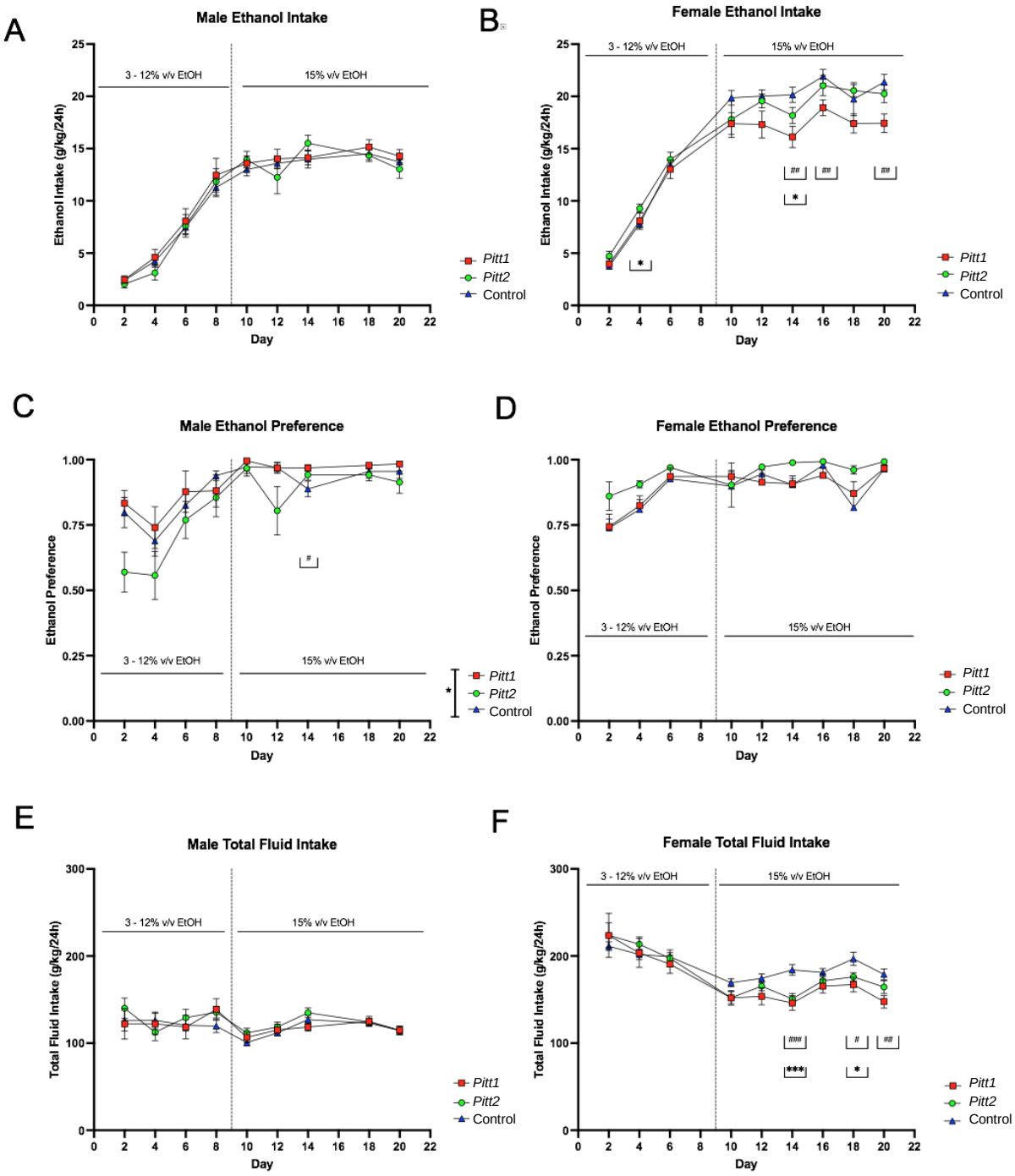

Figure 25: EOD-2BC drinking in *Pitt1*, *Pitt2*, and control mice. Left, males; right, females. (**A and D**) Ethanol intake (g/kg/24 h), (**B and E**) ethanol preference, and (**C and F**) total fluid intake (g/kg/24 h) in *Pitt1* mutant, *Pitt2* mutant, and control mice across time and concentration. N = 11 – 16/sex/genotype. Values represent Mean ± SEM. # or * $q < 0.05$, ## or **$q < 0.01$, and ### or ***$q < 0.001$ between *Pitt1* and control, and *Pitt2* and control, respectively.

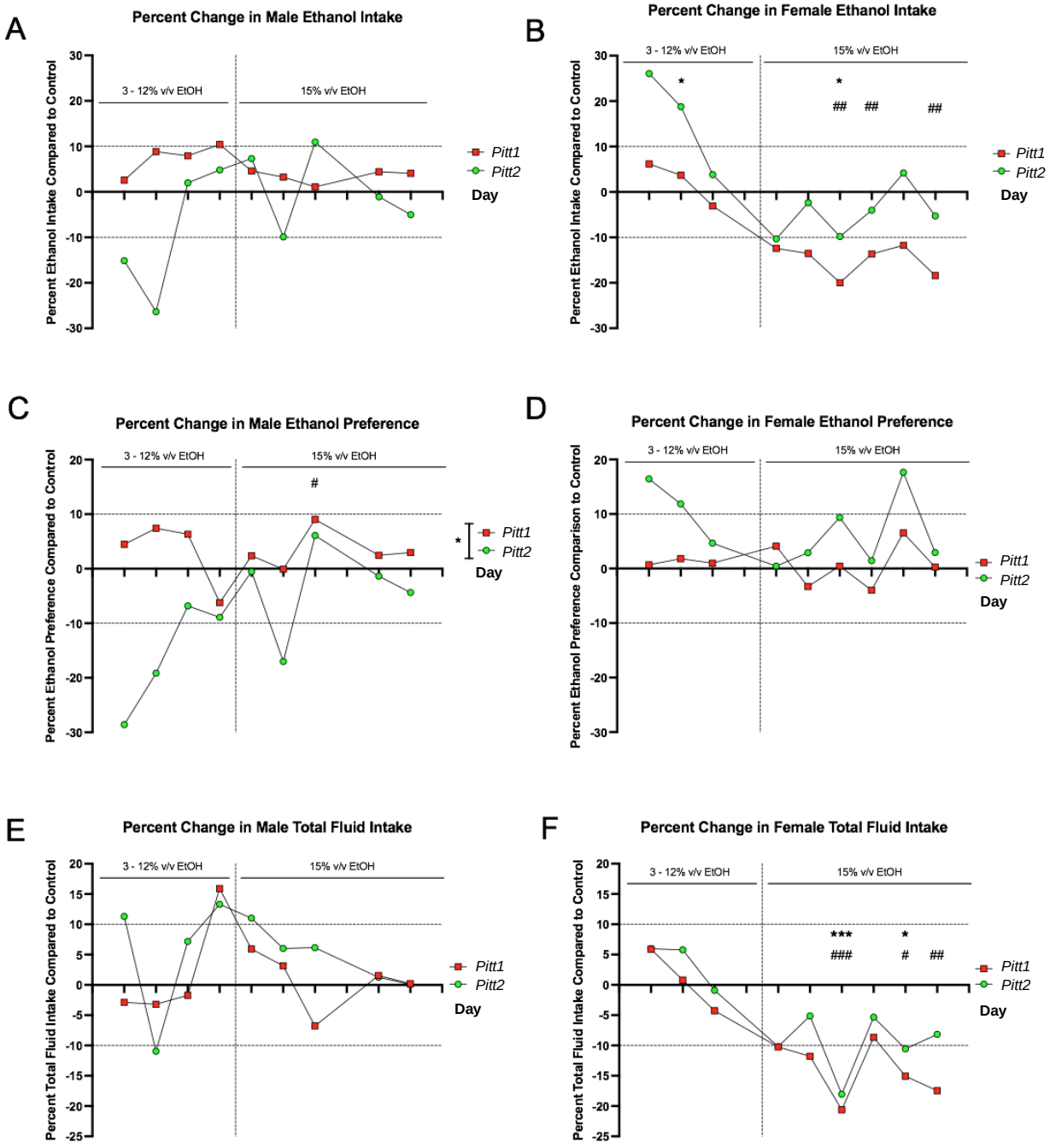

Figure 26: EOD-2BC data from *Pitt1*, *Pitt2*, and control mice transformed to reflect the percent change from control. (**A and D**) Ethanol intake (g/kg/24 h). (**B and E**) Ethanol preference. (**C and F**) Total fluid intake (g/kg/24 h). N = 11 – 16/sex/genotype. Values represent Mean ± SEM. # or * q < 0.05, ## or ** q < 0.01, and ### or *** q < 0.001 between *Pitt1* and control, and *Pitt2* and control, respectively.

3.2.3.2.5 Preference for Non-Ethanol Tastants

Changes in taste perception can alter ethanol consumption in mice[725-727]. Because female *Pitt1* and *Pitt2* displayed altered EOD-2BC ethanol consumption compared to controls, females were subjected to both sweet (*i.e.,* saccharin) and bitter (*i.e.,* quinine) tastants. A 24-hour 2BC assay was used to determine whether an alteration in taste perception could account for the observed changes in ethanol consumption in the mutant lines tested. No significant difference was observed between genotypes for either saccharin (**Figure 27A**) or quinine preference (**Figure 27B**).

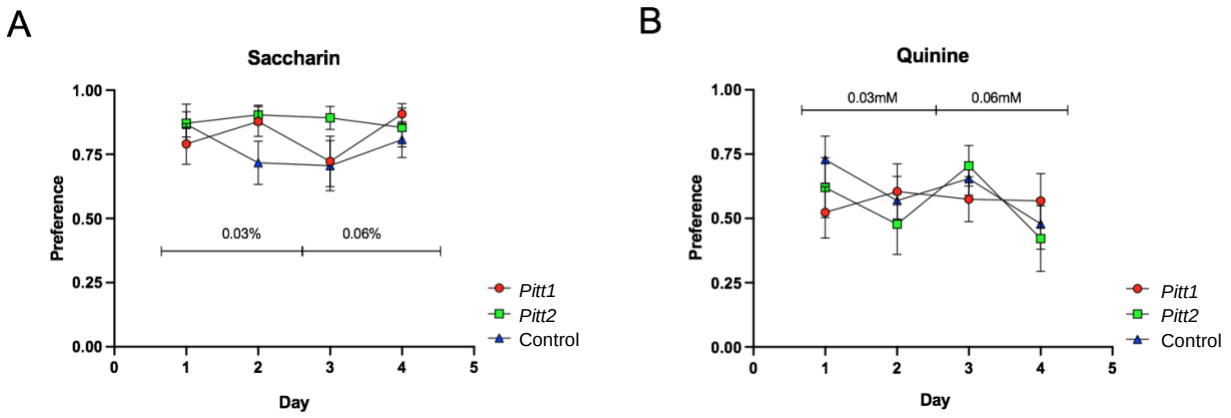

Figure 27: *Pitt1*, *Pitt2*, and control female mouse preference for non-ethanol tastants. (**A**) Saccharin tastant; first two days were presented at 0.03% w/v and the second two day were presented at 0.06% w/v. (**B**) Quinine tastant; the first two days were presented at 0.03mM w/v and the second two days were presented at 0.06mM w/v. N = 11 – 16/sex/genotype. Values represent Mean ± SEM.

3.2.3.3 CRISPy TAKOs – *Pitt3* and *Pitt4*

3.2.3.3.1 CRISPR/Cas9-Mediated Mutagenesis

A second cohort of mice targeting *Pitt3* and *Pitt4* (**Figure 28A and D**, respectively) were subsequently characterized and tested for behavior. Initial validation of gRNAs designed to target *Pitt3* and *Pitt4* occurred *in vitro* using electroporated embryos (**Figure 21C and D**, respectively) and demonstrated that both genes were mutated at a high frequency.

A total of 70 offspring for *Pitt3* and 62 offspring for *Pitt4* were generated on the C57BL/6J background using the CRISPy TAKO approach. All mice born from electroporated embryos were genotyped for gross indels using PCR and agarose gel electrophoresis. The *Pitt3* 581 bp WT PCR amplicon was readily apparent in WT control and 9 out of 70 *Pitt3* animals (data not shown). The remaining 61 mutants displayed gross indels encompassing the targeted region of interest. The indels from a random representative subset of *Pitt3* TAKOs varied from animal to animal and most appeared to be deletions, as evidenced by the PCR products being ~50 – 350 bp smaller than the 581 bp WT amplicons (**Figure 28B**). The *Pitt4* 583 bp WT PCR amplicon was readily apparent in WT control and 4 out of 62 *Pitt4* animals (data not shown). The remaining 58 mutants displayed gross indels encompassing the targeted region of interest. The indels from a random representative subset of *Pitt4* TAKOs demonstrated deletions ranging from ~50 – 350 bp smaller than the 583 bp WT amplicon (**Figure 28E**). Of the *Pitt3* and *Pitt4* mice produced, a subset (n = 15/sex/genotype) harboring large deletions spanning the putative promoter and first exon of *Pitt3* or *Pitt4* were selected for behavioral phenotyping.

A *Pitt3 – Gm15767*

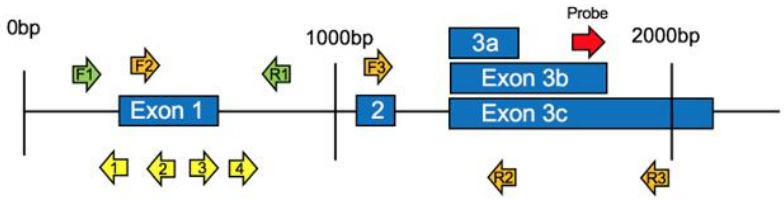

B

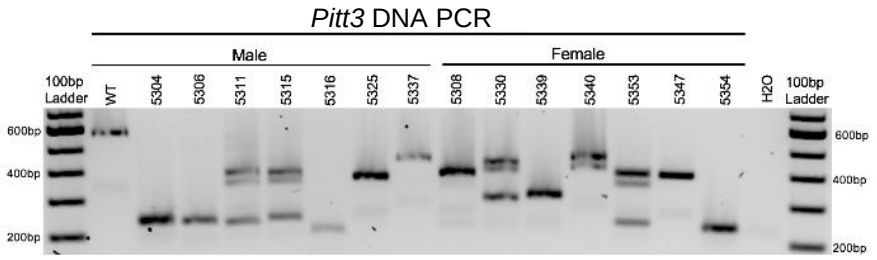

C

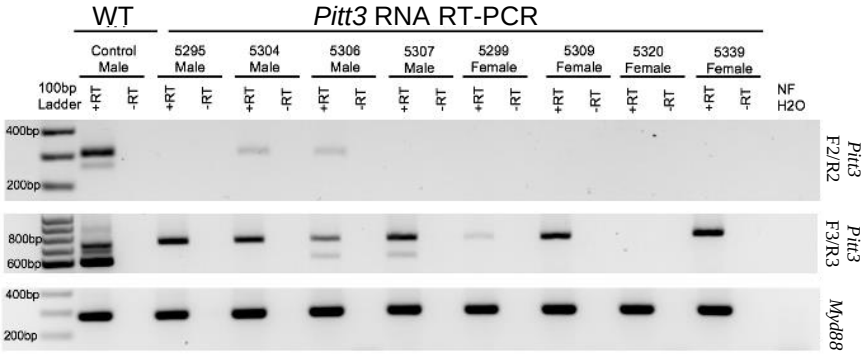

D *Pitt4 – Gm33447*

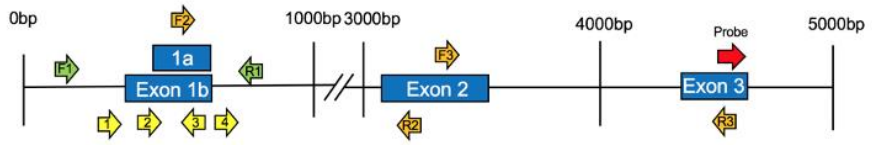

E

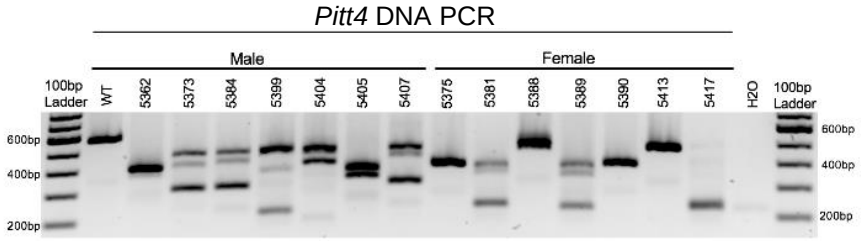

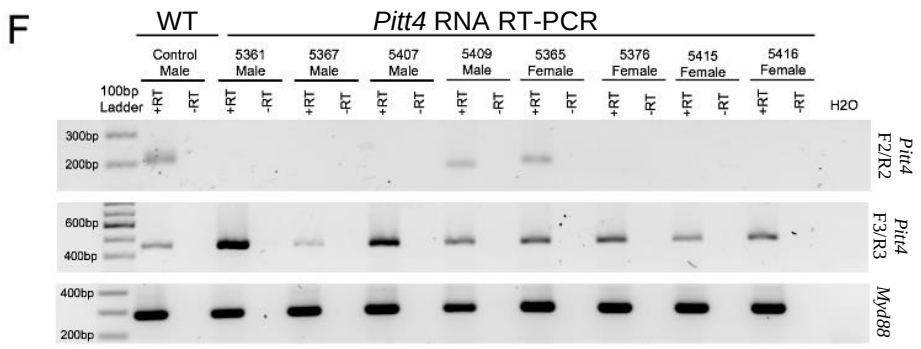

Figure 28: CRISPy TAKO schematics and genotypes for *Pitt3* and *Pitt4*. (**A**) *Pitt3* gene symbol and structure. The gRNAs, PCR primers, RT-PCR primers, and probe binding site are shown as yellow, green, orange, and red arrows, respectively. (**B**) Agarose gel electrophoresis of PCR amplicons of DNA from a random representative subset of *Pitt3* TAKOs. Individual mouse numbers are presented above the gel. (**C**) Random representative subset of RT-PCR results from *Pitt3* hippocampal brain tissue showing abnormal RNA transcripts in TAKO mice compared to WT control. (Top) RT-PCR of *Pitt3* exon 1 using the F2/R2 primers demonstrating the absence of the WT amplicon in most mice, although two animals (5304 and 5306) express a WT sized transcript at an apparently reduced level. (Middle) RT-PCR amplicons using F3/R3 primers spanning downstream *Pitt3* exons demonstrating abnormal RNA products in *Pitt3* mutant TAKOs compared to controls. (Bottom) RT-PCR of *Myd88* used as an internal control. (**D**) *Pitt4* gene symbol and structure. The gRNAs, PCR primers, RT-PCR primers, and probe binding site are shown as yellow, green, orange, and red arrows, respectively. (**E**) Agarose gel electrophoresis of PCR amplicons of DNA from a random representative subset of *Pitt4* TAKOs. Individual mouse numbers are presented above the gel. (**F**) Random representative subset of RT-PCR results from *Pitt4* hippocampal brain tissue showing abnormal RNA transcripts. (Top) RT-PCR of *Pitt4* exon 1 amplicons using the F2/R2 primers demonstrating that the mutations eliminate expression of the WT transcript in 7 of 8 *Pitt4* TAKOs analyzed. (Middle) RT-PCR amplicons of downstream *Pitt4* exons amplified with the F3/R3 primers demonstrating expression of normal sized transcripts in TAKOs compared to WT control. (Bottom) RT-PCR of *Myd88* amplicons used as an internal control.

As noted for *Pitt1* and *Pitt2* cohorts, *Pitt3* and *Pitt4* males and females consistently weighed significantly more than controls (**Figure 29**). Analysis of male *Pitt3*, *Pitt4*, and control weight over time revealed a main effect of day [$F(2.477, 104) = 412.1$; $p < 0.0001$], a main effect of genotype [$F(2, 42) = 19.48$; $p < 0.0001$], and day x genotype [$F(12, 252) = 3.599$; $p < 0.0001$]. *Post-hoc* analysis for both males and females, for all weeks, had a significant increase in weight compared to control ($q < 0.0001$).

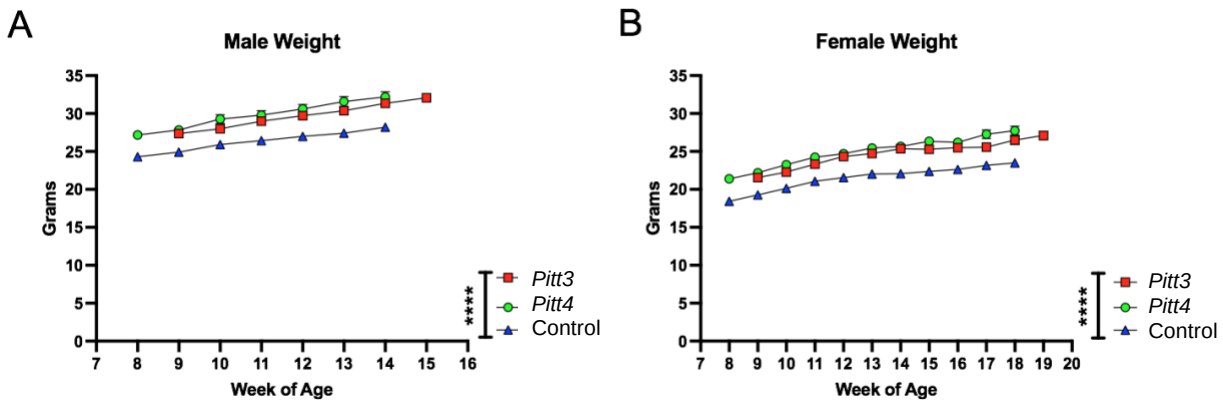

Figure 29: *Pitt3, Pitt4*, and control mouse weights over time. (**A**) Males, (**B**) females. N = 15/sex/genotype. Values represent Mean ± SEM.

3.2.3.3.2 RNA Analysis

Hippocampal RNA was isolated from a subset of mutant mice and analyzed by RT-PCR to validate that the DNA mutations surrounding the putative promoter and first exon of *Pitt3* and *Pitt4* disrupted expression. Two RT-PCR primer sets were used for each genotype to characterize the RNA transcript in TAKO versus control hippocampal RNA. F2/R2 RT-PCR primers were used to examine RNA at the site of mutation, and F3/R3 RT-PCR primers were used to characterize expression of the downstream exon containing the microarray probe-binding site (**Figure 28A and D**, respectively).

Pitt3 – The top panel of **Figure 28C** demonstrates that the exon 1 region in the control sample expressed both the expected 303 bp amplicon as well as an unexpected, slightly larger amplicon. These transcripts were not transcribed in 75% of the *Pitt3* TAKOs tested. Two of eight mice (25%; 5304 and 5306) still expressed the slightly larger RNA transcript from exon 1, but at an apparently reduced level. The middle panel highlights variability in expression between animals. Some TAKO mice (5306 and 5307) expressed two downstream transcripts, some only one transcript (5295, 5304, 5229, 5309, and 5339), and one had no downstream transcripts (5320). This is likely due to variability in deletions of poorly characterized regulatory sequences surrounding the mutation site. The bottom panel targeting *Myd88* was used as an internal control.

Pitt4 – The top panel of **Figure 28F** demonstrates that the targeted exon 1 region was not transcribed in 75% of *Pitt4* TAKOs tested. One sample, 5365, still expressed the control-sized transcript, and one sample, 5409, expressed a slightly smaller RNA transcript. This ~10 – 20 nt smaller RNA transcript likely reflects an internal mutation that was within the boundaries of the RT-PCR primers. The middle panel revealed that all *Pitt4* TAKO mice still produced the downstream *Pitt4* transcript, albeit at variable levels of expression. The bottom panel targeting *Myd88* was used as an internal control.

3.2.3.3.3 Drinking in the Dark (DID)

Mice were tested for binge-like drinking behavior using the DID ethanol consumption paradigm. Cohorts were separated and analyzed based on sex. No significant difference was observed between *Pitt3*, *Pitt4*, and control males (**Figure 30A**) or females (**Figure 30B**) for either the 2-hour training day (data not shown) or the 4-hour experimental day. Consistently, there were also no significant differences between *Pitt3*, *Pitt4*, and control male (**Figure 30C**) or female (**Figure 30D**) BECs following the 4-hour experimental day.

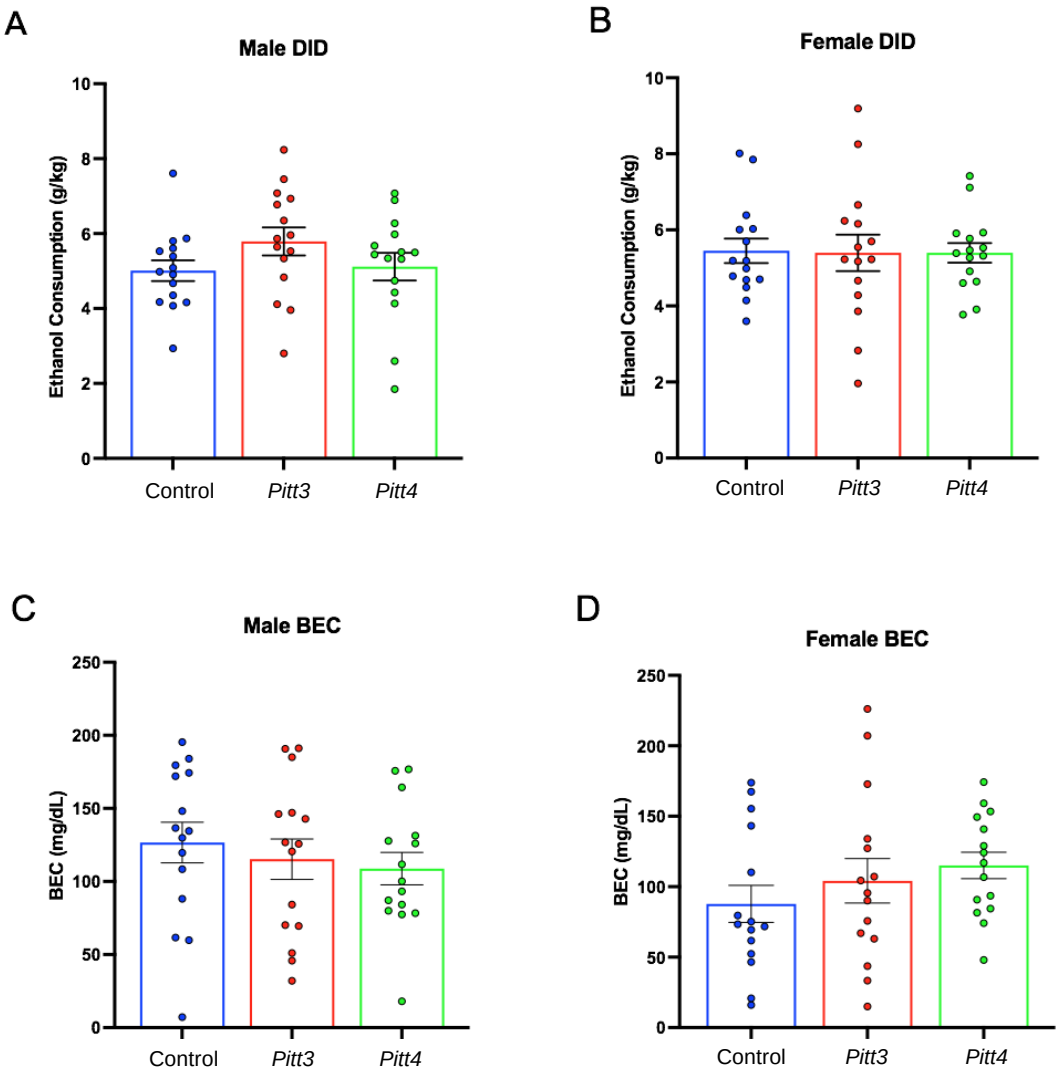

Figure 30: Effect of *Pitt3* and *Pitt4* mutation on the DID assay. Total ethanol consumption of *Pitt3*, *Pitt4*, and control male (**A**) and female (**B**) mice over a 4-hour experimental period (g/kg/4hr). Blood Ethanol Concentrations (mg/dL; 5µL) from plasma collected from all male (**C**) and female (**D**) mice immediately following the removal of ethanol-filled bottles. N = 15/sex/genotype. Values represent Mean ± SEM.

3.2.3.3.4 Every-Other-Day Two-Bottle Choice (EOD-2BC) Drinking

Pitt3, *Pitt4*, and control mice were tested for ethanol drinking using an EOD-2BC ethanol consumption assay. Because this set of TAKO animals did not present a significant difference in total fluid intake following 15% v/v ethanol, the experimental paradigm was expanded to include 20% v/v ethanol. Analysis of male *Pitt3*, *Pitt4*, and control ethanol intake revealed a main effect

of day [F (15, 625) = 335.2; $p < 0.0001$], but no effect of genotype or day x genotype (**Figure 31A**). Analysis of male ethanol preference revealed a main effect of day [F (15, 624) = 39.54; $p < 0.0001$], but no effect of genotype or day x genotype (**Figure 31C**). Consistently, analysis of male total fluid revealed a significant main effect of day [F (15, 624) = 19.39; $p < 0.0001$], but no effect of genotype or day x genotype (**Figure 31E**).

Analysis of ethanol intake in *Pitt3*, *Pitt4*, and control females revealed significant main effects of genotype [F (2, 42) = 3.302; $p < 0.05$], day [F (15, 630) = 248.6; $p < 0.0001$], and a day x genotype [F (30, 630) = 2.201; $p < 0.001$] (**Figure 31B**). *Post-hoc* analysis revealed that on day 22, 26, and 32 (20% v/v ethanol) *Pitt3* females consumed significantly less ethanol than controls ($q < 0.05$). On days 22 – 32 *Pitt4* females consumed significantly less than control females ($q < 0.01$, $q < 0.01$, $q < 0.01$, $q < 0.001$, $q < 0.01$, and $q < 0.01$, respectively). *Pitt3* females at both 15% and 20% v/v ethanol consumed up to 10% less ethanol compared to control. *Pitt4* females consumed up to 12% less at 15% v/v and reached a reduction of up to 18.5% at 20% v/v ethanol. Interestingly, both *Pitt3* and *Pitt4* females consumed ~50% more ethanol at 3% v/v (**Figure 32B**). Analysis of female ethanol preference revealed a significant main effect of day [F (15, 630) = 19.28; $p < 0.0001$] and day x genotype [F (30, 630) = 1.596; $p < 0.05$], but no effect of genotype (**Figure 31D**). *Post-hoc* analysis revealed a significant increase in ethanol preference compared to control on day 2 for both *Pitt3* and *Pitt4* ($q < 0.001$). Both *Pitt3* and *Pitt4* females had a preference ranging from 0 – 10% difference from control at 15% and 20% v/v ethanol, with ~35% increase at 3% v/v (**Figure 32D**). Considering total fluid intake in females, there was a significant main effect of day [F (15, 630) = 43.97; $p < 0.0001$] and day x genotype [F (30, 630) = 1.542; $p < 0.05$], but no effect of genotype (**Figure 31F**). *Post-hoc* analysis revealed that on day 4 *Pitt3* females consumed significantly less total fluid control females ($q < 0.01$) and on day 22 (20% v/v ethanol) both *Pitt3* and *Pitt4* females consumed significantly less total fluid than control females ($q < 0.01$). Both *Pitt3* and *Pitt4* females had reductions in total fluid intake by up to 19% in *Pitt3* and 16% in *Pitt4* females at 20% v/v ethanol (**Figure 32F**).

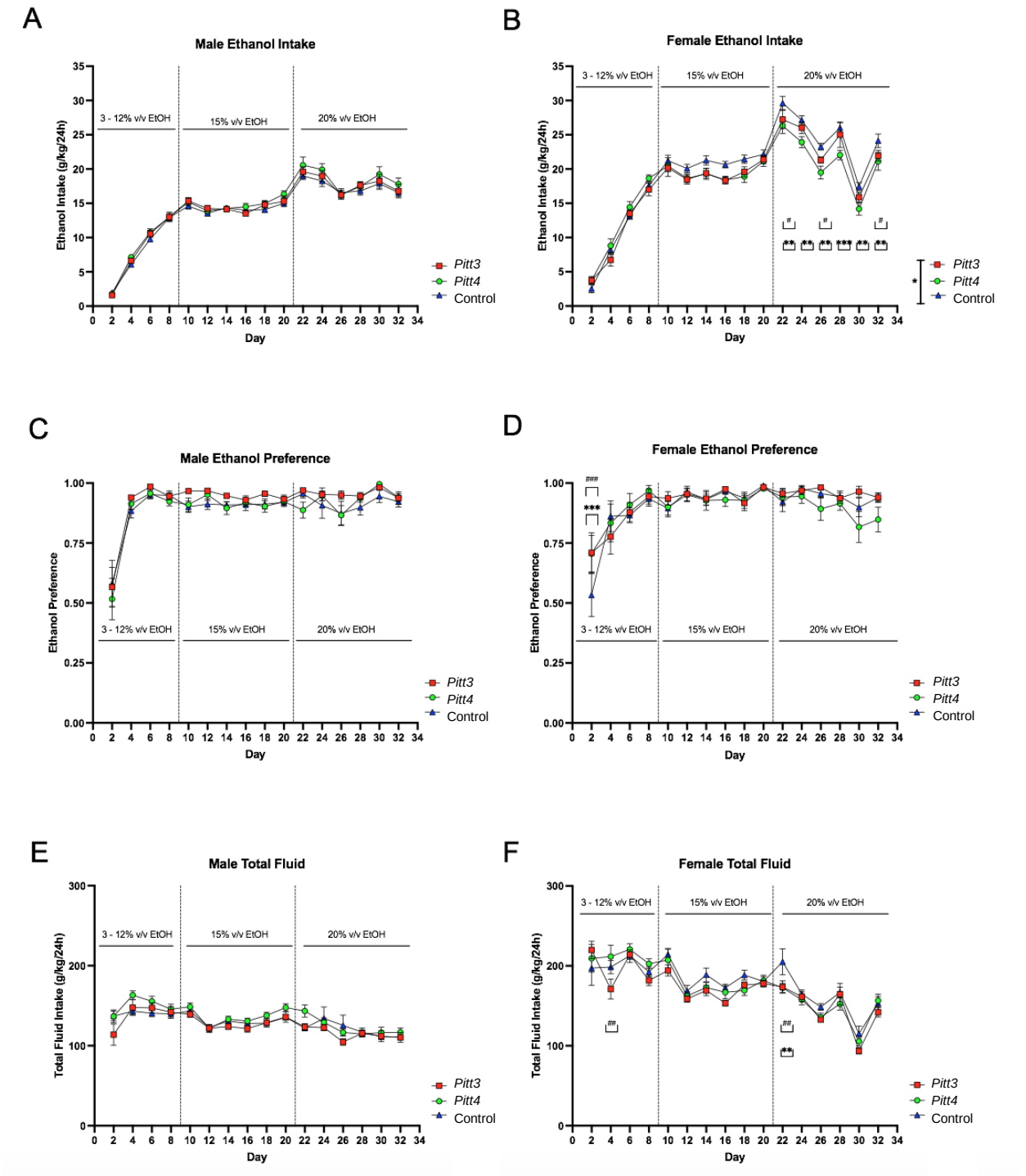

Figure 31: EOD-2BC drinking in *Pitt3, Pitt4,* and control mice. Left, males; right, females. (**A and D**) Ethanol intake (g/kg/24 h), (**B and E**) ethanol preference, and (**C and F**) total fluid intake (g/kg/24 h) in *Pitt3* mutant, *Pitt2* mutant and control mice across time and concentration. N = 15/sex/genotype.Values represent Mean ± SEM. # or * q < 0.05, ## or **q < 0.01, and ### or ***q < 0.001 between *Pitt3* and control, and *Pitt4* and control, respectively).

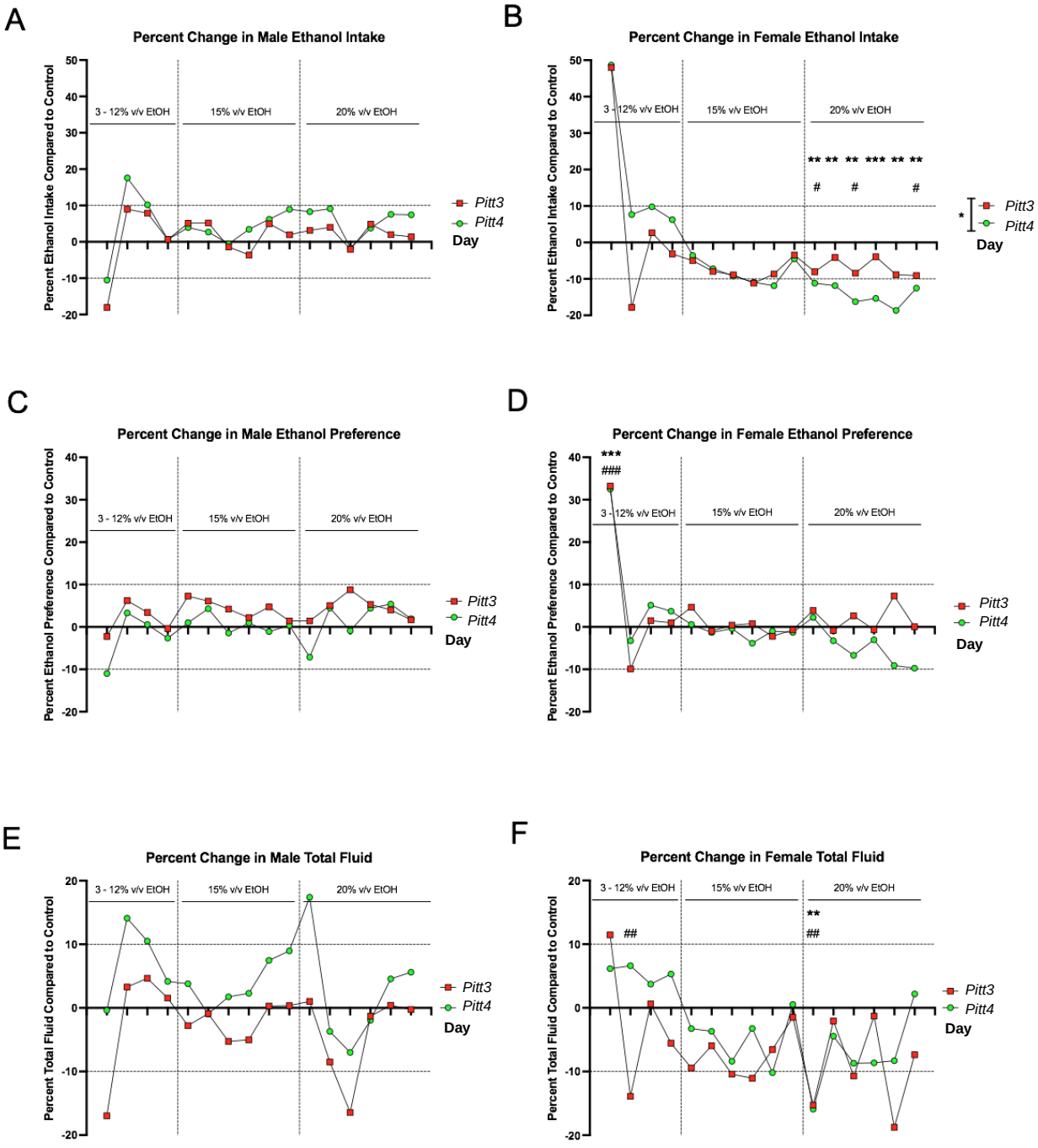

Figure 32: EOD-2BC data from *Pitt3*, *Pitt4*, and control mice transformed to reflect the percent change from control. (**A and D**) Ethanol intake (g/kg/24 h). (**B and E**) Ethanol preference. (**C and F**) Total fluid intake (g/kg/24 h). N = 15/sex/genotype. Values represent Mean ± SEM. # or * q < 0.05, ## or ** q < 0.01, and ### or *** q < 0.001 between *Pitt3* and control, and *Pitt4* and control, respectively.

3.2.3.3.5 Preference for Non-Ethanol Tastants

Since *Pitt3* and *Pitt4* females had altered EOD-2BC ethanol consumption when compared to controls, females were subject to both sweet (*i.e.*, saccharin) and bitter (*i.e.*, quinine) tastant preference analysis. No differences were observed between genotypes for saccharin preference (**Figure 33A**). For quinine preference, there was a significant main effect of day [$F(3, 126) = 3.444$; $p < 0.05$], but no main effect of genotype or day x genotype (**Figure 33B**).

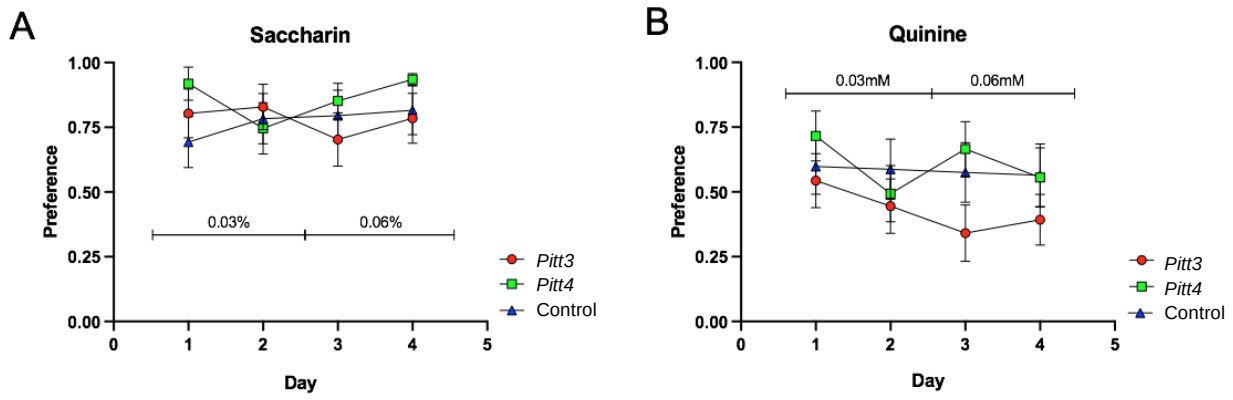

Figure 33: *Pitt3*, *Pitt4*, and control female mouse preference for non-ethanol tastants. 2BC paradigm at two different concentrations. (**A**) Saccharin tastant; first two days were presented at 0.03% w/v and the second two day were presented at 0.06% w/v. (**B**) Quinine tastant; the first two days were presented at 0.03mM w/v and the second two days were presented at 0.06mM w/v. N = 15/sex/genotype. Values represent Mean ± SEM.

3.2.4 Discussion

Identification of phenotypically relevant ethanol-responsive regulatory genes that control brain transcriptional networks offer valuable insight into the chronic effects of ethanol exposure and AUD. Microarray analysis of hippocampal RNA from male mice intermittently exposed to CIEV was used to discern ceRNA expression networks that included four prominent RNA subtypes: lncRNA, mRNA, miRNA, and circRNA (**Figure 19**). The top four ethanol-responsive hub lncRNAs were identified and selected for functional interrogation. These novel lncRNAs, named *Pitt1 – Pitt4*, interact and compete with a myriad of transcripts to modulate specific ceRNA networks. We hypothesized that directly altering the expression of these lncRNAs would change

downstream biological processes and change ethanol-related drinking behavior. Cohorts of *Pitt1* – *Pitt4* gene KO mice were created using the CRISPy TAKO method (see: **Chapter 3.1**) and subsequently screened for changes in ethanol drinking using the DID and EOD-2BC drinking assays. We observed female-specific reductions in ethanol consumption ranging from 10 – 20% in the EOD-2BC paradigm compared to control in three of the tested Pitt mutant lines; *Pitt1*, *Pitt3*, and *Pitt4*. Some of the observed changes were associated with reductions in total fluid consumption but they were not influenced by a change in taste perception. No changes in binge-like drinking in the DID paradigm were observed in either the male or female mutants for any Pitt TAKO genotype (**Table 7**).

The CRISPy TAKO approach was utilized to rapidly generate a cohort of mutant animals in a single generation (see: **Chapter 3.1**). This offers a quick approach to functionally screen novel lncRNAs of interest so the genes can be quickly tested for the ability to alter behavior, saving both time and resources. This is important when screening large numbers of genes with unknown function for ethanol-related behaviors and avoids the bottleneck of standard forward-genetic approaches. Electroporating embryos with 4 – 6 gRNAs targeting a > 1 kb region led to unique mutations from the various combinations of gRNAs in each animal produced. Those harboring desirable large mutations in their DNA were selected for behavioral experimentation, producing a cohort of uniquely mutated mice in one generation, all hypothesized to interfere with gene function.

Table 7: Summary table of *Pitt1* – *Pitt4* male and female behavioral results. Words in red represent unchanged behaviors, words in green represent changed behaviors.

Behavior	**M** *Pitt1*	**M** *Pitt2*	**M** *Pitt3*	**M** *Pitt4*	**F** *Pitt1*	**F** *Pitt2*	**F** *Pitt3*	**F** *Pitt4*
DID and BEC	No	No	No	No	No	No	No	No
Ethanol Intake	No	No	No	No	Yes (-20% - 6%)	Yes (-10% - 26%)	Yes (-18% - 49%)	Yes (-19% - 48%)
Ethanol Preference	Yes (-6% - 9%)	Yes (-28% - 6%)	No	No	No	No	Yes (-10% - 33%)	Yes (-10% - 33%)
Total Fluid	No	No	No	No	Yes (-21% - 6%)	Yes (-18% - 6%)	Yes (-19% - 11%)	Yes (-16% - 6%)

3.2.4.1 RNA Analysis

Hippocampal RNA was analyzed by RT-PCR to confirm that mutation of the putative promoter and first exon of each lncRNA gene disrupted gene expression from each targeted locus. Using primers that bind to the putative first exon (*Pitt1* and *Pitt3*) or exon 1 and exon 2 (*Pitt4*) we established that the CRISPy TAKO mutagenesis approach successfully disrupted gene expression of the targeted loci. Nearly all animals failed to amplify with these primer sets. It should be noted that *Pitt4* 5365 was the only mouse to express transcripts that appeared like WT, but likely at a reduced level of expression (**Figure 28F; top panel**). The other *Pitt4* mouse, 5409, expressed a slightly smaller transcript than WT, suggesting that an internal mutation within the boundaries of the RT-PCR primers may have been retained, or an alternate splice variant was expressed.

Each hippocampal RNA sample was also analyzed with RT-PCR using primers targeting the probe-binding exon used for the initial microarray analyses that identified these lncRNAs, downstream from the mutation site. This was conducted to determine if the full transcript had been knocked out, or if downstream sequences were still transcribed following mutagenesis of the putative promoter and first exonic region. Regions downstream of the *Pitt1*, *Pitt3*, and *Pitt4* mutations were expressed in the majority of animals. Surprisingly, the *Pitt1* downstream amplicon was not detectable in control samples but was consistently expressed in all *Pitt1* TAKO mice (**Figure 22C; middle panel**). These results are likely due to mutation of the putative promoter activating a normally silent promoter, or by altering downstream splicing events. *Pitt3* RT-PCR results revealed variable downstream RNA products; of the eight TAKOs used for RT-PCR, two TAKOs express two downstream transcripts (5306 and 5307), five TAKOs express only a single downstream transcript (5295, 5304, 5229, 5309, and 5339), and one TAKO does not express either downstream transcript (5320). Interestingly, none of the *Pitt3* TAKOs had similar RT-PCR results compared to WT (**Figure 28C; middle panel**). As detailed previously, CRISPy TAKO mutants harbor variable mutations (see: **Chapter 3.1**) and at some loci such as *Pitt3*, this can lead to expression of novel transcripts from the targeted locus. This could be the result of the mutations impacting the 5' splice site(s), or mutating splicer enhancer/repressor binding sites and therefore shifting splicing dynamics[728-732]. Analysis of downstream sequences in *Pitt4* mutants revealed that the downstream cDNA amplicon was readily detected in control and all TAKOs analyzed (**Figure 28F; middle panel**). The most parsimonious explanation for these results is that an alternate promoter is present that is driving this downstream transcript[733-735].

Unexpectedly, following extensive experimentation, the *Pitt2* transcript at the mutation site and probe-binding site were unable to be reliably amplified from either control or *Pitt2* TAKO cDNA. This could have occurred due to *Pitt2* RNA being expressed at very low levels, or the *Pitt2* gene structure could have been inaccurately annotated. These results highlight an important limitation of working with previously unstudied genes including the majority of lncRNAs. Current gene structure annotations may not accurately predict function and unexpected changes in gene expression may be observed when putative regulatory sequences are deleted form the genome.

The RT-PCR data provided a representative look into the potential transcriptome differences between the TAKO mice within a genotype, such as the three different variants of the downstream *Pitt3* amplicon(s). Whereas all *Pitt1* TAKOs tested produced identical amplicons for both the mutation site and downstream probe-binding region, it is possible that the *Pitt3* TAKO mice could be further divided into sub-genotypes based on their retained RNA transcripts and their expression levels. The observed *Pitt3* phenotype could be dampened by the variability of transcripts expressed in each TAKO. Variation in behaviors within a mutant line could be the result of small versus large mutations, novel transcripts being produced, altered expression levels of unmutated transcripts, altered or ablated lncRNA functionality, ethanol-responsive versus ethanol-unresponsive variations, or a combination of such molecular events. However, the spread of data points from all genotypes were similar to control and each other; they were well clustered together, suggesting that independent sub-genotypes did not differ in behavior significantly from each other. To discern these intricacies however, Sanger Sequencing, subcloning, and rigorous molecular testing and statistical analysis of the individual animals would be required.

3.2.4.2 Behavioral Results

Pitt1 – Pitt4 female TAKO mice all demonstrated at least a 10% difference from control in ethanol drinking behavior when tested with the EOD-2BC paradigm (**Table 7**). This includes ~20% decrease in ethanol consumption in *Pitt1* females at 15% v/v ethanol and in *Pitt4* females at 20% v/v ethanol. However, the associated reduction in total fluid intake at their respective concentrations could suggest an alternate reason for the ethanol consumption reduction beyond genotype and sex alone, such as a reduction in all fluid intake irrespective of content. Large changes in ethanol consumption and/or preference were also observed between mutant lines and controls during the initial ethanol ramping stage (**Figures 25 and 31**, respectively). *Pitt2, Pitt3,*

and *Pitt4* female mutants all showed increased ethanol consumption ranging from ~25 – 50% on ramping days with 3% and 6% v/v ethanol (**Figures 26 and 32**, respectively). While these results at lower ethanol concentrations are intriguing, our primary focus was the impact on the higher-level concentrations of 15% and 20% v/v ethanol. All four of the lncRNAs targeted are capable of modulating ethanol drinking behavior, with *Pitt1*, *Pitt3,* and *Pitt4* influencing ethanol consumption in a sex-specific manner.

While differences in ethanol intake were readily apparent throughout the EOD-2BC paradigm in all mutant lines, no differences were observed in DID ethanol consumption or the BECs of the animals immediately following DID (**Table 7**). This could be due to the obvious differences between the short-term binge-like paradigm and the long-term escalation-of-drinking paradigm and suggestive of specific behavioral patterns being altered by mutation of these lncRNAs that only present in one manner of ethanol consumption. The impacted ceRNA networks may function alternatively from control dependent on the paradigm employed, leading to the deviation in drinking behavior over time.

3.2.4.3 Sexual Dimorphism

Our data supports the identification and partial characterization of four novel ethanol-responsive lncRNAs that can alter ethanol drinking behavior, specifically in females. Sexually dimorphic behavioral responses to ethanol have been previously reported in the literature for alcohol[529,694,736-739]. LncRNA genes have shown sex-specific expression in reward pathways, cell signaling, structural plasticity, complex decision making, and behaviors[501-503]. Sexually dimorphic biology is present in many stages of drug addiction, including acute reinforcement, the transition to compulsive drug use, withdrawal-associated states of negative affect, craving, and relapse[521]. Further, there are known differences in neural systems related to addiction and reward behavior such as epigenetic organization, expression, and contingency that are sex-dependent[521]. This suggest that lncRNAs may be important in sexually dimorphic biology and behaviors associated with substance misuse.

The female-specific behavioral changes observed in ethanol drinking were somewhat unexpected as the ethanol-regulated lncRNAs studied were identified from microarray data that originated from a male-only cohort. Male samples were used because of tissue availability (hippocampal tissue originated from the sires described in Rathod *et al.*, 2020[719]). The sex

differences observed are likely either qualitative and/or based on underlying differences in mechanism(s) of action[521]. For example, there may be differences between the sexes in baseline or ethanol-induced expression levels of *Pitt1 – Pitt4* lncRNAs. To investigate possible expression differences, analogous female tissue would need to be collected, analyzed, and compared to the male microarray data. This would shed light on not only potential differences in *Pitt1 – Pitt4* expression between sexes and insight into the observed behavior presented, but also would allow for the identification of sex-independent and additional sex-specific genes.

3.2.4.4 LncRNAs and Conclusions

A handful of literature has already begun to study lncRNAs in relation to the neurobiology of AUD[314,401,473-476]. The biological functions of these novel ethanol-linked lncRNAs have been associated with altered gene networks and RNA co-expression[314], alternative splicing[401], and neural function[475]. The lncRNA *BDNF-antisense* has previously been described as a regulator of epigenetic events in the amygdala of humans with AUD[473]. Additionally, the lncRNA named *long non-coding RNA for alcohol preference* was identified as a hub gene whose mutation increased alcohol consumption and preference in Wister rats compared to controls[476]. While the field is growing, there are still over 125,000 lncRNA transcripts[448-452] that remain uncharacterized for their relevance to AUD and other human disorders but hold the potential to regulate multiple cellular mechanisms and behaviors.

Mutating these novel uncharacterized *Pitt1 – Pitt4* lncRNA genes may impact a number of molecular functions, such as subcellular localization, sequestration, scaffolding, and epigenetic regulation of gene expression[413,415,427,604,702]. Our study was specifically designed to test genes with no known molecular or behavioral functions related to models for AUD. We conducted these studies with the hypothesis that several, if not all, of the top-ranked genes would have the ability to alter ethanol drinking and provide an ideal candidate gene for more in-depth molecular characterization. By removing a large exonic region of these genes, many different mechanisms of action could have been altered that manifest as a change in ethanol drinking behavior. Future studies should delve into further ethanol-related behaviors and the mechanism(s) of action of these ethanol-responsive lncRNAs.

Here, we demonstrated that mutating and screening top-ranked ethanol-responsive hub lncRNA genes from chronic ethanol exposed mouse hippocampus led to altered ethanol drinking

behavior in all of the generated TAKO cohorts. Among the mutant lines tested, *Pitt4* appears to be the ideal target to generate a true breeding line for further studies. This would permit studying additional ethanol-related behaviors as well as an in-depth molecular analysis to discern the potential function(s) and mechanism of action(s) for this novel lncRNA. The data presented here add to the growing body of literature supporting the hypothesis that expression of specific lncRNAs is important for mediating addiction -related behaviors relevant to human health[467,614,703,707].

4.0 AIM 3: VIRAL-MEDIATED *Gas5* mPFC KNOCKDOWN IMPACT ON ETHANOL-DRINKING AND RELATED PHENOTYPES

4.1 INTRODUCTION

Chronic alcohol use strongly impacts the immune system[740-743]. Neuroimmune responses specifically have been suggested as critical targets of alcohol, causing dysregulation of the system[350,686,718,744,745]. Genetic and behavioral evidence suggest a neuroimmune hypothesis of alcohol addiction, positing that heavy alcohol consumption activates neuroimmune signaling and drives misuse[352,718].

Alcohol misuse impacts brain gene expression and regulation[396,411,746,747]; however, it is not well understood how such molecular changes underlie alcohol addiction. Chronic ethanol exposure directly alters gene expression and the molecular pathways that regulate neuroinflammation, which can lead to dysregulation of cellular homeostasis and prolonged impacts on brain function[718]. Transcriptome dysregulation is a suggested biological mechanism in the transition to addiction, and persistent transcriptional changes may contribute to Alcohol Use Disorder (AUD) progression and higher chances of relapse[396].

The noncoding RNA (ncRNA) transcriptome is a diverse class of epigenetic regulatory molecules linked to normal development and physiology[413,415,604,702], as well as to disease states[396,459,461,464,473,617,703,746]. While only ~2% of the human genome encodes protein, ~75-85% of the remaining genome actively transcribes ncRNA[748,749]. Long noncoding RNAs (lncRNAs) are an abundant ncRNA subclass > 200 nts that do not encode protein[411,427]. LncRNA expression is developmentally regulated, can show tissue- and cell-type specific expression, and is involved in numerous cellular pathways critical to normal function, as well as the pathophysiology of disease[411,427,462,470,473,609]. LncRNAs are quickly gaining attention, but the majority are still in the process of being fully characterized for their biological activity and roles in gene regulation[411,427,462].

LncRNA *Growth arrest-specific 5* (*Gas5*) is heavily linked to the pathogenesis of human disease[393,466,471,707,750-753]. *Gas5* has been shown to regulate gene expression, act as both a miRNA sponge[754-756] and ceRNA regulator of immune signaling[471], and is conserved between humans and

mice[757]. *Gas5* was also found consistently differentially expressed in autoimmune and inflammatory disorders[758,759]. Highlighting *Gas5*'s role in addiction, viral-mediated dysregulation of *Gas5* in neurons of the murine nucleus accumbens regulated cocaine-related behavior and transcriptome dysregulation in response to cocaine[707]. *Gas5* was also upregulated in the amygdala of individuals who suffered from AUD[393]. Lastly, RNA-sequencing (RNA-Seq) from the murine medial prefrontal cortex (mPFC) following Chronic Intermittent Ethanol Vapor (CIEV) exposure showed persistent and extended downregulation of *Gas5* expression during withdrawal, indicating a lasting *in vivo* response of *Gas5* to ethanol within the mPFC[752].

Gas5 is a lncRNA that can bind within the neuroimmune-linked glucocorticoid receptor (GR) DNA-binding domain to act as a repressive decoy, inhibiting GR function and regulating GR signaling[394]. Such impacted GR activity includes transcriptional activation of anti-inflammatory, immunosuppressive, and regulatory proteins[383-385]. Studies emphasize the importance of GR signaling in ethanol-drinking and addictive behaviors[386-392], and GR signaling has been strongly linked to AUD[386-391].

Here, I investigate the role of *Gas5* expression on ethanol drinking and ethanol-related behaviors. A CRISPR/Cas9 viral-mediated delivery approach was used to enable brain-region and cell-type specific *Gas5* gene perturbation in adulthood, substantially reducing the possibility of developmental and genetic compensation associated with embryonic gene mutation[760,761]. The mPFC was targeted[752], allowing for brain region-specific study of *Gas5* impact(s) on ethanol drinking behavior. Stereotaxic injection of neuron-targeting AAV1/2 virus[581] expressing two sgRNAs targeting the experimentally-verified *Gas5* promoter in the mPFC of adult, ethanol-naïve Cas9-expressing knockin mice (C57BL/6J background)[581] was used to knockdown (KD) *Gas5* expression. A battery of behavioral experiments was conducted that revealed a female-specific reduction in ethanol preference following mPFC KD of *Gas5*.

4.2 MATERIALS AND METHODS

4.2.1 Animals

All experiments were approved by the Institutional Animal Care and Use Committee of the University of Pittsburgh and conducted in accordance with the National Institutes of Health Guidelines for the Care and Use of Laboratory Animals. Homozygous Rosa26-Cas9-expressing knockin male and female mice (Stock No: 026179; C57BL/6J background; Cas9 KI)[581] were procured from The Jackson Laboratory (Bar Harbor, ME) and bred in-house. Mice were housed under 12-hour reverse light/dark cycles, with lights off at 10 AM and had *ad libitum* access to food (irradiated 5P76 ProLab IsoProRMH3000; LabDiet, St. Louis, MO) and water. Mice were single-housed throughout behavioral experimentation.

4.2.2 Guide RNA Design

Guide RNAs (gRNAs) were generated using a commercially available two-piece system termed ALT-R™ CRISPR/Cas9 Genome Editing System (IDT DNA). This system combines a custom CRISPR RNA (crRNA) for genomic specificity with an invariant trans-activating crRNA (tracrRNA) to produce gRNAs[535]. The experimentally-verified *Gas5* promoter (**Figure 34A and B**) was identified from EPDnewNC mouse (Eukaryotic Promoter Database new Non-Coding)[762,763] and selected as the target gRNA binding region. Bacterial *LacZ* gRNA[581] was used as a control *in vitro*. CRISPOR[764] was used to identify specific gRNA sequences predicted to have high on-target and minimal off-target activity[762,763]. Each crRNA was annealed separately with tracrRNA in a 1:2 molar ratio then combined into a single solution for each gene target.

Table 8: gRNA target sites and PCR primer sequences for Chapter 4. All sequences are written in a 5' to 3' orientation. Note: underlined sequence in the *Gas5* gRNA target site is the protospacer adjacent motif.

Name	Sequence
Gas5 gRNA1	GCGGCTGAGTCGAGTATATA AGG
Gas5 gRNA2	GAATGCCGCACAGCTCCGAA AGG
LacZ gRNA1	TGTTCGCATTATCCGAACCAT
Gas5 PCR Primer F1	CGGAAGGAAATCAGTCACCCTC
Gas5 PCR Primer R1	ACGCATGCTGAGTCGTCTTT
Gas5 RT-qPCR Primer F1	GGATAACAGAGCGAGCGCAAT
Gas5 RT-qPCR Primer R1	CCAGCCAAATGAACAAGCATG
β-Actin RT-qPCR Primer F1	GACCTCTATGCCAACACAGT
β-Actin RT-qPCR Primer R1	AGTACTTGCGCTCAGGAGGA

4.2.3 Primary Astrocyte Culture Isolation

Primary astrocytes were collected from brain of postnatal day (PD) 0 – 3 Cas9 KI mice. Following euthanasia and decapitation, the head was placed in a petri dish containing Hanks Buffered Saline Solution (HBSS; Gibco, #14025092) and 1% penicillin/streptomycin (P/S; Gibco, #15140122). Each brain was removed from the skull and placed in a clean dish of HBSS + 1% P/S. Individual brains were minced with a razor blade then placed into a 15mL conical tubes containing 3mL of 0.25% Trypsin-EDTA (Gibco, #25200056) and dissociated by pipetting up and down repeatedly. Tubes were placed in a 37°C incubator (containing 5% CO_2; Binder Inc. Bohemia, NY) for 15 minutes, inverted multiple times, and placed back in the incubator for 15 minutes. Upon removal from the incubator, 200µL of DNase I [Sigma, #10104159001; 5mg/mL in Dulbecco's Modified Eagle Media (DMEM; Gibco, #11965092)] followed by 3mL of complete media (DMEM + 10% heat inactivated fetal bovine serum (Gibco, #16000044) + 1% P/S) were added to each tube, and a homogenous mixture was ensured by pipetting up and down repeatedly with a 5mL serological pipette. Tubes were centrifuged at 1500 RPM for 5 minutes and the

supernatant discarded. The pellet was resuspended in 3mL of complete media and added to a poly-L-lysine (PLL; MP Biomedicals, #26124-78-7)-coated T75 flask containing 12mL of complete media. Flasks were placed back in the incubator for 14 days, with 15mL of complete media being replaced on the seventh day.

To isolate primary astrocytes from the mixed glial cultures, microglia were detached by shaking flasks on an orbital shaker for 2 hours at 200 RPM within a 37°C incubator. The supernatant was discarded and 10mL of 0.25% Trypsin-EDTA was added to each flask. Once all astrocytes had detached from the bottom of the flask, 10mL of complete media was added, the bottom of the flask rinsed, and the entire mixture added to a 50mL conical tube. The tube was centrifuged at 1500 RPM for 5 minutes, supernatant discarded, and pellet resuspended in 10mL of complete media. Approximately 3 x 10^5 astrocytes were plated into individual wells of a PLL-coated 12-well plate and used for gRNA validation.

4.2.4 *In Vitro* Transfection of *Gas5* Promoter-Targeting gRNAs

Primary astrocytes were transfected in triplicate for each construct tested 48 hours post-cell seeding (**Table 8;** two *Gas5* gRNAs or *LacZ* control gRNA[581]). Lipofectamine™ 2000 Transfection Reagent (Invitrogen, #11668019) was utilized according to manufacturer's instructions. Briefly, 0.8µg total gRNA was transfected per well of a 12-well plate. The plate was returned to a 37°C incubator for 48 hours before either DNA or RNA isolation.

4.2.5 DNA Isolation and Mutation Detection

Culture media was aspirated 48 hours post-transfection. Cells were washed with 1mL 37°C 0.9% phosphate-buffered saline (PBS; Gibco, #10010023), PBS aspirated, then trypsinized with 500µL Trypsin-EDTA for 15 minutes at 37°C. Fresh media was then added to the wells (1mL) and the cells were disassociated to a single-cell suspension by pipetting up and down with a p200 pipette tip. DNA was extracted with 200µL QuickExtract™ DNA Extraction Solution (Lucigen, #QE09050) per well. PCR was conducted on each DNA sample using the *Gas5* F1/F1 primers (**Table 8**) under the following settings: 95°C for 5 minutes (1x); 95°C for 30 seconds, 60°C for 30

seconds, 72°C for 1 minute (40x); 72°C for 10 minutes (1x), then Sanger Sequenced (Genewiz, South Plainfield, NJ). DNA chromatograms of the *Gas5* promoter from *Gas5*-gRNA transfected astrocytes were compared to DNA chromatograms from control *LacZ*-gRNA transfected astrocytes (**Figure 34C**).

4.2.6 RNA Precipitation

In vitro: Culture media was aspirated 48 hours post-transfection, cells were washed with 1mL 37°C PBS, then the cells were lysed with 250µL TRIzol (Invitrogen, #15596018). RNA was isolated using Direct-zol RNA Microprep kit (Zymo, #R2060) according to manufacturer's protocol.

In vivo: mPFC brain tissue microdissections from AAV-injected mice were used for RNA analysis. All mice had been injected a minimum of 3 weeks prior to RNA isolation. The Xite Florescence Flashlight System (Xite-GR; NIGHTSEA) was used to visualize mCherry-fluorescence (*i.e.,* AAV-expressing regions) and carefully dissected. Total RNA was isolated using TRIzol according to the manufacturer's protocol. RNA was subsequently purified with a TURBO DNA-*free*™ Kit (Invitrogen, AM1907).

4.2.7 cDNA Synthesis

Total RNA was analyzed for purity and concentration using a Nanodrop Spectrophotometer (Thermo Scientific). 1µg of purified RNA per sample was converted into cDNA using Superscript™ III First-Strand Synthesis System (Invitrogen, #18080051) with random hexamer primers. RT-PCR primers were used that span downstream Exons for *Gas5*^{753} (**Table 8**) to demonstrate RNA KD. A reaction that lacked reverse transcriptase was used as a negative control for each sample tested.

4.2.8 Reverse Transcription quantitative PCR (RT-qPCR)

Reactions were carried out in technical triplicate for each gene tested. *β-Actin* was used as an internal control for *Gas5*. All primers were optimized for 90% to 110% efficiency at the following conditions: 3 minutes at 95°C (initial denaturation) followed by 40 cycles of 15 seconds at 95°C (denaturation), 30 seconds at 60°C (annealing), and 30 seconds at 72°C (extension), then followed lastly from 55 – 95°C in 0.5°C increments every 30 seconds. Primer sequences for *Gas5* and *β-Actin* are shown in **Table 8**. RT-qPCR primers bind specifically to *Gas5* transcript 3 and span 4 exons (exon 4 to exon 7; **Figure 34A**). *Gas5* transcript 3 and 5 are predicted to be under the control of the EPDnewNC *Gas5* promoter; *Gas5* transcript 1, 2, and 4 have transcription start sites upstream of the EPDnewNC *Gas5* promoter (**Figure 34A and B**). Due to size constraints and shared exons between *Gas5* transcripts 1, 2, 4, and 5, *Gas5* transcript 3 was targeted as the measure for *Gas5* KD. SYBR green fluorescent master mix (Bio-Rad, #1708882) was added to each well and visualized using a Bio-Rad iCycler. Threshold cycle (Ct) values were calculated for each well and triplicate values averaged. The difference between *Gas5* and *β-Actin* (ΔCt) was calculated for each animal and normalized to the average of control *Gas5* expression (ΔΔCt). Fold change over controls was calculated for each animal using the following formula: $2^{-\Delta\Delta Ct}$. *In vitro* n = 3 – 4 biological replicates were used with n = 2 independent transfection experiments, and *in vivo* n = 3 – 8/sex/genotype biological replicates were used.

4.2.9 AAV1/2 DNA Vectors and Production

VectorBuilder (Chicago, IL) was utilized to design custom, ultra-purified AAV vectors and viruses. The AAV vectors used for stereotaxic injection into the mouse mPFC were cloned between the AAV2 serotype genome and packaged into the AAV1 capsid *(i.e.,* AAV1/2; **Figure 35A**). Two AAV vectors were designed, one *Gas5* and one Scrambled control (both contain two independent sgRNA sequences). The experimental AAV vector contains two *Gas5* promoter-targeting gRNAs and is fluorescently tagged with mCherry; *Gas5*-sgRNA1-*Gas5*-sgRNA2-mCherry (AAV-*Gas5*). The sgRNAs were cloned between AAV2 ITRs and were under the control of the ubiquitous U6 promoter for noncoding sgRNA transcription. mCherry was under control of a CMV promoter. The Scrambled control AAV vector was identical, except with scrambled gRNA

sequences that have no predictive binding site within the mouse genome; scrambled-sgRNA1-scrambled-sgRNA2-mCherry (AAV-Scrambled).

4.2.10 Stereotaxic Injection of AAV1/2

Cas9 KI mice (6 – 7-weeks of age) were anesthetized with isoflurane (Covetrus, #11695067772). The head was shaved using an electric razor (Oster Professional) and then immobilized using ear and tooth bars to a Stoelting stereotaxic apparatus. Normal body temperature was maintained throughout surgery by placing the mouse on a heating pad. The head was disinfected with betadine (Fisher Scientific, #19-066452) and ophthalmic ointment (Covetrus, #08897) was placed over the eyes. A 2 – 3cm cut was made on the anterior-posterior (A/P) plane to visualize the skull, the skull was aligned on all planes, and bregma was located. Bilateral holes were drilled into the skull at 1.7mm anterior and 0.3mm lateral to Bregma. Using a 33G cannula (Bilaney Consultants) attached to a Hamilton syringe (Hamilton Company; 1 μL), the needle was injected -2.2mm ventral to Bregma. AAV1/2 (0.05μL; 4.31 x 10^{13} genome copies/mL; 2.155 x 10^{10} genome copies/hemisphere) was injected bilaterally into the prelimbic cortex (PrL) of mPFC at a rate of 0.1μL/minute. The cannula remained in place for 5 minutes before and after injection. Following injection, the incision site was sutured, treated with triple antibiotic ointment (Fisher Scientific, #NC9074123), and the mouse was given a subcutaneous injection of 5mg/kg ketoprofen (Zoetis Inc.). Animals were placed in a pre-warmed cage and monitored until they achieved ambulatory recovery. Mice were administered 5mg/kg ketoprofen 24 hours post-surgery and monitored daily for one-week post-surgery. Mice that lost >20% body weight or were in clear distress were appropriately removed from the final cohort. Three independent cohorts were generated sequentially: male behavioral cohort (n = 11 – 14), female behavioral cohort (n = 13 – 14), and mPFC *Gas5* quantification cohort (n = 12 – 16).

4.2.11 Drinking in the Dark (DID)

Mice were given access to ethanol (20% v/v) two hours into the dark-cycle for two days. The first day was the training session and lasted for 2 hours. The second day was the experimental session and lasted for 4 hours. The amount of ethanol consumed by each mouse was recorded.

Empty cages with sipper bottles only were used to control for leakage, and leakage amount was subtracted from amount consumed by the mice. Following the experimental session, blood samples were collected via tail vein puncture and the plasma isolated. An Analox analyzer (Analox Instruments, United Kingdom) was used to measure the blood ethanol concentrations (BECs) within plasma (5μL) from each mouse.

4.2.12 Every-Other-Day Two-Bottle Choice (EOD-2BC) Drinking

Mice were given access to ethanol and water for 24-hour sessions every-other-day. Ethanol concentration (v/v) ramped from 3%, 6%, 9%, 12% until 15% was reached and maintained 6 days, followed by 20% for 12 days. Water alone was offered on off days. Purchased drinking bottles were 15mL with 3.5-inch sipper tubes (Amuza, San Diego). The side placement of the ethanol bottles was switched with each drinking session to avoid side preference. Ethanol solutions were prepared fresh daily. Bottles were weighed before placement and after removal from the experimental cages. Empty cages with sipper bottles only were used to control for leakage, and leakage amount was subtracted from amount consumed by the mice. The quantity of ethanol consumed, and total fluid intake was calculated as g/kg body weight per 24 hours. Preference was calculated as amount ethanol consumed divided by total fluid consumed per 24 hours. Ethanol solutions were prepared fresh daily.

4.2.13 Preference for Non-Ethanol Tastants

Mice were tested for saccharin (sweet tastant; Sigma-Aldrich, #240931) and quinine (bitter tastant; Sigma-Aldrich, #145912) and preference using a 24-hour Two-Bottle Choice (2BC) paradigm. One sipper bottle contained the tastant solution and the other contained water. Mice were offered two concentrations of saccharin (0.02% and 0.06%) and quinine (0.03mM and 0.09mM). For each tastant, the lower concentration was presented first followed by the higher concentration. Each concentration was presented for two days with at least 7 days of water-only washout between tastants. Empty cages with sipper bottles only were used to control for leakage, and leakage amount was subtracted from amount consumed by the mice. Solutions were prepared fresh daily.

4.2.14 Elevated Plus Maze (EPM)

The EPM paradigm was employed to measure basal anxiety-like behavior. Mice were taken to the testing room 30 minutes before experiment initiation to acclimate to the room and were tested between 12:00 PM and 4:00 PM under ambient room light. Each mouse was placed on the central platform of the maze facing an open arm and allowed to freely explore for 5 minutes while being video recorded. The following measurements were calculated manually for each mouse by two independent and blinded researchers: number of open arm entries, time spent in open arms (seconds), and number of fecal boli. The number of closed arm entries and the total time spent in the closed arms were not included. The subject was considered to be on the central platform or any arm when all four paws were within its perimeter.

4.2.15 Acute Functional Tolerance (AFT)

Within-session tolerance to ethanol was determined using an AFT assay. Mice were trained on an unmoving dowel (Ugo Basile, Gemonio, Province of Varese, Italy) for one minute then given an i.p. injection of 1.75g/kg ethanol (0.02mL/g injection volume) and immediately placed on the dowel again. The time until loss of function (falling off the dowel) and the time until the regaining of function was recorded (remain on the dowel for 30 seconds). Blood samples were taken via tail nick after initial recovery, followed by a second larger i.p. injection of 2.0g/kg ethanol. The time of the second dose and time until the second recovery were recorded. Blood samples were again taken via tail nick after the second recovery. The BECs were measured as detailed above. AFT was defined as BEC2 - BEC1, and the AFT Rate was defined as BEC2 - BEC1/ Recovery Time 2 - Recovery Time 1.

4.2.16 Loss of Righting Response (LORR)

Sensitivity to the sedative/hypnotic effects of ethanol (3.5g/kg; i.p.) was determined using a LORR assay. When mice became ataxic following ethanol injection, they were placed in the supine position in V-shaped plastic troughs until they were able to right themselves three times

within 30 seconds. LORR latency is the time it takes for the mice to become ataxic following the ethanol injection. LORR was defined as the time from being placed in the supine position until they regained their righting response. Normothermia was maintained with a heat lamp.

4.2.17 Ethanol Clearance

The rate of ethanol clearance was measured by determining the BECs in serial blood collections following a sedative/hypnotic dose of ethanol (3.5g/kg; i.p.). Blood was collected via tail vein puncture at 30, 60, 120, 180, and 240-minutes post-injection. BECs were measured as detailed above. Normothermia was maintained with a heat lamp.

4.2.18 Histological Analysis

Following behavioral experimentation, mice were anesthetized by i.p. injection of ketamine (Covetrus, #010177; 100 mg/kg) and xylazine (Covetrus, #033197; 100 mg/kg). Once anesthetized, the mice were immobilized and transcardially perfused with PBS followed by 4% paraformaldehyde (PFA; Sigma-Aldrich, #158127). Brains were harvested and post-fixed in 4% PFA for 18 – 24 hours at 4°C. After post-fixation brains were equilibrated in 30% sucrose (Fisher Scientific, #BP220212) for 2 days at 4°C. Brains were then cut into 40μm thick coronal sections on a cryostat (Leica Biosystems, Germany) and mounted on plus-coated slides (Fisher Scientific, #12-550-15). For each mouse used for behavioral experimentation, 20 – 30 40μm sections were analyzed. Sections were analyzed for injection site location using an epifluorescent microscope (Nikon Eclipse Ni). Fluorescent imaging was taken at 4x/0.20 using the Nikon DS-Qi2 camera (Nikon, Japan). Mice with improperly placed injections (*e.g.*, too posterior, angled cannula; **Figure 35D, bottom**) were removed from all behavioral data. A proper injection was defined as +1.7mm A/P ± 0.2mm to Bregma.

4.2.19 Statistical Analysis

Statistical analysis was performed using GraphPad Prism (GraphPad Software, Inc., La Jolla, CA). Unpaired t-tests were used for DID, BEC, EPM, AFT, and LORR. If a significant difference in variance was found, then the Mann-Whitney test was applied. Two-way ANOVA with multiple comparisons and repeated measures was used for EOD-2BC, non-ethanol tastants, and ethanol clearance assays. Significant main effects were subsequently analyzed with Benjamini, Krieger, and Yekutieli two-stage linear step up procedure *post-hoc* analysis[670]. Technical failures and outliers were appropriately removed from analysis (Grubbs outlier test[765]). Male and female behavioral cohorts were generated sequentially, so each sex was analyzed separately. Statistical significance was defined as $p \leq 0.05$ and $q \leq 0.05$. All data are presented as mean ± S.E.M.

4.3 RESULTS

4.3.1 *In Vitro* RNA Analysis

Genome database analysis for the *Gas5* gene displays five different transcript products that can be expressed from the *Gas5* gene (GRCm38/mm10; **Figure 34A**). *Gas5* exon 1a, 1b, 1c, 1d, and 1e are shown as blue boxes (**Figure 34B**). Two gRNAs (**Figure 34B**; yellow arrows) were designed to bind within the experimentally-validated *Gas5* promoter (**Figure 34B**; green boxes), identified from the Eukaryotic Promoter Database New NonCoding (EPDnewNC)[762,763]. Successful mutagenesis of the promoter was verified *in vitro* in Cas9-expressing primary astrocytes [astrocytes and neurons have similar levels of Gas5 expression (data not shown)], where DNA chromatograms of the *Gas5* promoter revealed clear signs DNA mutation following *Gas5* gRNA transfection, but not control *LacZ* gRNA transfection (**Figure 34C**). The two gRNAs (**Figure 34C**; green boxes) were tiled along a 51 bp region encompassing the 62 bp *Gas5* promoter region (**Figure 34C**; shaded in gray). *Gas5* RNA expression following gRNA transfection was quantified via RT-qPCR and compared to control. A statistically significant (~50%) *Gas5* KD was observed *in vitro* ($p < 0.001$; **Figure 34D**).

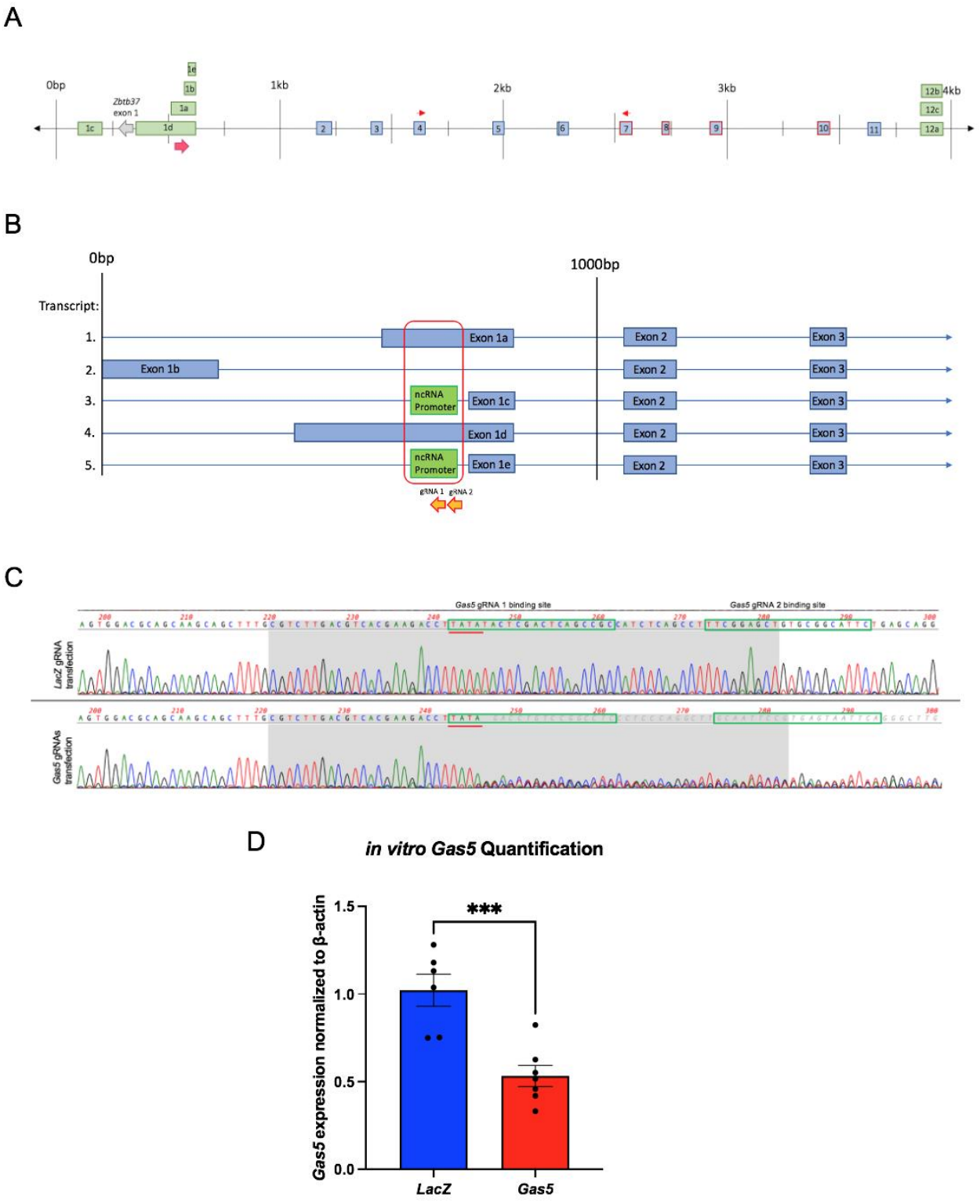

Figure 34: *In vitro Gas5* gene targeting. (**A**) *Gas5* genomic annotation showing *Zbtb37* location and EPDnewNC promoter location (pink arrow) and RT-qPCR primer binding sites (red arrows). Exons specific to transcript 3 are boxed in red (GRCm38/mm10). (**B**) Schematic of the first ~1.5kb of the *Gas5* gene, showing 5 different transcripts.

Gas5 exons are shown in blue and the promoter is shown in green. A red box shows the ncRNA promoter locus with respect to each transcript. The promoter applies to *Gas5* transcripts 3 and 5. The two *Gas5* gRNAs are shown as yellow arrows. (**C**) DNA chromatogram of the *Gas5* promoter region from *Gas5*-gRNA and *LacZ*-gRNA transfected Cas9-expressing cells. The *Gas5* promoter is shaded in grey. The two *Gas5*-gRNA-binding sites are shown in green boxes. A TATA box within the *Gas5* promoter and first *Gas5*-gRNA-binding site is underlined in red. The control *LacZ* gRNA transfected sample shows no sign of mutation at the *Gas5* promoter, as the control chromatogram shows single peaks for each nucleotide. Note the *Gas5* gRNA transfection sample shows clear signs of mutation beginning immediately downstream of the TATA box. (**D**) *Gas5* lncRNA quantification in *in vitro* transfected cells, showing *Gas5* gRNA-transfected cells express ~50% less *Gas5* lncRNA when compared to control. Values represent Mean ± SEM. Results encompass 2 independent experiments, with 3 – 4 biological replicates per experiment. *** $p < 0.001$.

It should be noted that prior to the use of the above method targeting two of the five *Gas5* transcripts via the EPDnewNC-verified promoter, an alternate approach was tested in an attempt to KD all *Gas5* transcript variants (data not shown). CRISPR inhibition (CRISPRi) was originally tested, using 6 gRNAs targeting a 38 – 155 bp region downstream of the putative bidirectional promoter (**Figure 34A,** Zbtb37_1; **Table 9**). The bidirectional promoter was hypothesized to promote expression of both *Gas5* as well as neighboring antisense gene *Zinc finger and BTB domain containing 37* (*Zbtb37)*[766]. The two antisense genes share overlapping complementary genomic regions, and the bidirectional promoter is within 250 bp of *Gas5* and *Zbtb37* transcription start sites (**Figure 34A**). A dCas9 plasmid was utilized and transfected into primary astrocytes along with 6 gRNAs (Addgene: #112233; **Table 9**). The intent was not to repress the promoter but to cause a repressive blockage downstream of the promoter to inhibit RNA Polymerase extension of *Gas5* transcription without altering *Zbtb37* transcription[767,768]. Unfortunately, this technique was deemed ineffective and the method was modified to CRISPR/Cas9 by using Cas9 KI animals and targeting the experimentally-verified *Gas5* promoter. By targeting the EPDnewNC *Gas5* promoter and not the upstream bidirectional promoter, it was hypothesized that only two of five *Gas5* transcripts would be targeted instead of all five, and the potential for impacting *Zbtb37* expression would be greatly minimized.

Table 9: gRNA target sites for *in vitro* CRISPRi in Chapter 4. All sequences are written in a 5' to 3' orientation. These gRNA target sites were deemed ineffective and were not used *in vivo*. Note: underlined sequence in the *Gas5* gRNA target site is the protospacer adjacent motif.

Name	Sequence
Gas5 gRNA1 CRISPRi	GGAGTTGCCGCGGGCACGAT AGG
Gas5 gRNA2 CRISPRi	CCTGCAAGGAAAGCGCTGG GGG
Gas5 gRNA3 CRISPRi	GGGCGGGCCTATCGTGCCCG CGG
Gas5 gRNA4 CRISPRi	TCTCGGGGGCGTGGCCAGA GGG
Gas5 gRNA5 CRISPRi	GTACTCCTCAGGGAGGCGG AGG
Gas5 gRNA6 CRISPRi	GTACTCCTCAGGGAGGCGG AGG

4.3.2 *In Vivo* RNA Analysis

A cohort of Cas9-KI mice were injected with AAV1/2 virus expressing either AAV-*Gas5* or AAV-Scrambled bilaterally into the mPFC. Mice recovered for 3 weeks to allow for maximal viral expression[581], then brains were harvested, mCherry-fluorescing mPFC was dissected, and *Gas5* expression levels were quantified (**Figure 35C**). A statistically significant (~40%) *Gas5* KD was observed in AAV-*Gas5* versus AAV-Scrambled injected samples ($p < 0.001$; **Figure 35E**).

A

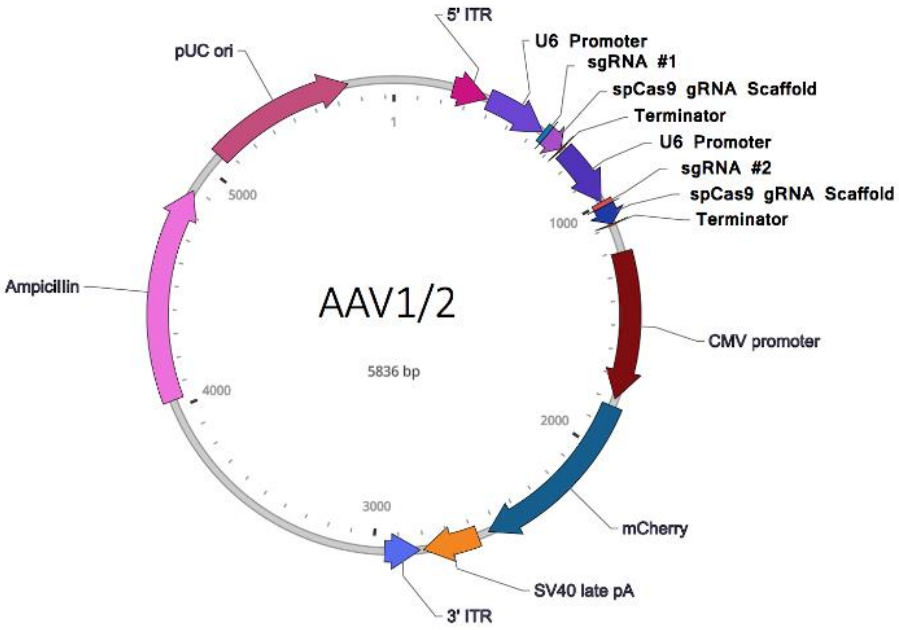
5' ITR
U6 Promoter
sgRNA #1
spCas9 gRNA Scaffold
Terminator
U6 Promoter
sgRNA #2
spCas9 gRNA Scaffold
Terminator
pUC ori
Ampicillin
AAV1/2
5836 bp
CMV promoter
mCherry
SV40 late pA
3' ITR
1
1000
2000
3000
4000
5000

B

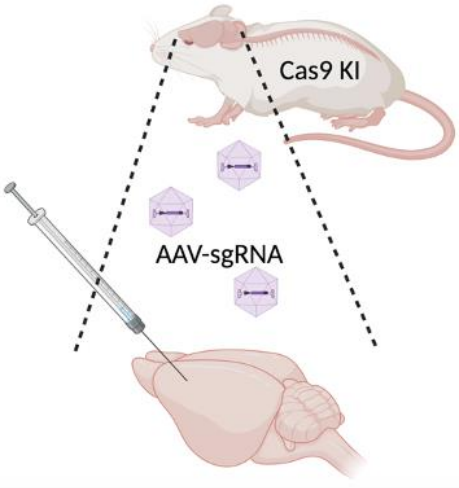
Cas9 KI
AAV-sgRNA

C

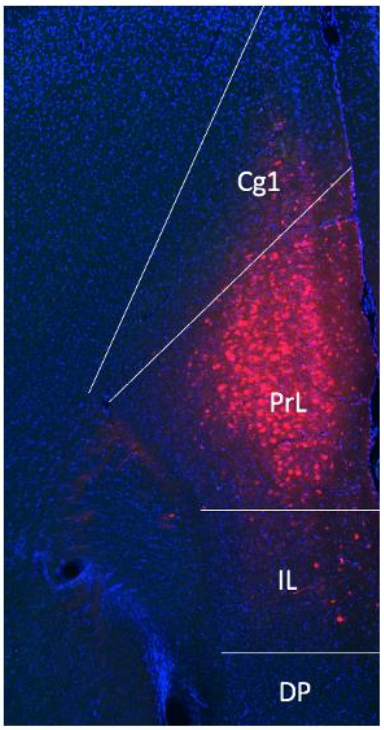
Cg1
PrL
IL
DP

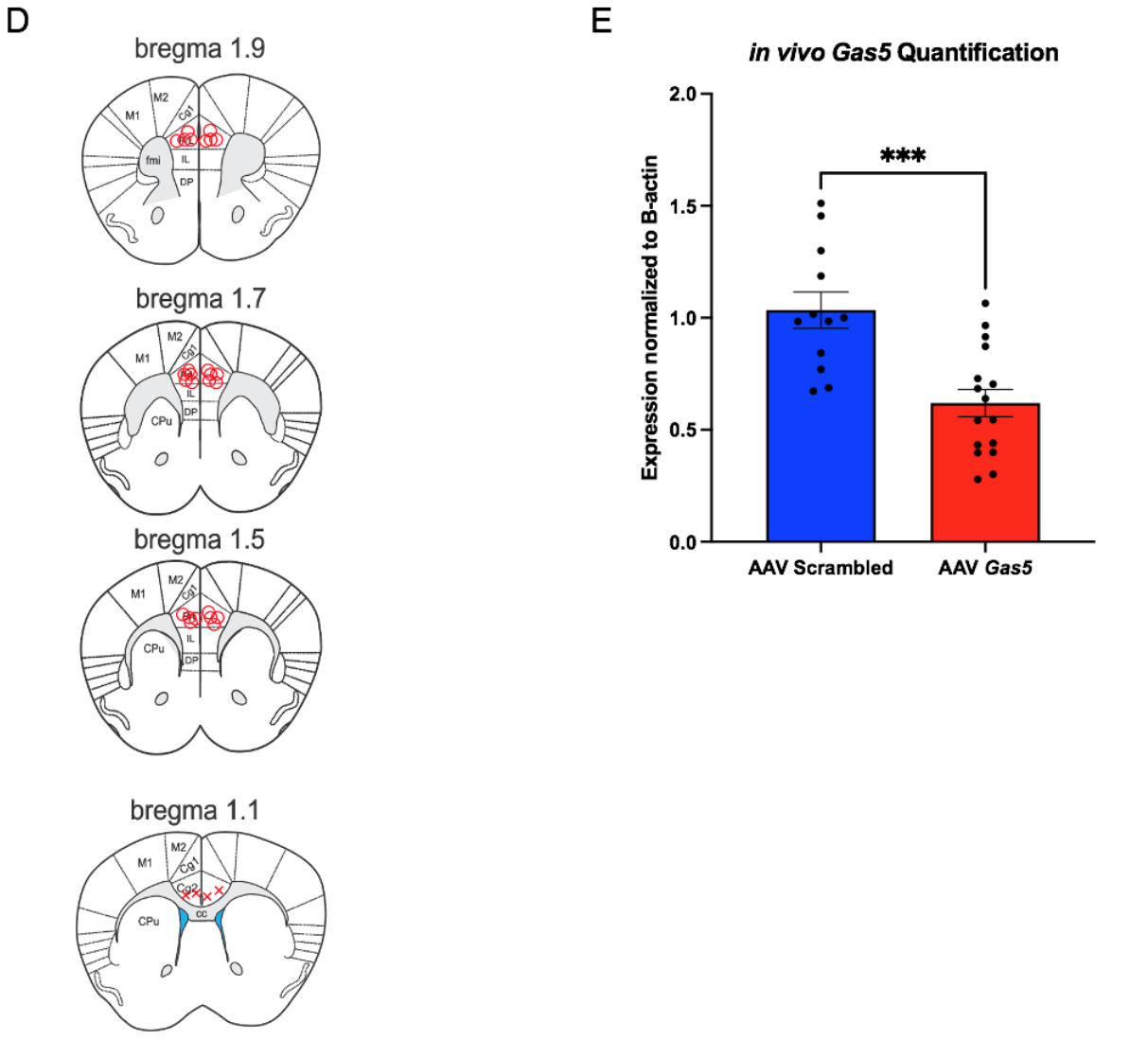

Figure 35: *In vivo Gas5* gene targeting. (**A**) Schematic of the plasmid used for AAV1/2 viral production. Two sgRNAs were encoded, each under the control of the U6 promoter. mCherry was encoded under the control of the CMV promoter. (**B**) Schematic of AAV-sgRNA injection into the mPFC of Cas9 KI mice. (**C**) Representative image of successful AAV expression in the PrL of the mPFC. DAPI is shown in blue and mCherry is shown in red. mCherry expression is indicative of viral expression within those cells. (**D**) Diagram of representative injection placement. Properly placed injections are shown as red circles, improperly placed injections are shown as red exes. Proper injections were defined as A/P: +1.7mm ± 0.2mm relative to bregma. (**E**) *Gas5* lncRNA quantification in mCherry-fluorescing AAV-injected mPFC tissue. *In vivo Gas5* expression was reduced by ~40% compared to control. N = 3 – 8/sex/genotype. Values represent Mean ± SEM. mPFC = medial prefrontal cortex; Cg1 = cingulate cortex 1; PrL = prelimbic cortex; IL = infralimbic cortex; DP = dorsal peduncular cortex.

4.3.3 Behavioral Experimentation

AAV-*Gas5* and AAV-Scrambled mice were injected bilaterally into the PrL of the mPFC in 6 – 7-week-old Cas9-KI mice. Three weeks following injection behavioral experimentation began. Only those with properly-placed injections were used for behavioral analysis (determined via histological analysis following all behavioral paradigms). Mice were weighed weekly throughout experimentation. No difference was observed between AAV-*Gas5* and AAV-Scrambled weights for either male (**Figure 36A**) or female (**Figure 36B**) mice.

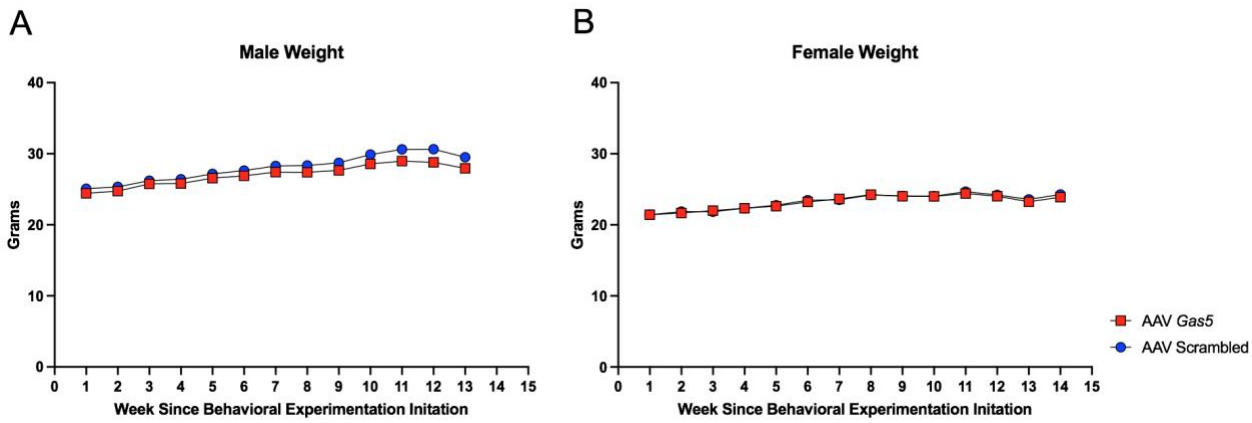

Figure 36: AAV-*Gas5* and AAV-Scrambled mouse weights over time. (**A**) Males, (**B**) females. No significant differences were observed between AAV-*Gas5* and AAV-Scrambled control for males or females. N = 11 – 14/sex/genotype. Values represent Mean ± SEM.

4.3.4 Drinking in the Dark (DID)

Mice were tested for binge-like drinking behavior using the DID ethanol consumption paradigm[283,284,769,770]. No significant difference was observed between AAV-*Gas5* and AAV-Scrambled males or females for either the 2-hour training day (data not shown) or the 4-hour experimental day (**Figure 37A and C**, respectively). AAV-*Gas5* and AAV-Scrambled males had no significant difference between BECs on the experimental day (**Figure 37B**). AAV-*Gas5* and AAV-Scrambled females presented a significant difference of variance using the unpaired t-test ($p < 0.01$), however the subsequent Mann-Whitney test p-value for female BECs was 0.0626 (**Figure 37D**).

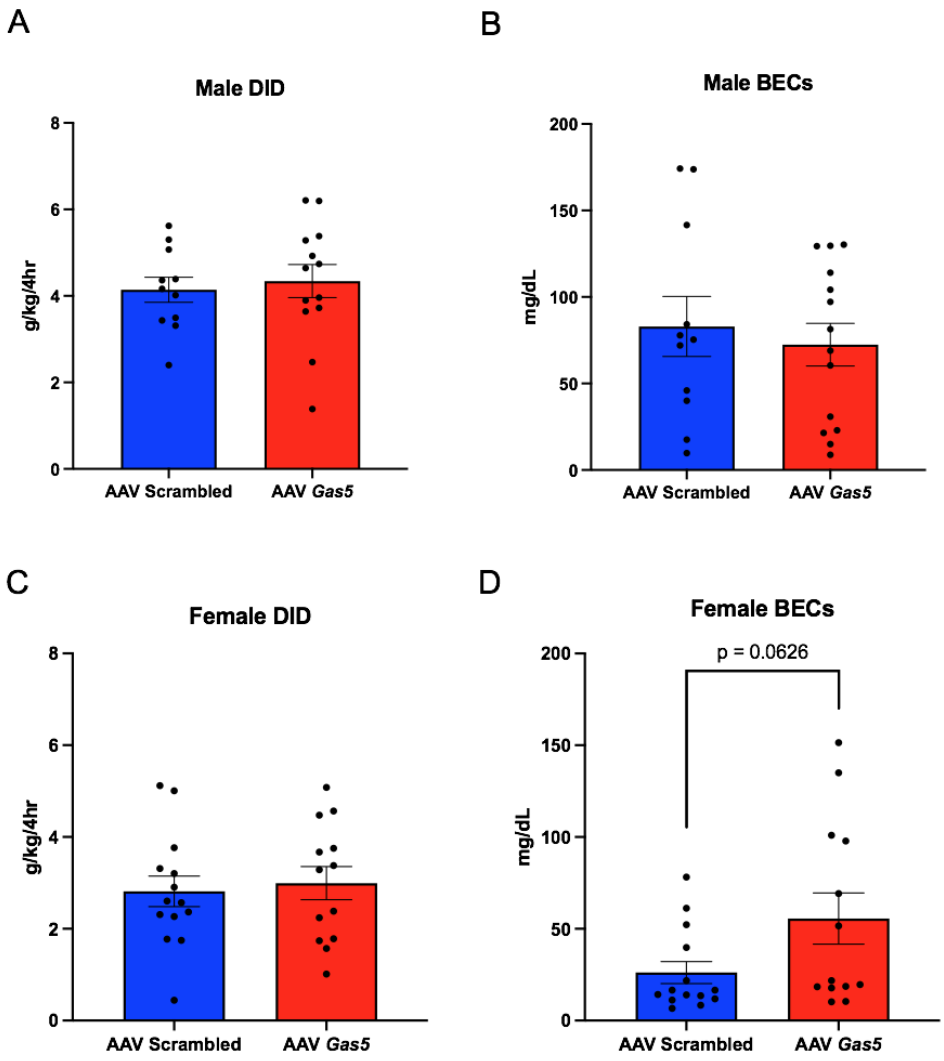

Figure 37: Effect of *Gas5* KD mutation on the DID assay. (**A and C**) Total ethanol consumption of AAV-*Gas5* and AAV-Scrambled male and female mice, respectively, over a 4-hour experimental period (g/kg/4hr). No significant differences were observed between AAV-*Gas5* and AAV-Scrambled control for males or females for ethanol consumption. (**B and D**) BECs (mg/dL; 5µL) from plasma collected from AAV-*Gas5* and AAV-Scrambled male and female mice, respectively, immediately following removal of ethanol-filled bottles. No significant differences were observed between AAV-*Gas5* and AAV-Scrambled control for males or females for BECs. N = 11 – 14/sex/genotype. Values represent Mean ± SEM.

4.3.5 Every-Other-Day Two-Bottle Choice (EOD-2BC) Drinking

AAV-*Gas5* and AAV-Scrambled mice were tested for ethanol drinking and preference using the EOD-2BC consumption assay[286]. Analysis of AAV-*Gas5* and AAV-Scrambled males revealed no difference in ethanol drinking, ethanol preference, or total fluid intake (**Figure 38A, B, and C**, respectively) for genotype or genotype x day, although the p-values for male ethanol intake and male ethanol preference on genotype were 0.0728 and 0.0701, respectively. There was, however, a significant day x concentration in males for ethanol drinking [$F (11, 250) = 258.2$; $p < 0.0001$], ethanol preference [$F (11, 249) = 15.16$; $p < 0.0001$], and total fluid intake [$F (11, 249) = 7.157$; $p < 0.0001$]. Female EOD-2BC analysis revealed no change in ethanol drinking or total fluid intake (**Figure 38D and F**, respectively) for genotype or day x genotype, but AAV-*Gas5* females had a significant decrease in ethanol preference when compared to AAV-Scrambled controls ($p < 0.05$). Analysis showed a day x genotype interaction [$F (11, 267) = 1.881$; $p > 0.05$] but no significant effect of genotype ($p = 0.0663$) (**Figure 38E**). *Post-hoc* analysis displayed significant reductions of ethanol preference on day's 1, 2, and 10 ($q < 0.05$) when comparing the AAV-*Gas5* females to AAV-Scrambled control. A significant day x concentration was also observed in female ethanol intake [$F (11, 270) = 140.1$; $p < 0.0001$], ethanol preference [$F (11, 267) = 8.682$; $p < 0.0001$], and total fluid intake [$F (11, 274) = 15.63$; $p < 0.0001$].

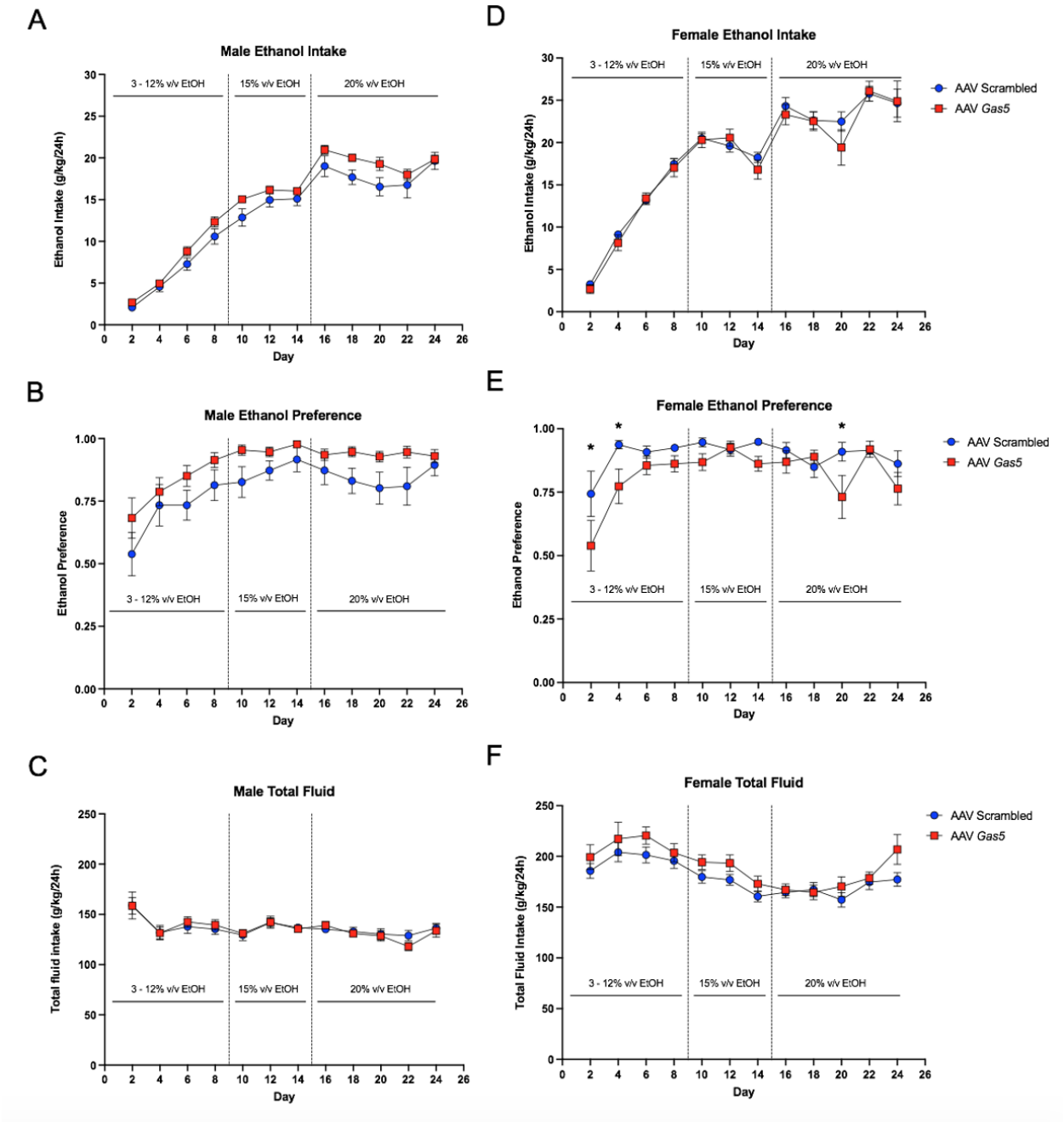

Figure 38: EOD-2BC drinking in AAV-*Gas5* and AAV-Scrambled mice. Left, males; right, females. (**A and D**) Ethanol intake (g/kg/24 h). No significant differences were observed between AAV-*Gas5* and AAV-Scrambled control for males or females. (**B and E**) Ethanol preference. No significant differences were observed between AAV-*Gas5* and AAV-Scrambled control males. AAV-*Gas5* females displayed significant day x genotype interaction that was followed by *post-hoc* analysis. (**C and F**) Total fluid intake (g/kg/24 h) across time and concentration. No significant differences were observed between AAV-*Gas5* and AAV-Scrambled control for males or females. * $q < 0.05$. N = 11 – 14/sex/genotype. Values represent Mean ± SEM.

4.3.6 Preference for Non-Ethanol Tastants

Male and female AAV-*Gas5* and AAV-Scrambled mice were subject to both sweet (saccharin) and bitter (quinine) tastant preference analysis under a 2BC paradigm. No differences were observed between males or females for saccharin (**Figure 39A and C**, respectively) or quinine (**Figure 39B and D**, respectively) preference at either concentration.

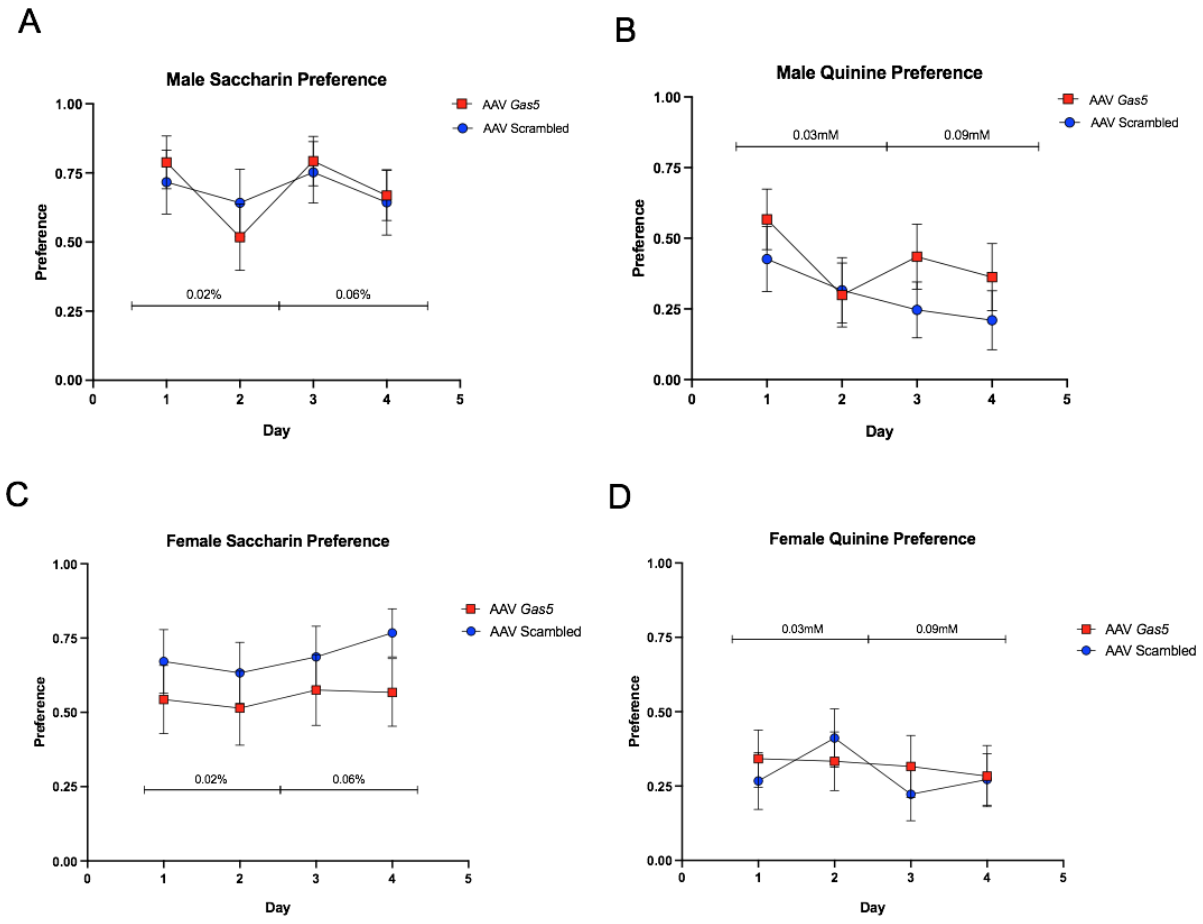

Figure 39: AAV-*Gas5* and AAV-Scrambled preference for non-ethanol tastants. (**A and C**) Saccharin tastant in males and females, respectively; first two days were presented at 0.02% w/v and the second two day were presented at 0.06% w/v. No significant differences were observed between AAV-*Gas5* and AAV-Scrambled control for males or females. (**B and D**) Quinine tastant in males and females, respectively; the first two days were presented at 0.03mM w/v and the second two days were presented at 0.09mM w/v. No significant differences were observed between AAV-*Gas5* and AAV-Scrambled control for males or females. N = 11 – 14/sex/genotype. Values represent Mean ± SEM.

4.3.7 Elevated Plus Maze (EPM)

AAV-*Gas5* and AAV-Scrambled mice were tested for anxiety-like behavior on the EPM because of well-known roles of GR action in anxiety-like behavior[771-773]. No differences were observed in the time spent in open arms (seconds), number of open arm entries, or number of fecal boli between male (**Figure 40A, B, and C**, respectively) or female (**Figure 40C, D, and E**, respectively) AAV-*Gas5* and AAV-Scrambled mice.

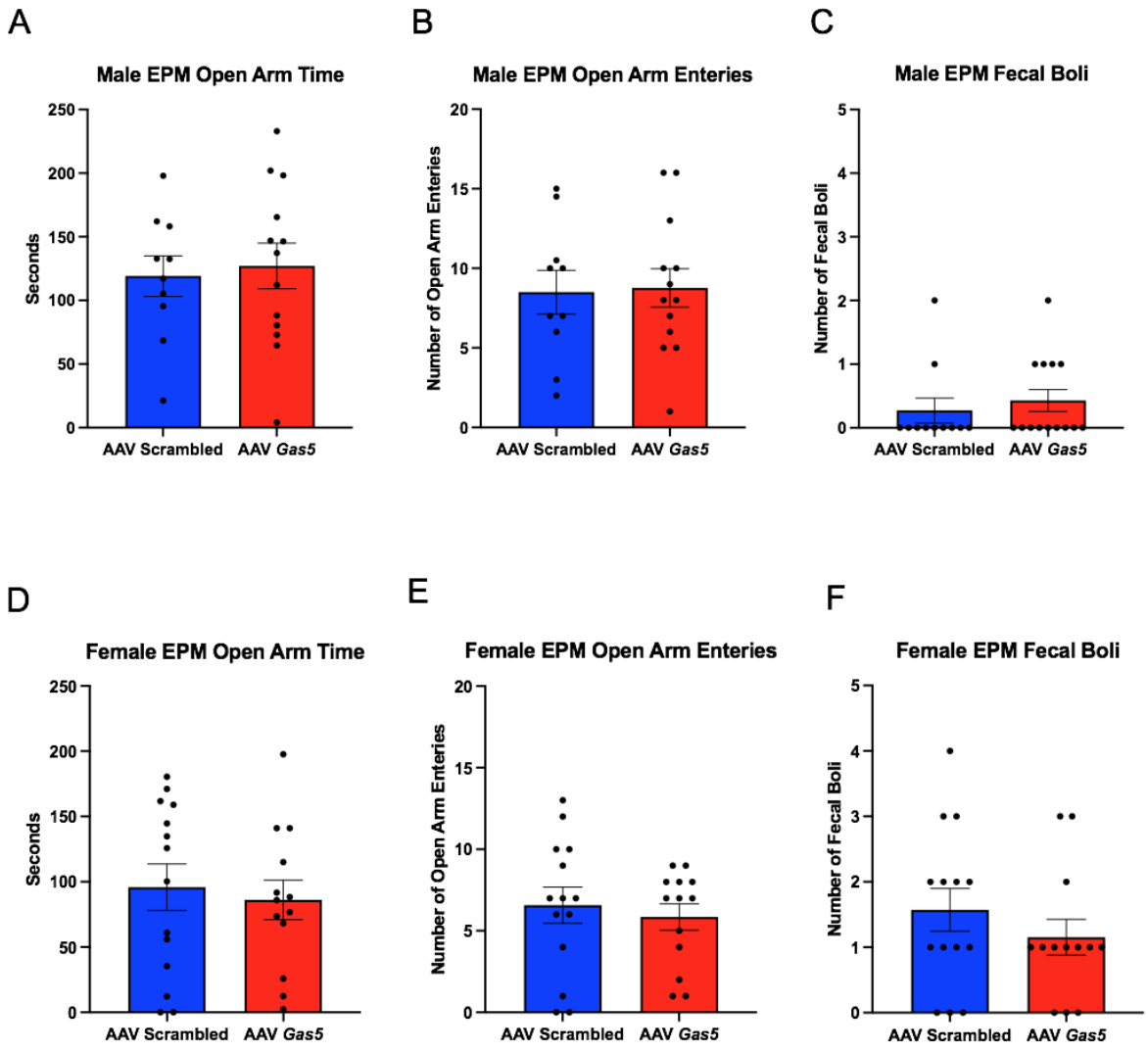

Figure 40: EPM behavior in AAV-*Gas5* and AAV-Scrambled mice. Top, males; bottom, females. (**A and D**) Amount of time spent in the open arms. (**B and E**) Number of entries onto the open arms. (**C and F**) Number of fecal boli excreted during the 5-minute test. No significant differences were observed between AAV-*Gas5* and AAV-

Scrambled control for males or females for any measures recorded. N = 11 – 14/sex/genotype. Values represent Mean ± SEM.

4.3.8 Acute Functional Tolerance (AFT)

The AFT assay was performed on the AAV-*Gas5* and AAV-Scrambled mice to measure within-session tolerance to ethanol[293]. There was no significant difference in AFT or AFT rate between male (**Figure 41A and B**, respectively) or female (**Figure 41C and D**, respectively) AAV-*Gas5* and AAV-Scrambled mice. Male mice did present a significant difference of variance for AFT rate ($p < 0.05$), however there was no significant difference identified between genotypes using the Mann-Whitney statistical test.

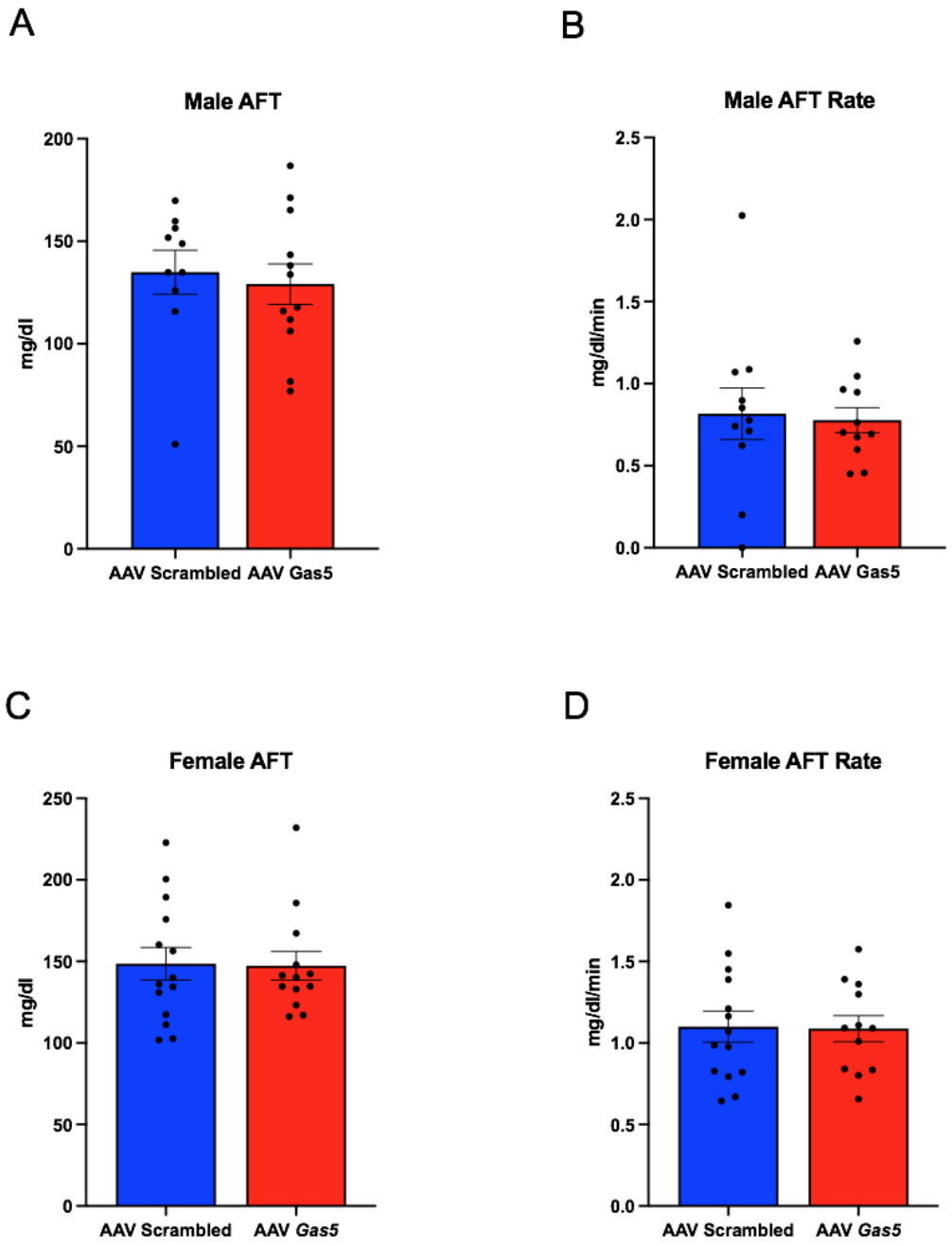

Figure 41: AFT to ethanol in AAV-*Gas5* and AAV-Scrambled mice. (**A and C**) AFT to ethanol (BEC2 – BEC1) in males and females, respectively. (**B and D**) AFT rate (AFT/Recovery time 2-recovery time 1) in males and females, respectively. No significant differences were observed between AAV-*Gas5* and AAV-Scrambled control for males or females for either AFT or AFT rate. N = 11 – 14/sex/genotype. Values represent Mean ± SEM.

4.3.9 Loss of Righting Response (LORR)

To measure sensitivity to the hypnotic/sedative effects of ethanol, AAV-*Gas5* and AAV-Scrambled mice were subjected to a LORR assay[291]. There was no significant difference in latency or duration of ethanol LORR between male (**Figure 42A and B**, respectively) or female (**Figure 42C and D**, respectively) AAV-*Gas5* and AAV-Scrambled mice. Female mice did present a significant difference of variance for LORR latency ($p < 0.05$), however there was no significant difference identified between genotypes using the Mann-Whitney statistical test.

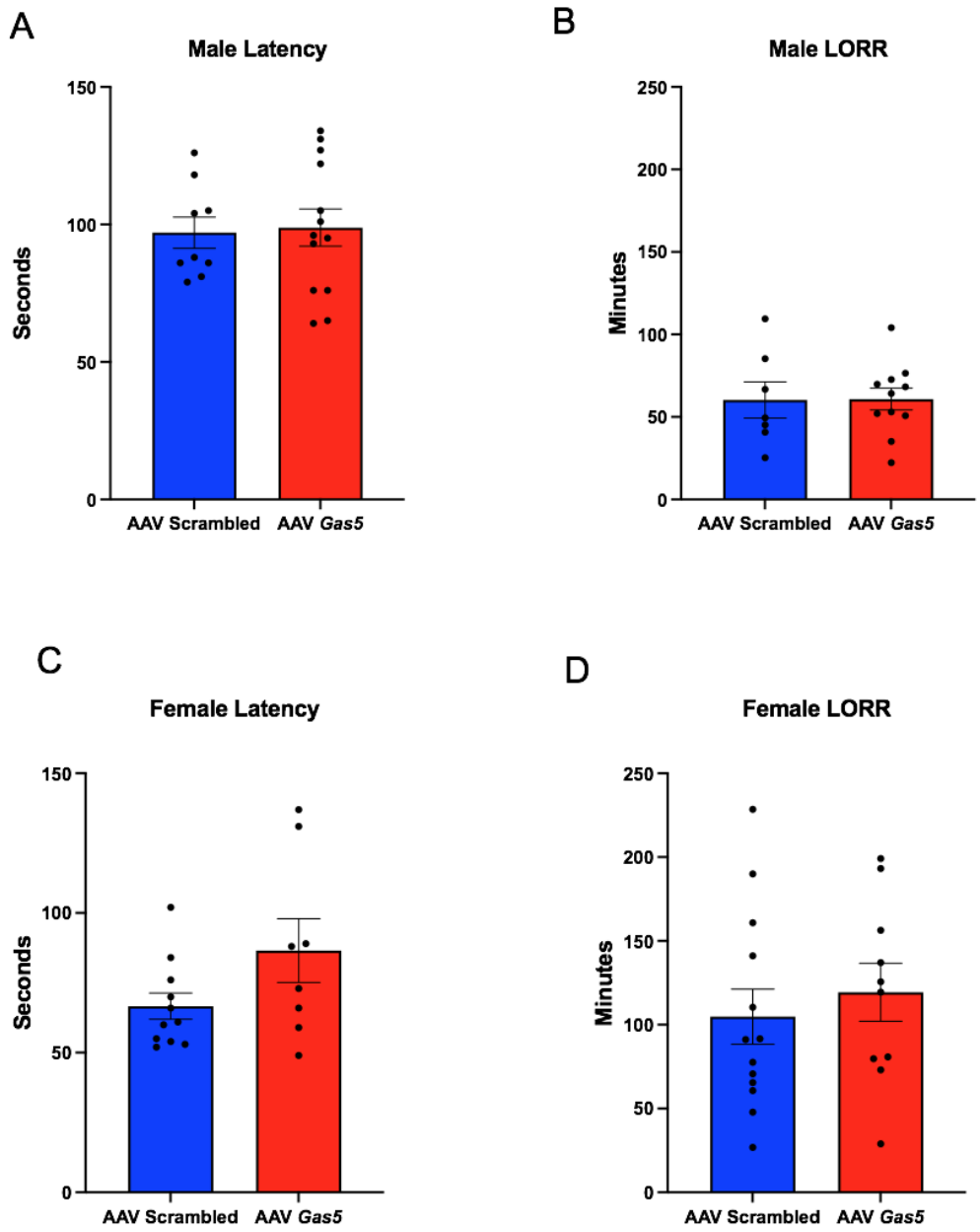

Figure 42: Ethanol-induced LORR in AAV-*Gas5* and AAV-Scrambled mice. 3.5g/kg ethanol; i.p. injection. Duration of LORR latency male (**A**) and female (**C**) mice. Duration of LORR in male (**B**) and female (**D**) mice. No significant differences were observed between AAV-*Gas5* and AAV-Scrambled control for males or females for either latency or LORR. N = 11 – 14/sex/genotype. Values represent Mean ± SEM.

4.3.10 Ethanol Clearance

The female AAV-*Gas5* mice had significantly increased BECs following DID compared to AAV-Scrambled females prior to removal of improperly injected mice from analysis ($p < 0.05$; after removal of improperly injected mice following the battery of behavioral experimentation the p-value rose to 0.0626), so they were subjected to an ethanol clearance assay to measure metabolism rate[774]. There was no difference in ethanol clearance between AAV-*Gas5* and AAV-Scrambled female mice (**Figure 43**).

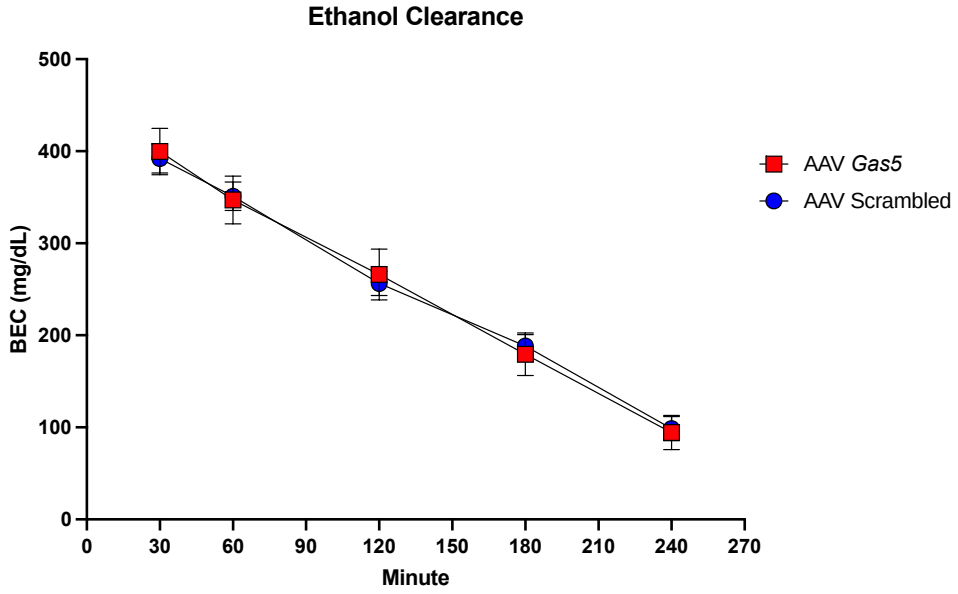

Figure 43: Ethanol clearance rate in AAV-*Gas5* and AAV-Scrambled female mice. 3.5g/kg ethanol, i.p. injection. Blood was collected via tail vein puncture at 30, 60, 120, 180, and 240-min post-ethanol injection. No significant difference was observed between AAV-*Gas5* and AAV-Scrambled control females, N = 13 – 14/genotype. Values represent Mean ± SEM.

4.3.11 Histological Analysis

Coronal brain sections were analyzed from each mouse used for behavioral experimentation to confirm mCherry fluorescence and to locate the injection sites (**Figure 35C**). It should be noted that variability is expected when it comes to bilateral viral injections[775-777].

Variability can occur as asymmetric viral expression or viral spread differences. The targeted subregion of the mPFC was the prelimbic cortex (PrL) because it is a brain area associated with substance misuse[778], drug seeking, and drug relapse[779,780]. However, viral spread into neighboring subregions of mPFC [*e.g.*, infralimbic cortex (IL) and the cingulate cortex area 1 (Cg1)] was expected. Mice with improperly placed injections were removed from behavioral analysis (see: **Methods 4.2.11**; **Figure 35D**). Each cohort had n = 2 – 4 mice removed from analysis, with final n-values of 11 – 14.

4.4 DISCUSSION

LncRNAs are critical epigenetic regulators for cellular and molecular maintenance. LncRNA *Gas5* specifically has many known roles in the neuroimmune system and disease biology, including cancers and addiction[393,466,471,707,750-752,758]. Previous data of *Gas5* expression in the mPFC of adult mice chronically exposed to CIEV demonstrated a pronounced reduction in *Gas5* lncRNA expression (~15%) that was still observed one week after the extinction of vapor exposure[752]. To mimic this observed reduction and measure behavioral outcomes in response to ethanol (and because of well-known roles of the mPFC in ethanol action[329,331,332,334,335,781-783]), *Gas5* was selectively knocked down in neuronal cells within the mPFC of adult, ethanol-naïve mice via viral AAV injection targeting the noncoding *Gas5* promoter and compared to controls.

A battery of behavioral tests revealed that under the EOD-2BC paradigm, female AAV-*Gas5* mice had significant genotype x day interaction demonstrating reduced ethanol preference compared to AAV-Scrambled controls (**Figure 38E**). Differences in variance were observed between AAV-*Gas5* and AAV-Scrambled females for BECs and LORR latency, and between male AFT rates. Beyond these results, there was no significant difference observed in all additional behavioral experiments conducted between AAV-*Gas5* and AAV-Scrambled males or females.

These data suggest that alterations in neuronal mPFC *Gas5* expression may hold minor roles in ethanol preference that is sex dependent, specifically under an escalation of drinking behavioral paradigm. Out of the seven assays run to characterize different facets of ethanol action, only the EOD-2BC yielded significant results. *Gas5* did not alter binge-like ethanol drinking, BECs following DID (although female BEC had an effect of genotype p-value of 0.0626), acute

tolerance to ethanol, sensitivity to the sedative/hypnotic effects of ethanol, ethanol clearance rates (tested in females only), or anxiety-like behavior. The significant analysis of variance observed sex-specifically under female DID, female LORR latency, and male AFT rate demonstrate differential degrees of separation from the mean between genotypes (*i.e.*, while there was no significant difference in behavior, there was differential spread of data points across genotypes). AAV-*Gas5* females have a larger spread of data points than AAV-Scrambled females for both BEC and LORR latency (**Figure 37D and 42C**, respectively), whereas AAV-*Gas5* males have smaller spread than AAV-Scrambled control for AFT rate (**Figure 41B**). Only genotype x day female ethanol preference behavior was reduced in response to neuronal mPFC *Gas5* KD, however, it should be noted that the effect of genotype p-value was 0.0663 for females, and AAV-*Gas5* males were trending toward a significant increase in both ethanol consumption and preference (p = 0.0728 and 0.0701, respectively). These results may hold biological relevance while not specifically being a statistically significant discovery[784,785].

This study has its limitations; the first is the targeted promoter. *Gas5* is hypothesized to have multiple promoters, at least one bidirectional[766]. Due to this molecular handicap, certain *Gas5* transcripts cannot be targeted without the potential for altering other genes sharing the promoter. Initial attempts to KD all five *Gas5* transcripts proved ineffective, therefore the EPDnewNC was used to identify the experimentally verified *Gas5* promoter and it was targeted for mutation. The EPDnewNC *Gas5* promoter falls downstream of three *Gas5* transcription start sites and upstream of two (**Figure 34A**). Due to this, it is likely that not all *Gas5* transcript expression levels were altered by the injected sgRNAs, and a subset of *Gas5* transcripts will still be expressed in the animals. Long-read sequencing strategies would need to be employed in order to establish which *Gas5* transcripts were still being expressed following AAV injection. Next, a neuronal-specific chimeric AAV1/2 was used for viral delivery, so not all cells within the mPFC will harbor a mutation at the *Gas5* promoter. Neurons were the selected the cellular target because of *Gas5*'s well documented roles within disease-state neurons[786-791]. Glial cells were not targeted, which may have impacted the observed phenotype. Another limitation of this study was the variability of AAV1/2 expression between animals. Each animal was injected manually, bilaterally, and with the same viral volume (*i.e.*, genomic copies). Slightly differential mPFC mCherry expression was noted across animals (*i.e.*, differential or asymmetric expression; unpublished observations). Variability could be due to such things as AAV nuclear shuttling events, transduction efficiency,

cellular protein expression, and host-encoded replication factors[775,792] and it presented as slightly differential expression profiles across injected animals[775-777]. These points of potential variability could account for the significantly larger variance observed with AAV-*Gas5* females for BEC and LORR latency. While expected, this is a caveat for interpreting these viral data.

Neuronal mPFC *Gas5* KD in adulthood of ethanol-naïve mice revealed a subtle ethanol drinking phenotype that is sex-dependent. While it has been shown that *Gas5* is involved in AUD-related behaviors, the phenotype reported herein is mild. This does not mean that *Gas5* does not still hold interest for addiction research and deserves further characterization. Future directions could include analysis of ethanol-responsive *Gas5* miRNA-binding partners, *Gas5* KD in alternate brain regions linked to AUD, additional behavioral paradigms of chronic ethanol dependence to probe the phenotype detailed herein, and further analysis of *Gas5* action within other substance use disorders. Taken together, it has been demonstrated that mPFC KD of *Gas5* reduces ethanol preference in females only.

5.0 FINAL DISCUSSION

Individual lncRNA molecules have proven to be critical regulators of normal cellular function[415,427,445,793], as well as disease states[413,420,453-455]. However, the foundation on which to build research projects on is limited when it comes to lncRNAs and the AUD field. It was therefore of high importance to target and characterize novel lncRNAs to determine their roles in ethanol action. This project design was relatively high-risk/high-reward, with the potential to observe no significant changes after applying complex CRISPR/Cas9 techniques to study individual lncRNAs *in vivo*. However, as this is a relatively novel area of research, positive results could shine a light on ncRNAs and AUD. Excitingly, all six lncRNA gene-targeted groups displayed significant alterations in behavior when compared to control (**Table 10**). These data highlight the importance of lncRNA physiology, the impact lncRNA mutation has on ethanol action, and adds to the foundation of lncRNA research in the AUD field.

Table 10 Summary table of the final results from the three main dissertation chapters.

Chapter	lncRNA	CRISPR/Cas9 Method	Final Results	Sex
2	*Tx2*	Traditional, global	EOD-2C: Reduced Ethanol Intake and Preference	♂
			LORR: Reduced Ethanol-, Gaboxadol-, and Zolpidem-induced LORR. Chronic Ethanol-Induced LORR: No tolerance index.	♂/♀
			Electrophysiology consistent with altered GABA Transmission and $GABA_AR$ Subunit Composition	♂/NA
			Cortical *Tx2* expressed similarly in males and females. *Tx2* expressed in low levels in multiple brain regions. *Tx2* expressed primarily in the cytoplasm of neurons and microglia. Alternative annotation from NCBI.	♂/♀
3	*Pitt1*	CRISPy TAKO, global	EOD-2BC: Reduced Ethanol Intake and Total Fluid	♀
			EOD-2BC: Altered Ethanol Preference	♂
	Pitt2	CRISPy TAKO, global	EOD-2BC: Altered Ethanol Intake and Reduced Total Fluid	♀
			EOD-2BC: Altered Ethanol Preference	♂
	Pitt3	CRISPy TAKO, global	EOD-2BC: Reduced Ethanol Intake and Total Fluid	♀
			EOD-2BC: Altered Ethanol Preference	♀
	Pitt4	CRISPy TAKO, global	EOD-2BC: Reduced Ethanol Intake and Total Fluid	♀
			EOD-2BC: Altered Ethanol Preference	♀

4	*Gas5*	AAV1/2, brain region- and cell-specific	EOD-2BC: Reduced Ethanol Preference	♀

The overall hypothesis I set forth to test, that individual ethanol-responsive lncRNAs act as determinants of ethanol consumption and ethanol-related behaviors, has been proven correct. These six lncRNAs have all shown the ability to modulate ethanol drinking and ethanol-induced behavioral responses (**Table 10**).

5.1 SIGNIFICANCE AND FUTURE DIRECTIONS

These chapters are highly significant, demonstrating the importance of lncRNAs in the regulation of ethanol drinking behavior. Of the six ethanol-responsive, neuroimmune-linked lncRNAs detailed in this dissertation, five were novel and uncharacterized. This is the first record of their function and lays down a foundation for future lncRNA AUD research.

5.1.1 Gene Mutation versus Gene KO (*Tx2*, *Pitt1*, *Pitt2*, *Pitt3*, *Pitt4*)

This dissertation describes research set forth to identify lncRNAs that impact ethanol-drinking behavior. While none of these lncRNAs were completely knocked out, they have all been implicated in ethanol action. Based on the annotations available at the time for *Tx2*, *Pitt1*, *Pitt2*, *Pitt3* and *Pitt4*, the putative promoter and exon 1 were targeted for mutagenesis. All gene-targeted cohorts no longer express the WT transcript(s), but instead each cohort now expressed mutant RNA. Unfortunately, *Pitt2* TAKOs could not reliably produce RT-PCR products for *Pitt2* lncRNA, therefore the mutated RNA product(s), or lack-there-of, are unknown. Knowing these facts, several questions come to mind. (1) What conclusions can be drawn about these lncRNAs with respect to ethanol action? (2) What is the impact of gene mutation versus gene KO on analysis of gene function and analysis of the observed phenotypes? (3) How could a complete gene KO be created and lncRNA function identified?

What conclusions can be drawn about the function of these lncRNAs researched herein with respect to ethanol action? Important information was gleaned about the ethanol-responsive lncRNA genes researched herein that are relevant to ethanol action. Alcohol dysregulates gene expression[752,794,795] and alters splicing events[620,796]; therefore characterizing mutant lncRNA products from an ethanol-responsive gene offers its own set of insights when compared to full gene KO, such as implicating specific genomic regions or specific lncRNA gene transcripts as being functionally linked to ethanol action. While individual lncRNA mechanisms remains elusive, Exon 1 of *Tx2*, *Pitt1*, *Pitt2*, *Pitt3*, and *Pitt4*, and *Gas5* transcripts 3 and 5, have been linked to ethanol drinking behavior and put forth all six lncRNAs as determinants of ethanol action.

What is the impact of gene mutation versus gene KO on analysis of gene function and analysis of the observed phenotypes? It has been shown that mutation of these genes resulted in mutant lncRNA transcript(s) (*Tx2*, *Pitt1*, *Pitt3*, and *Pitt4*). As the gene was not knocked out, it makes hypothesizing about lncRNA function more challenging. The observed phenotypes could be due to disruption of the original transcript or novel functionality of the mutant transcript(s). The gene mutation(s) harbored could alter a variety of factors involved in lncRNA biology, such as dysregulated expression, altered function, disruption of regulatory splice sites, or deletion of an important region for tertiary structure formation, subcellular shuttling, or molecular partner binding. While no complete mechanism can be reached about specific gene function based on the data presented herein, conclusions can be drawn about the impacts that result from gene disruption and the importance of Exon 1 expression. All mutant lncRNAs researched herein regulated ethanol drinking behavior, implicating them in ethanol action. This supports the hypothesis that specific genomic regions and lncRNA transcript dysregulation are enough to alter ethanol-related behavior.

How could a complete gene KO be created and lncRNA function be identified? There are several approaches that could be used to create a complete gene KO (for reviews, see: [797-799]). (1) Identify the full transcript and relevant regulatory regions of each gene (*i.e.*, promoter). This would greatly aid in gRNA design and gene characterization. (2) Target the promoter in the same manner that *Gas5* was targeted. This would allow for KO or KD of the gene, dependent on gene complexity. (3) Perform large-scale mutagenesis to remove the entire gene (this technique would remove multi-kilobase regions and is dependent on the genomic neighborhood of individual genes). (4) Gain-of-function or loss-of-function studies to gain insight on *cis*- or *trans*-mechanisms. (5) Lastly, functional molecular experiments could be applied to determine lncRNA

characteristics (*e.g.,* RT-PCR for analysis of differential expression in tissues, ISH for cellular and subcellular localization, column binding experiments to identify molecular partners, sequence analysis for repeat regions, computational tertiary structure formation).

Transcript sequencing. The gene annotations for *Tx2* and *Pitt2* were proven incorrect and will require sequencing strategies to generate the correct annotation. There are several techniques that could be employed to discern this information; such as: short-read RNA-Seq[800], long-read RNA-Seq[801], direct RNA-Seq[802], and targeted RNA-Seq[803] (for reviews, see: [804,805]). However, lncRNAs are known to be expressed up to 10-fold less than mRNA[806] and are not always poly-adenylated[807], which is a limitation for short-read RNA-Seq strategies. Targeted RNA-Seq, a derivative of long-read RNA-Seq that allows for custom oligonucleotide probe design, would be the most ideal option for sequencing *Tx2* and *Pitt2*. This method can further be coupled with techniques to specifically enrich for lncRNA (*e.g.,* SeqCap RNA Enrichment System[808] and RNA Capture Long-Read Sequencing[809-811]). Using techniques coupled to long-read RNA-Seq overcomes several limitations associated with short-read sequencing, such as the inability to identify novel transcript isoforms and structural variants[812].

Promoter identification. Gene promoters are generally located directly upstream of the 5' transcription start site. However, this is not always the case. Genes can have multiple promoters[813-816], multiple transcripts variants[817,818], and experimentally-unverified annotations[819-821] (for reviews, see: [822-827]). Promoters too have been shown to interact in a *trans*-fashion[828-831], which can make promoter identification challenging. Due to limitations surrounding novel gene annotation, the first Exon and the surrounding intronic region was targeted for *Tx2*, *Pitt1, Pitt2*, *Pitt3*, and *Pitt4*. The hypothesis being that disruption of this putative promoter region would result in KO of the gene. This was proven incorrect, as all genes targeted in this manner still maintained expression of the now mutant gene. Functional experiments to identify and validate promoters are time-consuming[832-834], therefore computational tools are available and improving to identify lncRNA promoters, such as DeepLncPro[835], DeePromoter[836], and FastText N-Grams coupled with deep learning[837]. Chromatin Immunoprecipitation Sequencing could also be applied and analyzed to identify lncRNA genomic regions bound to transcription factors that could then be used to identify specific regulatory regions of interest based on genomic location (*e.g.,* promoter or exonic enhancer regions)[838-840]. The promoter could then be targeted with CRISPR/Cas9 or CRISPRi and the lncRNA expression quantified, in the same manner that *Gas5* was targeted in Aim 3. This

would also give insight into a potential mechanism if the phenotypes differ from those detailed herein, as multiple animal models are helpful at deciphering lncRNA function[838].

Large-scale genome deletion. Another option for complete gene KO would be removal of the entire gene (*i.e.*, large-scale kilobase whole-gene deletion)[538,841-843]. This is dependent on correct genomic annotations and the genomic neighborhood of the target gene (*i.e.*, this would not be possible for *Tx2* due to antisense gene *Osmr*). Large, multi-kilobase deletions also hold the potential to remove important intronic regulatory regions necessary for other genes, so careful genome analysis would be required prior to complete genomic deletion or exonic deletion.

Gain-of-function and loss-of-function studies. LncRNAs are complex molecules that can require multiple gain- or loss-of-function genetic models to fully characterize the lncRNA mechanism. Examples include the use of short interfering RNAs[844,845] and antisense oligonucleotides[846,847] to KD RNA, reporter assays to ablate the gene[793,848,849], insertion of a polyadenylation termination cassette downstream of the transcription start site to truncate the lncRNA[850-853], and ectopic transgene expression[854-856]. Many lncRNAs have been researched using various combination of these techniques in order to tease apart gene function, such as the *Linc-p21* locus[857-859] and *Xist*[860-863]. The benefit of RNA interference is that it allows for RNA expression modulation independent of the gene locus, however, there are downsides associated with off-target effects[864-869]. Loss-of-function studies allow for analysis of neighboring gene expression, which could give insight into potential *cis*-mechanisms of the lncRNA. Following loss-of-function analysis, rescue and reinstatement experiments could then be applied to determine if regulation is restored with ectopic expression of the lncRNA being researched. This technique could give insight into potential *trans*-mechanisms of the lncRNA. Overall, multiple genetic approaches can be utilized to tease apart lncRNA mechanisms of action.

Computational and functional analysis. There is a large breadth of potential lncRNA roles, making identification of specific mechanisms challenging and exploration-based. LncRNA transcripts could be analyzed computationally in detail for repeat regions (indicative of a sponging site[870]), analyzed for predicted structural conformation (this could glean information on how mutation altered the lncRNA[871]), analysis of the ceRNA networks for *Pitt1*, *Pitt2*, *Pitt3*, and *Pitt4* for insight into specific ncRNA partners and pathways[872], and RNA-centric column binding assays to probe for protein[873] or RNA[588] binding partners. For example, MechRNA[874], a prediction tool for lncRNA molecular interactions, could be applied to *Tx2* which could have value for

hypothesizing specific functions or pathways that could then be functionally interrogated. Lastly, there is RT-PCR, RT-qPCR, and ISH techniques that can be applied to characterize lncRNA expression and localization in different tissue and cell types.

Looking back at the original project design, I do not think these approaches would have been advantageous at project onset. It was not a necessity to perform them, as the functional link to ethanol action was not yet confirmed for *Tx2*, *Pitt1*, *Pitt2*, *Pitt3*, and *Pitt4*. Now knowing these data presented herein, there is more of a logical need to clearly understand these genes with respect to AUD. These potential avenues of exploration detailed above represent future directions for characterization of these lncRNAs. Now that these novel genes have been linked to ethanol drinking behavior, it is of interest moving forward to know how the lncRNAs function and how they propagate the observed phenotypes.

5.1.2 Aim 1

A 306 bp deletion within the presumed first Exon of the *Tx2* gene was able to produce very compelling alterations in behavior. The mutation resulted in significant ethanol-related behavioral changes from control. A 36% reduction in ethanol consumption and 42% reduction in ethanol preference at 15% v/v ethanol was observed only in males when compared to control. Changes in LORR responses were similar in both males and females, ranging from 38 – 46% reduction in ethanol-induced LORR (3.6 and 3.8g/kg ethanol) and reduced tolerance index to chronic LORR compared to control, suggesting that both males and females displayed similar pharmacodynamics in response to a debilitating dose of ethanol. When a free-choice ethanol drinking model was introduced however, the females were not opposed to ethanol drinking the way their male counterparts were.

Out of the three aims detailed herein, Aim 1 presents the most mechanistic insight for lncRNA function. *Tx2*, a previously novel, uncharacterized, and inaccurately-annotated lncRNA, when mutated, shows significant behavioral alterations to ethanol and GABAergic drugs, significantly altered GABA transmission, and is consistent with altered $GABA_AR$ composition. This suggests that *Tx2* is normally involved in these pathways and presents a new hypothesis for future *Tx2* research to build on.

As touched upon above, there are many questions about *Tx2* that became evident during experimentation. What are the molecular impacts of the still transcribed regions of *Tx2*? How does mutant *Tx2* differ from WT? Are there other important regions of *Tx2* that dictate ethanol-related behavior? These questions are all reliant on first identifying the full transcript(s) of *Tx2* RNA and solidifying the WT genomic annotation. The mutation altered GABAergic function and reduced ethanol sensitivity, therefore once the annotation is better understood, then specific hypotheses can be made about tertiary structure, binding partners, and function (*i.e.*, are there repetitive regions that are indicative of miRNA sponging sites? Does a computational model of tertiary structure have predictive value of function? Does the deletion interfere with regulation, function, or structure?). There are many questions about *Tx2* characterization with respect to normal physiology and in response to ethanol that deserve attention, however, to move this project forward in the future from a pharmacological standpoint, future directions could include moving towards a more translational approach to modulate *Tx2* and analyze ethanol-associated behaviors. This could be done by targeting *Tx2* in a similar manner to *Gas5*. A viral-mediated method would allow for more specific probing of *Tx2* effects, and could allow for brain-specific, brain-region-specific, and/or cell-type-specific modulation of *Tx2* in adult, ethanol-naïve mice. The translatability has already been shown (human *LINC01265* was the ethanol-responsive target identified for functional analysis through RNA-Seq and bioinformatic analysis), so there is promise for continuing this project and digging deeper into the annotation, mechanisms, and precise physiology of *Tx2*.

5.1.3 Aim 2

The purpose of this Aim was to develop a novel CRISPR/Cas9 technique and apply it to multiple ethanol-responsive lncRNA genes. The CRISPy TAKO method was designed to rapidly screen AUD gene targets for altered ethanol-drinking phenotypes with the goal of identifying at least one lncRNA that can significantly modulate ethanol drinking behavior for in-depth analysis and characterization. The amount of time and effort that goes into generating a traditional gene-targeted animal cohort does not always outweigh the potential for the genotype to be inconsequential. Overcoming the limitations of time, cost, and animal number, the CRISPy TAKO technique was used to measure ethanol self-administration in four different gene-targeted groups in both males and females in the same amount of time it would take to generate a true-breeding

line. Not only does the technique hold high significance and potential for the genetic engineering field as a whole, but all four genes studied using this technique had significant and sexually dimorphic ethanol drinking behavioral differences from control. The novel lncRNA genes discussed in Aim 2 offer the regulatory potential to reduce ethanol consumption by up to 20% in an extended and escalating ethanol drinking paradigm in females alone.

When considering the methodology and data produced from Aim 2, one predominant question comes to mind: why are the results female-specific when the ceRNA network analysis was derived from male samples? It is possible that these genes may have underlying divergent sex-specific expression, which could contribute toward the sexually dimorphic phenotypes observed (see: **Chapter 1.6 and 5.1.5**). It is also possible that, while identified in hippocampal tissue, global mutation of these genes resulted in alternative cellular compensation and/or differential functionality between the sexes. In order to decipher why male-derived ceRNA networks that identified *Pitt1 – Pitt4* produced little-to-no ethanol drinking behavioral changes in males but produced complex female-specific results, comparative experimentation is needed. First, the initial CIEV paradigm used for microarray analysis would need to be repeated in females. Second, the male hippocampi would need a detailed comparison of gene expression to the female hippocampi exposed to the same paradigm (this could be done by RT-qPCR of *Pitt1 – Pitt4* as well as other potential genes of interest, or repetition of the microarray analysis for large-scale transcriptome comparisons). It is possible that while CIEV exposure resulted in the significant reduction of *Pitt1 – Pitt4* expression in males, it produced alternative expression changes in females. It is also possible that males exhibit a form of protection, or conversely that females are more vulnerable to the mutation of these specific genes.

The RT-PCR results of *Pitt1*, *Pitt3*, and *Pitt4* demonstrated three differential gene expression outcomes: alternate transcript variant present in mutants (*Pitt1*), multiple differential RNA transcript outcomes (*Pitt3*), and maintained transcript (*Pitt4*). These data also highlight the novelty and unannotated nature of these lncRNA genes, such as the variable and inconsistent RT-PCR results noted for *Pitt2*, resulting in the inability to analyze the lncRNA. Phenotypically, sub-genotypes could be generated based on gene transcription and expression levels that could then be statistically analyzed against each other (*e.g.*, of the *Pitt3* TAKOs used for RNA analysis, three different downstream transcriptional outcomes were produced). Molecularly, the individual gRNAs as well as the combinations of gRNAs employed to produce the observed sub-genotypes

would need characterization and Sanger sequenced to determine how the variants were produced and how they differ from one another.

The RT-PCR results also provide new research questions that can be used to build future projects off of. What is the impact of the observed changes in gene expression on the interpretation of the results? Taking *Pitt1* as an example, is the observed phenotype due to the lack of the transcript targeted or due to expression of the new transcript? Why does the WT sample not produce a PCR product from the probe binding site? There is potential that mutation caused significant upregulation of the gene, leading to a sizable PCR product for all mutants that muted the WT band (potential mutation of a repressor sequence motif$^{875\text{-}878}$). This question could be addressed functionally by modulating the RT-PCR reaction components and thermocycler settings to maximize efficiency and performing a nesting RT-PCR followed by Sanger sequencing and RT-qPCR. *Pitt3* TAKO RT-PCR products could be subcloned to sequence the novel transcripts being produced and compared to WT *Pitt3*. This could provide information on potential regulatory regions that harbored a mutation, resulting in differential RNA products between *Pitt3* TAKOs. Considering *Pitt4*, it would be of interest to perform RT-qPCR to quantify *Pitt4* expression to determine if certain retained mutations modulate expression patterns.

As it is very difficult to predict individual lncRNA function, to move this project forward in the future, it would be ideal to perform a battery of exploratory behavioral and molecular experiments to probe for lncRNAs role. First a true breeding line would need to be created and EOD-2BC and DID repeated to validate the phenotype. Then a similar behavioral battery that was done for *Tx2* and *Gas5* (*e.g.*, LORR, AFT, EPM, rotarod) and ISH for cellular and subcellular localization could be used as a starting point. Detailed bioinformatic analysis of the top predicted binding partners from the ceRNA network analyses would also be of interest and could be used to predict network interactions that were dysregulated by TAKO mutation. This is important when trying to characterize a novel lncRNA and glean information about potential binding partners and network connectivity. Future directions for this project are two-fold: (1) continue using the TAKO method to screen AUD-linked genes of interest, and (2) generate true breeding lines for the Pitt gene of highest interest and begin the detailed behavioral, molecular, and off-target analysis that was originally set forth as a future direction at project conception. As *Pitt4* produced the most compelling results with respect to ethanol intake and preference, I believe *Pitt4* is of the highest interest when considering all four groups and is deserving of future in-depth analysis.

5.1.4 Aim 3

Unlike the lncRNAs detailed in Aim 1 and Aim 2, *Gas5* was not novel, had been previously studied, and had known functions on which to build a detailed hypothesis on[394,471,707,750,751,753,754,759,766,788,790,791,879-889]. *Gas5* is conserved between humans and mice[757] regulates gene expression, sponges miRNA, and is a ceRNA regulator of immune signaling[471]. *Gas5* is also heavily linked to the pathogenesis of human disease (*e.g.*, multiple cancers[471,750,766,879,881] stroke[791], Parkinson's Disease[788]) and substance use disorders (SUDs)[707,752,890]. The largest DNA methylation epigenome-wide association study analysis available for AUD found that a top probe consistently associated across all cohorts was located within the *GAS5* gene[393,395]. Further, *Gas5* binding partners have been linked to addiction (GR[386,387,390,391,890-894] and miRNAs[895,896]), so KD of *Gas5* lncRNA could contribute towards dysregulation of those systems already linked to SUDs. As *Gas5* was already implicated in ethanol action, a more specialized study was designed to functionally research *Gas5* in relation to ethanol drinking behavior.

In the context of AUD, Aim 3 offers a functional analysis of specific *Gas5* gene transcript KD. According to the UCSC genome browser (GRCm38/mm10; **Figure 34A and B**) *Gas5* transcripts 3 and 5 are predicted to be under control of the EPDnewNC promoter, and *Gas5* transcript 3 is the only transcript to express all 12 *Gas5* exons (and is the transcript targeted by RT-qPCR). Unfortunately, due to size constraints of targetable exons (most exons range in size from 20 – 40 bps), RT-qPCR size requirements, and exon similarity across all *Gas5* transcripts, it was not possible to design RT-PCR primers to distinguish between the individual *Gas5* transcripts beyond transcript 3. One possible future direction would be to analyze exons 7, 8, 9, and 10 with respect to ethanol (transcript 3 is the only *Gas5* transcript to express all 4 of these exons, and transcript 5 does not express any), as it was shown herein that KD of *Gas5* transcript 3 and 5 alters ethanol drinking behavior.

While not all data was negative, the behavioral responses to *Gas5* KD were underwhelming. There was a female-specific reduction in ethanol preference with mPFC *Gas5* KD however, which does further implicate *Gas5* in ethanol action. It also cannot be discounted that the AAV-*Gas5* males were trending towards significance on the EOD-2BC assay for ethanol consumption and preference that may have been unmasked with a larger sample size.

Several questions are produced from these results, highlighting potential avenues for future *Gas5*-AUD studies. Other brain regions besides the mPFC have implicated *Gas5* in addiction[707,890], so how would these alternative regions involved in addiction respond to *Gas5* KD (*e.g.*, NAc, BLA, amygdala)? *Gas5* could also be targeted for KD throughout the brain via the Cre-lox system. Would the results differ from those observed in neuron-specific mPFC *Gas5* KD? It should be noted that the TAKO method was used for *Gas5* by fellow laboratory-mate and graduate student Rachel Rice, creating a global *Gas5* mutant using the same gRNAs detailed herein. There was almost complete (92%) KD of *Gas5* (data not shown), however no significant phenotype was observed under identical ethanol-drinking paradigms. This could be indicative of cellular compensation or the importance of analyzing specific brain regions. Future directions for this project could involve probing for an ethanol-responsive *Gas5* network including glucocorticoids, GR, and miRNA. Can specific ethanol-responsive, *Gas5*-binding miRNAs be identified for transcripts 3 and 5, and can a pharmacologically-targetable pathway be unveiled? While the results presented herein are modest, it doesn't discount *Gas5* as a regulator of ethanol action.

5.1.5 Sexual Dimorphism

LncRNAs[465,513,515], ethanol[527,528], and other drugs of abuse (for reviews, see: [521,721,897-900]) are known to differentially impact the sexes. Along with the well-detailed anatomical, hormonal, and chemical differences between the biological sexes (for reviews, see: [901-903]), there is also sexual dimorphism in mammalian gene expression[904] and neural mechanisms[521,897,905,906]. Examples include: differential gene expression (DGE) networks[907], sexually dimorphic sensory neural populations[908], ovarian hormone fluctuation[897], DGE and inter-cellular distribution of genes[909], and female-predominant DGE has been linked to inflammatory synaptic transmission and extracellular matrix reorganization that can exacerbate neuroinflammation[908]. It has been shown here that ethanol-related behavioral phenotypes can be sex-specific, underscoring the necessity of female sample inclusion in addiction research. While all behavioral data presented herein explores both male and female responses, it is important to note that all lncRNA targets were identified from male transcriptome data. Since many targets identified from male samples presented female-specific responses, it will be of importance moving forward to analyze both male and female transcriptome data so that a more complete analysis of the target gene can be understood.

Hormonal cycles were not deemed as a confounding variable herein because, while important for social behaviors[910], hormone cycles were not as critical to monitor for the ethanol-related behavior conducted within these chapters. C57BL/6J female mice have shown stable behavioral patterns across all stages of the estrus cycle (proestrus, estrus, metestrus, diestrus repeated every 4 – 5 days[911]; the only exception being depressive-like behavior)[912], two different rat strains both demonstrated no estrus cycle impact on voluntary ethanol consumption (when cycles were not synchronized)[913,914], and it has been found in humans that ethanol consumption and the subjective effects of ethanol did not differ across four menstrual cycle phases[915]. However, it should be noted that links between specific estrous stages and differential ethanol consumption have been observed[916,917]. While hormone cycles were not monitored herein while measuring behavioral responses to ethanol, ovarian hormones could present as an interesting avenue of exploration for sex-specific, ethanol-related molecular dysregulation in the future, as ethanol is known to alter female hormone fluctuation[918,919] and alter reproductive hormone synthesis, processing, and secretion[920]. Ovarian hormone fluctuation in females can modulate the mesolimbic reward system, influence reward- and drug-directed behavior, and has been linked to faster SUD progression[897]. For example, sex-specific DGE in the NAc was noted both at baseline and in response to cocaine exposure and cocaine withdrawal in males and in females under three differing hormonal paradigms[921]. Further, endogenous circulating female sex hormones were neuroprotective in models of traumatic brain injury[922]. Estrogen specifically has long been known to be neuroprotective in CNS disorders[897,923-928], and could potentially be involved in the observed sex-specific behavior. Moving forward, it would be of interest to measure circulating hormones levels in males and females throughout experimentation, as well as estrus cycle, to identify further potential alterations in pharmacokinetics and pharmacodynamics across sex and estrus cycle.

Mutation of all six lncRNAs presented in this dissertation resulted in sex-specific changes in ethanol drinking behavior when compared to control. This is highly significant, as it is broadly known that males and females respond differently to psychiatric disorders and addictions, as well as to molecular insults. This data presented herein underscores the importance of researching both sexes in pharmacological settings. Not only are females historically underrepresented in scientific research (for reviews, see: [929-932]) but comparing female responses to male responses and assuming the same result discounts a wide breadth of possible sex-specific pharmacokinetics and

pharmacodynamics. This is important for both preclinical research as well as clinical testing of pharmacological therapeutics.

5.2 CRISPR/CAS9 TECHNIQUE COMPARISON

To broaden my training, several CRISPR/Cas9 techniques were applied for the development and research of gene-targeted mouse models (**Table 11**). Four different CRISPR derivatives were applied (traditional CRISPR/Cas9, CRISPy TAKO, CRISPRi, and AAV-CRISPR) to generate gene-targeted mutant mouse cohorts. Aim 1 used the classical CRISPR/Cas9 technique to generate a global mutant line for *Tx2*. Aim 2 was developed to overcome the limitations associated with this technique observed in Aim 1, applying an accelerated CRISPR/Cas9 technique via utilization of ~4x the gRNAs and Cas9 protein and a third of the time. Unlike Aim 1 and Aim 2 which used global mutant animals, Aim 3 was designed with CRISPR/Cas9 mutagenesis to be cell-type and brain-region specific via AAV1/2. Aim 3 was built off of current literature in the field implicating *Gas5* and *Gas5* binding partners in ethanol action. While not all methods were successful (*i.e.,* CRISPRi), learning the specific nuances of the different techniques and applications was invaluable for understanding molecular genetics and pharmacology.

Traditional global KO approaches are best suited for when a compelling hypothesis of lncRNA localization and function is unknown (*i.e.,* novel, uncharacterized lncRNAs). It is a relatively straight-forward method to assess overall behavioral and cellular impacts of gene function. Unfortunately, there is a large bottleneck between the acquisition of novel transcriptome data and researcher's ability to functionally characterize identified genes. Standard CRISPR/Cas9 generation of KO animals takes 9 – 12 months, with no certainty of identifying a significant regulator of ethanol-related behavior. The CRISPy TAKO method was developed herein, which allows for novel candidate genes to rapidly be screened for robust changes in ethanol drinking behavior to subsequently identify those suitable for generation of a true breeding line or removed from the list of candidate genes. I developed, validated, and applied this novel technique to four top-ranked genes of interest rapidly and two at a time. This screening method for novel genes of interest allows for multiple cohorts to be generated sequentially and within one generation.

Whereas Aim 1 took ~11 months to generate the first homozygous *Tx2* mutant cohort for experimentation, Aim 2 cohorts were generated and ready for experimentation within 3 months of embryo injection. While this technique does have limitations (**Table 11**), it is in the nature of the technique design to not be precise.

Table 11 Summary table of the advantages and disadvantages of each CRISPR/Cas9 method employed.

Chapter	CRISPR/Cas9 Method	Advantages	Limitations
2	Traditional CRISPR/Cas9	Whole-body KO	9 – 12 months to generate a colony
		Each animal is genetically identical (within its sex)	Potential for cellular compensation
3	CRISPy TAKO	Whole-body KO	Each animal harbors a unique mutation
		3 months to generate a colony	Potential for cellular compensation
4	CRISPRi	KD of all *Gas5* transcripts	Potential for impacting neighboring gene expression
			Repressive KRAB domain could not be employed
4	AAV1/2	Increased translatability	Requires extensive technical training
		Multiple AAV serotypes	Equipment and reagents are costly
		Can be brain region- and cell-specific	Variability of viral spread between subjects is expected

Viral-mediated delivery of CRISPR/Cas9 components in adult, ethanol-naïve mice to selectively KD a specific gene was of great interest for me to master. It allowed for learning translational AAV approaches and a more specified understanding of neuronal mPFC *Gas5* KD impact on behavior. This technique also minimized the potential for genetic compensation by injecting adult, ethanol-naïve mice[760,761,933]. Further, viral-mediated therapeutics are clinically relevant in the pharmacology field, therefore understanding AAV design and dynamics was a highly relevant technical skill of great interest for me to learn.

CRISPR/Cas9 can be used to target and modulate gene expression, allowing for increased precision medicine in humans. AAVs have emerged as safe and highly effective tools for the study of neurological disorders[597,934-937]. Differential capsid composition and multiple serotypes offer their own individual and distinct transduction profiles[597]. The majority of AAV stereotypes cannot

reliably cross the blood-brain-barrier which does limit access into the CNS, however systemic delivery through the circulatory system has shown success[597,935,938]. Additionally, there is current research on systemic delivery of the AAV9 serotype that suggests it is highly efficient at crossing the blood-brain-barrier to transduce neural cells[939-941]. Further preclinical exploration of this stereotype (and potential novel chimeric AAVs derived from AAV9) is therefore of great interest. If successful, it could improve CRISPR/Cas9 therapeutics and potentially be used for treatment of neural diseases and disorders that could not previously be targeted.

The future for CRISPR/Cas9 gene-targeted animals is expanding. More precise techniques and alternative Cas proteins (*e.g.*, saCas9[942,943], Cas12[944], Cas13[945]) allow for increased specificity and alternative targets, improving the gene-editing toolbox. Further, CRISPR/Cas9 components can be virally packaged for delivery and can be coupled with genetically engineered lines (*e.g.*, Cre-lox lines[946]) to analyze and tease apart molecular mechanisms in specific tissues or cells. Three techniques were used successfully throughout this dissertation to assess specific hypotheses. Each CRIPSR/Cas9 technique applied was tailored to its specific Aim, and each came with its own set of advantages and limitations (**Table 11**). While the variety of techniques for gene-targeting keeps growing, careful methodology selection and project design like those applied herein can allow for CRISPR/Cas9 to be exploited and utilized for a wide array of translational preclinical pharmacology research.

5.3 FINAL CONCLUSIONS

LncRNAs have the ability to regulate ethanol drinking. Of the six ethanol-responsive, neuroimmune-linked lncRNA genes researched, *Tx2*, *Pitt1*, *Pitt2*, *Pitt3*, *Pitt4*, and *Gas5*, all six demonstrated the ability to alter ethanol drinking behavior in C57BL/6J mice. These data presented within this dissertation demonstrates that lncRNAs act as determinants of ethanol consumption and ethanol-related behaviors. These data increase the number of individual lncRNAs functionally assessed for alcohol-related phenotypes and pushes the AUD field forward by laying down a foundation on which future projects can be built.

Appendix A *Tx2* sgRNA Off-Target Analysis Information

Appendix Table 1 Off target site analysis for *Tx2* sgRNA1. The top 14 scoring off targets based on the MIT Off Target (mitOfftarget) Score for the truncated[947] *Tx2* sgRNA1 (ATTTGCAATTCTCTTCCA GGG) were analyzed by PCR/Sanger sequencing. Note: sgRNA1 Off Target (OT) 11 failed to amplify and could not be analyzed. The protospacer adjacent motif sequence is underlined.

Off Target	Off Target Seq	Mismatch Count	mitOff-target Score	Chromosome	Start	End	Locus Description	F primer	R primer	amplicon
OT1	AAATT TGGAA TTCTC TTCCA GGA	2	7.09	Chr12	47324 365	47324 387	intergenic: Gm25051-Gm1818	TGCCA TCAAC AAAAT GTGTC A	TTGCA GAAGC CAACA CCTCA	484
OT2	CAGTT TCCAA TTCTC TTCCA AGG	2	4.05	Chr6	98640 082	98640 104	intergenic: Gm24387-Foxp1	TCCCA CCTTCC TTCCTT CCT	GAACC CTTCCT CTGTG GCTC	360
OT3	CCCTT TGCAT TTCTC TTCCA CAG	3	2.43	Chr13	35156 631	35156 653	intergenic: Eci2-Gm22674	ACTTG AGTTG AGTGT GCCCC	AGGTC CAGGT TTCTGT TGCT	397
OT4	CCTTT TGCAC TTCTC TTCCA TAG	3	2.43	ChrX	16117 6304	16117 6326	intron: Scml2	GTCTG CTTGC ATTCAT GGCA	ACATT CTGCCT GGTTT GAACA	411
OT5	CAATT CTCAA TTCTC TTCCA AGA	2	2.16	Chr11	63584 04	46358 426	intron: Itk	GGCCT CATGT ACACC CACAA	ACCCA CTTGA AAGCC AACCA	376
OT6	CACTT TTGAA TTCTC TTCCA GAG	3	1.63	Chr13	18315 910	18315 932	intron: Pou6f2	CCCAG GGCAT CAGAG GAAAG	TGTCCT CTCCTA GCTCA GGG	495
OT7	GAACT TGCGA TTCTC TTCCA GAG	3	1.63	Chr14	45308 151	45308 173	intron: Ero1l	AGGAT AGCCA AGCGT CATGG	ACCTCT CCAGT CCCCA CTTT	421
OT8	CAGCT TGCTA TTCTC TTCCA GGG	3	1.53	Chr8	11033 3585	11033 3607	intron: Hydin	TGTAA GTCCC GGGAA ACAGC	CAAGG CAAGG AAGGG TAGGG	306
OT9	CCATT TGCTT TTCTC TTCCA TAG	3	1.50	Chr12	10127 681	10127 703	intergenic: Gm22845-Nt5c1b	CCCCTC ATTGTC ACTGC CTT	TCATG CTGCTT GAAAC CCCC	273
OT10	TCATT TGCAA TTCTC TTCCT AGG	3	1.49	Chr9	29904 398	29904 420	intron: Ntm	CCAGG TCACCT CAGGT TCTC	TAAGA GCTAG GGACA GGCCA	343

OT11	CACTA TGCAA GTCTC TTCCA GAG	3	1.46	Chr1	11913 5305	11913 5327	intergenic: Gm26831-Gm8321	GCCAG CCTGG TCTAC AAAGT	ACCCA GATTC GGAGC ATGTG	348
OY12	CAATT TCTAT TTCTC TTCCA TGA	3	1.46	Chr2	94891 919	94891 941	intergenic: Gm26396-Gm13795	GCCTG AAATT GCCTT ACCCC	TGAGC CAAAC CACAT GGGAA	368
OT13	CAACT TGCTG TTCTC TTCCA GAG	3	1.43	Chr14	77718 314	77718 336	intron: Enox1	AAGAG AAGAG CGTGC AGAGG	GGGTG TTTTGC CTGCTT GTT	300
OT14	CAAAT TGAAA TTCTC TTCCC AGG	3	1.40	Chr3	85895 899	85895 921	intergenic: Glt28d2/Arfip1-Gm26204	GCCTG GCAGA ATCTA GCCTT	GTCTG GAACT GGAAG CAGCT	413

Appendix Table 2 Off target site analysis for *Tx2* sgRNA2. The top 10 scoring off targets (OT) based on the MIT Off Target (mitOfftarget) Score for the truncated[947] *Tx2* sgRNA2 (AATAAACAGGTGTGACGG TGG) were analyzed by PCR/Sanger sequencing. The protospacer adjacent motif sequence is underlined.

Off Target	Off Target Seq	Mismatch Count	mitOff-target Score	Chromosome	Start	End	Locus Description	F primer	R primer	amplicon
OT1	AGACT AAACA GGTGT GAAGG GGA	2	2.39	Chr8	92814 712	92814 734	intergenic: Gm3272-Mmp2	AGGAG AGGGA GAAGG CAGAG	AGAGA GACTG GAGGC TGAGG	442
OT2	ATGAG AAACT GGTGT GACGG AGG	4	1.24	Chr11	50448 43	50448 65	Intergenic: Ap1b1-Gas2l1	ATTCTC CATGA GCCCT CCCT	TACTG GAGGG AGATG AGCCC	384
OT3	AGCAT AGACA GGTGT GACGA GGG	3	0.94	Chr10	44451 590	44451 612	intron: Prdm1	GGCCA CTCTCA TGACA GGTG	CCTGG GACCG GAAAG TGTAG	379
OT4	AGAAG AACCA GGTGT GAAGG GGG	3	0.58	Chr7	98826 975	98826 997	intergenic: Prkrir-Wnt11	TTGGA TTCTCG TCAGG CCTG	ACACC CTGAA CAGTC TCCCT	275
OT5	AGAAA AATCA GGTGT GATGG AGG	3	0.58	Chr9	51509 342	51509 364	intergenic:1810046K07Rik-Gm7293	CTGTA AGAGG GAGCG GATGC	GTCCT GGGAA AGCCA CCTAC	405
	ACAGA ATTCA GGTGT GACGG AGG	5	0.57	Chr14	52264 028	52264 050	exon: Rab2b	Not analyzed (5 mismatches)		
OT6	AGAAA AGCAA GGTGT GACGG TGG	4	0.54	Chr15	63661 274	63661 296	intergenic: Gm5473-Gsdmc	GGGTG CTTATG TGTGC ATGC	GAGCG TATGG GTCTG GGAAG	301

OT7	CAGATAAACAGGTGTGACCGCGG	4	0.52	Chr5	135447515	135447537	intron: Hip1	CAGGCTCTCCTTTCCTTGGG	TCCTTCTGTCATGGGTCCCA	257
	AAATCAAGGAGGTGTGACGGGGG	5	0.51	Chr9	50255933	50255955	intergenic: Gm8907-Rpl10-ps3	Not analyzed (5 mismatches)		
OT8	ATAATACACGTGTGTGACGGTGG	4	0.50	Chr14	32905122	32905144	intron: Vstm4	TCTCTGTGCATGTCCACCAC	AGGCTCTGTGACTTGGATGC	426
OT9	ATAAAAATCAGGTGTGACAGAGG	4	0.50	Chr9	43998520	43998542	intergenic: Gm23326-Thy1	GATCAGCCTGGGAGTCCAAG	GCCAACAAGACCTATTGGCC	292
OT10	AGAATACAGAGTTGTGACGGAGG	3	0.50	Chr19	38131365	38131387	intergenic: Rbp4-Pde6c	CTGCCCGGATACAGGACATC	TTCCCAGGCGAACAGAACTC	405

Bibliography

1 McGovern, P. E. *et al.* Fermented beverages of pre-and proto-historic China. *Proceedings of the National Academy of Sciences* **101**, 17593-17598 (2004).

2 McGovern, P. *et al.* Early neolithic wine of Georgia in the South Caucasus. *Proceedings of the National Academy of Sciences* **114**, E10309-E10318 (2017).

3 Correa-Ascencio, M., Robertson, I. G., Cabrera-Cortés, O., Cabrera-Castro, R. & Evershed, R. P. Pulque production from fermented agave sap as a dietary supplement in Prehispanic Mesoamerica. *Proceedings of the National Academy of Sciences* **111**, 14223-14228 (2014).

4 Logan, A. L., Hastorf, C. A. & Pearsall, D. M. "Let's drink together": Early ceremonial use of maize in the Titicaca Basin. *Latin American Antiquity* **23**, 235-258 (2012).

5 Smith, R. C., Parker, E. S. & Noble, E. P. Alcohol and affect in dyadic social interaction. *Psychosomatic Medicine* (1975).

6 Diao, Y. *et al.* Long-term low-dose ethanol intake improves healthspan and resists high-fat diet-induced obesity in mice. *Aging (Albany NY)* **12**, 13128 (2020).

7 Fernandez-Sola, J. *et al.* Low-dose ethanol consumption allows strength recovery in chronic alcoholic myopathy. *QJM* **93**, 35-40 (2000).

8 St Leger, A., Cochrane, A. & Moore, F. Factors associated with cardiac mortality in developed countries with particular reference to the consumption of wine. *The Lancet* **313**, 1017-1020 (1979).

9 Topiwala, A. *et al.* Moderate alcohol consumption as risk factor for adverse brain outcomes and cognitive decline: longitudinal cohort study. *bmj* **357** (2017).

10 Beulens, J. *et al.* Alcohol consumption and risk of type 2 diabetes in European men and women: influence of beverage type and body sizeThe EPIC–InterAct study. *Journal of internal medicine* **272**, 358-370 (2012).

11 Ouchi, E. *et al.* Frequent alcohol drinking is associated with lower prevalence of self-reported common cold: a retrospective study. *BMC public health* **12**, 1-8 (2012).

12 Thakur, L. *et al.* Alcohol consumption and development of acute respiratory distress syndrome: a population-based study. *International journal of environmental research and public health* **6**, 2426-2435 (2009).

13 Łowicka-Smolarek, M. *et al.* Analysis of Patients with Alcohol Dependence Treated in Silesian Intensive Care Units. *International Journal of Environmental Research and Public Health* **19**, 5914 (2022).

14 Saitz, R., Ghali, W. A. & Moskowitz, M. A. The impact of alcohol-related diagnoses on pneumonia outcomes. *Archives of internal medicine* **157**, 1446-1452 (1997).

15 Baum, M. K. *et al.* Alcohol use accelerates HIV disease progression. *AIDS research and human retroviruses* **26**, 511-518 (2010).

16 Delgado-Rodríguez, M., Gómez-Ortega, A., Mariscal-Ortiz, M., Palma-Pérez, S. & Sillero-Arenas, M. Alcohol drinking as a predictor of intensive care and hospital mortality in general surgery: a prospective study. *Addiction* **98**, 611-616 (2003).

17 Dry, M. J., Burns, N. R., Nettelbeck, T., Farquharson, A. L. & White, J. M. Dose-related effects of alcohol on cognitive functioning. *PloS one* **7**, e50977 (2012).

18 Bisby, J. A., Leitz, J. R., Morgan, C. J. & Curran, H. V. Decreases in recollective experience following acute alcohol: A dose–response study. *Psychopharmacology* **208**, 67-74 (2010).
19 Jääskeläinen, I. P., Schröger, E. & Näätänen, R. Electrophysiological indices of acute effects of ethanol on involuntary attention shifting. *Psychopharmacology* **141**, 16-21 (1999).
20 Breitmeier, D., Seeland-Schulze, I., Hecker, H. & Schneider, U. CLINICAL STUDY: The influence of blood alcohol concentrations of around 0.03% on neuropsychological functions—a double-blind, placebo-controlled investigation. *Addiction biology* **12**, 183-189 (2007).
21 Cui, C. & Koob, G. F. Titrating tipsy targets: the neurobiology of low-dose alcohol. *Trends in pharmacological sciences* **38**, 556-568 (2017).
22 Griswold, M. G. *et al.* Alcohol use and burden for 195 countries and territories, 1990–2016: a systematic analysis for the Global Burden of Disease Study 2016. *The Lancet* **392**, 1015-1035 (2018).
23 Organization, W. H. *Global status report on alcohol and health 2018*. (World Health Organization, 2019).
24 Centers for Disease Control and Prevention (CDC). Alcohol and Public Health: Alcohol-Related Disease Impact (ARDI). Annual Average for United States 2011–2015 Alcohol-Attributable Deaths Due to Excessive Alcohol Use, All Ages. (2020).
25 Mokdad, A. H., Marks, J. S., Stroup, D. F. & Gerberding, J. L. Correction: actual causes of death in the United States, 2000. *Jama* **293**, 293-294 (2005).
26 Mokdad, A. H., Marks, J. S., Stroup, D. F. & Gerberding, J. L. Actual causes of death in the United States, 2000. *Jama* **291**, 1238-1245 (2004).
27 Edition, F. Diagnostic and statistical manual of mental disorders. *Am Psychiatric Assoc* **21**, 591-643 (2013).
28 Organization, W. H. International statistical classification of diseases and related health problems, Tenth revision, Fifth edition, 2016. *World Health Organization* (2015).
29 Carvalho, A. F., Heilig, M., Perez, A., Probst, C. & Rehm, J. Alcohol use disorders. *The Lancet* **394**, 781-792 (2019).
30 Whiteford, H. A. *et al.* Global burden of disease attributable to mental and substance use disorders: findings from the Global Burden of Disease Study 2010. *The lancet* **382**, 1575-1586 (2013).
31 Rehm, J. *et al.* Global burden of disease and injury and economic cost attributable to alcohol use and alcohol-use disorders. *The lancet* **373**, 2223-2233 (2009).
32 SAMHSA, C. f. B. H. S. a. Q. *National Survey on Drug Use and Health*, <https://www.samhsa.gov/data/sites/default/files/reports/rpt29394/NSDUHDetailedTabs2019/NSDUHDetTabsSect5pe2019.htm#tab5-4a> (2019).
33 Collaborators, G. R. F. Global, regional, and national comparative risk assessment of 79 behavioural, environmental and occupational, and metabolic risks or clusters of risks in 188 countries, 1990–2013: a systematic analysis for the Global Burden of Disease Study 2013. *Lancet (London, England)* **386**, 2287 (2015).
34 Tucker, J. A., Cheong, J., James, T. G., Jung, S. & Chandler, S. D. Preresolution drinking problem severity profiles associated with stable moderation outcomes of natural recovery attempts. *Alcoholism: Clinical and Experimental Research* **44**, 738-745 (2020).

35 Dawson, D. A. *et al.* Recovery from DSM-IV alcohol dependence: United States, 2001–2002. *Addiction* **100**, 281-292 (2005).
36 Bischof, G., Rumpf, H. J., Hapke, U., Meyer, C. & John, U. Types of natural recovery from alcohol dependence: a cluster analytic approach. *Addiction* **98**, 1737-1746 (2003).
37 Zhu, S., Wu, J., Hu, J. Non-coding RNA in alcohol use disorder by affecting synaptic plasticity. *Experimental Brain Research*, doi:https://doi.org/10.1007/s00221-022-06305-x (2022).
38 Cargiulo, T. Understanding the health impact of alcohol dependence. *American journal of health-system pharmacy* **64**, S5-S11 (2007).
39 De Graaf, R., Bijl, R. V., Smit, F., Vollebergh, W. A. & Spijker, J. Risk factors for 12-month comorbidity of mood, anxiety, and substance use disorders: findings from the Netherlands Mental Health Survey and Incidence Study. *American Journal of Psychiatry* **159**, 620-629 (2002).
40 Grant, B. F. *et al.* Prevalence and co-occurrence of substance use disorders and independentmood and anxiety disorders: Results from the national epidemiologic survey on alcohol and relatedconditions. *Archives of general psychiatry* **61**, 807-816 (2004).
41 Gazzieri, D. *et al.* Ethanol dilates coronary arteries and increases coronary flow via transient receptor potential vanilloid 1 and calcitonin gene-related peptide. *Cardiovascular research* **70**, 589-599 (2006).
42 Tawakol, A., Omland, T. & Creager, M. A. Direct effect of ethanol on human vascular function. *American Journal of Physiology-Heart and Circulatory Physiology* **286**, H2468-H2473 (2004).
43 De Oliveira e Silva, E. R. *et al.* Alcohol consumption raises HDL cholesterol levels by increasing the transport rate of apolipoproteins AI and A-II. *Circulation* **102**, 2347-2352 (2000).
44 Marmillot, P. *et al.* Long-term ethanol consumption impairs reverse cholesterol transport function of high-density lipoproteins by depleting high-density lipoprotein sphingomyelin both in rats and in humans. *Metabolism* **56**, 947-953 (2007).
45 Cardet, J. C. *et al.* Alcohol-induced respiratory symptoms are common in patients with aspirin exacerbated respiratory disease. *The Journal of Allergy and Clinical Immunology: In Practice* **2**, 208-213. e202 (2014).
46 Myou, S. *et al.* Effect of ethanol on airway caliber and nonspecific bronchial responsiveness in patients with alcohol-induced asthma. *Allergy* **51**, 52-55 (1996).
47 Ting, S., Rauls, D., Ashbaugh, P. & Mansfield, L. Ethanol-induced urticaria: a case report. *Annals of allergy* **60**, 527-530 (1988).
48 Ramachandran, V., Cline, A., Summey, B. T. & Feldman, S. R. Systemic contact dermatitis related to alcoholic beverage consumption. *Dermatology online journal* **25** (2019).
49 Wolverton, W. & Gada, S. Systemic contact dermatitis to ethanol. *The Journal of Allergy and Clinical Immunology: In Practice* **1**, 195-196 (2013).
50 Watanabe, T. Mechanism of ethanol-induced bronchoconstriction in Japanese asthmatic patients. *Arerugi* **40**, 1210-1217 (1991).
51 Bouchier, I. A., Hislop, W. & Prescott, R. J. A prospective study of alcoholic liver disease and mortality. *Journal of hepatology* **16**, 290-297 (1992).
52 Becker, U. *et al.* Prediction of risk of liver disease by alcohol intake, sex, and age: a prospective population study. *Hepatology* **23**, 1025-1029 (1996).

53 Bellentani, S. *et al.* Drinking habits as cofactors of risk for alcohol induced liver damage. *Gut* **41**, 845-850 (1997).
54 Koch, O. R. *et al.* Role of the life span determinant P66shcA in ethanol-induced liver damage. *Laboratory investigation* **88**, 750-760 (2008).
55 Wang, A.-L. *et al.* A dual effect of N-acetylcysteine on acute ethanol-induced liver damage in mice. *Hepatology research* **34**, 199-206 (2006).
56 Nakano, M., Worner, T. M. & Lieber, C. S. Perivenular fibrosis in alcoholic liver injury: ultrastructure and histologic progression. *Gastroenterology* **83**, 777-785 (1982).
57 Ward, R. J., Lallemand, F. & De Witte, P. Biochemical and neurotransmitter changes implicated in alcohol-induced brain damage in chronic or 'binge drinking'alcohol abuse. *Alcohol & Alcoholism* **44**, 128-135 (2009).
58 Lee, K., Hardt, F., Møller, L., Haubek, A. & Jensen, E. Alcohol-induced brain damage and liver damage in young males. *The Lancet* **314**, 759-761 (1979).
59 Alfonso-Loeches, S., Pascual, M. & Guerri, C. Gender differences in alcohol-induced neurotoxicity and brain damage. *Toxicology* **311**, 27-34 (2013).
60 Page, R. D. & Cleveland, M. F. Cognitive dysfunction and aging among male alcoholics and social drinkers. *Alcoholism: Clinical and Experimental Research* **11**, 376-384 (1987).
61 Harper, C. The neuropathology of alcohol-related brain damage. *Alcohol & Alcoholism* **44**, 136-140 (2009).
62 Tillonen, J., Homann, N., Rautio, M., Jousimies-Somer, H. & Salaspuro, M. Role of Yeasts in the Salivary Acetaldehyde Production From Ethanol Among Risk Groups for Ethanol-Associated Oral Cavity Cancer. *Alcoholism: Clinical and Experimental Research* **23**, 1409-1411, doi:10.1111/j.1530-0277.1999.tb04364.x (1999).
63 Homann, N., Tillonen, J. & Salaspuro, M. Microbially produced acetaldehyde from ethanol may increase the risk of colon cancer via folate deficiency. *International Journal of Cancer* **86**, 169-173, doi:10.1002/(sici)1097-0215(20000415)86:2<169::Aid-ijc4>3.0.Co;2-3 (2000).
64 Malik, D. e. s. & · Rhiannon M. David1, N. J. G.
65 Seitz, H. K. & Stickel, F. Acetaldehyde as an underestimated risk factor for cancer development: role of genetics in ethanol metabolism. *Genes Nutr* **5**, 121-128, doi:10.1007/s12263-009-0154-1 (2010).
66 Rumgay, H. *et al.* Global burden of cancer in 2020 attributable to alcohol consumption: a population-based study. *The Lancet Oncology* **22**, 1071-1080, doi:10.1016/s1470-2045(21)00279-5 (2021).
67 Kokkinakis, M. *et al.* Carcinogenic, ethanol, acetaldehyde and noncarcinogenic higher alcohols, esters, and methanol compounds found in traditional alcoholic beverages. A risk assessment approach. *Toxicol Rep* **7**, 1057-1065, doi:10.1016/j.toxrep.2020.08.017 (2020).
68 Pfeiffer A, H. B., Kaess H. Effect of ethanol and commonly injested alcoholic beverages on gastric emptying and gastrointenstinal transit *The Clinical Investigator* **70**, 5 (1992).
69 Scroggs, R., Abruzzo, M. & Advokat, C. Effects of ethanol on gastrointestinal transit in mice. *Alcohol Clin Exp Res* **10**, 452-456, doi:10.1111/j.1530-0277.1986.tb05123.x (1986).
70 Wegener M, S. J., Dilger U, Coenen C, Wedmann B, Schmidt G. Gastrointestinal transit of solid-liquid meal in chronic alcoholics. *Digestive Diseases and Sciences* **36**, 7 (1991).
71 Bluemel, S. *et al.* Intestinal and hepatic microbiota changes associated with chronic ethanol administration in mice. *Gut Microbes* **11**, 265-275, doi:10.1080/19490976.2019.1595300 (2020).

72 Beiranvand, M. & Bahramikia, S. Ameliorating and protective effects mesalazine on ethanol-induced gastric ulcers in experimental rats. *Eur J Pharmacol* **888**, 173573, doi:10.1016/j.ejphar.2020.173573 (2020).
73 Wong SH, C. C., Ogle CW. Protection by zinc sulphate against ethanol-induced ulceration: Preservation of the Gastric Mucosal Barrier. *Pharmacology* **33**, 9 (1986).
74 Gould, L., Zahir, M., DeMartino, A., Gomprecht, R. F. & Jaynal, F. Hemodynamic effects of ethanol in patients with cardiac disease. *Quarterly journal of studies on alcohol* **33**, 714-721 (1972).
75 Regan, T. J. & Morvai, V. Experimental models for studying the effects of ethanol on the myocardium. *Acta Medica Scandinavica* **221**, 107-113 (1987).
76 Richardson, P., Wodak, A., Atkinson, L., Saunders, J. & Jewitt, D. Relation between alcohol intake, myocardial enzyme activity, and myocardial function in dilated cardiomyopathy. Evidence for the concept of alcohol induced heart muscle disease. *Heart* **56**, 165-170 (1986).
77 Jones KL, S. D. Recognition of the fetal alcohol syndrome in early infancy. *The Lancet* **302**, 3 (1973).
78 Stratton K, H. C., Battaglia FC. Fetal alcohol syndrome: diagnosis, epidemiology, prevention, and treatment. *National Academies Press* (1996).
79 Williams, J. F., Smith, V. C. & Committee On Substance, A. Fetal Alcohol Spectrum Disorders. *Pediatrics* **136**, e1395-1406, doi:10.1542/peds.2015-3113 (2015).
80 Nixon, S. J., Tivis, R. & Parsons, O. A. Behavioral dysfunction and cognitive efficiency in male and female alcoholics. *Alcoholism: Clinical and Experimental Research* **19**, 577-581 (1995).
81 Dar, M. Central adenosinergic system involvement in ethanol-induced motor incoordination in mice. *Journal of Pharmacology and Experimental Therapeutics* **255**, 9 (1990).
82 VS Barwick, M. D. Adenosinergic modulation of ethanol-induced motor incoordination in the rat motor cortex. *Progress in Neuro-Psychopharmacology and Biological Psychiatry* **22**, 21 (1998).
83 Blednov, Y. A. *et al.* Mutation of the inhibitory ethanol site in GABAA ρ1 receptors promotes tolerance to ethanol-induced motor incoordination. *Neuropharmacology* **123**, 201-209 (2017).
84 Auta, J. *et al.* Essential role for neuronal nitric oxide synthase in acute ethanol-induced motor impairment. *Nitric Oxide* **100-101**, 50-56, doi:10.1016/j.niox.2020.04.003 (2020).
85 Rezayof, A., Shirazi-Zand, Z., Zarrindast, M. R. & Nayer-Nouri, T. Nicotine improves ethanol-induced memory impairment: the role of dorsal hippocampal NMDA receptors. *Life Sci* **86**, 260-266, doi:10.1016/j.lfs.2009.12.008 (2010).
86 S Gönenç, N. U., O Açikgöz, BM Kayatekin, A Sönmez, M Kiray, I Aksu, B Güleçer, A Topçu, I Semin. Effects of melatonin on oxidative stress and spatial memory impairment induced by acute ethanol treatment in rats. *Physiological Research* **54**, 8 (2005).
87 Sanday, L. *et al.* Ethanol-induced memory impairment in a discriminative avoidance task is state-dependent. *Alcohol Clin Exp Res* **37 Suppl 1**, E30-39, doi:10.1111/j.1530-0277.2012.01905.x (2013).
88 Boulouard, M., Lelong, V., Daoust, M. & Naassila, M. Chronic ethanol consumption induces tolerance to the spatial memory impairing effects of acute ethanol administration in rats. *Behavioural brain research* **136**, 239-246 (2002).

89 JW Wright, A. M., JR Reichert, GD Turner, SE Meighan, PC Meighan, JW Harding. Ethanol-induced impairment of spatial memory and brain matrix metalloproteinases. *Brain Research* **963**, 10 (2003).
90 Wu, G. *et al.* Ethanol attenuates sensory stimulus-evoked responses in cerebellar granule cells via activation of GABA(A) receptors in vivo in mice. *Neurosci Lett* **561**, 107-111, doi:10.1016/j.neulet.2013.12.049 (2014).
91 Markwiese, B. J., Acheson, S. K., Levin, E. D., Wilson, W. A. & Swartzwelder, H. S. Differential Effects of Ethanol on Memory in Adolescent and Adult Rats. *Alcoholism: Clinical and Experimental Research* **22**, 416-421, doi:10.1111/j.1530-0277.1998.tb03668.x (1998).
92 Odlaug, B. *et al.* Alcohol dependence, co-occurring conditions and attributable burden. *Alcohol and Alcoholism* **51**, 201-209 (2016).
93 Neighbors, B., Kempton, T. & Forehand, R. Co-occurence of substance abuse with conduct, anxiety, and depression disorders in juvenile delinquents. *Addictive behaviors* **17**, 379-386 (1992).
94 Yao, H. *et al.* Chronic ethanol exposure induced depressive-like behavior in male C57BL/6 N mice by downregulating GluA1. *Physiology & Behavior* **234**, 113387 (2021).
95 Boden, J. M. & Fergusson, D. M. Alcohol and depression. *Addiction* **106**, 906-914 (2011).
96 Ciccocioppo, R. *et al.* Antidepressant-like effect of ethanol revealed in the forced swimming test in Sardinian alcohol-preferring rats. *Psychopharmacology* **144**, 151-157 (1999).
97 Deykin, E. Y., Levy, J. C. & Wells, V. Adolescent depression, alcohol and drug abuse. *American Journal of Public Health* **77**, 178-182 (1987).
98 Grant, B. F. & Harford, T. C. Comorbidity between DSM-IV alcohol use disorders and major depression: results of a national survey. *Drug and alcohol dependence* **39**, 197-206 (1995).
99 Doremus, T. L., Brunell, S. C., Varlinskaya, E. I. & Spear, L. P. Anxiogenic effects during withdrawal from acute ethanol in adolescent and adult rats. *Pharmacology Biochemistry and Behavior* **75**, 411-418 (2003).
100 Langen, B., Dietze, S. & Fink, H. Acute effect of ethanol on anxiety and 5-HT in the prefrontal cortex of rats. *Alcohol* **27**, 135-141 (2002).
101 Kushner, M. G., Abrams, K., Thuras, P. & Hanson, K. L. Individual differences predictive of drinking to manage anxiety among non-problem drinkers with panic disorder. *Alcoholism: Clinical and Experimental Research* **24**, 448-458 (2000).
102 LaBuda, C. J. & Fuchs, P. N. Aspirin attenuates the anxiolytic actions of ethanol. *Alcohol* **21**, 287-290 (2000).
103 Chan, T., Wall, R. A. & Sutter, M. C. Chronic ethanol consumption, stress, and hypertension. *Hypertension* **7**, 519-524 (1985).
104 Pando, J. M. *et al.* Ethanol-induced stress response of Staphylococcus aureus. *Canadian journal of microbiology* **63**, 745-757 (2017).
105 Becker, H. C. Influence of stress associated with chronic alcohol exposure on drinking. *Neuropharmacology* **122**, 115-126 (2017).
106 Colrain, I. M., Nicholas, C. L. & Baker, F. C. Alcohol and the sleeping brain. *Handbook of clinical neurology* **125**, 415-431 (2014).
107 Rundell, O. H., Lester, B. K., Griffiths, W. J. & Williams, H. L. Alcohol and sleep in young adults. *Psychopharmacologia* **26**, 201-218 (1972).

108 Van Reen, E., Jenni, O. G. & Carskadon, M. A. Effects of alcohol on sleep and the sleep electroencephalogram in healthy young women. *Alcoholism: Clinical and Experimental Research* **30**, 974-981 (2006).
109 Chan, J. K., Trinder, J., Andrewes, H. E., Colrain, I. M. & Nicholas, C. L. The acute effects of alcohol on sleep architecture in late adolescence. *Alcoholism: Clinical and Experimental Research* **37**, 1720-1728 (2013).
110 Melchior, M., Prokofyeva, E., Younès, N., Surkan, P. J. & Martins, S. S. Treatment for illegal drug use disorders: the role of comorbid mood and anxiety disorders. *BMC psychiatry* **14**, 1-9 (2014).
111 Pignataro, L., Varodayan, F. P., Tannenholz, L. E. & Harrison, N. L. The regulation of neuronal gene expression by alcohol. *Pharmacology & therapeutics* **124**, 324-335 (2009).
112 Health, N. I. o. (NIH, 2014).
113 Waller, M., McBride, W., Lumeng, L. & Li, T.-K. Initial sensitivity and acute tolerance to ethanol in the P and NP lines of rats. *Pharmacology Biochemistry and Behavior* **19**, 683-686 (1983).
114 Scholz, H., Ramond, J., Singh, C. M. & Heberlein, U. Functional ethanol tolerance in Drosophila. *Neuron* **28**, 261-271 (2000).
115 Becker, H. C. & Lopez, M. F. Increased ethanol drinking after repeated chronic ethanol exposure and withdrawal experience in C57BL/6 mice. *Alcoholism: Clinical and Experimental Research* **28**, 1829-1838 (2004).
116 Moskowitz, G., Chalmers, T. C., Sacks, H. S., Fagerstrom, R. M. & Smith Jr, H. Deficiencies of clinical trials of alcohol withdrawal. *Alcoholism: Clinical and Experimental Research* **7**, 42-46 (1983).
117 Heinz, A. *et al.* Influence of dopaminergic transmission on severity of withdrawal syndrome in alcoholism. *Journal of studies on alcohol* **57**, 471-474 (1996).
118 Boness, C. L., Lane, S. P. & Sher, K. J. Assessment of withdrawal and hangover is confounded in the Alcohol Use Disorder and Associated Disabilities Interview Schedule: Withdrawal prevalence is likely inflated. *Alcoholism: Clinical and Experimental Research* **40**, 1691-1699 (2016).
119 Becker, H. C. Alcohol dependence, withdrawal, and relapse. *Alcohol Research & Health* (2008).
120 Muncie Jr, H. L., Yasinian, Y. & Oge, L. K. Outpatient management of alcohol withdrawal syndrome. *American family physician* **88**, 589-595 (2013).
121 Bayard, M., Mcintyre, J., Hill, K. & Woodside, J. Alcohol withdrawal syndrome. *American family physician* **69**, 1443-1450 (2004).
122 Perry, E. C. Inpatient management of acute alcohol withdrawal syndrome. *CNS drugs* **28**, 401-410 (2014).
123 Hayashida, M. *et al.* Comparative effectiveness and costs of inpatient and outpatient detoxification of patients with mild-to-moderate alcohol withdrawal syndrome. *New England Journal of Medicine* **320**, 358-365 (1989).
124 Mainerova, B. *et al.* Alcohol withdrawal delirium-diagnosis, course and treatment. *Biomedical Papers of the Medical Faculty of Palacky University in Olomouc* **159** (2015).
125 Saitz, R. Unhealthy alcohol use. *New England Journal of Medicine* **352**, 596-607 (2005).
126 Mayo-Smith, M. F. Pharmacological management of alcohol withdrawal: a meta-analysis and evidence-based practice guideline. *Jama* **278**, 144-151 (1997).

127 M Piasecki, T., M Robertson, B. & J Epler, A. Hangover and risk for alcohol use disorders: Existing evidence and potential mechanisms. *Current drug abuse reviews* **3**, 92-102 (2010).
128 RA Johnson, EC Noll & Rodney, W. Survival after a serum ethanol concentration of 1 1/2%. *The Lancet* **320**, 1394 (1982).
129 Sellers, E. M. & Kalant, H. Alcohol intoxication and withdrawal. *New England Journal of Medicine* **294**, 757-762 (1976).
130 A Poklis & Pearson, M. An unusually high blood ethanol level in a living patient. *Clinical Toxicology* **10**, 429-431 (1977).
131 KB Hammond, B. R., DO Rodgerson. Blood ethanol: a report of unusually high levels in a living patient. *JAMA* **226**, 2, doi:10.1001/jama.1973.03230010039009 (1973).
132 Berild, D. & Hasselbalch, H. Survival after a blood alcohol of 1127 mg/dl. *The Lancet* **318**, 363 (1981).
133 Urso, T., Gavaler, J. & Van Thiel, D. Blood ethanol levels in sober alcohol users seen in an emergency room. *Life sciences* **28**, 1053-1056 (1981).
134 Harris, R. & Mihic, S. Alcohol and inhibitory receptors: unexpected specificity from a nonspecific drug. *Proceedings of the National Academy of Sciences* **101**, 2-3 (2004).
135 Fairbanks, J. *et al.* in *Mayo Clinic Proceedings.* 1964-1977 (Elsevier).
136 Kim, Y., Hack, L. M., Ahn, E. S. & Kim, J. Practical outpatient pharmacotherapy for alcohol use disorder. *Drugs in context* **7** (2018).
137 SAMHSA, C. f. B. H. S. a. Q. *National Survey on Drug Use and Health*, <https://www.datafiles.samhsa.gov/dataset/national-survey-drug-use-and-health-2020-nsduh-2020-ds0001> (2020).
138 Mark, T. L., Kassed, C. A., Vandivort-Warren, R., Levit, K. R. & Kranzler, H. R. Alcohol and opioid dependence medications: prescription trends, overall and by physician specialty. *Drug and alcohol dependence* **99**, 345-349 (2009).
139 Harris, A. H., Kivlahan, D. R., Bowe, T. & Humphreys, K. N. Pharmacotherapy of alcohol use disorders in the Veterans Health Administration. *Psychiatric Services* **61**, 392-398 (2010).
140 Kalk, N. J. & Lingford-Hughes, A. R. The clinical pharmacology of acamprosate. *British journal of clinical pharmacology* **77**, 315-323 (2014).
141 Littleton, J. Acamprosate in alcohol dependence: how does it work? *Addiction* **90**, 1179-1188 (1995).
142 Saivin, S. *et al.* Clinical pharmacokinetics of acamprosate. *Clinical pharmacokinetics* **35**, 331-345 (1998).
143 Sass, H., Potgieter, A. & Lehert, P. Results from a pooled analysis of 11 European trials comparing acamprosate and placebo in the treatment of alcohol dependence. *Alcohol Alcohol* **30**, 551 (1995).
144 Paille, F. M. *et al.* Double-blind randomized multicentre trial of acamprosate in maintaining abstinence from alcohol. *Alcohol and Alcoholism* **30**, 239-247 (1995).
145 Whitworth, A. B. *et al.* Comparison of acamprosate and placebo in long-term treatment of alcohol dependence. *The Lancet* **347**, 1438-1442 (1996).
146 Poldrugo, F., Chabac, S. & Lehert, P. Acamprosate in the long-term treatment of alcoholism: is its use recommended within the psycho-social approach. *Alcohol Clin Exp Res* **18**, 43A (1994).

147 Pelc, I., Bon, O. L., Verbanck, P., Lehert, P. & Opsomer, L. in *Novel pharmacological interventions for alcoholism* 348-352 (Springer, 1992).
148 Poldrugo, F. Acamprosate treatment in a long-term community-based alcohol rehabilitation programme. *Addiction* **92**, 1537-1546 (1997).
149 Rösner, S. *et al.* Acamprosate for alcohol dependence. *Cochrane Database of Systematic Reviews* (2010).
150 Bouza C, Magro A, Muñoz A & M, A. J. Efficacy and safety of naltrexone and acamprosate in the treatment of alcohol dependence: a systematic review. *Addiction* **99**, 811-828 (2004).
151 Mann, K., Lehert, P. & Morgan, M. Y. The efficacy of acamprosate in the maintenance of abstinence in alcohol-dependent individuals: results of a meta-analysis. *Alcoholism: Clinical and Experimental Research* **28**, 51-63 (2004).
152 Kranzler, H. R. & Van Kirk, J. Efficacy of naltrexone and acamprosate for alcoholism treatment: a meta-analysis. *Alcoholism: Clinical and Experimental Research* **25**, 1335-1341 (2001).
153 Mason, B. J. & Ownby, R. L. Acamprosate for the treatment of alcohol dependence: a review of double-blind, placebo-controlled trials. *CNS spectrums* **5**, 58-69 (2000).
154 Rösner, S., Leucht, S., Lehert, P. & Soyka, M. Acamprosate supports abstinence, naltrexone prevents excessive drinking: evidence from a meta-analysis with unreported outcomes. *Journal of Psychopharmacology* **22**, 11-23 (2008).
155 Mason, B. J. & Heyser, C. J. The neurobiology, clinical efficacy and safety of acamprosate in the treatment of alcohol dependence. *Expert opinion on drug safety* **9**, 177-188 (2010).
156 Donoghue, K. *et al.* The efficacy of acamprosate and naltrexone in the treatment of alcohol dependence, Europe versus the rest of the world: a meta-analysis. *Addiction* **110**, 920-930 (2015).
157 Anton, R. F. *et al.* Combined pharmacotherapies and behavioral interventions for alcohol dependence: the COMBINE study: a randomized controlled trial. *Jama* **295**, 2003-2017 (2006).
158 Morley, K. C. *et al.* Naltrexone versus acamprosate in the treatment of alcohol dependence: a multi-centre, randomized, double-blind, placebo-controlled trial. *Addiction* **101**, 1451-1462 (2006).
159 Chick, J., Howlett, H., Morgan, M. & Ritson, B. United Kingdom Multicentre Acamprosate Study (UKMAS): a 6-month prospective study of acamprosate versus placebo in preventing relapse after withdrawal from alcohol. *Alcohol and Alcoholism* **35**, 176-187 (2000).
160 Namkoong, K., Lee, B.-O., Lee, P.-G., Choi, M.-J. & Lee, E. Acamprosate in Korean alcohol-dependent patients: a multi-centre, randomized, double-blind, placebo-controlled study. *Alcohol and alcoholism* **38**, 135-141 (2003).
161 Verheul, R., Lehert, P., Geerlings, P. J., Koeter, M. W. & van den Brink, W. Predictors of acamprosate efficacy: results from a pooled analysis of seven European trials including 1485 alcohol-dependent patients. *Psychopharmacology* **178**, 167-173 (2005).
162 Donoghue, K., Hermann, L., Brobbin, E. & Drummond, C. The rates and measurement of adherence to acamprosate in randomised controlled clinical trials: A systematic review. *PloS one* **17**, e0263350 (2022).
163 Mason, B. J., Goodman, A. M., Chabac, S. & Lehert, P. Effect of oral acamprosate on abstinence in patients with alcohol dependence in a double-blind, placebo-controlled trial: the role of patient motivation. *Journal of psychiatric research* **40**, 383-393 (2006).

164 Gonzalez JP, B. R. Naltrexone: a review of its pharmacodynamics and pharmacokinetic properties and therapeutic efficacy in the management of opioid dependence. *Drugs* **35**, 192-213 (1988).
165 McCaul, M. E., Wand, G. S., Stauffer, R., Lee, S. M. & Rohde, C. A. Naltrexone dampens ethanol-induced cardiovascular and hypothalamic-pituitary-adrenal axis activation. *Neuropsychopharmacology* **25**, 537-547 (2001).
166 Pettinati, H. M. *et al.* The status of naltrexone in the treatment of alcohol dependence: specific effects on heavy drinking. *Journal of clinical psychopharmacology* **26**, 610-625 (2006).
167 O'Malley SS *et al.* Naltrexone and coping skills therapy for alcohol dependence: a controlled study. *Archives of general psychiatry* **49**, 881-887 (1992).
168 Ray, L. A., Krull, J. L. & Leggio, L. The effects of naltrexone among alcohol non-abstainers: results from the COMBINE Study. *Frontiers in psychiatry* **1**, 26 (2010).
169 Krystal, J. H., Cramer, J. A., Krol, W. F., Kirk, G. F. & Rosenheck, R. A. Naltrexone in the treatment of alcohol dependence. *New England Journal of Medicine* **345**, 1734-1739 (2001).
170 Kranzler, H. R., Modesto-Lowe, V. & Van Kirk, J. Naltrexone vs. nefazodone for treatment of alcohol dependence: A placebo-controlled trial. *Neuropsychopharmacology* **22**, 493-503 (2000).
171 Volpicelli, J. R., Clay, K. L., Watson, N. T. & O'Brien, C. P. Naltrexone in the treatment of alcoholism: predicting response to naltrexone. *The Journal of clinical psychiatry* (1995).
172 Volpicelli, J. R., Alterman, A. I., Hayashida, M. & O'Brien, C. P. Naltrexone in the treatment of alcohol dependence. *Archives of general psychiatry* **49**, 876-880 (1992).
173 Chick, J. *et al.* A multicentre, randomized, double-blind, placebo-controlled trial of naltrexone in the treatment of alcohol dependence or abuse. *Alcohol and alcoholism* **35**, 587-593 (2000).
174 Jaffe, A. J. *et al.* Naltrexone, relapse prevention, and supportive therapy with alcoholics: an analysis of patient treatment matching. *Journal of consulting and clinical psychology* **64**, 1044 (1996).
175 Jørgensen, C. H., Pedersen, B. & Tønnesen, H. The efficacy of disulfiram for the treatment of alcohol use disorder. *Alcoholism: Clinical and Experimental Research* **35**, 1749-1758 (2011).
176 Barth, K. S. & Malcolm, R. J. Disulfiram: an old therapeutic with new applications. *CNS & Neurological Disorders-Drug Targets (Formerly Current Drug Targets-CNS & Neurological Disorders)* **9**, 5-12 (2010).
177 Lash, E. & Hack, J. B. Disulfiram and Hypotension in a 53-year-old Woman. *Rhode Island Medical Journal* **102**, 44-46 (2019).
178 De Sousa, A. & De Sousa, A. A one-year pragmatic trial of naltrexone vs disulfiram in the treatment of alcohol dependence. *Alcohol and Alcoholism* **39**, 528-531 (2004).
179 De Sousa, A. & De Sousa, A. An open randomized study comparing disulfiram and acamprosate in the treatment of alcohol dependence. *Alcohol and Alcoholism* **40**, 545-548 (2005).
180 De Sousa, A. & De Sousa, A. An open randomized trial comparing disulfiram and naltrexone in adolescents with alcohol dependence. *Journal of Substance Use* **13**, 382-388 (2008).

181 De Sousa, A. A., De Sousa, J. & Kapoor, H. An open randomized trial comparing disulfiram and topiramate in the treatment of alcohol dependence. *Journal of substance abuse treatment* **34**, 460-463 (2008).
182 Skinner, M. D., Lahmek, P., Pham, H. & Aubin, H.-J. Disulfiram efficacy in the treatment of alcohol dependence: a meta-analysis. *PloS one* **9**, e87366 (2014).
183 Niederhofer, H. & Staffen, W. Comparison of disulfiram and placebo in treatment of alcohol dependence of adolescents. *Drug and Alcohol Review* **22**, 295-297 (2003).
184 Laaksonen, E., Koski-Jännes, A., Salaspuro, M., Ahtinen, H. & Alho, H. A randomized, multicentre, open-label, comparative trial of disulfiram, naltrexone and acamprosate in the treatment of alcohol dependence. *Alcohol & Alcoholism* **43**, 53-61 (2008).
185 Fuller, R. K. *et al.* Disulfiram treatment of alcoholism: A Veterans Administration cooperative study. *Jama* **256**, 1449-1455 (1986).
186 Ulrichsen, J., Nielsen, M. K. & Ulrichsen, M. Disulfiram in severe alcoholism—An open controlled study. *Nordic journal of psychiatry* **64**, 356-362 (2010).
187 Huffman, J. C. & Stern, T. A. Disulfiram use in an elderly man with alcoholism and heart disease: a discussion. *Primary Care Companion to the Journal of Clinical Psychiatry* **5**, 41 (2003).
188 Nucifora, G., Cassin, M., Brun, F. & Nicolosi, G. L. Anterior myocardial infarction in a chronic alcoholic man on disulfiram therapy: a case report. *Italian Heart journal. Supplement: Official Journal of the Italian Federation of Cardiology* **5**, 900-904 (2004).
189 Mohapatra, S., Sahoo, M. R. & Rath, N. Disulfiram-induced neuropathy: a case report. *General Hospital Psychiatry* **37**, 97. e95-97. e96 (2015).
190 Bevilacqua, J. A., Díaz, M., Díaz, V., Silva, C. & Fruns, M. Disulfiram neuropathy. Report of 3 cases. *Revista Medica de Chile* **130**, 1037-1042 (2002).
191 Dupuy, O. *et al.* Disulfiram (Esperal) toxicity. Apropos of 3 original cases. *La Revue de Medecine Interne* **16**, 67-72 (1995).
192 Kulkarni, R. R., Pradeep, A. & Bairy, B. K. Disulfiram-induced combined irreversible anterior ischemic optic neuropathy and reversible peripheral neuropathy: a prospective case report and review of the literature. *The Journal of neuropsychiatry and clinical neurosciences* **25**, 339-342 (2013).
193 Orakzai, A., Guerin, M. & Beatty, S. Disulfiram-induced transient optic and peripheral neuropathy: a case report. *Irish journal of medical science* **176**, 319-321 (2007).
194 Alonzo, M. M., Lewis, T. V. & Miller, J. L. Disulfiram-like reaction with metronidazole: an unsuspected culprit. *The Journal of Pediatric Pharmacology and Therapeutics* **24**, 445-449 (2019).
195 Penick SB & Carrier RN, S. J. Metronidazole in the treatment of alcoholism. *American Journal of Psychiatry* **125**, 1063-1066 (1969).
196 Taylor, J. Metronidazole--a new agent for combined somatic and psychic therapy of alcoholism. A case study and preliminary report. *Bulletin of the Los Angeles Neurological Society* **29**, 158-162 (1964).
197 Goodwin, D. Metronidazole in the treatment of alcoholism: a negative report. *American Journal of Psychiatry* **123**, 1276-1278 (1967).
198 Lehmann, H., Ban, T. & Naltchayan, E. Metronidazole in the treatment of the alcoholic. *European Neurology* **152**, 395-401 (1966).

199 Semer, J., Friedland, P., Vaisberg, M. & Greenberg, A. The use of metronidazole in the treatment of alcoholism: a pilot study. *American Journal of Psychiatry* **123**, 722-724 (1966).
200 Santhakumar, V., Wallner, M. & Otis, T. S. Ethanol acts directly on extrasynaptic subtypes of GABAA receptors to increase tonic inhibition. *Alcohol* **41**, 211-221 (2007).
201 Suzdak, P. D., Paul, S. M. & Crawley, J. N. Effects of Ro15-4513 and other benzodiazepine receptor inverse agonists on alcohol-induced intoxication in the rat. *Journal of Pharmacology and Experimental Therapeutics* **245**, 880-886 (1988).
202 Mhatre, M., Mehta, A. K. & Ticku, M. K. Chronic ethanol administration increases the binding of the benzodiazepine inverse agonist and alcohol antagonist [3H] RO15-4513 in rat brain. *European journal of pharmacology* **153**, 141-145 (1988).
203 Linden, A.-M. *et al.* Ro 15-4513 antagonizes alcohol-induced sedation in mice through αβγ2-type GABAA receptors. *Frontiers in neuroscience* **5**, 3 (2011).
204 Pym, L., Cook, S., Rosahl, T., McKernan, R. & Atack, J. Selective labelling of diazepam-insensitive GABAA receptors in vivo using [3H] Ro 15-4513. *British journal of pharmacology* **146**, 817-825 (2005).
205 Shen, Y. *et al.* Dihydromyricetin as a novel anti-alcohol intoxication medication. *Journal of Neuroscience* **32**, 390-401 (2012).
206 Getachew, B., Csoka, A. B. & Tizabi, Y. Dihydromyricetin Protects Against Ethanol-Induced Toxicity in SH-SY5Y Cell Line: Role of GABAA Receptor. *Neurotoxicity Research* **40**, 892-899 (2022).
207 Carry, E. *et al.* Identification of dihydromyricetin and metabolites in serum and brain associated with acute anti-ethanol intoxicating effects in mice. *International journal of molecular sciences* **22**, 7460 (2021).
208 Myrick, H. *et al.* A double-blind trial of gabapentin versus lorazepam in the treatment of alcohol withdrawal. *Alcoholism: Clinical and Experimental Research* **33**, 1582-1588 (2009).
209 Mariani, J. J., Rosenthal, R. N., Tross, S., Singh, P. & Anand, O. P. A randomized, open-label, controlled trial of gabapentin and phenobarbital in the treatment of alcohol withdrawal. *American Journal on Addictions* **15**, 76-84 (2006).
210 Furieri, F. A. & Nakamura-Palacios, E. M. Gabapentin reduces alcohol consumption and craving: a randomized, double-blind, placebo-controlled trial. *Journal of Clinical Psychiatry* **68**, 1691 (2007).
211 Mason, B. J. *et al.* Gabapentin treatment for alcohol dependence: a randomized clinical trial. *JAMA internal medicine* **174**, 70-77 (2014).
212 Kranzler, H. R., Feinn, R., Morris, P. & Hartwell, E. E. A meta-analysis of the efficacy of gabapentin for treating alcohol use disorder. *Addiction* **114**, 1547-1555 (2019).
213 Reynolds, K. *et al.* Trends in gabapentin and baclofen exposures reported to US poison centers. *Clinical toxicology* **58**, 763-772 (2020).
214 Saitz, R., Friedman, L. S. & Mayo-Smith, M. F. Alcohol withdrawal. *Journal of general internal medicine* **10**, 479-487 (1995).
215 Alling, C. *et al.* in *Toward a Molecular Basis of Alcohol Use and Abuse* 19-28 (Springer, 1994).
216 Cederbaum, A. I. Alcohol metabolism. *Clinics in liver disease* **16**, 667-685 (2012).
217 Rajendram, R., Rajendram, R. & Preedy, V. R. in *Neuropathology of Drug Addictions and Substance Misuse* 377-388 (Elsevier, 2016).

218 Singh, A. K., Jiang, Y., Gupta, S. & Benlhabib, E. Effects of chronic ethanol drinking on the blood–brain barrier and ensuing neuronal toxicity in alcohol-preferring rats subjected to intraperitoneal LPS injection. *Alcohol & Alcoholism* **42**, 385-399 (2007).
219 Phillips, S. Does ethanol damage the blood-brain barrier? *Journal of the neurological sciences* **50**, 81-87 (1981).
220 Carrino, D. *et al.* Alcohol-induced blood-brain barrier impairment: An in vitro study. *International Journal of Environmental Research and Public Health* **18**, 2683 (2021).
221 Lovinger, D., White, G. & Weight, F. Ethanol (EtOH) inhibition of NMDA-activated ion current is not voltage-dependent and EtOH does not interact with other binding sites on the NMDA receptor/ionophore complex. *FASEB Journal (Federation of American Societies for Experimental Biology);(United States)* **4** (1990).
222 Lovinger, D. M., White, G. & Weight, F. F. Ethanol inhibits NMDA-activated ion current in hippocampal neurons. *Science* **243**, 1721-1724 (1989).
223 Vairappan, B. in *Molecular Aspects of Alcohol and Nutrition* 187-200 (Elsevier, 2016).
224 Nagoshi, C. & Wilson, J. R. Long-term repeatability of human alcohol metabolism, sensitivity and acute tolerance. *Journal of studies on alcohol* **50**, 162-169 (1989).
225 Wilkinson, P. K., Sedman, A. J., Sakmar, E., Kay, D. R. & Wagner, J. G. Pharmacokinetics of ethanol after oral administration in the fasting state. *Journal of pharmacokinetics and biopharmaceutics* **5**, 207-224 (1977).
226 Wiener, S. W., Olmedo, R., Howland, M., Nelson, L. & Hoffman, R. Ethanol elimination kinetics following massive ingestion in an ethanol naive child. *Hum Exp Toxicol* **32**, 775-777, doi:10.1177/0960327112468171 (2013).
227 Holford, N. H. Clinical pharmacokinetics of ethanol. *Clinical pharmacokinetics* **13**, 273-292 (1987).
228 Woo, K. Determination of low molecular weight alcohols including fusel oil in various samples by diethyl ether extraction and capillary gas chromatography. *Journal of AOAC International* **88**, 1419-1427 (2005).
229 Abrahao, K. P., Salinas, A. G. & Lovinger, D. M. Alcohol and the brain: neuronal molecular targets, synapses, and circuits. *Neuron* **96**, 1223-1238 (2017).
230 Allan, A. M. & Harris, R. A. Acute and chronic ethanol treatments alter GABA receptor-operated chloride channels. *Pharmacology Biochemistry and Behavior* **27**, 665-670 (1987).
231 RD Schwartz, P. S., SM Paul gamma-Aminobutyric acid (GABA)-and barbiturate-mediated 36Cl-uptake in rat brain synaptoneurosomes: evidence for rapid desensitization of the GABA receptor-coupled chloride ion channel. *Molecular pharmacology* **30**, 419-426 (1986).
232 Roberto, M., Madamba, S. G., Stouffer, D. G., Parsons, L. H. & Siggins, G. R. Increased GABA release in the central amygdala of ethanol-dependent rats. *Journal of Neuroscience* **24**, 10159-10166 (2004).
233 Steffensen, S. C. *et al.* Contingent and non-contingent effects of low-dose ethanol on GABA neuron activity in the ventral tegmental area. *Pharmacology Biochemistry and Behavior* **92**, 68-75 (2009).
234 Wirkner, K., Eberts, C., Poelchen, W., Allgaier, C. & Illes, P. Mechanism of inhibition by ethanol of NMDA and AMPA receptor channel functions in cultured rat cortical neurons. *Naunyn-Schmiedeberg's archives of pharmacology* **362** (2000).
235 Wong, S. M., Fong, E., Tauck, D. L. & Kendig, J. J. Ethanol as a general anesthetic: actions in spinal cord. *European journal of pharmacology* **329**, 121-127 (1997).

236 Nie, Z., Madamba, S. G. & Siggins, G. R. Ethanol inhibits glutamatergic neurotransmission in nucleus accumbens neurons by multiple mechanisms. *Journal of Pharmacology and Experimental Therapeutics* **271**, 1566-1573 (1994).
237 Nagy, J. Alcohol related changes in regulation of NMDA receptor functions. *Current neuropharmacology* **6**, 39-54 (2008).
238 Xu, M., Smothers, C. T., Trudell, J. & Woodward, J. J. Ethanol inhibition of constitutively open N-methyl-D-aspartate receptors. *Journal of Pharmacology and Experimental Therapeutics* **340**, 218-226 (2012).
239 Ye, Q. *et al.* Enhancement of glycine receptor function by ethanol is inversely correlated with molecular volume at position α267. *Journal of Biological Chemistry* **273**, 3314-3319 (1998).
240 Cardoso, R. A. *et al.* Effects of Ethanol on Recombinant Human Neuronal Nicotinic Acetylcholine Receptors Expressed in XenopusOocytes. *Journal of Pharmacology and Experimental Therapeutics* **289**, 774-780 (1999).
241 Campbell, A., Kohl, R. & McBride, W. Serotonin-3 receptor and ethanol-stimulated somatodendritic dopamine release. *Alcohol* **13**, 569-574 (1996).
242 Messing, R. O., Carpenter, C. L., Diamond, I. & Greenberg, D. A. Ethanol regulates calcium channels in clonal neural cells. *Proceedings of the National Academy of Sciences* **83**, 6213-6215 (1986).
243 Di Chiara, G. & Imperato, A. Drugs abused by humans preferentially increase synaptic dopamine concentrations in the mesolimbic system of freely moving rats. *Proceedings of the National Academy of Sciences* **85**, 5274-5278 (1988).
244 Imperato, A. & Di Chiara, G. Preferential stimulation of dopamine release in the nucleus accumbens of freely moving rats by ethanol. *Journal of Pharmacology and Experimental Therapeutics* **239**, 219-228 (1986).
245 Gessa, G. L., Muntoni, F., Collu, M., Vargiu, L. & Mereu, G. Low doses of ethanol activate dopaminergic neurons in the ventral tegmental area. *Brain research* **348**, 201-203 (1985).
246 Thanos, P. K., Dimitrakakis, E. S., Rice, O., Gifford, A. & Volkow, N. D. Ethanol self-administration and ethanol conditioned place preference are reduced in mice lacking cannabinoid CB1 receptors. *Behavioural brain research* **164**, 206-213 (2005).
247 Fernández-Solari, J. *et al.* Alcohol inhibits luteinizing hormone-releasing hormone release by activating the endocannabinoid system. *Proceedings of the National Academy of Sciences* **101**, 3264-3268 (2004).
248 Morikawa, H. & Morrisett, R. A. Ethanol action on dopaminergic neurons in the ventral tegmental area: interaction with intrinsic ion channels and neurotransmitter inputs. *International review of neurobiology* **91**, 235-288 (2010).
249 Weiss, F., Lorang, M. T., Bloom, F. E. & Koob, G. F. Oral alcohol self-administration stimulates dopamine release in the rat nucleus accumbens: genetic and motivational determinants. *Journal of Pharmacology and Experimental Therapeutics* **267**, 250-258 (1993).
250 Theile, J. W., Morikawa, H., Gonzales, R. A. & Morrisett, R. A. Ethanol enhances GABAergic transmission onto dopamine neurons in the ventral tegmental area of the rat. *Alcoholism: Clinical and Experimental Research* **32**, 1040-1048 (2008).
251 Guan, Y. *et al.* GABAergic actions mediate opposite ethanol effects on dopaminergic neurons in the anterior and posterior ventral tegmental area. *Journal of Pharmacology and Experimental Therapeutics* **341**, 33-42 (2012).

252 Tateno, T. & Robinson, H. P. The mechanism of ethanol action on midbrain dopaminergic neuron firing: a dynamic-clamp study of the role of I h and GABAergic synaptic integration. *Journal of neurophysiology* **106**, 1901-1922 (2011).
253 Harrison, N. L. *et al.* Effects of acute alcohol on excitability in the CNS. *Neuropharmacology* **122**, 36-45 (2017).
254 Kerns, R. T. *et al.* Ethanol-responsive brain region expression networks: implications for behavioral responses to acute ethanol in DBA/2J versus C57BL/6J mice. *Journal of Neuroscience* **25**, 2255-2266 (2005).
255 Kim, K.-W., Kim, K., Lee, H. & Suh, B.-C. Ethanol elevates excitability of superior cervical ganglion neurons by inhibiting Kv7 channels in a cell type-specific and PI (4, 5) P2-dependent manner. *International journal of molecular sciences* **20**, 4419 (2019).
256 Badanich, K. A., Mulholland, P. J., Beckley, J. T., Trantham-Davidson, H. & Woodward, J. J. Ethanol reduces neuronal excitability of lateral orbitofrontal cortex neurons via a glycine receptor dependent mechanism. *Neuropsychopharmacology* **38**, 1176-1188 (2013).
257 Criswell, H. E. & Breese, G. R. A conceptualization of integrated actions of ethanol contributing to its GABAmimetic profile: a commentary. *Neuropsychopharmacology* **30**, 1407-1425 (2005).
258 Breese, G. *et al.* Basis of the gabamimetic profile of ethanol. *Alcoholism: clinical and experimental research* **30**, 731-744 (2006).
259 Lobo, I. A. & Harris, R. A. GABAA receptors and alcohol. *Pharmacology Biochemistry and Behavior* **90**, 90-94 (2008).
260 Liljequist, S. & Engel, J. Effects of GABAergic agonists and antagonists on various ethanol-induced behavioral changes. *Psychopharmacology* **78**, 71-75 (1982).
261 ı Stórustovu, S. & Ebert, B. Gaboxadol: in vitro interaction studies with benzodiazepines and ethanol suggest functional selectivity. *European journal of pharmacology* **467**, 49-56 (2003).
262 Ticku, M., Burch, T. & Davis, W. The interactions of ethanol with the benzodiazepine-GABA receptor-ionophore complex. *Pharmacology Biochemistry and Behavior* **18**, 15-18 (1983).
263 Aguayo, L. G., Peoples, R. W., Yeh, H. H. & Yevenes, G. E. GABA-A receptors as molecular sites of ethanol action. Direct or indirect actions? *Current topics in medicinal chemistry* **2**, 869-885 (2002).
264 Aguayo, L. G. Ethanol potentiates the GABAA-activated Cl− current in mouse hippocampal and cortical neurons. *European journal of pharmacology* **187**, 127-130 (1990).
265 Aguayo, L. G., Pancetti, F. C., Klein, R. L. & Harris, R. A. Differential effects of GABAergic ligands in mouse and rat hippocampal neurons. *Brain research* **647**, 97-105 (1994).
266 Grobin, A. C., Matthews, D. B., Devaud, L. L. & Morrow, A. L. The role of GABAA receptors in the acute and chronic effects of ethanol. *Psychopharmacology* **139**, 2-19 (1998).
267 Löf, E., Ericson, M., Stomberg, R. & Söderpalm, B. Characterization of ethanol-induced dopamine elevation in the rat nucleus accumbens. *European journal of pharmacology* **555**, 148-155 (2007).
268 Gianoulakis, C. Influence of the endogenous opioid system on high alcohol consumption and genetic predisposition to alcoholism. *Journal of psychiatry & neuroscience* (2001).

269 Acquas, E., Meloni, M. & Di Chiara, G. Blockade of δ-opioid receptors in the nucleus accumbens prevents ethanol-induced stimulation of dopamine release. *European journal of pharmacology* **230**, 239-241 (1993).
270 Jamensky, N. T. & Gianoulakis, C. Content of Dynorphins and k-Opioid Receptors in Distinct Brain Regions of C57BL/6 and DBA/2 Mice. *Alcoholism: Clinical and Experimental Research* **21**, 1455-1464 (1997).
271 de Waele, J.-P., Kiianmaa, K. & Gianoulakis, C. Distribution of the mu and delta opioid binding sites in the brain of the alcohol-preferring AA and alcohol-avoiding ANA lines of rats. *Journal of Pharmacology and Experimental Therapeutics* **275**, 518-527 (1995).
272 Froehlich, J., Zweifel, M., Harts, J., Lumeng, L. & Li, T.-K. Importance of delta opioid receptors in maintaining high alcohol drinking. *Psychopharmacology* **103**, 467-472 (1991).
273 Hyytiä, P. Involvement of μ-opioid receptors in alcohol drinking by alcohol-preferring AA rats. *Pharmacology Biochemistry and Behavior* **45**, 697-701 (1993).
274 Foddai, M., Dosia, G., Spiga, S. & Diana, M. Acetaldehyde increases dopaminergic neuronal activity in the VTA. *Neuropsychopharmacology* **29**, 530-536 (2004).
275 Quertemont, E. & Didone, V. Role of acetaldehyde in mediating the pharmacological and behavioral effects of alcohol. *Alcohol Research & Health* **29**, 258 (2006).
276 Lewis, M. J. Alcohol reinforcement and neuropharmacological. *Alcohol & Alcoholism* **31**, 17-25 (1996).
277 June, H. L. *et al.* The reinforcing properties of alcohol are mediated by GABAA1 receptors in the ventral pallidum. *Neuropsychopharmacology* **28**, 2124-2137 (2003).
278 Johnson, B. A. & Cowen, P. J. Alcohol-induced reinforcement: Dopamine and 5-HT3 receptor interactions in animals and humans. *Drug Development Research* **30**, 153-169 (1993).
279 Ding, Z.-M., Ingraham, C. M., Rodd, Z. A. & McBride, W. J. The reinforcing effects of ethanol within the nucleus accumbens shell involve activation of local GABA and serotonin receptors. *Journal of Psychopharmacology* **29**, 725-733 (2015).
280 Cui, C., Shurtleff, D. & Harris, R. A. Neuroimmune mechanisms of alcohol and drug addiction. *Int Rev Neurobiol* **118**, 1-12, doi:10.1016/B978-0-12-801284-0.00001-4 (2014).
281 Becker, H. C. & Ron, D. Animal models of excessive alcohol consumption: recent advances and future challenges. *Alcohol (Fayetteville, NY)* **48**, 205 (2014).
282 Mayfield, J., Arends, M. A., Harris, R. A. & Blednov, Y. A. Genes and alcohol consumption: studies with mutant mice. *International review of neurobiology* **126**, 293-355 (2016).
283 Thiele, T. E., Crabbe, J. C. & Boehm, S. L., 2nd. "Drinking in the Dark" (DID): a simple mouse model of binge-like alcohol intake. *Curr Protoc Neurosci* **68**, 9 49 41-49 49 12, doi:10.1002/0471142301.ns0949s68 (2014).
284 Thiele, T. E. & Navarro, M. "Drinking in the dark" (DID) procedures: a model of binge-like ethanol drinking in non-dependent mice. *Alcohol* **48**, 235-241, doi:10.1016/j.alcohol.2013.08.005 (2014).
285 Blizard, D. A., Vandenbergh, D. J., Lionikas, A. & McClearn, G. E. Learning in the 2-bottle alcohol preference test. *Alcoholism: Clinical and Experimental Research* **32**, 2041-2046 (2008).
286 Hwa, L. S. *et al.* Persistent escalation of alcohol drinking in C57BL/6J mice with intermittent access to 20% ethanol. *Alcoholism: Clinical and Experimental Research* **35**, 1938-1947 (2011).

287 Melendez, R. I. Intermittent (every-other-day) drinking induces rapid escalation of ethanol intake and preference in adolescent and adult C57BL/6J mice. *Alcoholism: Clinical and Experimental Research* **35**, 652-658 (2011).
288 Karkhanis, A. N., Rose, J. H., Huggins, K. N., Konstantopoulos, J. K. & Jones, S. R. Chronic intermittent ethanol exposure reduces presynaptic dopamine neurotransmission in the mouse nucleus accumbens. *Drug and alcohol dependence* **150**, 24-30 (2015).
289 Griffin, W. C., Lopez, M. F., Yanke, A. B., Middaugh, L. D. & Becker, H. C. Repeated cycles of chronic intermittent ethanol exposure in mice increases voluntary ethanol drinking and ethanol concentrations in the nucleus accumbens. *Psychopharmacology* **201**, 569-580 (2009).
290 Osterndorff-Kahanek, E., Ponomarev, I., Blednov, Y. A. & Harris, R. A. Gene expression in brain and liver produced by three different regimens of alcohol consumption in mice: comparison with immune activation. *PLoS One* **8**, e59870, doi:10.1371/journal.pone.0059870 (2013).
291 Ozburn, A. R., Harris, R. A. & Blednov, Y. A. Chronic voluntary alcohol consumption results in tolerance to sedative/hypnotic and hypothermic effects of alcohol in hybrid mice. *Pharmacol Biochem Behav* **104**, 33-39, doi:10.1016/j.pbb.2012.12.025 (2013).
292 Rustay, N. R., Wahlsten, D. & Crabbe, J. C. Influence of task parameters on rotarod performance and sensitivity to ethanol in mice. *Behavioural brain research* **141**, 237-249 (2003).
293 Erwin, V. G. & Deitrich, R. A. Genetic selection and characterization of mouse lines for acute functional tolerance to ethanol. *Journal of Pharmacology and Experimental Therapeutics* **279**, 1310-1317 (1996).
294 Walf, A. A. & Frye, C. A. The use of the elevated plus maze as an assay of anxiety-related behavior in rodents. *Nature protocols* **2**, 322-328 (2007).
295 Miller, S. M., Piasecki, C. C. & Lonstein, J. S. Use of the light-dark box to compare the anxiety-related behavior of virgin and postpartum female rats. *Pharmacol Biochem Behav* **100**, 130-137, doi:10.1016/j.pbb.2011.08.002 (2011).
296 Bourin, M. & Hascoet, M. The mouse light/dark box test. *Eur J Pharmacol* **463**, 55-65, doi:10.1016/s0014-2999(03)01274-3 (2003).
297 Kurtuncu, M., Luka, L., Dimitrijevic, N., Uz, T. & Manev, H. Reliability assessment of an automated forced swim test device using two mouse strains. *Journal of neuroscience methods* **149**, 26-30 (2005).
298 Choleris, E., Thomas, A., Kavaliers, M. & Prato, F. A detailed ethological analysis of the mouse open field test: effects of diazepam, chlordiazepoxide and an extremely low frequency pulsed magnetic field. *Neuroscience & Biobehavioral Reviews* **25**, 235-260 (2001).
299 Oscar-Berman, M. & Marinkovic, K. Alcoholism and the brain: an overview. *Alcohol Research & Health* **27**, 125 (2003).
300 Chanraud, S. *et al.* Brain morphometry and cognitive performance in detoxified alcohol-dependents with preserved psychosocial functioning. *Neuropsychopharmacology* **32**, 429-438 (2007).
301 Pfefferbaum, A., Sullivan, E. V., Rosenbloom, M. J., Mathalon, D. H. & Lim, K. O. A controlled study of cortical gray matter and ventricular changes in alcoholic men over a 5-year interval. *Archives of general psychiatry* **55**, 905-912 (1998).

302 Pfefferbaum, A. *et al.* Brain gray and white matter volume loss accelerates with aging in chronic alcoholics: a quantitative MRI study. *Alcoholism: Clinical and Experimental Research* **16**, 1078-1089 (1992).
303 El Marroun, H. *et al.* Alcohol use and brain morphology in adolescence: A longitudinal study in three different cohorts. *European Journal of Neuroscience* **54**, 6012-6026 (2021).
304 Mavromatis, L. A. *et al.* Association Between Brain Structure and Alcohol Use Behaviors in Adults: A Mendelian Randomization and Multiomics Study. *JAMA psychiatry* **79**, 869-878 (2022).
305 Topiwala, A., Ebmeier, K. P., Maullin-Sapey, T. & Nichols, T. E. Alcohol consumption and MRI markers of brain structure and function: Cohort study of 25,378 UK Biobank participants. *NeuroImage: Clinical* **35**, 103066 (2022).
306 Daviet, R. *et al.* Associations between alcohol consumption and gray and white matter volumes in the UK Biobank. *Nature Communications* **13**, 1175 (2022).
307 Wang, Y., Zhao, Y., Nie, H., Liu, C. & Chen, J. Disrupted brain network efficiency and decreased functional connectivity in multi-sensory modality regions in male patients with alcohol use disorder. *Frontiers in human neuroscience* **12**, 513 (2018).
308 Beck, A. *et al.* Effect of brain structure, brain function, and brain connectivity on relapse in alcohol-dependent patients. *Archives of general psychiatry* **69**, 842-852 (2012).
309 Welch, K. A., Carson, A. & Lawrie, S. M. Brain structure in adolescents and young adults with alcohol problems: systematic review of imaging studies. *Alcohol and alcoholism* **48**, 433-444 (2013).
310 Crespi, C. *et al.* Executive impairment in alcohol use disorder reflects structural changes in large-scale brain networks: A joint independent component analysis on gray-matter and white-matter features. *Frontiers in Psychology* **10**, 2479 (2019).
311 Benegal, V., Antony, G., Venkatasubramanian, G. & Jayakumar, P. N. Imaging study: gray matter volume abnormalities and externalizing symptoms in subjects at high risk for alcohol dependence. *Addiction biology* **12**, 122-132 (2007).
312 Dager, A. D. *et al.* Shared genetic factors influence amygdala volumes and risk for alcoholism. *Neuropsychopharmacology* **40**, 412-420 (2015).
313 O'Brien, J. W. & Hill, S. Y. Neural predictors of substance use disorders in Young adulthood. *Psychiatry Research: Neuroimaging* **268**, 22-26 (2017).
314 Drake, J. *et al.* Assessing the role of long noncoding rna in nucleus accumbens in subjects with alcohol dependence. *Alcoholism: Clinical and Experimental Research* **44**, 2468-2480 (2020).
315 Flatscher-Bader, T., Harrison, E., Matsumoto, I. & Wilce, P. A. Genes associated with alcohol abuse and tobacco smoking in the human nucleus accumbens and ventral tegmental area. *Alcoholism: Clinical and Experimental Research* **34**, 1291-1302 (2010).
316 Fowler, A.-K. *et al.* Differential sensitivity of prefrontal cortex and hippocampus to alcohol-induced toxicity. *PLoS One* **9**, e106945 (2014).
317 Mackey, S. *et al.* Mega-analysis of gray matter volume in substance dependence: general and substance-specific regional effects. *American Journal of Psychiatry* **176**, 119-128 (2019).
318 Chye, Y. *et al.* Subcortical surface morphometry in substance dependence: An ENIGMA addiction working group study. *Addiction Biology* **25**, e12830 (2020).

319 Zou, X., Durazzo, T. C. & Meyerhoff, D. J. Regional brain volume changes in alcohol-dependent individuals during short-term and long-term abstinence. *Alcoholism: clinical and experimental research* **42**, 1062-1072 (2018).
320 Makris, N. *et al.* Decreased volume of the brain reward system in alcoholism. *Biological psychiatry* **64**, 192-202 (2008).
321 Moselhy, H. F., Georgiou, G. & Kahn, A. Frontal lobe changes in alcoholism: a review of the literature. *Alcohol and alcoholism* **36**, 357-368 (2001).
322 Sullivan, E. V., Harris, R. A. & Pfefferbaum, A. Alcohol's effects on brain and behavior. *Alcohol Research & Health* (2010).
323 Oscar-Berman, M. & Marinkovic, K. Alcohol: effects on neurobehavioral functions and the brain. *Neuropsychol Rev* **17**, 239-257, doi:10.1007/s11065-007-9038-6 (2007).
324 Pfefferbaum, A., Sullivan, E. V., Mathalon, D. H. & Lim, K. O. Frontal lobe volume loss observed with magnetic resonance imaging in older chronic alcoholics. *Alcoholism: Clinical and Experimental Research* **21**, 521-529 (1997).
325 Crews, F. T. & Boettiger, C. A. Impulsivity, frontal lobes and risk for addiction. *Pharmacology Biochemistry and Behavior* **93**, 237-247 (2009).
326 Goldstein, R. Z. & Volkow, N. D. Dysfunction of the prefrontal cortex in addiction: neuroimaging findings and clinical implications. *Nature reviews neuroscience* **12**, 652-669 (2011).
327 Fein, G. *et al.* Cortical gray matter loss in treatment-naive alcohol dependent individuals. *Alcoholism: Clinical and Experimental Research* **26**, 558-564 (2002).
328 Narendran, R. *et al.* Decreased prefrontal cortical dopamine transmission in alcoholism. *American Journal of Psychiatry* **171**, 881-888 (2014).
329 Klenowski, P. M. Emerging role for the medial prefrontal cortex in alcohol-seeking behaviors. *Addictive behaviors* **77**, 102-106 (2018).
330 Riga, D. *et al.* Optogenetic dissection of medial prefrontal cortex circuitry. *Front Syst Neurosci* **8**, 230, doi:10.3389/fnsys.2014.00230 (2014).
331 Koob, G. F. & Volkow, N. D. Neurocircuitry of addiction. *Neuropsychopharmacology* **35**, 217-238 (2010).
332 Dayas, C. V., Liu, X., Simms, J. A. & Weiss, F. Distinct patterns of neural activation associated with ethanol seeking: effects of naltrexone. *Biological psychiatry* **61**, 979-989 (2007).
333 Arruda-Carvalho, M., Wu, W.-C., Cummings, K. A. & Clem, R. L. Optogenetic examination of prefrontal-amygdala synaptic development. *Journal of Neuroscience* **37**, 2976-2985 (2017).
334 Crofton, E. J. *et al.* Medial prefrontal cortex-basolateral amygdala circuit dysfunction in chronic alcohol-exposed male rats. *Neuropharmacology* **205**, 108912, doi:10.1016/j.neuropharm.2021.108912 (2022).
335 Keistler, C. R. *et al.* Regulation of alcohol extinction and cue-induced reinstatement by specific projections among medial prefrontal cortex, nucleus accumbens, and basolateral amygdala. *Journal of Neuroscience* **37**, 4462-4471 (2017).
336 Kai, Y. *et al.* A medial prefrontal cortex-nucleus acumens corticotropin-releasing factor circuitry for neuropathic pain-increased susceptibility to opioid reward. *Translational Psychiatry* **8**, 1-12 (2018).
337 Pascucci, T., Ventura, R., Latagliata, E. C., Cabib, S. & Puglisi-Allegra, S. The medial prefrontal cortex determines the accumbens dopamine response to stress through the

opposing influences of norepinephrine and dopamine. *Cereb Cortex* **17**, 2796-2804, doi:10.1093/cercor/bhm008 (2007).

338 West, E. A., Saddoris, M. P., Kerfoot, E. C. & Carelli, R. M. Prelimbic and infralimbic cortical regions differentially encode cocaine-associated stimuli and cocaine-seeking before and following abstinence. *European Journal of Neuroscience* **39**, 1891-1902 (2014).

339 Chaudhri, N., Sahuque, L. L., Schairer, W. W. & Janak, P. H. Separable roles of the nucleus accumbens core and shell in context-and cue-induced alcohol-seeking. *Neuropsychopharmacology* **35**, 783-791 (2010).

340 Palombo, P. *et al.* Inactivation of the prelimbic cortex impairs the context-induced reinstatement of ethanol seeking. *Frontiers in pharmacology* **8**, 725 (2017).

341 Avchalumov, Y. & Mandyam, C. D. Plasticity in the Hippocampus, Neurogenesis and Drugs of Abuse. *Brain Sciences* **11**, 404 (2021).

342 Goodman, J. & Packard, M. G. Memory systems and the addicted brain. *Frontiers in psychiatry* **7**, 24 (2016).

343 Kutlu, M. G. & Gould, T. J. Effects of drugs of abuse on hippocampal plasticity and hippocampus-dependent learning and memory: contributions to development and maintenance of addiction. *Learning & memory* **23**, 515-533 (2016).

344 Han, H. *et al.* Opioid addiction and withdrawal differentially drive long-term depression of inhibitory synaptic transmission in the hippocampus. *Sci Rep* **5**, 9666, doi:10.1038/srep09666 (2015).

345 Thompson, A., Swant, J., Gosnell, B. & Wagner, J. Modulation of long-term potentiation in the rat hippocampus following cocaine self-administration. *Neuroscience* **127**, 177-185 (2004).

346 Zhou, Z., Yuan, Q., Mash, D. C. & Goldman, D. Substance-specific and shared transcription and epigenetic changes in the human hippocampus chronically exposed to cocaine and alcohol. *Proc Natl Acad Sci U S A* **108**, 6626-6631, doi:10.1073/pnas.1018514108 (2011).

347 Basu, S. & Suh, H. Role of hippocampal neurogenesis in alcohol withdrawal seizures. *Brain plasticity*, 1-13 (2020).

348 Taffe, M. A. *et al.* Long-lasting reduction in hippocampal neurogenesis by alcohol consumption in adolescent nonhuman primates. *Proc Natl Acad Sci U S A* **107**, 11104-11109, doi:10.1073/pnas.0912810107 (2010).

349 Erickson, E. K., Grantham, E. K., Warden, A. S. & Harris, R. Neuroimmune signaling in alcohol use disorder. *Pharmacology Biochemistry and Behavior* **177**, 34-60 (2019).

350 Robinson, G. *et al.* Neuroimmune pathways in alcohol consumption: evidence from behavioral and genetic studies in rodents and humans. *International review of neurobiology* **118**, 13-39 (2014).

351 Peng, Q., Bizon, C., Gizer, I. R., Wilhelmsen, K. C. & Ehlers, C. L. Genetic loci for alcohol-related life events and substance-induced affective symptoms: indexing the "dark side" of addiction. *Translational Psychiatry* **9**, 71 (2019).

352 Mayfield, J. & Harris, R. A. The neuroimmune basis of excessive alcohol consumption. *Neuropsychopharmacology* **42**, 376 (2017).

353 Szelényi, J. Cytokines and the central nervous system. *Brain research bulletin* **54**, 329-338 (2001).

354 Mosley, B. *et al.* Dual oncostatin M (OSM) receptors: cloning and characterization of an alternative signaling subunit conferring OSM-specific receptor activation. *Journal of Biological Chemistry* **271**, 32635-32643 (1996).
355 Chen, S. H. & Benveniste, E. N. Oncostatin M: a pleiotropic cytokine in the central nervous system. *Cytokine Growth Factor Rev* **15**, 379-391, doi:10.1016/j.cytogfr.2004.06.002 (2004).
356 Hermanns, H. M. Oncostatin M and interleukin-31: cytokines, receptors, signal transduction and physiology. *Cytokine & growth factor reviews* **26**, 545-558 (2015).
357 Du, Q., Qian, Y. & Xue, W. Molecular simulation of oncostatin M and receptor (OSM–OSMR) interaction as a potential therapeutic target for inflammatory bowel disease. *Frontiers in molecular biosciences* **7**, 29 (2020).
358 Turner, R. C. *et al.* Single low-dose lipopolysaccharide preconditioning: neuroprotective against axonal injury and modulates glial cells. *Neuroimmunol Neuroinflamm* **4**, 6-15, doi:10.20517/2347-8659.2016.40 (2017).
359 Yu, Z. *et al.* Oncostatin M receptor, positively regulated by SP1, promotes gastric cancer growth and metastasis upon treatment with Oncostatin M. *Gastric Cancer* **22**, 955-966 (2019).
360 Kortylewski, M. *et al.* Interleukin-6 and oncostatin M-induced growth inhibition of human A375 melanoma cells is STAT-dependent and involves upregulation of the cyclin-dependent kinase inhibitor p27/Kip1. *Oncogene* **18**, 3742-3753 (1999).
361 Pan, C.-M., Wang, M.-L., Chiou, S.-H., Chen, H.-Y. & Wu, C.-W. Oncostatin M suppresses metastasis of lung adenocarcinoma by inhibiting SLUG expression through coordination of STATs and PIASs signalings. *Oncotarget* **7**, 60395 (2016).
362 Douglas, A. M. *et al.* Oncostatin M induces the differentiation of breast cancer cells. *International journal of cancer* **75**, 64-73 (1998).
363 Halfter, H. *et al.* Inhibition of growth and induction of differentiation of glioma cell lines by oncostatin M (OSM). *Growth Factors* **15**, 135-147 (1998).
364 Sharanek, A. *et al.* OSMR controls glioma stem cell respiration and confers resistance of glioblastoma to ionizing radiation. *Nature communications* **11**, 1-16 (2020).
365 Hermanns, H. *et al.* Deficiency of the oncostatin M receptor affects the pathogenesis of non-alcoholic fatty liver disease in a context dependent manner. *Zeitschrift für Gastroenterologie* **53**, A3_2 (2015).
366 Gao, J.-X. *et al.* Overexpression of microRNA-183 promotes apoptosis of substantia nigra neurons via the inhibition of OSMR in a mouse model of Parkinson's disease. *International journal of molecular medicine* **43**, 209-220 (2019).
367 Moidunny, S. *et al.* Oncostatin M promotes excitotoxicity by inhibiting glutamate uptake in astrocytes: implications in HIV-associated neurotoxicity. *J Neuroinflammation* **13**, 144, doi:10.1186/s12974-016-0613-8 (2016).
368 Richards, C. D. The enigmatic cytokine oncostatin m and roles in disease. *ISRN Inflamm* **2013**, 512103, doi:10.1155/2013/512103 (2013).
369 Robson, M. J. *et al.* SN79, a sigma receptor antagonist, attenuates methamphetamine-induced astrogliosis through a blockade of OSMR/gp130 signaling and STAT3 phosphorylation. *Exp Neurol* **254**, 180-189, doi:10.1016/j.expneurol.2014.01.020 (2014).
370 Kapoor, M. *et al.* Analysis of whole genome-transcriptomic organization in brain to identify genes associated with alcoholism. *Translational psychiatry* **9**, 1-11 (2019).

371 Burns, K. *et al.* MyD88, an adapter protein involved in interleukin-1 signaling. *Journal of biological chemistry* **273**, 12203-12209 (1998).
372 Deguine, J. & Barton, G. M. MyD88: a central player in innate immune signaling. *F1000prime reports* **6** (2014).
373 Janssens, S. & Beyaert, R. A universal role for MyD88 in TLR/IL-1R-mediated signaling. *Trends in biochemical sciences* **27**, 474-482 (2002).
374 Yan, H. *et al.* Inhibition of myeloid differentiation primary response protein 88 provides neuroprotection in early brain injury following experimental subarachnoid hemorrhage. *Scientific Reports* **7**, 1-11 (2017).
375 Treon, S. P. *et al.* MYD88 L265P somatic mutation in Waldenström's macroglobulinemia. *New England Journal of Medicine* **367**, 826-833 (2012).
376 Ngo, V. N. *et al.* Oncogenically active MYD88 mutations in human lymphoma. *Nature* **470**, 115-119 (2011).
377 Wang, J. Q., Jeelall, Y. S., Ferguson, L. L. & Horikawa, K. Toll-like receptors and cancer: MYD88 mutation and inflammation. *Frontiers in immunology* **5**, 367 (2014).
378 Blednov, Y. A. *et al.* Ethanol Consumption in Mice Lacking CD14, TLR2, TLR4, or MyD88. *Alcohol Clin Exp Res* **41**, 516-530, doi:10.1111/acer.13316 (2017).
379 Plasil, S. L., Seth, A. & Homanics, G. E. CRISPR Turbo Accelerated KnockOut (CRISPy TAKO) for Rapid in vivo Screening of Gene Function. *Frontiers in Genome Editing* **2**, doi:10.3389/fgeed.2020.598522 (2020).
380 Blednov, Y. A. *et al.* Sedative and Motor Incoordination Effects of Ethanol in Mice Lacking CD14, TLR2, TLR4, or MyD88. *Alcohol Clin Exp Res* **41**, 531-540, doi:10.1111/acer.13314 (2017).
381 Saikh, K. U. MyD88 and beyond: A perspective on MyD88-targeted therapeutic approach for modulation of host immunity. *Immunologic Research* **69**, 117-128 (2021).
382 Di Padova, F., Quesniaux, V. F. & Ryffel, B. MyD88 as a therapeutic target for inflammatory lung diseases. *Expert Opinion on Therapeutic Targets* **22**, 401-408 (2018).
383 Strehl, C., Ehlers, L., Gaber, T. & Buttgereit, F. Glucocorticoids-All-Rounders Tackling the Versatile Players of the Immune System. *Front Immunol* **10**, 1744, doi:10.3389/fimmu.2019.01744 (2019).
384 Quatrini, L. & Ugolini, S. New insights into the cell- and tissue-specificity of glucocorticoid actions. *Cell Mol Immunol* **18**, 269-278, doi:10.1038/s41423-020-00526-2 (2021).
385 Busillo, J. M., Azzam, K. M. & Cidlowski, J. A. Glucocorticoids sensitize the innate immune system through regulation of the NLRP3 inflammasome. *J Biol Chem* **286**, 38703-38713, doi:10.1074/jbc.M111.275370 (2011).
386 Gatta, E. *et al.* Genome-wide methylation in alcohol use disorder subjects: implications for an epigenetic regulation of the cortico-limbic glucocorticoid receptors (NR3C1). *Mol Psychiatry* **26**, 1029-1041, doi:10.1038/s41380-019-0449-6 (2021).
387 Richardson, H. N., Lee, S. Y., O'Dell, L. E., Koob, G. F. & Rivier, C. L. Alcohol self-administration acutely stimulates the hypothalamic-pituitary-adrenal axis, but alcohol dependence leads to a dampened neuroendocrine state. *European Journal of Neuroscience* **28**, 1641-1653 (2008).
388 McGinn, M. A. *et al.* Glucocorticoid receptor modulators decrease alcohol self-administration in male rats. *Neuropharmacology*, 108510, doi:10.1016/j.neuropharm.2021.108510 (2021).

389 Vendruscolo, L. F. *et al.* Glucocorticoid receptor antagonism decreases alcohol seeking in alcohol-dependent individuals. *The Journal of clinical investigation* **125**, 3193-3197 (2015).
390 McGinn, M. A., Edwards, K. & Edwards, S. Glucocorticoid Receptor-Dependent Gene Expression in the Central Amygdala of Alcohol-Dependent Animals. *The FASEB Journal* **32**, 878.877-878.877 (2018).
391 Vendruscolo, L. F. *et al.* Corticosteroid-dependent plasticity mediates compulsive alcohol drinking in rats. *J Neurosci* **32**, 7563-7571, doi:10.1523/JNEUROSCI.0069-12.2012 (2012).
392 Rose, A., Shaw, S., Prendergast, M. & Little, H. The importance of glucocorticoids in alcoholdependence and neurotoxicity. *Alcoholism: Clinical and Experimental Research* **34**, 2011-2018 (2010).
393 Lohoff, F. W. *et al.* Epigenome-wide association study and multi-tissue replication of individuals with alcohol use disorder: evidence for abnormal glucocorticoid signaling pathway gene regulation. *Mol Psychiatry*, doi:10.1038/s41380-020-0734-4 (2020).
394 Kino, T., Hurt, D. E., Ichijo, T., Nader, N. & Chrousos, G. P. Noncoding RNA gas5 is a growth arrest- and starvation-associated repressor of the glucocorticoid receptor. *Sci Signal* **3**, ra8, doi:10.1126/scisignal.2000568 (2010).
395 Wedemeyer, F. *et al.* Prospects of Genetics and Epigenetics of Alcohol Use Disorder. *Current Addiction Reports* **7**, 446-452, doi:10.1007/s40429-020-00331-x (2020).
396 Farris, S. P., Arasappan, D., Hunicke-Smith, S., Harris, R. A. & Mayfield, R. D. Transcriptome organization for chronic alcohol abuse in human brain. *Mol Psychiatry* **20**, 1438-1447, doi:10.1038/mp.2014.159 (2015).
397 Lim, Y. *et al.* Exploration of alcohol use disorder-associated brain miRNA–mRNA regulatory networks. *Translational psychiatry* **11**, 1-10 (2021).
398 Warden, A. S. & Mayfield, R. D. Gene expression profiling in the human alcoholic brain. *Neuropharmacology* **122**, 161-174 (2017).
399 Farris, S. P. & Mayfield, R. D. RNA-Seq reveals novel transcriptional reorganization in human alcoholic brain. *International review of neurobiology* **116**, 275-300 (2014).
400 Chen, W.-Y. *et al.* Transcriptomics identifies STAT3 as a key regulator of hippocampal gene expression and anhedonia during withdrawal from chronic alcohol exposure. *Translational psychiatry* **11**, 1-12 (2021).
401 Van Booven, D. *et al.* Alcohol use disorder causes global changes in splicing in the human brain. *Translational psychiatry* **11**, 1-9 (2021).
402 Rao, X. *et al.* Allele-specific expression and high-throughput reporter assay reveal functional genetic variants associated with alcohol use disorders. *Molecular psychiatry*, 1-10 (2019).
403 Kisby, B. R. *et al.* Alcohol Dependence in Rats Is Associated with Global Changes in Gene Expression in the Central Amygdala. *Brain sciences* **11**, 1149 (2021).
404 Baratta, A. M., Brandner, A., Plasil, S. L., Rice, R. C. & Farris, S. Advancements in Genomic and Behavioral Neuroscience Analysis for the Study of Normal and Pathological Brain Function. *Frontiers in Molecular Neuroscience*, 310.
405 Zhao, W. *et al.* Comparison of RNA-Seq by poly (A) capture, ribosomal RNA depletion, and DNA microarray for expression profiling. *BMC genomics* **15**, 1-11 (2014).

406 Lee, M. R. *et al.* Effect of alcohol use disorder on oxytocin peptide and receptor mRNA expression in human brain: A post-mortem case-control study. *Psychoneuroendocrinology* **85**, 14-19 (2017).
407 Lieberman, R., Kranzler, H. R., Levine, E. S. & Covault, J. Examining the effects of alcohol on GABAA receptor mRNA expression and function in neural cultures generated from control and alcohol dependent donor induced pluripotent stem cells. *Alcohol* **66**, 45-53 (2018).
408 Bach, H. *et al.* Alcoholics have more tryptophan hydroxylase 2 mRNA and protein in the dorsal and median raphe nuclei. *Alcoholism: Clinical and Experimental Research* **38**, 1894-1901 (2014).
409 Even-Chen, O. *et al.* FGF2 is an endogenous regulator of alcohol reward and consumption. *Addiction biology*, e13115.
410 Mayfield, J., Arends, M. A., Harris, R. A. & Blednov, Y. A. Genes and Alcohol Consumption: Studies with Mutant Mice. *Int Rev Neurobiol* **126**, 293-355, doi:10.1016/bs.irn.2016.02.014 (2016).
411 Mayfield, R. D. Emerging roles for ncRNAs in alcohol use disorders. *Alcohol* **60**, 31-39, doi:10.1016/j.alcohol.2017.01.004 (2017).
412 Atianand, M. K., Caffrey, D. R. & Fitzgerald, K. A. Immunobiology of long noncoding RNAs. *Annual review of immunology* **35**, 177-198 (2017).
413 Beermann, J., Piccoli, M. T., Viereck, J. & Thum, T. Non-coding RNAs in Development and Disease: Background, Mechanisms, and Therapeutic Approaches. *Physiol Rev* **96**, 1297-1325, doi:10.1152/physrev.00041.2015 (2016).
414 Mercer, T. R., Dinger, M. E., Sunkin, S. M., Mehler, M. F. & Mattick, J. S. Specific expression of long noncoding RNAs in the mouse brain. *Proc Natl Acad Sci U S A* **105**, 716-721, doi:10.1073/pnas.0706729105 (2008).
415 Kopp, F. & Mendell, J. T. Functional Classification and Experimental Dissection of Long Noncoding RNAs. *Cell* **172**, 393-407, doi:10.1016/j.cell.2018.01.011 (2018).
416 Kazimierczyk, M., Kasprowicz, M. K., Kasprzyk, M. E. & Wrzesinski, J. Human long noncoding RNA interactome: detection, characterization and function. *International journal of molecular sciences* **21**, 1027 (2020).
417 Vornholt, E. *et al.* Identifying a novel biological mechanism for alcohol addiction associated with circRNA networks acting as potential miRNA sponges. *Addiction biology* **26**, e13071 (2021).
418 Zhang, P., Wu, W., Chen, Q. & Chen, M. Non-coding RNAs and their integrated networks. *Journal of integrative bioinformatics* **16** (2019).
419 Mahnke, A. H., Miranda, R. C. & Homanics, G. E. Epigenetic mediators and consequences of excessive alcohol consumption. *Alcohol (Fayetteville, NY)* **60**, 1 (2017).
420 Nie, J.-H., Li, T.-X., Zhang, X.-Q. & Liu, J. Roles of non-coding RNAs in normal human brain development, brain tumor, and neuropsychiatric disorders. *Non-coding RNA* **5**, 36 (2019).
421 Ling, H. *et al.* Junk DNA and the long non-coding RNA twist in cancer genetics. *Oncogene* **34**, 5003-5011 (2015).
422 Palazzo, A. F. & Lee, E. S. Non-coding RNA: what is functional and what is junk? *Frontiers in genetics* **6**, 2 (2015).
423 Liu, J., Liu, T., Wang, X. & He, A. Circles reshaping the RNA world: from waste to treasure. *Molecular cancer* **16**, 1-12 (2017).

424 Bautista-Becerril, B. *et al.* miRNAs, from evolutionary junk to possible prognostic markers and therapeutic targets in COVID-19. *Viruses* **14**, 41 (2021).
425 Oldham, M. C. *et al.* Functional organization of the transcriptome in human brain. *Nature neuroscience* **11**, 1271-1282 (2008).
426 Hawrylycz, M. J. *et al.* An anatomically comprehensive atlas of the adult human brain transcriptome. *Nature* **489**, 391-399 (2012).
427 Quinn, J. J. & Chang, H. Y. Unique features of long non-coding RNA biogenesis and function. *Nat Rev Genet* **17**, 47-62, doi:10.1038/nrg.2015.10 (2016).
428 Salmena, L., Poliseno, L., Tay, Y., Kats, L. & Pandolfi, P. P. A ceRNA hypothesis: the Rosetta Stone of a hidden RNA language? *Cell* **146**, 353-358 (2011).
429 Tay, Y., Rinn, J. & Pandolfi, P. P. The multilayered complexity of ceRNA crosstalk and competition. *Nature* **505**, 344-352 (2014).
430 Nunez, Y. O. *et al.* Positively correlated miRNA-mRNA regulatory networks in mouse frontal cortex during early stages of alcohol dependence. *BMC genomics* **14**, 1-21 (2013).
431 Wang, L. *et al.* Long noncoding RNA (lncRNA)-mediated competing endogenous RNA networks provide novel potential biomarkers and therapeutic targets for colorectal cancer. *International journal of molecular sciences* **20**, 5758 (2019).
432 Wang, Q.-C., Wang, Z.-Y., Xu, Q., Chen, X.-L. & Shi, R.-Z. lncRNA expression profiles and associated ceRNA network analyses in epicardial adipose tissue of patients with coronary artery disease. *Scientific Reports* **11**, 1-10 (2021).
433 Xu, J., Xu, J., Liu, X. & Jiang, J. The role of lncRNA-mediated ceRNA regulatory networks in pancreatic cancer. *Cell Death Discovery* **8**, 1-11 (2022).
434 Zhou, M. *et al.* Construction and analysis of dysregulated lncRNA-associated ceRNA network identified novel lncRNA biomarkers for early diagnosis of human pancreatic cancer. *Oncotarget* **7**, 56383 (2016).
435 Wu, X., Sui, Z., Zhang, H., Wang, Y. & Yu, Z. Integrated Analysis of lncRNA–Mediated ceRNA Network in Lung Adenocarcinoma. *Frontiers in oncology* **10**, 554759 (2020).
436 Zhou, M. *et al.* Characterization of long non-coding RNA-associated ceRNA network to reveal potential prognostic lncRNA biomarkers in human ovarian cancer. *Oncotarget* **7**, 12598 (2016).
437 Plasil, S. L., Collins, V. J., Baratta, A. M., Farris, S. P. & Homanics, G. E. Hippocampal ceRNA networks from chronic intermittent ethanol vapor-exposed male mice and functional analysis of top-ranked lncRNA genes for ethanol drinking phenotypes. *Advances in Drug and Alcohol Research*, 10 (2022).
438 Gurtan, A. M. & Sharp, P. A. The role of miRNAs in regulating gene expression networks. *Journal of molecular biology* **425**, 3582-3600 (2013).
439 Gorini, G., Nunez, Y. O. & Mayfield, R. D. Integration of miRNA and protein profiling reveals coordinated neuroadaptations in the alcohol-dependent mouse brain. *PLoS One* **8**, e82565 (2013).
440 Darcq, E. *et al.* MicroRNA-30a-5p in the prefrontal cortex controls the transition from moderate to excessive alcohol consumption. *Mol Psychiatry* **20**, 1219-1231, doi:10.1038/mp.2014.120 (2015).
441 Ureña-Peralta, J., Alfonso-Loeches, S., Cuesta-Diaz, C., García-García, F. & Guerri, C. Deep sequencing and miRNA profiles in alcohol-induced neuroinflammation and the TLR4 response in mice cerebral cortex. *Scientific reports* **8**, 1-17 (2018).

442 Li, J. *et al.* Profiling circular RNA in methamphetamine-treated primary cortical neurons identified novel circRNAs related to methamphetamine addiction. *Neuroscience Letters* **701**, 146-153 (2019).
443 Zhang, H. *et al.* Circular RNA expression profiling in the nucleus accumbens: Effects of electroacupuncture treatment on morphine-induced conditioned place preference. *Addiction Biology* **25**, e12794 (2020).
444 Bu, Q. *et al.* Cocaine induces differential circular RNA expression in striatum. *Translational psychiatry* **9**, 1-11 (2019).
445 Statello, L., Guo, C.-J., Chen, L.-L. & Huarte, M. Gene regulation by long non-coding RNAs and its biological functions. *Nature Reviews Molecular Cell Biology* **22**, 96-118 (2021).
446 Chen, L.-L. Linking long noncoding RNA localization and function. *Trends in biochemical sciences* **41**, 761-772 (2016).
447 Dong, P. *et al.* Long non-coding RNA NEAT1: a novel target for diagnosis and therapy in human tumors. *Frontiers in genetics* **9**, 471 (2018).
448 Benetatos, L., Benetatou, A. & Vartholomatos, G. Long non-coding RNAs and MYC association in hematological malignancies. *Annals of Hematology*, 1-12 (2020).
449 Salviano-Silva, A., Lobo-Alves, S. C., Almeida, R. C. d., Malheiros, D. & Petzl-Erler, M. L. Besides pathology: Long non-coding RNA in cell and tissue homeostasis. *Non-coding RNA* **4**, 3 (2018).
450 Spurlock, C. F. *et al.* Profiles of long noncoding RNAs in human naive and memory T cells. *The Journal of Immunology* **199**, 547-558 (2017).
451 Marchese, F. P. & Huarte, M. Long non-coding RNAs and chromatin modifiers: their place in the epigenetic code. *Epigenetics* **9**, 21-26 (2014).
452 Volders, P.-J. *et al.* LNCipedia 5: towards a reference set of human long non-coding RNAs. *Nucleic acids research* **47**, D135-D139 (2019).
453 Prabhakar, B., Zhong, X.-b. & Rasmussen, T. P. Exploiting long noncoding RNAs as pharmacological targets to modulate epigenetic diseases. *The Yale journal of biology and medicine* **90**, 73 (2017).
454 Denham, A. N. *et al.* Long Non-Coding RNAs: The New Frontier into Understanding the Etiology of Alcohol Use Disorder. *Non-coding RNA* **8**, 59 (2022).
455 Aznaourova, M., Schmerer, N., Schmeck, B. & Schulte, L. N. Disease-causing mutations and rearrangements in long non-coding RNA gene loci. *Frontiers in genetics* **11**, 527484 (2020).
456 Shen, Y. *et al.* Focusing on long non-coding RNA dysregulation in newly diagnosed multiple myeloma. *Life sciences* **196**, 133-142 (2018).
457 Liu, S. *et al.* The Potential Roles of Long Noncoding RNAs (lncRNA) in Glioblastoma Development. *Mol Cancer Ther* **15**, 2977-2986, doi:10.1158/1535-7163.MCT-16-0320 (2016).
458 Dinescu, S. *et al.* Epitranscriptomic Signatures in lncRNAs and Their Possible Roles in Cancer. *Genes (Basel)* **10**, doi:10.3390/genes10010052 (2019).
459 Tian, T. *et al.* The Impact of lncRNA Dysregulation on Clinicopathology and Survival of Breast Cancer: A Systematic Review and Meta-analysis. *Mol Ther Nucleic Acids* **12**, 359-369, doi:10.1016/j.omtn.2018.05.018 (2018).

460 Shan, Y. *et al.* LncRNA SNHG7 sponges miR-216b to promote proliferation and liver metastasis of colorectal cancer through upregulating GALNT1. *Cell death & disease* **9**, 1-13 (2018).
461 Huo, X. *et al.* Dysregulated long noncoding RNAs (lncRNAs) in hepatocellular carcinoma: implications for tumorigenesis, disease progression, and liver cancer stem cells. *Mol Cancer* **16**, 165, doi:10.1186/s12943-017-0734-4 (2017).
462 Elkouris, M. *et al.* Long non-coding rnas associated with neurodegeneration-linked genes are reduced in Parkinson's disease patients. *Frontiers in cellular neuroscience* **13**, 58 (2019).
463 Faghihi, M. A. *et al.* Evidence for natural antisense transcript-mediated inhibition of microRNA function. *Genome biology* **11**, 1-13 (2010).
464 Liu, Y. *et al.* Non-coding RNA dysregulation in the amygdala region of schizophrenia patients contributes to the pathogenesis of the disease. *Transl Psychiatry* **8**, 44, doi:10.1038/s41398-017-0030-5 (2018).
465 Issler, O. *et al.* Sex-specific role for the long non-coding RNA LINC00473 in depression. *Neuron* **106**, 912-926. e915 (2020).
466 Haiyang Xu, A. N. B., Nicholas J. Waddell, Xiaochuan Liu, Graham J. Kaplan, Javed M. Chitaman, Victoria Stockman, Rachel L. Hedinger, Ryan Adams, Kristen Abreu, Li Shen, Rachael Neve, Zuoxin Wang, Eric J. Nestler, Jian Feng. Role of long non-coding RNA Gas5 in cocaine action *Biological Psychiatry* (2020).
467 Zhu, L. *et al.* Methamphetamine induces alterations in the long non-coding RNAs expression profile in the nucleus accumbens of the mouse. *BMC neuroscience* **16**, 1-13 (2015).
468 Bu, Q. *et al.* Transcriptome analysis of long non-coding RNAs of the nucleus accumbens in cocaine-conditioned mice. *Journal of neurochemistry* **123**, 790-799 (2012).
469 Bannon, M. J. *et al.* Identification of long noncoding RNAs dysregulated in the midbrain of human cocaine abusers. *J Neurochem* **135**, 50-59, doi:10.1111/jnc.13255 (2015).
470 Deng, M. *et al.* LncRNA MRAK159688 facilitates morphine tolerance by promoting REST-mediated inhibition of mu opioid receptor in rats. *Neuropharmacology* **206**, 108938, doi:10.1016/j.neuropharm.2021.108938 (2022).
471 Ji, J., Dai, X., Yeung, S. J. & He, X. The role of long non-coding RNA GAS5 in cancers. *Cancer Manag Res* **11**, 2729-2737, doi:10.2147/CMAR.S189052 (2019).
472 Goustin, A. S., Thepsuwan, P., Kosir, M. A. & Lipovich, L. The growth-arrest-specific (GAS)-5 long non-coding RNA: a fascinating lncRNA widely expressed in cancers. *Non-coding RNA* **5**, 46 (2019).
473 Bohnsack, J. P., Teppen, T., Kyzar, E. J., Dzitoyeva, S. & Pandey, S. C. The lncRNA BDNF-AS is an epigenetic regulator in the human amygdala in early onset alcohol use disorders. *Transl Psychiatry* **9**, 34, doi:10.1038/s41398-019-0367-z (2019).
474 Zheng, H. *et al.* Alcohol and hepatitis virus-dysregulated lncRNAs as potential biomarkers for hepatocellular carcinoma. *Oncotarget* **9**, 224 (2018).
475 Zhou, A., Wang, Y., Liu, Y., Feng, W. & Edenberg, H. J. in *2016 IEEE International Conference on Bioinformatics and Biomedicine (BIBM)*. 167-173 (IEEE).
476 Saba, L. M. *et al.* A long non-coding RNA (Lrap) modulates brain gene expression and levels of alcohol consumption in rats. *Genes, Brain and Behavior* **20**, e12698 (2021).
477 Winkle, M., El-Daly, S. M., Fabbri, M. & Calin, G. A. Noncoding RNA therapeutics—challenges and potential solutions. *Nature Reviews Drug Discovery*, 1-23 (2021).

478 Gomes, C. P. *et al.* The function and therapeutic potential of long non-coding RNAs in cardiovascular development and disease. *Molecular Therapy-Nucleic Acids* **8**, 494-507 (2017).
479 Connelly, C. M., Moon, M. H. & Schneekloth Jr, J. S. The emerging role of RNA as a therapeutic target for small molecules. *Cell chemical biology* **23**, 1077-1090 (2016).
480 Harries, L. W. RNA biology provides new therapeutic targets for human disease. *Frontiers in genetics* **10**, 205 (2019).
481 Wang, S.-W., Liu, Z. & Shi, Z.-S. Non-coding RNA in acute ischemic stroke: mechanisms, biomarkers and therapeutic targets. *Cell transplantation* **27**, 1763-1777 (2018).
482 Tamang, S. *et al.* SNHG12: an LncRNA as a potential therapeutic target and biomarker for human cancer. *Frontiers in oncology* **9**, 901 (2019).
483 Fatima, R., Akhade, V. S., Pal, D. & Rao, S. M. Long noncoding RNAs in development and cancer: potential biomarkers and therapeutic targets. *Mol Cell Ther* **3**, 5, doi:10.1186/s40591-015-0042-6 (2015).
484 Gutschner, T., Richtig, G., Haemmerle, M. & Pichler, M. From biomarkers to therapeutic targets-the promises and perils of long non-coding RNAs in cancer. *Cancer Metastasis Rev* **37**, 83-105, doi:10.1007/s10555-017-9718-5 (2018).
485 MM Kumar, R. G. LncRNA as a Therapeutic Target for Angiogenesis. *Current Topics in Medicinal Chemistry* **17**, 8, doi:10.2174/1568026617666161116447444 (2017).
486 Di Martino, M. T. R., C.;, Scionti, F. G., K.; Polerà, N.;, Caracciolo, D. A., M.; & Tagliaferri, P. T., P. miRNAs and lncRNAs as Novel Therapeutic Targets to Improve Cancer Immunotherapy. *Cancers* **23**, doi:10.3390/
cancers13071587 (2021).
487 Dizaji, F. Strategies to target long non-coding RNAs in cancer treatment: progress and challenges. *Egyptian Journal of Medical Human Genetics* **21**, doi:10.1186/s43042-020-00074-4 (2020).
488 Damase, T. R. *et al.* The limitless future of RNA therapeutics. *Frontiers in Bioengineering and Biotechnology*, 161 (2021).
489 Kapoor, M. *et al.* Analysis of whole genome-transcriptomic organization in brain to identify genes associated with alcoholism. *Transl Psychiatry* **9**, 89, doi:10.1038/s41398-019-0384-y (2019).
490 Finegersh, A. & Homanics, G. E. Acute ethanol alters multiple histone modifications at model gene promoters in the cerebral cortex. *Alcoholism: Clinical and Experimental Research* **38**, 1865-1873 (2014).
491 Veazey, K. J. *et al.* Disconnect between alcohol-induced alterations in chromatin structure and gene transcription in a mouse embryonic stem cell model of exposure. *Alcohol* **60**, 121-133 (2017).
492 Ignacio, C. *et al.* Alterations in serum microRNA in humans with alcohol use disorders impact cell proliferation and cell death pathways and predict structural and functional changes in brain. *BMC neuroscience* **16**, 1-18 (2015).
493 Pietrzykowski, A. Z. *et al.* Posttranscriptional regulation of BK channel splice variant stability by miR-9 underlies neuroadaptation to alcohol. *Neuron* **59**, 274-287 (2008).
494 Most, D., Leiter, C., Blednov, Y. A., Harris, R. A. & Mayfield, R. D. Synaptic microRNAs coordinately regulate synaptic mRNAs: perturbation by chronic alcohol consumption. *Neuropsychopharmacology* **41**, 538-548 (2016).

495 Tapocik, J. D. *et al.* microRNA-206 in rat medial prefrontal cortex regulates BDNF expression and alcohol drinking. *Journal of Neuroscience* **34**, 4581-4588 (2014).
496 Tian, H. *et al.* SVCT2, a potential therapeutic target, protects against oxidative stress during ethanol-induced neurotoxicity via JNK/p38 MAPKs, NF-κB and miRNA125a-5p. *Free Radical Biology and Medicine* **96**, 362-373 (2016).
497 Darcq, E. *et al.* MicroRNA-30a-5p in the prefrontal cortex controls the transition from moderate to excessive alcohol consumption. *Molecular psychiatry* **20**, 1240-1250 (2015).
498 Tapocik, J. D. *et al.* Coordinated dysregulation of mRNAs and microRNAs in the rat medial prefrontal cortex following a history of alcohol dependence. *The pharmacogenomics journal* **13**, 286-296 (2013).
499 Grantham, E. K. & Farris, S. P. Bioinformatic and biological avenues for understanding alcohol use disorder. *Alcohol* **74**, 65-71 (2019).
500 Bogenpohl, J. W. *et al.* Cross-species co-analysis of prefrontal cortex chronic ethanol transcriptome responses in mice and monkeys. *Frontiers in molecular neuroscience* **12**, 197 (2019).
501 Shansky, R. M. & Murphy, A. Z. Considering sex as a biological variable will require a global shift in science culture. *Nature Neuroscience*, doi:10.1038/s41593-021-00806-8 (2021).
502 Shansky, R. M. Estrogen, stress and the brain: progress toward unraveling gender discrepancies in major depressive disorder. *Expert review of neurotherapeutics* **9**, 967-973 (2009).
503 Farrell, M. R., Gruene, T. M. & Shansky, R. M. The influence of stress and gonadal hormones on neuronal structure and function. *Hormones and behavior* **76**, 118-124 (2015).
504 Yagi, S. *et al.* Sex Differences in Maturation and Attrition of Adult Neurogenesis in the Hippocampus. *eNeuro* **7**, doi:10.1523/ENEURO.0468-19.2020 (2020).
505 Lu, T. & Mar, J. C. Investigating transcriptome-wide sex dimorphism by multi-level analysis of single-cell RNA sequencing data in ten mouse cell types. *Biol Sex Differ* **11**, 61, doi:10.1186/s13293-020-00335-2 (2020).
506 Mecklenburg, J. *et al.* Transcriptomic sex differences in sensory neuronal populations of mice. *Sci Rep* **10**, 15278, doi:10.1038/s41598-020-72285-z (2020).
507 Mozhui, K., Lu, L., Armstrong, W. E. & Williams, R. W. Sex-specific modulation of gene expression networks in murine hypothalamus. *Front Neurosci* **6**, 63, doi:10.3389/fnins.2012.00063 (2012).
508 Lee, C. W.-S. & Ho, I. Sex differences in opioid analgesia and addiction; interactions among opioid receptors and estrogen receptors. *Molecular Pain* **9**, 10 (2013).
509 Varì, R. *et al.* Significance of Sex Differences in ncRNAs Expression and Function in Pregnancy and Related Complications. *Biomedicines* **9**, 1509 (2021).
510 Zhu, J. *et al.* Whole-Transcriptome Analysis Identifies Gender Dimorphic Expressions of Mrnas and Non-Coding Rnas in Chinese Soft-Shell Turtle (Pelodiscus sinensis). *Biology* **11**, 834 (2022).
511 Chernov, A. V. & Shubayev, V. I. Sexual Dimorphism of Early Transcriptional Reprogramming in Dorsal Root Ganglia After Peripheral Nerve Injury. *Frontiers in molecular neuroscience* **14**, 779024 (2021).
512 Yoon, J. & Kim, H. Multi-tissue observation of the long non-coding RNA effects on sexually biased gene expression in cattle. *Asian-Australasian journal of animal sciences* **32**, 1044 (2019).

513 Keshavarz, M. & Tautz, D. The imprinted lncRNA Peg13 regulates sexual preference and the sex-specific brain transcriptome in mice. *Proceedings of the National Academy of Sciences* **118** (2021).
514 Rastetter, R. H., Smith, C. A. & Wilhelm, D. The role of non-coding RNAs in male sex determination and differentiation. *Reproduction* **150**, R93-R107 (2015).
515 Gururajan, A. Sex differences in susceptibility to depression: a role for LncRNAs. *Neuron* **106**, 871-872 (2020).
516 Fiselier, A., Byeon, B., Ilnytskyy, Y., Kovalchuk, I. & Kovalchuk, O. Sex-Specific Expression of Non-Coding RNA Fragments in Frontal Cortex, Hippocampus and Cerebellum of Rats. *Epigenomes* **6**, 11 (2022).
517 Madrer, N. & Soreq, H. Cholino-ncRNAs modulate sex-specific-and age-related acetylcholine signals. *FEBS letters* **594**, 2185-2198 (2020).
518 Cerase, A., Pintacuda, G., Tattermusch, A. & Avner, P. Xist localization and function: new insights from multiple levels. *Genome biology* **16**, 1-12 (2015).
519 Johansson, M. M. *et al.* Novel Y-chromosome long non-coding RNAs expressed in human male CNS during early development. *Frontiers in Genetics* **10**, 891 (2019).
520 Chernov, A. V. & Shubayev, V. I. Sexually dimorphic transcriptional programs of early-phase response in regenerating peripheral nerves. *Frontiers in Molecular Neuroscience*, 381 (2022).
521 Becker, J. B. & Chartoff, E. Sex differences in neural mechanisms mediating reward and addiction. *Neuropsychopharmacology* **44**, 166-183, doi:10.1038/s41386-018-0125-6 (2019).
522 Kokane, S. S. & Perrotti, L. I. Sex Differences and the Role of Estradiol in Mesolimbic Reward Circuits and Vulnerability to Cocaine and Opiate Addiction. *Front Behav Neurosci* **14**, 74, doi:10.3389/fnbeh.2020.00074 (2020).
523 LaRese, T. P., Rheaume, B. A., Abraham, R., Eipper, B. A. & Mains, R. E. Sex-Specific Gene Expression in the Mouse Nucleus Accumbens Before and After Cocaine Exposure. *J Endocr Soc* **3**, 468-487, doi:10.1210/js.2018-00313 (2019).
524 Pfefferbaum, A., Rosenbloom, M., Deshmukh, A. & Sullivan, E. V. Sex differences in the effects of alcohol on brain structure. *American Journal of Psychiatry* **158**, 188-197 (2001).
525 Darnieder, L. M. *et al.* Female-specific decreases in alcohol binge-like drinking resulting from GABA(A) receptor delta-subunit knockdown in the VTA. *Sci Rep* **9**, 8102, doi:10.1038/s41598-019-44286-0 (2019).
526 Przybycien-Szymanska, M. M., Rao, Y. S. & Pak, T. R. Binge-pattern alcohol exposure during puberty induces sexually dimorphic changes in genes regulating the HPA axis. *Am J Physiol Endocrinol Metab* **298**, E320-328, doi:10.1152/ajpendo.00615.2009 (2010).
527 Li, J. *et al.* Differences between male and female rats in alcohol drinking, negative affects and neuronal activity after acute and prolonged abstinence. *International Journal of Physiology, Pathophysiology and Pharmacology* **11**, 163 (2019).
528 Sneddon, E. A., White, R. D. & Radke, A. K. Sex Differences in Binge-Like and Aversion-Resistant Alcohol Drinking in C57 BL/6J Mice. *Alcoholism: clinical and experimental research* **43**, 243-249 (2019).
529 Jury, N. J., DiBerto, J. F., Kash, T. L. & Holmes, A. Sex differences in the behavioral sequelae of chronic ethanol exposure. *Alcohol* **58**, 53-60 (2017).

530 Barker, J. M., Bryant, K. G., Osborne, J. I. & Chandler, L. J. Age and Sex Interact to Mediate the Effects of Intermittent, High-Dose Ethanol Exposure on Behavioral Flexibility. *Front Pharmacol* **8**, 450, doi:10.3389/fphar.2017.00450 (2017).
531 Middaugh, L. D., Kelley, B. M., Bandy, A.-L. E. & McGroarty, K. K. Ethanol consumption by C57BL/6 mice: influence of gender and procedural variables. *Alcohol* **17**, 175-183 (1999).
532 Karp, N. A. & Reavey, N. Sex bias in preclinical research and an exploration of how to change the status quo. *British journal of pharmacology* **176**, 4107-4118 (2019).
533 Zucker, I. & Beery, A. K. Males still dominate animal studies. *Nature* **465**, 690-690 (2010).
534 Beery, A. K. Inclusion of females does not increase variability in rodent research studies. *Current opinion in behavioral sciences* **23**, 143-149 (2018).
535 Homanics, G. E. Gene-edited CRISPy Critters for alcohol research. *Alcohol* **74**, 11-19 (2019).
536 Jinek, M. *et al.* A programmable dual-RNA–guided DNA endonuclease in adaptive bacterial immunity. *science* **337**, 816-821 (2012).
537 Wefers, B., Bashir, S., Rossius, J., Wurst, W. & Kühn, R. Gene editing in mouse zygotes using the CRISPR/Cas9 system. *Methods* **121**, 55-67 (2017).
538 Kosicki, M., Tomberg, K. & Bradley, A. Repair of double-strand breaks induced by CRISPR–Cas9 leads to large deletions and complex rearrangements. *Nature biotechnology* **36**, 765-771 (2018).
539 Josephs, E. A. *et al.* Structure and specificity of the RNA-guided endonuclease Cas9 during DNA interrogation, target binding and cleavage. *Nucleic Acids Res* **43**, 8924-8941, doi:10.1093/nar/gkv892 (2015).
540 Kuscu, C., Arslan, S., Singh, R., Thorpe, J. & Adli, M. Genome-wide analysis reveals characteristics of off-target sites bound by the Cas9 endonuclease. *Nature biotechnology* **32**, 677-683 (2014).
541 Duan, J. *et al.* Genome-wide identification of CRISPR/Cas9 off-targets in human genome. *Cell research* **24**, 1009-1012 (2014).
542 Fu, Y. *et al.* High-frequency off-target mutagenesis induced by CRISPR-Cas nucleases in human cells. *Nature biotechnology* **31**, 822-826 (2013).
543 Hsu, P. D. *et al.* DNA targeting specificity of RNA-guided Cas9 nucleases. *Nature biotechnology* **31**, 827-832 (2013).
544 Anderson, K. R. *et al.* CRISPR off-target analysis in genetically engineered rats and mice. *Nature methods* **15**, 512-514 (2018).
545 Lee, J., Ma, J. & Lee, K. Direct delivery of adenoviral CRISPR/Cas9 vector into the blastoderm for generation of targeted gene knockout in quail. *Proceedings of the National Academy of Sciences* **116**, 13288-13292 (2019).
546 Akcakaya, P. *et al.* In vivo CRISPR editing with no detectable genome-wide off-target mutations. *Nature* **561**, 416-419 (2018).
547 Iyer, V. *et al.* Off-target mutations are rare in Cas9-modified mice. *Nature methods* **12**, 479-479 (2015).
548 Nakajima, K. *et al.* Exome sequencing in the knockin mice generated using the CRISPR/Cas system. *Scientific reports* **6**, 34703 (2016).
549 Iyer, V. *et al.* No unexpected CRISPR-Cas9 off-target activity revealed by trio sequencing of gene-edited mice. *PLoS genetics* **14**, e1007503 (2018).

550 Yang, H. *et al.* One-step generation of mice carrying reporter and conditional alleles by CRISPR/Cas-mediated genome engineering. *Cell* **154**, 1370-1379 (2013).
551 Hay, E. A. *et al.* An analysis of possible off target effects following CAS9/CRISPR targeted deletions of neuropeptide gene enhancers from the mouse genome. *Neuropeptides* **64**, 101-107 (2017).
552 Shen, B. *et al.* Efficient genome modification by CRISPR-Cas9 nickase with minimal off-target effects. *Nature methods* **11**, 399-402 (2014).
553 Wu, X. *et al.* Genome-wide binding of the CRISPR endonuclease Cas9 in mammalian cells. *Nature biotechnology* **32**, 670-676 (2014).
554 Han, H. A., Pang, J. K. S. & Soh, B.-S. Mitigating off-target effects in CRISPR/Cas9-mediated in vivo gene editing. *Journal of Molecular Medicine* **98**, 615-632 (2020).
555 Manghwar, H. *et al.* CRISPR/Cas systems in genome editing: methodologies and tools for sgRNA design, off-target evaluation, and strategies to mitigate off-target effects. *Advanced science* **7**, 1902312 (2020).
556 Vakulskas, C. A. *et al.* A high-fidelity Cas9 mutant delivered as a ribonucleoprotein complex enables efficient gene editing in human hematopoietic stem and progenitor cells. *Nat Med* **24**, 1216-1224, doi:10.1038/s41591-018-0137-0 (2018).
557 Thakore, P. I. *et al.* Highly specific epigenome editing by CRISPR-Cas9 repressors for silencing of distal regulatory elements. *Nat Methods* **12**, 1143-1149, doi:10.1038/nmeth.3630 (2015).
558 Okada, K. *et al.* Key sequence features of CRISPR RNA for dual-guide CRISPR-Cas9 ribonucleoprotein complexes assembled with wild-type or HiFi Cas9. *Nucleic Acids Research* **50**, 2854-2871 (2022).
559 Kleinstiver, B. P. *et al.* High-fidelity CRISPR-Cas9 nucleases with no detectable genome-wide off-target effects. *Nature* **529**, 490-495, doi:10.1038/nature16526 (2016).
560 Doench, J. G. *et al.* Optimized sgRNA design to maximize activity and minimize off-target effects of CRISPR-Cas9. *Nat Biotechnol* **34**, 184-191, doi:10.1038/nbt.3437 (2016).
561 Henderson, H. CRISPR clinical trials: a 2022 update. *Innovative Genomics Institute* (2022).
562 Uddin, F., Rudin, C. M. & Sen, T. CRISPR gene therapy: applications, limitations, and implications for the future. *Frontiers in oncology* **10**, 1387 (2020).
563 Gillmore, J. D. *et al.* CRISPR-Cas9 in vivo gene editing for transthyretin amyloidosis. *New England Journal of Medicine* **385**, 493-502 (2021).
564 Doudna, J. A. & Charpentier, E. The new frontier of genome engineering with CRISPR-Cas9. *Science* **346** (2014).
565 Zhang, Y. *et al.* CRISPR/gRNA-directed synergistic activation mediator (SAM) induces specific, persistent and robust reactivation of the HIV-1 latent reservoirs. *Sci Rep* **5**, 16277, doi:10.1038/srep16277 (2015).
566 Luo, N. W. Z., W; Li, J; Zhai, Z; Lu, J; Dong, R. Targeted activation of HNF4α/HGF1/FOXA2 reverses hepatic fibrosis via exosome-mediated delivery of CRISPR/dCas9-SAM system. *Nanomedicine* **17**, 17, doi:https://doi.org/10.2217/nnm-2022-0083 (2022).
567 Yuan, H. *et al.* Regenerating Urethral Striated Muscle by CRISPRi/dCas9-KRAB-Mediated Myostatin Silencing for Obesity-Associated Stress Urinary Incontinence. *CRISPR J* **3**, 562-572, doi:10.1089/crispr.2020.0077 (2020).

568 Parsi, K. H., E; Kearns, N; Maehr, R. *Using an Inducible CRISPR-dCas9-KRAB Effector System to Dissect Transcriptional Regulation in Human Embryonic Stem Cells*. Vol. 1507 (2016).
569 Li, A. *et al.* Using the dCas9-KRAB system to repress gene expression in hiPSC-derived NGN2 neurons. *STAR Protoc* **2**, 100580, doi:10.1016/j.xpro.2021.100580 (2021).
570 Ma, H. *et al.* Multiplexed labeling of genomic loci with dCas9 and engineered sgRNAs using CRISPRainbow. *Nat Biotechnol* **34**, 528-530, doi:10.1038/nbt.3526 (2016).
571 Tanenbaum, M. E., Gilbert, L. A., Qi, L. S., Weissman, J. S. & Vale, R. D. A protein-tagging system for signal amplification in gene expression and fluorescence imaging. *Cell* **159**, 635-646, doi:10.1016/j.cell.2014.09.039 (2014).
572 Hashimoto, M., Yamashita, Y. & Takemoto, T. Electroporation of Cas9 protein/sgRNA into early pronuclear zygotes generates non-mosaic mutants in the mouse. *Developmental biology* **418**, 1-9 (2016).
573 Wang, W. *et al.* Delivery of Cas9 protein into mouse zygotes through a series of electroporation dramatically increases the efficiency of model creation. *Journal of Genetics and Genomics* **43**, 319-327 (2016).
574 Chen, S., Lee, B., Lee, A. Y.-F., Modzelewski, A. J. & He, L. Highly efficient mouse genome editing by CRISPR ribonucleoprotein electroporation of zygotes. *Journal of Biological Chemistry* **291**, 14457-14467 (2016).
575 Valadkhan, S. & Valencia-Hipólito, A. in *Long Non-coding RNAs in Human Disease* 203-236 (Springer, 2015).
576 Lau, C.-H. & Suh, Y. In vivo epigenome editing and transcriptional modulation using CRISPR technology. *Transgenic research* **27**, 489-509 (2018).
577 Liao, H.-K. *et al.* In vivo target gene activation via CRISPR/Cas9-mediated trans-epigenetic modulation. *Cell* **171**, 1495-1507. e1415 (2017).
578 Kabadi, A. M., Ousterout, D. G., Hilton, I. B. & Gersbach, C. A. Multiplex CRISPR/Cas9-based genome engineering from a single lentiviral vector. *Nucleic Acids Res* **42**, e147, doi:10.1093/nar/gku749 (2014).
579 Bäck, S. *et al.* Neuron-specific genome modification in the adult rat brain using CRISPR-Cas9 transgenic rats. *Neuron* **102**, 105-119. e108 (2019).
580 Stoica, L., Ahmed, S. S., Gao, G. & Esteves, M. S. AAV-mediated gene transfer to the mouse CNS. *Current protocols in microbiology*, Unit14D. 15 (2013).
581 Platt, R. J. *et al.* CRISPR-Cas9 knockin mice for genome editing and cancer modeling. *Cell* **159**, 440-455 (2014).
582 Bero, A. W. *et al.* Early remodeling of the neocortex upon episodic memory encoding. *Proceedings of the National Academy of Sciences* **111**, 11852-11857 (2014).
583 Grieger, J. C. & Samulski, R. J. Adeno-associated virus vectorology, manufacturing, and clinical applications. *Methods in enzymology* **507**, 229-254 (2012).
584 Haery, L. *et al.* Adeno-associated virus technologies and methods for targeted neuronal manipulation. *Frontiers in neuroanatomy* **13**, 93 (2019).
585 Penaud-Budloo, M. *et al.* Adeno-associated virus vector genomes persist as episomal chromatin in primate muscle. *Journal of virology* **82**, 7875-7885 (2008).
586 Li, Q. *et al.* In vivo PCSK9 gene editing using an all-in-one self-cleavage AAV-CRISPR system. *Molecular Therapy-Methods & Clinical Development* **20**, 652-659 (2021).
587 Hunker, A. C. *et al.* Conditional single vector CRISPR/SaCas9 viruses for efficient mutagenesis in the adult mouse nervous system. *Cell reports* **30**, 4303-4316. e4306 (2020).

588 Bak, R. O. & Porteus, M. H. CRISPR-mediated integration of large gene cassettes using AAV donor vectors. *Cell reports* **20**, 750-756 (2017).
589 Yang, Y. *et al.* A dual AAV system enables the Cas9-mediated correction of a metabolic liver disease in newborn mice. *Nature biotechnology* **34**, 334-338 (2016).
590 Liang, S.-Q. *et al.* AAV5 delivery of CRISPR-Cas9 supports effective genome editing in mouse lung airway. *Molecular Therapy* **30**, 238-243 (2022).
591 Xu, C. L., Ruan, M. Z., Mahajan, V. B. & Tsang, S. H. Viral delivery systems for CRISPR. *Viruses* **11**, 28 (2019).
592 Yang, Y., Xu, J., Ge, S. & Lai, L. CRISPR/Cas: advances, limitations, and applications for precision cancer research. *Frontiers in Medicine* **8**, 649896 (2021).
593 Haggerty, D. L., Grecco, G. G., Reeves, K. C. & Atwood, B. Adeno-associated viral vectors in neuroscience research. *Molecular Therapy-Methods & Clinical Development* **17**, 69-82 (2020).
594 Choi, V. W., McCarty, D. M. & Samulski, R. J. AAV hybrid serotypes: improved vectors for gene delivery. *Current gene therapy* **5**, 299-310 (2005).
595 Kiyota, T. *et al.* AAV1/2-mediated CNS gene delivery of dominant-negative CCL2 mutant suppresses gliosis, β-amyloidosis, and learning impairment of APP/PS1 mice. *Molecular Therapy* **17**, 803-809 (2009).
596 Ip, C. W. *et al.* AAV1/2-induced overexpression of A53T-α-synuclein in the substantia nigra results in degeneration of the nigrostriatal system with Lewy-like pathology and motor impairment: a new mouse model for Parkinson's disease. *Acta neuropathologica communications* **5**, 1-12 (2017).
597 Bourdenx, M., Dutheil, N., Bezard, E. & Dehay, B. Systemic gene delivery to the central nervous system using Adeno-associated virus. *Frontiers in molecular neuroscience* **7**, 50 (2014).
598 Gessler, D. J., Tai, P. W., Li, J. & Gao, G. Intravenous infusion of AAV for widespread gene delivery to the nervous system. *Methods in molecular biology (Clifton, NJ)* **1950**, 143 (2019).
599 Correia, P. A., Matias, S. & Mainen, Z. F. Stereotaxic adeno-associated virus injection and cannula implantation in the dorsal raphe nucleus of mice. *Bio-protocol* **7** (2017).
600 Hana, S. *et al.* Highly efficient neuronal gene knockout in vivo by CRISPR-Cas9 via neonatal intracerebroventricular injection of AAV in mice. *Gene Therapy*, 1-13 (2021).
601 Hung, S. S. *et al.* AAV-mediated CRISPR/Cas gene editing of retinal cells in vivo. *Investigative Ophthalmology & Visual Science* **57**, 3470-3476 (2016).
602 Osterndorff-Kahanek, E. A. *et al.* Chronic ethanol exposure produces time- and brain region-dependent changes in gene coexpression networks. *PLoS One* **10**, e0121522, doi:10.1371/journal.pone.0121522 (2015).
603 Sarropoulos, I., Marin, R., Cardoso-Moreira, M. & Kaessmann, H. Developmental dynamics of lncRNAs across mammalian organs and species. *Nature* **571**, 510-514, doi:10.1038/s41586-019-1341-x (2019).
604 Jarroux, J., Morillon, A. & Pinskaya, M. History, Discovery, and Classification of lncRNAs. *Adv Exp Med Biol* **1008**, 1-46, doi:10.1007/978-981-10-5203-3_1 (2017).
605 Chen, L.-L. Linking long noncoding RNA localization and function. *Trends in Biochem Sci* **41**, 761-772 (2016).
606 Anderson, D. M. *et al.* A micropeptide encoded by a putative long noncoding RNA regulates muscle performance. *Cell* **160**, 595-606, doi:10.1016/j.cell.2015.01.009 (2015).

607 Raveendra, B. L. *et al.* Long noncoding RNA GM12371 acts as a transcriptional regulator of synapse function. *Proc Natl Acad Sci U S A* **115**, E10197-E10205, doi:10.1073/pnas.1722587115 (2018).
608 Elkouris, M. *et al.* Long non-coding RNAs associated with neurodegeneration-linked genes are reduced in Parkinson's disease patients. *Front Cell Neurosci* **13**, 58 (2019).
609 Liu, J. *et al.* Systematic Analysis of RNA Regulatory Network in Rat Brain after Ischemic Stroke. *Biomed Res Int* **2018**, 8354350, doi:10.1155/2018/8354350 (2018).
610 Shen, Y. *et al.* Focusing on long non-coding RNA dysregulation in newly diagnosed multiple myeloma. *Life Sci* **196**, 133-142, doi:10.1016/j.lfs.2018.01.025 (2018).
611 Shan, Y. *et al.* LncRNA SNHG7 sponges miR-216b to promote proliferation and liver metastasis of colorectal cancer through upregulating GALNT1. *Cell Death Dis* **9**, 722, doi:10.1038/s41419-018-0759-7 (2018).
612 Elkouris, M. *et al.* Long Non-coding RNAs Associated With Neurodegeneration-Linked Genes Are Reduced in Parkinson's Disease Patients. *Front Cell Neurosci* **13**, 58, doi:10.3389/fncel.2019.00058 (2019).
613 Dallner, O. S. *et al.* Dysregulation of a long noncoding RNA reduces leptin leading to a leptin-responsive form of obesity. *Nat Med* **25**, 507-516, doi:10.1038/s41591-019-0370-1 (2019).
614 Bannon, M. J. *et al.* Identification of long noncoding RNA s dysregulated in the midbrain of human cocaine abusers. *Journal of neurochemistry* **135**, 50-59 (2015).
615 Khalil, A. M. *et al.* Many human large intergenic noncoding RNAs associate with chromatin-modifying complexes and affect gene expression. *Proceedings of the National Academy of Sciences* **106**, 11667-11672 (2009).
616 Guttman, M. & Rinn, J. L. Modular regulatory principles of large non-coding RNAs. *Nature* **482**, 339-346 (2012).
617 Yu, V. *et al.* RNA-seq analysis identifies key long non-coding RNAs connected to the pathogenesis of alcohol-associated head and neck squamous cell carcinoma. *Oncol Lett* **12**, 2846-2853, doi:10.3892/ol.2016.4972 (2016).
618 Ignacio, C. *et al.* Alterations in serum microRNA in humans with alcohol use disorders impact cell proliferation and cell death pathways and predict structural and functional changes in brain. *BMC neuroscience* **16**, 55 (2015).
619 Kapoor, M. *et al.* Analysis of whole genome-transcriptomic organization in brain genes associated with alcoholism. doi:10.1101/500439 (2018).
620 Van Booven, D. *et al.* Alcohol use disorder causes global changes in splicing in the human brain. *Translational psychiatry* **11**, 1-9 (2021).
621 Fu, Y., Sander, J. D., Reyon, D., Cascio, V. M. & Joung, J. K. Improving CRISPR-Cas nuclease specificity using truncated guide RNAs. *Nat Biotechnol* **32**, 279-284, doi:10.1038/nbt.2808 (2014).
622 Bassett, Andrew R., Tibbit, C., Ponting, Chris P. & Liu, J.-L. Highly efficient targeted mutagenesis of Drosophila with the CRISPR/Cas9 system. *Cell Reports* **4**, 220-228, doi:10.1016/j.celrep.2013.06.020 (2013).
623 Blednov, Y. A. *et al.* GABA A receptors containing ρ1 subunits contribute to in vivo effects of ethanol in mice. *PloS one* **9**, e85525 (2014).
624 Yang, H., Wang, H. & Jaenisch, R. Generating genetically modified mice using CRISPR/Cas-mediated genome engineering. *Nat Protoc* **9**, 1956-1968, doi:10.1038/nprot.2014.134 (2014).

625 Melendez, R. I. Intermittent (every-other-day) drinking induces rapid escalation of ethanol intake and preference in adolescent and adult C57BL/6J mice. *Alcohol Clin Exp Res* **35**, 652-658, doi:10.1111/j.1530-0277.2010.01383.x (2011).
626 Griffin, W. C., 3rd, Lopez, M. F. & Becker, H. C. Intensity and duration of chronic ethanol exposure is critical for subsequent escalation of voluntary ethanol drinking in mice. *Alcohol Clin Exp Res* **33**, 1893-1900, doi:10.1111/j.1530-0277.2009.01027.x (2009).
627 Ma, Y.-Y. *et al.* Regional and cell-type-specific effects of DAMGO on striatal D1 and D2 dopamine receptor-expressing medium-sized spiny neurons. *ASN neuro* **4**, AN20110063 (2012).
628 Tepper, J. M. & Bolam, J. P. Functional diversity and specificity of neostriatal interneurons. *Current opinion in neurobiology* **14**, 685-692 (2004).
629 Tepper, J. M., Tecuapetla, F., Koós, T. & Ibáñez-Sandoval, O. Heterogeneity and diversity of striatal GABAergic interneurons. *Frontiers in neuroanatomy* **4**, 150 (2010).
630 Tepper, J. M. *et al.* Heterogeneity and diversity of striatal GABAergic interneurons: update 2018. *Frontiers in neuroanatomy* **12**, 91 (2018).
631 Modzelewski, A. J. *et al.* Efficient mouse genome engineering by CRISPR-EZ technology. *Nature protocols* **13**, 1253-1274 (2018).
632 Kralic, J. *et al.* GABAA receptor alpha-1 subunit deletion alters receptor subtype assembly, pharmacological and behavioral responses to benzodiazepines and zolpidem. *Neuropharmacology* **43**, 685-694 (2002).
633 Siddiqui, S. V., Chatterjee, U., Kumar, D., Siddiqui, A. & Goyal, N. Neuropsychology of prefrontal cortex. *Indian journal of psychiatry* **50**, 202 (2008).
634 Del Arco, A. & Mora, F. Neurotransmitters and prefrontal cortex–limbic system interactions: implications for plasticity and psychiatric disorders. *Journal of neural transmission* **116**, 941-952 (2009).
635 Wassum, K. M. & Izquierdo, A. The basolateral amygdala in reward learning and addiction. *Neuroscience & Biobehavioral Reviews* **57**, 271-283 (2015).
636 Goto, Y. & Grace, A. A. Limbic and cortical information processing in the nucleus accumbens. *Trends in neurosciences* **31**, 552-558 (2008).
637 Kryger, R. & Wilce, P. The effects of alcoholism on the human basolateral amygdala. *Neuroscience* **167**, 361-371 (2010).
638 Gilpin, N. W. & Koob, G. F. Neurobiology of alchohol dependence. *Alcohol Res Health* (2014).
639 Martin, C. S. & Winters, K. C. Diagnosis and assessment of alcohol use disorders among adolescents. *Alcohol health and research world* **22**, 95 (1998).
640 Fritz, B. M., Grahame, N. J. & Boehm, S. L. Selection for high alcohol preference drinking in mice results in heightened sensitivity and rapid development of acute functional tolerance to alcohol's ataxic effects. *Genes, Brain and Behavior* **12**, 78-86 (2013).
641 Elvig, S. K. *et al.* Tolerance to alcohol: A critical yet understudied factor in alcohol addiction. *Pharmacology Biochemistry and Behavior* **204**, 173155 (2021).
642 Sancar, F., Ericksen, S. S., Kucken, A. M., Teissere, J. A. & Czajkowski, C. Structural determinants for high-affinity zolpidem binding to GABA-A receptors. *Molecular pharmacology* **71**, 38-46 (2007).
643 Crestani, F., Martin, J. R., Mohler, H. & Rudolph, U. Mechanism of action of the hypnotic zolpidem in vivo. *Br J Pharmacol* **131**, 1251-1254, doi:10.1038/sj.bjp.0703717 (2000).

644 Chandra, D. *et al.* GABAA receptor α4 subunits mediate extrasynaptic inhibition in thalamus and dentate gyrus and the action of gaboxadol. *Proceedings of the National Academy of Sciences* **103**, 15230-15235 (2006).
645 Chandra, D. *et al.* $GABA_A$ receptor α4 subunits mediate extrasynaptic inhibition in thalamus and dentate gyrus and the action of gaboxadol. *Proc Natl Acad Sci U S A* **103**, 15230-15235 (2006).
646 Meera, P., Wallner, M. & Otis, T. S. Molecular basis for the high THIP/gaboxadol sensitivity of extrasynaptic GABA(A) receptors. *J Neurophysiol* **106**, 2057-2064, doi:10.1152/jn.00450.2011 (2011).
647 Olsen, R. W. & Liang, J. Role of GABA(A) receptors in alcohol use disorders suggested by chronic intermittent ethanol (CIE) rodent model. *Mol Brain* **10**, 45, doi:10.1186/s13041-017-0325-8 (2017).
648 Forstera, B., Castro, P. A., Moraga-Cid, G. & Aguayo, L. G. Potentiation of Gamma Aminobutyric Acid Receptors (GABAAR) by Ethanol: How Are Inhibitory Receptors Affected? *Front Cell Neurosci* **10**, 114, doi:10.3389/fncel.2016.00114 (2016).
649 Sou, J. H., Chan, M. H. & Chen, H. H. Ketamine, but not propofol, anaesthesia is regulated by metabotropic glutamate 5 receptors. *Br J Anaesth* **96**, 597-601, doi:10.1093/bja/ael046 (2006).
650 Sato, Y. *et al.* Chronopharmacological studies of ketamine in normal and NMDA epsilon1 receptor knockout mice. *Br J Anaesth* **92**, 859-864, doi:10.1093/bja/aeh144 (2004).
651 Chen, X., Shu, S. & Bayliss, D. A. HCN1 channel subunits are a molecular substrate for hypnotic actions of ketamine. *J Neurosci* **29**, 600-609, doi:10.1523/JNEUROSCI.3481-08.2009 (2009).
652 Zhou, C. *et al.* Forebrain HCN1 channels contribute to hypnotic actions of ketamine. *Anesthesiology* **118**, 785-795, doi:10.1097/ALN.0b013e318287b7c8 (2013).
653 Leung, L. S., Chu, L., Prado, M. A. M. & Prado, V. F. Forebrain Acetylcholine Modulates Isoflurane and Ketamine Anesthesia in Adult Mice. *Anesthesiology* **134**, 588-606, doi:10.1097/ALN.0000000000003713 (2021).
654 Arama, J. *et al.* GABAA receptor activity shapes the formation of inhibitory synapses between developing medium spiny neurons. *Frontiers in cellular neuroscience* **9**, 290 (2015).
655 Maguire, E. P. *et al.* Tonic inhibition of accumbal spiny neurons by extrasynaptic α4βδ GABAA receptors modulates the actions of psychostimulants. *Journal of Neuroscience* **34**, 823-838 (2014).
656 Labrakakis, C., Rudolph, U. & De Koninck, Y. The heterogeneity in GABAA receptor-mediated IPSC kinetics reflects heterogeneity of subunit composition among inhibitory and excitatory interneurons in spinal lamina II. *Frontiers in cellular neuroscience* **8**, 424 (2014).
657 Smith, A. J. *et al.* Effect of α Subunit on Allosteric Modulation of Ion Channel Function in Stably Expressed Human Recombinant γ-Aminobutyric AcidA Receptors Determined Using36Cl Ion Flux. *Molecular Pharmacology* **59**, 1108-1118 (2001).
658 Dixon, C., Sah, P., Lynch, J. W. & Keramidas, A. GABAA receptor α and γ subunits shape synaptic currents via different mechanisms. *Journal of Biological Chemistry* **289**, 5399-5411 (2014).

659 Zhang, H. *et al.* LncRNA Nqo1-AS1 Attenuates Cigarette Smoke-Induced Oxidative Stress by Upregulating its Natural Antisense Transcript Nqo1. *Front Pharmacol* **12**, 729062, doi:10.3389/fphar.2021.729062 (2021).
660 Plasil, S. L., Collins, V. J., Baratta, A. M., Farris, S. P. & Homanics, G. E. Hippocampal ceRNA networks from chronic intermittent ethanol vapor-exposed male mice and functional analysis of top-ranked lncRNA genes for ethanol drinking phenotypes. *Advances in Drug and Alcohol Research* **2**, 10831, doi:10.3389/adar.2022.10831 (2022).
661 Denham, A. N. *et al.* Long Non-Coding RNAs: The New Frontier into Understanding the Etiology of Alcohol Use Disorder. *Noncoding RNA* **8**, doi:10.3390/ncrna8040059 (2022).
662 Childs-Disney, J. L. *et al.* Targeting RNA structures with small molecules. *Nat Rev Drug Discov* **21**, 736-762, doi:10.1038/s41573-022-00521-4 (2022).
663 Falese, J. P., Donlic, A. & Hargrove, A. E. Targeting RNA with small molecules: from fundamental principles towards the clinic. *Chem Soc Rev* **50**, 2224-2243, doi:10.1039/d0cs01261k (2021).
664 Michels, B. E. *et al.* Pooled In Vitro and In Vivo CRISPR-Cas9 Screening Identifies Tumor Suppressors in Human Colon Organoids. *Cell Stem Cell* (2020).
665 Khan, D. H. *et al.* Mitochondrial carrier homolog 2 (MTCH2) is necessary for AML survival. *Blood Journal*, blood. 2019000106 (2020).
666 Muir, A. M. *et al.* Bi-allelic Loss-of-Function Variants in NUP188 Cause a Recognizable Syndrome Characterized by Neurologic, Ocular, and Cardiac Abnormalities. *The American Journal of Human Genetics* (2020).
667 Wu, Y. *et al.* Inhibiting the TLR4-MyD88 signalling cascade by genetic or pharmacological strategies reduces acute alcohol-induced sedation and motor impairment in mice. *British journal of pharmacology* **165**, 1319-1329 (2012).
668 Stemmer, M., Thumberger, T., del Sol Keyer, M., Wittbrodt, J. & Mateo, J. L. CCTop: an intuitive, flexible and reliable CRISPR/Cas9 target prediction tool. *PloS one* **10** (2015).
669 Labuhn, M. *et al.* Refined sgRNA efficacy prediction improves large-and small-scale CRISPR–Cas9 applications. *Nucleic acids research* **46**, 1375-1385 (2018).
670 Benjamini, Y., Krieger, A. & Yekutieli, D. Adaptive linear step-up false discovery rate controlling procedures. *Biometrika* **93**, 491-507 (2006).
671 Hou, B., Reizis, B. & DeFranco, A. L. Toll-like receptor-mediated dendritic cell-dependent and-independent stimulation of innate and adaptive immunity. *Immunity* **29**, 272 (2008).
672 Modzelewski, A. J. *et al.* Efficient mouse genome engineering by CRISPR-EZ technology. *Nat Protoc* **13**, 1253-1274, doi:10.1038/nprot.2018.012 (2018).
673 Zuo, E. *et al.* One-step generation of complete gene knockout mice and monkeys by CRISPR/Cas9-mediated gene editing with multiple sgRNAs. *Cell research* **27**, 933-945 (2017).
674 Wahlsten, D., Bachmanov, A., Finn, D. A. & Crabbe, J. C. Stability of inbred mouse strain differences in behavior and brain size between laboratories and across decades. *Proceedings of the national academy of sciences* **103**, 16364-16369 (2006).
675 Crabbe, J. C., Wahlsten, D. & Dudek, B. C. Genetics of mouse behavior: interactions with laboratory environment. *Science* **284**, 1670-1672 (1999).
676 Willi, M., Smith, H. E., Wang, C., Liu, C. & Hennighausen, L. Mutation frequency is not increased in CRISPR–Cas9-edited mice. *Nature methods* **15**, 756-758 (2018).
677 Dong, Y. *et al.* Genome-wide off-target analysis in CRISPR-Cas9 modified mice and their offspring. *G3: Genes, Genomes, Genetics* **9**, 3645-3651 (2019).

678 Jones, C., Paulozzi, L. & Mack, K. Centers for Disease Control and Prevention (CDC) Alcohol involvement in opioid pain reliever and benzodiazepine drug abuse-related emergency department visits and drug-related deaths-United States, 2010. *MMWR Morb Mortal Wkly Rep* **63**, 881-885 (2014).
679 Sacks, J. J., Gonzales, K. R., Bouchery, E. E., Tomedi, L. E. & Brewer, R. D. 2010 national and state costs of excessive alcohol consumption. *American journal of preventive medicine* **49**, e73-e79 (2015).
680 Mira, R. G. *et al.* Effect of alcohol on hippocampal-dependent plasticity and behavior: Role of glutamatergic synaptic transmission. *Frontiers in Behavioral Neuroscience* **13**, 288 (2020).
681 Sun, W., Li, X., Tang, C. & An, L. Acute low alcohol disrupts hippocampus-striatum neural correlate of learning strategy by inhibition of PKA/CREB pathway in rats. *Frontiers in pharmacology* **9**, 1439 (2018).
682 White, A. M., Matthews, D. B. & Best, P. J. Ethanol, memory, and hippocampal function: a review of recent findings. *Hippocampus* **10**, 88-93 (2000).
683 Montesinos, J., Alfonso-Loeches, S. & Guerri, C. Impact of the innate immune response in the actions of ethanol on the central nervous system. *Alcoholism: Clinical and Experimental Research* **40**, 2260-2270 (2016).
684 Geil, C. R. *et al.* Alcohol and adult hippocampal neurogenesis: promiscuous drug, wanton effects. *Progress in Neuro-Psychopharmacology and Biological Psychiatry* **54**, 103-113 (2014).
685 Zahr, N. M. *et al.* Brain injury and recovery following binge ethanol: evidence from in vivo magnetic resonance spectroscopy. *Biological psychiatry* **67**, 846-854 (2010).
686 Grifasi, I. R. *et al.* Characterization of the hippocampal neuroimmune response to binge-like ethanol consumption in the drinking in the dark model. *Neuroimmunomodulation* **26**, 19-32 (2019).
687 Macht, V., Crews, F. T. & Vetreno, R. P. Neuroimmune and epigenetic mechanisms underlying persistent loss of hippocampal neurogenesis following adolescent intermittent ethanol exposure. *Curr Opin Pharmacol* **50**, 9-16, doi:10.1016/j.coph.2019.10.007 (2020).
688 Edenberg, H. J. *et al.* Gene expression in the hippocampus of inbred alcohol-preferring and -nonpreferring rats. *Genes Brain Behav* **4**, 20-30, doi:10.1111/j.1601-183X.2004.00091.x (2005).
689 Taffe, M. A. *et al.* Long-lasting reduction in hippocampal neurogenesis by alcohol consumption in adolescent nonhuman primates. *Proceedings of the National Academy of Sciences* **107**, 11104-11109, doi:10.1073/pnas.0912810107 (2010).
690 Basu, S. & Suh, H. Role of Hippocampal Neurogenesis in Alcohol Withdrawal Seizures. *Brain Plast* **6**, 27-39, doi:10.3233/BPL-200114 (2020).
691 Zhou, Z., Yuan, Q., Mash, D. C. & Goldman, D. Substance-specific and shared transcription and epigenetic changes in the human hippocampus chronically exposed to cocaine and alcohol. *Proceedings of the National Academy of Sciences* **108**, 6626-6631, doi:10.1073/pnas.1018514108 (2011).
692 Saba, L. *et al.* in *ALCOHOLISM-CLINICAL AND EXPERIMENTAL RESEARCH*. 190A-190A (WILEY-BLACKWELL 111 RIVER ST, HOBOKEN 07030-5774, NJ USA).
693 Osterndorff-Kahanek, E. A. *et al.* Chronic ethanol exposure produces time-and brain region-dependent changes in gene coexpression networks. *PloS one* **10**, e0121522 (2015).

694 Blednov, Y. A. *et al.* Perturbation of chemokine networks by gene deletion alters the reinforcing actions of ethanol. *Behavioural brain research* **165**, 110-125 (2005).
695 Mitsuyama, H., Little, K. Y., Sieghart, W., Devaud, L. L. & Morrow, A. L. GABAA, Receptor α1, α4, and β3 Subunit mRNA and Protein Expression in the Frontal Cortex of Human Alcoholics. *Alcoholism: Clinical and Experimental Research* **22**, 815-822 (1998).
696 Bhandage, A. K. *et al.* GABA-A and NMDA receptor subunit mRNA expression is altered in the caudate but not the putamen of the postmortem brains of alcoholics. *Frontiers in Cellular Neuroscience* **8**, 415 (2014).
697 Jin, Z. *et al.* Selective changes of GABAA channel subunit mRNAs in the hippocampus and orbitofrontal cortex but not in prefrontal cortex of human alcoholics. *Frontiers in cellular neuroscience* **5**, 30 (2012).
698 Osterndorff-Kahanek, E. A. *et al.* Long-term ethanol exposure: Temporal pattern of microRNA expression and associated mRNA gene networks in mouse brain. *PloS one* **13**, e0190841 (2018).
699 Kyzar, E. J., Bohnsack, J. P., Zhang, H. & Pandey, S. C. MicroRNA-137 drives epigenetic reprogramming in the adult amygdala and behavioral changes after adolescent alcohol exposure. *Eneuro* (2019).
700 Wyczechowska, D. *et al.* A miRNA signature for cognitive deficits and alcohol use disorder in persons living with HIV/AIDS. *Frontiers in molecular neuroscience* **10**, 385 (2017).
701 Kryger, R., Fan, L., Wilce, P. A. & Jaquet, V. MALAT-1, a non protein-coding RNA is upregulated in the cerebellum, hippocampus and brain stem of human alcoholics. *Alcohol* **46**, 629-634 (2012).
702 Mercer, T. R., Dinger, M. E., Sunkin, S. M., Mehler, M. F. & Mattick, J. S. Specific expression of long noncoding RNAs in the mouse brain. Proc. Natl. Acad. Sci. 105, 716–721 (2008). Specific expression of long noncoding RNAs in the mouse brain.
703 Sartor, G. C., St Laurent, G., 3rd & Wahlestedt, C. The Emerging Role of Non-Coding RNAs in Drug Addiction. *Front Genet* **3**, 106, doi:10.3389/fgene.2012.00106 (2012).
704 Dallner, O. S. *et al.* Dysregulation of a long noncoding RNA reduces leptin leading to a leptin-responsive form of obesity. *Nature medicine* **25**, 507-516 (2019).
705 Plasil SL, F. S., Blednov Y, Harris RA, Messing R, Aziz HC, Lambeth PS, Mangieri RA, Mayfield D, Homanics GE. Long Noncoding RNA and AUD; Molecular Pharmacology, Behavior, and Electrophysiology of *TX2* Knockout Mice. *Alcoholism: Clinical and Experimental Research* **44**, doi:https://doi.org/10.1111/acer.14358 (June 2020).
706 Carrizales, D. *et al.* Deletion of an Alcohol-Responsive Long Non-Coding RNA," TX1", has Sexually Divergent Effects on NMDA Receptor-Mediated Transmission in Hippocampal Area CA1 of Mice. *Alcoholism-Clinical and Experimental Research* **43**, 93A-93A, doi:https://doi.org/10.1111/acer.14058 (2019).
707 Xu, H. *et al.* Role of Long Noncoding RNA Gas5 in Cocaine Action. *Biol Psychiatry* **88**, 758-766, doi:10.1016/j.biopsych.2020.05.004 (2020).
708 Rusconi, F., Battaglioli, E. & Venturin, M. Psychiatric Disorders and lncRNAs: A Synaptic Match. *International Journal of Molecular Sciences* **21**, 3030 (2020).
709 Zhou, Y., Lutz, P.-E., Wang, Y. C., Ragoussis, J. & Turecki, G. Global long non-coding RNA expression in the rostral anterior cingulate cortex of depressed suicides. *Translational psychiatry* **8**, 1-13 (2018).

710 Pirogov, S. A., Gvozdev, V. A. & Klenov, M. S. Long noncoding RNAs and stress response in the nucleolus. *Cells* **8**, 668 (2019).
711 Kartha, R. V. & Subramanian, S. Competing endogenous RNAs (ceRNAs): new entrants to the intricacies of gene regulation. *Frontiers in genetics* **5**, 8 (2014).
712 Ala, U. Competing endogenous RNAs, non-coding RNAs and diseases: An intertwined story. *Cells* **9**, 1574 (2020).
713 Moreno-García, L. *et al.* Competing endogenous RNA networks as biomarkers in neurodegenerative diseases. *International Journal of Molecular Sciences* **21**, 9582 (2020).
714 Lan, C., Peng, H., Hutvagner, G. & Li, J. Construction of competing endogenous RNA networks from paired RNA-seq data sets by pointwise mutual information. *BMC genomics* **20**, 1-10 (2019).
715 Ala, U. *et al.* Integrated transcriptional and competitive endogenous RNA networks are cross-regulated in permissive molecular environments. *Proceedings of the National Academy of Sciences* **110**, 7154-7159 (2013).
716 Mitra, A., Pfeifer, K. & Park, K.-S. Circular RNAs and competing endogenous RNA (ceRNA) networks. *Translational cancer research* **7**, S624 (2018).
717 Pandey, A. K., Lu, L., Wang, X., Homayouni, R. & Williams, R. W. Functionally enigmatic genes: a case study of the brain ignorome. *PloS one* **9**, e88889 (2014).
718 Erickson, E. K., Grantham, E. K., Warden, A. S. & Harris, R. A. Neuroimmune signaling in alcohol use disorder. *Pharmacol Biochem Behav* **177**, 34-60, doi:10.1016/j.pbb.2018.12.007 (2019).
719 Rathod, R. S. *et al.* Effects of Paternal Preconception Vapor Alcohol Exposure Paradigms on Behavioral Responses in Offspring. *Brain Sci* **10**, doi:10.3390/brainsci10090658 (2020).
720 Ritchie, M. E. *et al.* limma powers differential expression analyses for RNA-sequencing and microarray studies. *Nucleic acids research* **43**, e47-e47 (2015).
721 Becker, J. B. & Koob, G. F. Sex differences in animal models: focus on addiction. *Pharmacological reviews* **68**, 242-263 (2016).
722 Finn, D. A. *et al.* Binge ethanol drinking produces sexually divergent and distinct changes in nucleus accumbens signaling cascades and pathways in adult C57BL/6J mice. *Frontiers in genetics* **9**, 325 (2018).
723 Gelineau, R. R. *et al.* The behavioral and physiological effects of high-fat diet and alcohol consumption: Sex differences in C57 BL 6/J mice. *Brain and behavior* **7**, e00708 (2017).
724 Glover, E. J., Starr, E. M., Chao, Y., Jhou, T. C. & Chandler, L. J. Inhibition of the rostromedial tegmental nucleus reverses alcohol withdrawal-induced anxiety-like behavior. *Neuropsychopharmacology* **44**, 1896-1905, doi:10.1038/s41386-019-0406-8 (2019).
725 Belknap, J. K., Crabbe, J. C. & Young, E. Voluntary consumption of ethanol in 15 inbred mouse strains. *Psychopharmacology* **112**, 503-510 (1993).
726 Blednov, Y. *et al.* Perception of sweet taste is important for voluntary alcohol consumption in mice. *Genes, brain and behavior* **7**, 1-13 (2008).
727 Blednov, Y. *et al.* Hybrid mice as genetic models of high alcohol consumption. *Behavior genetics* **40**, 93-110 (2010).
728 Koren, E., Lev-Maor, G. & Ast, G. The emergence of alternative 3′ and 5′ splice site exons from constitutive exons. *PLoS computational biology* **3**, e95 (2007).

729 Nolte, C. & Staiger, D. RNA around the clock–regulation at the RNA level in biological timing. *Frontiers in Plant Science* **6**, 311 (2015).
730 Roca, X., Krainer, A. R. & Eperon, I. C. Pick one, but be quick: 5′ splice sites and the problems of too many choices. *Genes & development* **27**, 129-144 (2013).
731 Anna, A. & Monika, G. Splicing mutations in human genetic disorders: examples, detection, and confirmation. *Journal of applied genetics* **59**, 253-268 (2018).
732 Fredericks, A. M., Cygan, K. J., Brown, B. A. & Fairbrother, W. G. RNA-binding proteins: splicing factors and disease. *Biomolecules* **5**, 893-909 (2015).
733 Landry, J.-R., Mager, D. L. & Wilhelm, B. T. Complex controls: the role of alternative promoters in mammalian genomes. *TRENDS in Genetics* **19**, 640-648 (2003).
734 Wang, J., Zhang, S., Lu, H. & Xu, H. Differential regulation of alternative promoters emerges from unified kinetics of enhancer-promoter interaction. *Nature Communications* **13**, 1-14 (2022).
735 Singer, G. A. *et al.* Genome-wide analysis of alternative promoters of human genes using a custom promoter tiling array. *BMC genomics* **9**, 1-15 (2008).
736 Finn, D. A. *et al.* Increased drinking during withdrawal from intermittent ethanol exposure is blocked by the CRF receptor antagonist D-Phe-CRF (12–41). *Alcoholism: Clinical and Experimental Research* **31**, 939-949 (2007).
737 Souza, T. P. *et al.* Acute effects of ethanol on behavioral responses of male and female zebrafish in the open field test with the influence of a non-familiar object. *Behavioural Processes* **191**, 104474 (2021).
738 Barker, J. M., Bryant, K. G., Osborne, J. I. & Chandler, L. Age and sex interact to mediate the effects of intermittent, high-dose ethanol exposure on behavioral flexibility. *Frontiers in Pharmacology* **8**, 450 (2017).
739 Darnieder, L. *et al.* Female-specific decreases in alcohol binge-like drinking resulting from GABAA receptor delta-subunit knockdown in the VTA. *Scientific reports* **9**, 1-11 (2019).
740 Pasala, S., Barr, T. & Messaoudi, I. Impact of alcohol abuse on the adaptive immune system. *Alcohol research: current reviews* **37**, 185 (2015).
741 Romeo, J. *et al.* Moderate alcohol consumption and the immune system: a review. *British Journal of Nutrition* **98**, S111-S115 (2007).
742 Sarkar, D., Jung, M. K. & Wang, H. J. Alcohol and the immune system. *Alcohol research: current reviews* **37**, 153 (2015).
743 Molina, P. E., Happel, K. I., Zhang, P., Kolls, J. K. & Nelson, S. Focus on: alcohol and the immune system. *Alcohol Research & Health* **33**, 97 (2010).
744 Barr, T., Helms, C., Grant, K. & Messaoudi, I. Opposing effects of alcohol on the immune system. *Progress in Neuro-Psychopharmacology and Biological Psychiatry* **65**, 242-251 (2016).
745 Marshall, S. A., McKnight, K. H., Blose, A. K., Lysle, D. T. & Thiele, T. E. Modulation of binge-like ethanol consumption by IL-10 signaling in the basolateral amygdala. *Journal of Neuroimmune Pharmacology* **12**, 249-259 (2017).
746 Bednářová, A. *et al.* Lost in translation: defects in transfer RNA modifications and neurological disorders. *Frontiers in molecular neuroscience* **10**, 135 (2017).
747 Chen, W. Y. *et al.* Transcriptomics identifies STAT3 as a key regulator of hippocampal gene expression and anhedonia during withdrawal from chronic alcohol exposure. *Transl Psychiatry* **11**, 298, doi:10.1038/s41398-021-01421-8 (2021).
748 Djebali, S. *et al.* Landscape of transcription in human cells. *Nature* **489**, 101-108 (2012).

749 Clark, M. B. *et al.* The reality of pervasive transcription. *PLoS Biol* **9**, e1000625 (2011).
750 Weng, W. C. *et al.* Impact of Gene Polymorphisms in GAS5 on Urothelial Cell Carcinoma Development and Clinical Characteristics. *Diagnostics (Basel)* **10**, doi:10.3390/diagnostics10050260 (2020).
751 Chang, Z., Yan, G., Zheng, J. & Liu, Z. The lncRNA GAS5 Inhibits the Osteogenic Differentiation and Calcification of Human Vascular Smooth Muscle Cells. *Calcif Tissue Int* **107**, 86-95, doi:10.1007/s00223-020-00696-1 (2020).
752 Farris, S. P. *et al.* Transcriptome analysis of alcohol drinking in non-dependent and dependent mice following repeated cycles of forced swim stress exposure. *Brain sciences* **10**, 275 (2020).
753 Yu, F. *et al.* Long Non-coding RNA Growth Arrest-specific Transcript 5 (GAS5) Inhibits Liver Fibrogenesis through a Mechanism of Competing Endogenous RNA. *J Biol Chem* **290**, 28286-28298, doi:10.1074/jbc.M115.683813 (2015).
754 Li, M. *et al.* The long noncoding RNA GAS5 negatively regulates the adipogenic differentiation of MSCs by modulating the miR-18a/CTGF axis as a ceRNA. *Cell death & disease* **9**, 554 (2018).
755 Zhang, Z. *et al.* Negative regulation of lncRNA GAS5 by miR-21. *Cell Death & Differentiation* **20**, 1558-1568 (2013).
756 Cui, J., Wang, Y. & Xue, H. Long non-coding RNA GAS5 contributes to the progression of nonalcoholic fatty liver disease by targeting the microRNA-29a-3p/NOTCH2 axis. *Bioengineered* **13**, 8370-8381 (2022).
757 Smith, C. M. & Steitz, J. A. Classification of gas5 as a multi-small-nucleolar-RNA (snoRNA) host gene and a member of the 5′-terminal oligopyrimidine gene family reveals common features of snoRNA host genes. *Molecular and cellular biology* **18**, 6897-6909 (1998).
758 Mayama, T., Marr, A. & Kino, T. Differential expression of glucocorticoid receptor noncoding RNA repressor Gas5 in autoimmune and inflammatory diseases. *Hormone and Metabolic Research* **48**, 550-557 (2016).
759 Sun, D. *et al.* LncRNA GAS5 inhibits microglial M2 polarization and exacerbates demyelination. *EMBO reports* **18**, 1801-1816 (2017).
760 El-Brolosy, M. A. & Stainier, D. Y. Genetic compensation: A phenomenon in search of mechanisms. *PLoS genetics* **13**, e1006780 (2017).
761 Ma, Z. *et al.* PTC-bearing mRNA elicits a genetic compensation response via Upf3a and COMPASS components. *Nature* **568**, 259-263 (2019).
762 Dreos, R., Ambrosini, G., Périer, R. C. & Bucher, P. The Eukaryotic Promoter Database: expansion of EPDnew and new promoter analysis tools. *Nucleic acids research* **43**, D92-D96 (2015).
763 Dreos, R., Ambrosini, G., Groux, R., Cavin Périer, R. & Bucher, P. The eukaryotic promoter database in its 30th year: focus on non-vertebrate organisms. *Nucleic acids research* **45**, D51-D55 (2017).
764 Concordet, J.-P. & Haeussler, M. CRISPOR: intuitive guide selection for CRISPR/Cas9 genome editing experiments and screens. *Nucleic acids research* **46**, W242-W245 (2018).
765 Grubbs, F. E. Sample criteria for testing outlying observations. *The Annals of Mathematical Statistics*, 27-58 (1950).
766 Renganathan, A. *et al.* GAS5 long non-coding RNA in malignant pleural mesothelioma. *Molecular cancer* **13**, 1-12 (2014).

767 Vigouroux, A., Oldewurtel, E., Cui, L., Bikard, D. & van Teeffelen, S. Tuning dCas9's ability to block transcription enables robust, noiseless knockdown of bacterial genes. *Molecular Systems Biology* **14**, e7899 (2018).
768 Widom, J. R., Rai, V., Rohlman, C. E. & Walter, N. G. Versatile transcription control based on reversible dCas9 binding. *Rna* **25**, 1457-1469 (2019).
769 Rhodes, J. S., Best, K., Belknap, J. K., Finn, D. A. & Crabbe, J. C. Evaluation of a simple model of ethanol drinking to intoxication in C57BL/6J mice. *Physiol Behav* **84**, 53-63, doi:10.1016/j.physbeh.2004.10.007 (2005).
770 Rhodes, J. S. *et al.* Mouse inbred strain differences in ethanol drinking to intoxication. *Genes Brain Behav* **6**, 1-18, doi:10.1111/j.1601-183X.2006.00210.x (2007).
771 Boyle, M. P., Kolber, B. J., Vogt, S. K., Wozniak, D. F. & Muglia, L. J. Forebrain glucocorticoid receptors modulate anxiety-associated locomotor activation and adrenal responsiveness. *J Neurosci* **26**, 1971-1978, doi:10.1523/JNEUROSCI.2173-05.2006 (2006).
772 Tronche, F. *et al.* Disruption of the glucocorticoid receptor gene in the nervous system results in reduced anxiety. *Nature genetics* **23**, 99-103 (1999).
773 Walf, A. A. & Frye, C. A. The use of the elevated plus maze as an assay of anxiety-related behavior in rodents. *Nat Protoc* **2**, 322-328, doi:10.1038/nprot.2007.44 (2007).
774 Deltour, L., Foglio, M. H. & Duester, G. Metabolic deficiencies in alcohol dehydrogenase Adh1, Adh3, and Adh4 null mutant mice: Overlapping roles of Adh1 and Adh4 in ethanol clearance and metabolism of retinol to retinoic acid. *Journal of Biological Chemistry* **274**, 16796-16801 (1999).
775 Xu, R. *et al.* Quantitative comparison of expression with adeno-associated virus (AAV-2) brain-specific gene cassettes. *Gene therapy* **8**, 1323-1332 (2001).
776 Albert, K. *et al.* Downregulation of tyrosine hydroxylase phenotype after AAV injection above substantia nigra: Caution in experimental models of Parkinson's disease. *Journal of neuroscience research* **97**, 346-361 (2019).
777 Mendoza, S. D., El-Shamayleh, Y. & Horwitz, G. D. AAV-mediated delivery of optogenetic constructs to the macaque brain triggers humoral immune responses. *Journal of Neurophysiology* **117**, 2004-2013 (2017).
778 Rubio, F. J. *et al.* Prelimbic cortex is a common brain area activated during cue-induced reinstatement of cocaine and heroin seeking in a polydrug self-administration rat model. *European Journal of Neuroscience* **49**, 165-178 (2019).
779 Moorman, D. E., James, M. H., McGlinchey, E. M. & Aston-Jones, G. Differential roles of medial prefrontal subregions in the regulation of drug seeking. *Brain research* **1628**, 130-146 (2015).
780 Van den Oever, M. C., Spijker, S., Smit, A. B. & De Vries, T. J. Prefrontal cortex plasticity mechanisms in drug seeking and relapse. *Neuroscience & Biobehavioral Reviews* **35**, 276-284 (2010).
781 McCalley, D. M. *et al.* Medial prefrontal cortex theta burst stimulation improves treatment outcomes in alcohol use disorder: a double-blind, sham-controlled neuroimaging study. *Biological Psychiatry Global Open Science* (2022).
782 Shang, P. *et al.* Chronic alcohol exposure induces aberrant mitochondrial morphology and inhibits respiratory capacity in the medial prefrontal cortex of mice. *Frontiers in Neuroscience* **14**, 561173 (2020).

783 Wei, G., Sirohi, S. & Walker, B. M. Dysregulated kappa-opioid receptors in the medial prefrontal cortex contribute to working memory deficits in alcohol dependence. *Addiction Biology* **27**, e13138 (2022).
784 Nakagawa, S. & Cuthill, I. C. Effect size, confidence interval and statistical significance: a practical guide for biologists. *Biological reviews* **82**, 591-605 (2007).
785 Lovell, D. P. Biological importance and statistical significance. *Journal of agricultural and food chemistry* **61**, 8340-8348 (2013).
786 Cao, Y., Jiang, C., Lin, H. & Chen, Z. Silencing of Long Noncoding RNA Growth Arrest–Specific 5 Alleviates Neuronal Cell Apoptosis and Inflammatory Responses Through Sponging microRNA-93 to Repress PTEN Expression in Spinal Cord Injury. *Frontiers in Cellular Neuroscience* **15**, 646788 (2021).
787 Deng, Y. *et al.* Silencing of long non-coding RNA GAS5 suppresses neuron cell apoptosis and nerve injury in ischemic stroke through inhibiting DNMT3B-dependent MAP4K4 methylation. *Translational stroke research* **11**, 950-966 (2020).
788 Ma, J. *et al.* The long noncoding RNA GAS5 potentiates neuronal injury in Parkinson's disease by binding to microRNA-150 to regulate Fosl1 expression. *Experimental Neurology* **347**, 113904 (2022).
789 Zhang, X.-C. *et al.* YY1/LncRNA GAS5 complex aggravates cerebral ischemia/reperfusion injury through enhancing neuronal glycolysis. *Neuropharmacology* **158**, 107682 (2019).
790 Liu, Y. & Sun, Y. High expression of GAS5 promotes neuronal death after cerebral infarction by regulating miR-365a-3p. *Eur Rev Med Pharmacol Sci* **22**, 5270-5277 (2018).
791 Chen, F., Zhang, L., Wang, E., Zhang, C. & Li, X. LncRNA GAS5 regulates ischemic stroke as a competing endogenous RNA for miR-137 to regulate the Notch1 signaling pathway. *Biochemical and biophysical research communications* **496**, 184-190 (2018).
792 Duan, D. *et al.* Dynamin is required for recombinant adeno-associated virus type 2 infection. *Journal of virology* **73**, 10371-10376 (1999).
793 Sauvageau, M. *et al.* Multiple knockout mouse models reveal lincRNAs are required for life and brain development. *elife* **2**, e01749 (2013).
794 Farris, S. P., Arasappan, D., Hunicke-Smith, S., Harris, R. A. & Mayfield, R. D. Transcriptome organization for chronic alcohol abuse in human brain. *Molecular psychiatry* **20**, 1438-1447 (2015).
795 Petruccelli, E., Brown, T., Waterman, A., Ledru, N. & Kaun, K. R. Alcohol causes lasting differential transcription in Drosophila mushroom body neurons. *Genetics* **215**, 103-116 (2020).
796 Huggett, S. B., Ikeda, A. S., Yuan, Q., Benca-Bachman, C. E. & Palmer, R. H. Genome- and transcriptome-wide splicing associations with alcohol use disorder. *Scientific Reports* **13**, 3950 (2023).
797 Rinn, J. L. & Chang, H. Y. Long noncoding RNAs: molecular modalities to organismal functions. *Annual review of biochemistry* **89**, 283-308 (2020).
798 Bassett, A. R. *et al.* Considerations when investigating lncRNA function in vivo. *elife* **3**, e03058 (2014).
799 Andergassen, D. & Rinn, J. L. From genotype to phenotype: genetics of mammalian long non-coding RNAs in vivo. *Nature Reviews Genetics* **23**, 229-243 (2022).
800 Mortazavi, A., Williams, B. A., McCue, K., Schaeffer, L. & Wold, B. Mapping and quantifying mammalian transcriptomes by RNA-Seq. *Nature methods* **5**, 621-628 (2008).

801 Byrne, A. *et al.* Nanopore long-read RNAseq reveals widespread transcriptional variation among the surface receptors of individual B cells. *Nature communications* **8**, 16027 (2017).
802 Garalde, D. R. *et al.* Highly parallel direct RNA sequencing on an array of nanopores. *Nature methods* **15**, 201-206 (2018).
803 Fu, C. *et al.* Targeted RNAseq assay incorporating unique molecular identifiers for improved quantification of gene expression signatures and transcribed mutation fraction in fixed tumor samples. *BMC cancer* **21**, 1-10 (2021).
804 Baratta, A. M., Brandner, A. J., Plasil, S. L., Rice, R. C. & Farris, S. P. Advancements in Genomic and Behavioral Neuroscience Analysis for the Study of Normal and Pathological Brain Function. *Front Mol Neurosci* **15**, 905328, doi:10.3389/fnmol.2022.905328 (2022).
805 Shin, J., Ming, G.-l. & Song, H. Decoding neural transcriptomes and epigenomes via high-throughput sequencing. *Nature neuroscience* **17**, 1463-1475 (2014).
806 Cabili, M. N. *et al.* Integrative annotation of human large intergenic noncoding RNAs reveals global properties and specific subclasses. *Genes & development* **25**, 1915-1927 (2011).
807 Fatica, A. & Bozzoni, I. Long non-coding RNAs: new players in cell differentiation and development. *Nature Reviews Genetics* **15**, 7-21 (2014).
808 Tan, J. C., Bouriakov, V. D., Feng, L., Richmond, T. A. & Burgess, D. Targeted lncRNA sequencing with the SeqCap RNA enrichment system. *Long Non-Coding RNAs: Methods and Protocols*, 73-100 (2016).
809 Lagarde, J. *et al.* High-throughput annotation of full-length long noncoding RNAs with capture long-read sequencing. *Nature genetics* **49**, 1731-1740 (2017).
810 Curion, F. *et al.* Targeted RNA sequencing enhances gene expression profiling of ultra-low input samples. *RNA biology* **17**, 1741-1753 (2020).
811 Bussotti, G. *et al.* Improved definition of the mouse transcriptome via targeted RNA sequencing. *Genome research* **26**, 705-716 (2016).
812 Whiteford, N. *et al.* An analysis of the feasibility of short read sequencing. *Nucleic acids research* **33**, e171-e171 (2005).
813 Timmusk, T. *et al.* Multiple promoters direct tissue-specific expression of the rat BDNF gene. *Neuron* **10**, 475-489 (1993).
814 Breslin, M. B., Geng, C.-D. & Vedeckis, W. V. Multiple promoters exist in the human GR gene, one of which is activated by glucocorticoids. *Molecular Endocrinology* **15**, 1381-1395 (2001).
815 Crofts, L., Hancock, M., Morrison, N. & Eisman, J. Multiple promoters direct the tissue-specific expression of novel N-terminal variant human vitamin D receptor gene transcripts. *Proceedings of the National Academy of Sciences* **95**, 10529-10534 (1998).
816 Koenigsberger, C., Chicca, J. J., Amoureux, M.-C., Edelman, G. M. & Jones, F. S. Differential regulation by multiple promoters of the gene encoding the neuron-restrictive silencer factor. *Proceedings of the National Academy of Sciences* **97**, 2291-2296 (2000).
817 Pal, S. *et al.* Alternative transcription exceeds alternative splicing in generating the transcriptome diversity of cerebellar development. *Genome research* **21**, 1260-1272 (2011).
818 Pruunsild, P., Kazantseva, A., Aid, T., Palm, K. & Timmusk, T. Dissecting the human BDNF locus: bidirectional transcription, complex splicing, and multiple promoters. *Genomics* **90**, 397-406 (2007).

819 Zhu, Y. *et al.* Computational identification of eukaryotic promoters based on cascaded deep capsule neural networks. *Briefings in Bioinformatics* **22**, bbaa299 (2021).
820 Bengtsson-Palme, J. *et al.* Strategies to improve usability and preserve accuracy in biological sequence databases. *Proteomics* **16**, 2454-2460 (2016).
821 Yandell, M. *et al.* A computational and experimental approach to validating annotations and gene predictions in the Drosophila melanogaster genome. *Proceedings of the National Academy of Sciences* **102**, 1566-1571 (2005).
822 Pedersen, A. G., Baldi, P., Chauvin, Y. & Brunak, S. The biology of eukaryotic promoter prediction—a review. *Computers & chemistry* **23**, 191-207 (1999).
823 Ayoubi, T. A. & Van De Yen, W. J. Regulation of gene expression by alternative promoters. *The FASEB Journal* **10**, 453-460 (1996).
824 Volders, P.-J. *et al.* LNCipedia: a database for annotated human lncRNA transcript sequences and structures. *Nucleic acids research* **41**, D246-D251 (2013).
825 Pal, S., Gupta, R. & Davuluri, R. V. Alternative transcription and alternative splicing in cancer. *Pharmacology & therapeutics* **136**, 283-294 (2012).
826 Ulveling, D., Francastel, C. & Hubé, F. When one is better than two: RNA with dual functions. *Biochimie* **93**, 633-644 (2011).
827 Sassone-Corsi, P. & Borrelli, E. Transcriptional regulation by trans-acting factors. *Trends in Genetics* **2**, 215-219 (1986).
828 Eszterhas, S. K., Bouhassira, E. E., Martin, D. I. & Fiering, S. Transcriptional interference by independently regulated genes occurs in any relative arrangement of the genes and is influenced by chromosomal integration position. *Molecular and Cellular Biology* **22**, 469-479 (2002).
829 Coste, A. T., Crittin, J., Bauser, C., Rohde, B. & Sanglard, D. Functional analysis of cis-and trans-acting elements of the Candida albicans CDR2 promoter with a novel promoter reporter system. *Eukaryotic Cell* **8**, 1250-1267 (2009).
830 Mignotte, V., Eleouet, J. F., Raich, N. & Romeo, P.-H. Cis-and trans-acting elements involved in the regulation of the erythroid promoter of the human porphobilinogen deaminase gene. *Proceedings of the National Academy of Sciences* **86**, 6548-6552 (1989).
831 Lee, J., Tam, J., Tsai, M. & Tsai, S. Identification of cis-and trans-acting factors regulating the expression of the human insulin receptor gene. *Journal of Biological Chemistry* **267**, 4638-4645 (1992).
832 Whitfield, T. W. *et al.* Functional analysis of transcription factor binding sites in human promoters. *Genome biology* **13**, 1-16 (2012).
833 Khambata-Ford, S. *et al.* Identification of promoter regions in the human genome by using a retroviral plasmid library-based functional reporter gene assay. *Genome research* **13**, 1765-1774 (2003).
834 Olson, N. J. *et al.* Functional identification of the promoter for the gene encoding the alpha subunit of calcium/calmodulin-dependent protein kinase II. *Proceedings of the National Academy of Sciences* **92**, 1659-1663 (1995).
835 Zhang, T., Tang, Q., Nie, F., Zhao, Q. & Chen, W. DeepLncPro: an interpretable convolutional neural network model for identifying long non-coding RNA promoters. *Briefings in Bioinformatics* **23**, bbac447 (2022).
836 Oubounyt, M., Louadi, Z., Tayara, H. & Chong, K. T. DeePromoter: robust promoter predictor using deep learning. *Frontiers in genetics* **10**, 286 (2019).

837 Le, N. Q. K., Yapp, E. K. Y., Nagasundaram, N. & Yeh, H.-Y. Classifying promoters by interpreting the hidden information of DNA sequences via deep learning and combination of continuous FastText N-grams. *Frontiers in bioengineering and biotechnology*, 305 (2019).
838 Birnbaum, R. Y. *et al.* Coding exons function as tissue-specific enhancers of nearby genes. *Genome research* **22**, 1059-1068 (2012).
839 Chen, M.-J. M. *et al.* Integrating RNA-seq and ChIP-seq data to characterize long non-coding RNAs in Drosophila melanogaster. *BMC genomics* **17**, 1-14 (2016).
840 Yang, J.-H., Li, J.-H., Jiang, S., Zhou, H. & Qu, L.-H. ChIPBase: a database for decoding the transcriptional regulation of long non-coding RNA and microRNA genes from ChIP-Seq data. *Nucleic acids research* **41**, D177-D187 (2013).
841 Basar, R. *et al.* Large-scale GMP-compliant CRISPR-Cas9–mediated deletion of the glucocorticoid receptor in multivirus-specific T cells. *Blood advances* **4**, 3357-3367 (2020).
842 Song, Y. *et al.* Efficient dual sgRNA-directed large gene deletion in rabbit with CRISPR/Cas9 system. *Cellular and molecular life sciences* **73**, 2959-2968 (2016).
843 Eleveld, T. F. *et al.* Engineering large-scale chromosomal deletions by CRISPR-Cas9. *Nucleic Acids Research* **49**, 12007-12016 (2021).
844 Vaidya, A. M. *et al.* Systemic delivery of tumor-targeting siRNA nanoparticles against an oncogenic LncRNA facilitates effective triple-negative breast cancer therapy. *Bioconjugate chemistry* **30**, 907-919 (2019).
845 Liu, S. *et al.* LncRNA NONRATT021972 siRNA regulates neuropathic pain behaviors in type 2 diabetic rats through the P2X7 receptor in dorsal root ganglia. *Molecular brain* **9**, 1-13 (2016).
846 Meng, L. *et al.* Towards a therapy for Angelman syndrome by targeting a long non-coding RNA. *Nature* **518**, 409-412 (2015).
847 Amodio, N. *et al.* Drugging the lncRNA MALAT1 via LNA gapmeR ASO inhibits gene expression of proteasome subunits and triggers anti-multiple myeloma activity. *Leukemia* **32**, 1948-1957 (2018).
848 Lai, K.-M. V. *et al.* Diverse phenotypes and specific transcription patterns in twenty mouse lines with ablated LincRNAs. *PLoS One* **10**, e0125522 (2015).
849 Groff, A. F., Barutcu, A. R., Lewandowski, J. P. & Rinn, J. L. Enhancers in the Peril lincRNA locus regulate distant but not local genes. *Genome biology* **19**, 1-14 (2018).
850 Paralkar, V. R. *et al.* Unlinking an lncRNA from its associated cis element. *Molecular cell* **62**, 104-110 (2016).
851 Sleutels, F., Zwart, R. & Barlow, D. P. The non-coding Air RNA is required for silencing autosomal imprinted genes. *Nature* **415**, 810-813 (2002).
852 Ballarino, M. *et al.* Deficiency in the nuclear long noncoding RNA Charme causes myogenic defects and heart remodeling in mice. *The EMBO Journal* **37**, e99697 (2018).
853 Ang, C. E. *et al.* The novel lncRNA lnc-NR2F1 is pro-neurogenic and mutated in human neurodevelopmental disorders. *Elife* **8**, e41770 (2019).
854 Grote, P. *et al.* The tissue-specific lncRNA Fendrr is an essential regulator of heart and body wall development in the mouse. *Developmental cell* **24**, 206-214 (2013).
855 Andersen, R. E. *et al.* The long noncoding RNA Pnky is a trans-acting regulator of cortical development in vivo. *Developmental cell* **49**, 632-642. e637 (2019).

856 Lewandowski, J. P. *et al.* The Firre locus produces a trans-acting RNA molecule that functions in hematopoiesis. *Nature communications* **10**, 5137 (2019).
857 Groff, A. F. *et al.* In vivo characterization of Linc-p21 reveals functional cis-regulatory DNA elements. *Cell reports* **16**, 2178-2186 (2016).
858 Huarte, M. *et al.* A large intergenic noncoding RNA induced by p53 mediates global gene repression in the p53 response. *Cell* **142**, 409-419 (2010).
859 Dimitrova, N. *et al.* LincRNA-p21 activates p21 in cis to promote Polycomb target gene expression and to enforce the G1/S checkpoint. *Molecular cell* **54**, 777-790 (2014).
860 Yildirim, E. *et al.* Xist RNA is a potent suppressor of hematologic cancer in mice. *Cell* **152**, 727-742 (2013).
861 Yang, L., Kirby, J. E., Sunwoo, H. & Lee, J. T. Female mice lacking Xist RNA show partial dosage compensation and survive to term. *Genes & development* **30**, 1747-1760 (2016).
862 Adrianse, R. L. *et al.* Perturbed maintenance of transcriptional repression on the inactive X-chromosome in the mouse brain after Xist deletion. *Epigenetics & chromatin* **11**, 1-13 (2018).
863 Yang, L., Yildirim, E., Kirby, J. E., Press, W. & Lee, J. T. Widespread organ tolerance to Xist loss and X reactivation except under chronic stress in the gut. *Proceedings of the National Academy of Sciences* **117**, 4262-4272 (2020).
864 Jackson, A. L. & Linsley, P. S. Recognizing and avoiding siRNA off-target effects for target identification and therapeutic application. *Nature reviews Drug discovery* **9**, 57-67 (2010).
865 Neumeier, J. & Meister, G. siRNA specificity: RNAi mechanisms and strategies to reduce off-target effects. *Frontiers in Plant Science* **11**, 526455 (2021).
866 Jackson, A. L. *et al.* Expression profiling reveals off-target gene regulation by RNAi. *Nature biotechnology* **21**, 635-637 (2003).
867 Svoboda, P. Off-targeting and other non-specific effects of RNAi experiments in mammalian cells. *Current opinion in molecular therapeutics* **9**, 248 (2007).
868 Yoshida, T. *et al.* Evaluation of off-target effects of gapmer antisense oligonucleotides using human cells. *Genes to Cells* **24**, 827-835 (2019).
869 Yoshida, T. *et al.* Estimated number of off-target candidate sites for antisense oligonucleotides in human mRNA sequences. *Genes to Cells* **23**, 448-455 (2018).
870 Wang, J., Zhang, C., Wu, Y., He, W. & Gou, X. Identification and analysis of long non-coding RNA related miRNA sponge regulatory network in bladder urothelial carcinoma. *Cancer cell international* **19**, 1-19 (2019).
871 Wang, J., Wang, J., Huang, Y. & Xiao, Y. 3dRNA v2.0: an updated web server for RNA 3D structure prediction. *International journal of molecular sciences* **20**, 4116 (2019).
872 Zhang, Y. *et al.* Identification of an lncRNA-miRNA-mRNA interaction mechanism in breast cancer based on bioinformatic analysis. *Molecular medicine reports* **16**, 5113-5120 (2017).
873 Ramanathan, M., Porter, D. F. & Khavari, P. A. Methods to study RNA–protein interactions. *Nature methods* **16**, 225-234 (2019).
874 Gawronski, A. R. *et al.* MechRNA: prediction of lncRNA mechanisms from RNA–RNA and RNA–protein interactions. *Bioinformatics* **34**, 3101-3110 (2018).
875 Gebelein, B. & Urrutia, R. Sequence-specific transcriptional repression by KS1, a multiple-zinc-finger–Kruppel-associated box protein. *Molecular and cellular biology* **21**, 928-939 (2001).

876 Weickert, M. J. & Chambliss, G. H. Site-directed mutagenesis of a catabolite repression operator sequence in Bacillus subtilis. *Proceedings of the National Academy of Sciences* **87**, 6238-6242 (1990).
877 Weber, J. R. & Skene, J. P. Identification of a novel repressive element that contributes to neuron-specific gene expression. *Journal of Neuroscience* **17**, 7583-7593 (1997).
878 Saito, K., Yoneyama, H. & Nakae, T. nalB-type mutations causing the overexpression of the MexAB-OprM efflux pump are located in the mexR gene of the Pseudomonas aeruginosa chromosome. *FEMS microbiology letters* **179**, 67-72 (1999).
879 Miao, Y. *et al.* lncRNA GAS5, as a ceRNA, inhibits the proliferation of diffuse large B-cell lymphoma cells by regulating the miR-18a-5p/RUNX1 axis. *Int J Oncol* **59**, doi:10.3892/ijo.2021.5274 (2021).
880 Wang, L., Zhang, Z. & Wang, H. Downregulation of lncRNA GAS5 prevents mitochondrial apoptosis and hypoxic-ischemic brain damage in neonatal rats through the microRNA-128-3p/Bax/Akt/GSK-3beta axis. *Neuroreport* **32**, 1395-1402, doi:10.1097/WNR.0000000000001730 (2021).
881 Goustin, A. S., Thepsuwan, P., Kosir, M. A. & Lipovich, L. The Growth-Arrest-Specific (GAS)-5 Long Non-Coding RNA: A Fascinating lncRNA Widely Expressed in Cancers. *Noncoding RNA* **5**, doi:10.3390/ncrna5030046 (2019).
882 Jin, F. *et al.* Downregulation of Long Noncoding RNA Gas5 Affects Cell Cycle and Insulin Secretion in Mouse Pancreatic beta Cells. *Cell Physiol Biochem* **43**, 2062-2073, doi:10.1159/000484191 (2017).
883 Liu, X., She, Y., Wu, H., Zhong, D. & Zhang, J. Long non-coding RNA Gas5 regulates proliferation and apoptosis in HCS-2/8 cells and growth plate chondrocytes by controlling FGF1 expression via miR-21 regulation. *J Biomed Sci* **25**, 18, doi:10.1186/s12929-018-0424-6 (2018).
884 Liu, L. *et al.* lncRNA GAS5 Inhibits Cell Migration and Invasion and Promotes Autophagy by Targeting miR-222-3p via the GAS5/PTEN-Signaling Pathway in CRC. *Mol Ther Nucleic Acids* **17**, 644-656, doi:10.1016/j.omtn.2019.06.009 (2019).
885 Mayama, T., Marr, A. K. & Kino, T. Differential Expression of Glucocorticoid Receptor Noncoding RNA Repressor Gas5 in Autoimmune and Inflammatory Diseases. *Horm Metab Res* **48**, 550-557, doi:10.1055/s-0042-106898 (2016).
886 Geng, X. *et al.* LncRNA GAS5 promotes apoptosis as a competing endogenous RNA for miR-21 via thrombospondin 1 in ischemic AKI. *Cell Death Discov* **6**, 19, doi:10.1038/s41420-020-0253-8 (2020).
887 Shi, Y. *et al.* Stabilization of lncRNA GAS5 by a Small Molecule and Its Implications in Diabetic Adipocytes. *Cell Chem Biol* **26**, 319-330 e316, doi:10.1016/j.chembiol.2018.11.012 (2019).
888 Tang, R. *et al.* LncRNA GAS5 attenuates fibroblast activation through inhibiting Smad3 signaling. *American Journal of Physiology-Cell Physiology* **319**, C105-C115 (2020).
889 Tu, J., Tian, G., Cheung, H. H., Wei, W. & Lee, T. L. Gas5 is an essential lncRNA regulator for self-renewal and pluripotency of mouse embryonic stem cells and induced pluripotent stem cells. *Stem Cell Res Ther* **9**, 71, doi:10.1186/s13287-018-0813-5 (2018).
890 Lohoff, F. W. *et al.* Epigenome-wide association study and multi-tissue replication of individuals with alcohol use disorder: evidence for abnormal glucocorticoid signaling pathway gene regulation. *Mol Psychiatry* **26**, 2224-2237, doi:10.1038/s41380-020-0734-4 (2021).

891 Arnett, M. G. *et al.* The role of glucocorticoid receptor-dependent activity in the amygdala central nucleus and reversibility of early-life stress programmed behavior. *Transl Psychiatry* **5**, e542, doi:10.1038/tp.2015.35 (2015).
892 McGinn, M. A. *et al.* Glucocorticoid receptor modulators decrease alcohol self-administration in male rats. *Neuropharmacology* **188**, 108510 (2021).
893 Rose, A. K., Shaw, S. G., Prendergast, M. A. & Little, H. J. The importance of glucocorticoids in alcohol dependence and neurotoxicity. *Alcohol Clin Exp Res* **34**, 2011-2018, doi:10.1111/j.1530-0277.2010.01298.x (2010).
894 Vendruscolo, L. F. *et al.* Glucocorticoid receptor antagonism decreases alcohol seeking in alcohol-dependent individuals. *J Clin Invest* **125**, 3193-3197, doi:10.1172/JCI79828 (2015).
895 Kyzar, E. J., Bohnsack, J. P., Zhang, H. & Pandey, S. C. MicroRNA-137 Drives Epigenetic Reprogramming in the Adult Amygdala and Behavioral Changes after Adolescent Alcohol Exposure. *eNeuro* **6**, doi:10.1523/ENEURO.0401-19.2019 (2019).
896 Beech, R. D. *et al.* Stress-related alcohol consumption in heavy drinkers correlates with expression of miR-10a, miR-21, and components of the TAR-RNA-binding protein-associated complex. *Alcohol Clin Exp Res* **38**, 2743-2753, doi:10.1111/acer.12549 (2014).
897 Kokane, S. S. & Perrotti, L. I. Sex differences and the role of estradiol in mesolimbic reward circuits and vulnerability to cocaine and opiate addiction. *Frontiers in behavioral neuroscience* **14**, 74 (2020).
898 Becker, J. B. Sex differences in addiction. *Dialogues in clinical neuroscience* (2022).
899 McHugh, R. K., Votaw, V. R., Sugarman, D. E. & Greenfield, S. F. Sex and gender differences in substance use disorders. *Clinical psychology review* **66**, 12-23 (2018).
900 Becker, J. B., McClellan, M. L. & Reed, B. G. Sex differences, gender and addiction. *Journal of neuroscience research* **95**, 136-147 (2017).
901 Ngun, T. C., Ghahramani, N., Sánchez, F. J., Bocklandt, S. & Vilain, E. The genetics of sex differences in brain and behavior. *Frontiers in neuroendocrinology* **32**, 227-246 (2011).
902 Miguel-Aliaga, I. Let's talk about (biological) sex. *Nature Reviews Molecular Cell Biology* **23**, 227-228 (2022).
903 Szadvári, I., Ostatníková, D. & Durdiaková, J. Sex differences matter: Males and females are equal but not the same. *Physiology & Behavior*, 114038 (2022).
904 Rinn, J. L. & Snyder, M. Sexual dimorphism in mammalian gene expression. *Trends in Genetics* **21**, 298-305 (2005).
905 Clarkson, T., Karvay, Y., Quarmley, M. & Jarcho, J. M. Sex differences in neural mechanisms of social and non-social threat monitoring. *Developmental cognitive neuroscience* **52**, 101038 (2021).
906 Nair, S. *et al.* Sex, age, and handedness modulate the neural correlates of active learning. *Frontiers in Neuroscience* **13**, 961 (2019).
907 Mozhui, K., Lu, L., Armstrong, W. E. & Williams, R. W. Sex-specific modulation of gene expression networks in murine hypothalamus. *Frontiers in neuroscience* **6**, 63 (2012).
908 Mecklenburg, J. *et al.* Transcriptomic sex differences in sensory neuronal populations of mice. *Scientific reports* **10**, 1-18 (2020).
909 Lu, T. & Mar, J. C. Investigating transcriptome-wide sex dimorphism by multi-level analysis of single-cell RNA sequencing data in ten mouse cell types. *Biology of sex differences* **11**, 1-20 (2020).

910 Chari, T., Griswold, S., Andrews, N. A. & Fagiolini, M. The stage of the estrus cycle is critical for interpretation of female mouse social interaction behavior. *Frontiers in behavioral neuroscience* **14**, 113 (2020).
911 Byers, S. L., Wiles, M. V., Dunn, S. L. & Taft, R. A. Mouse estrous cycle identification tool and images. *PloS one* **7**, e35538 (2012).
912 Meziane, H., Ouagazzal, A. M., Aubert, L., Wietrzych, M. & Krezel, W. Estrous cycle effects on behavior of C57BL/6J and BALB/cByJ female mice: implications for phenotyping strategies. *Genes, Brain and Behavior* **6**, 192-200 (2007).
913 Priddy, B. M. *et al.* Sex, strain, and estrous cycle influences on alcohol drinking in rats. *Pharmacology Biochemistry and Behavior* **152**, 61-67 (2017).
914 Roberts, A., Smith, A., Weiss, F., Rivier, C. & Koob, G. Estrous cycle effects on operant responding for ethanol in female rats. *Alcoholism: Clinical and Experimental Research* **22**, 1564-1569 (1998).
915 Holdstock, L. & de Wit, H. Effects of ethanol at four phases of the menstrual cycle. *Psychopharmacology* **150**, 374-382 (2000).
916 Forger, N. G. & Morin, L. Reproductive state modulates ethanol intake in rats: effects of ovariectomy, ethanol concentration, estrous cycle and pregnancy. *Pharmacology Biochemistry and Behavior* **17**, 323-331 (1982).
917 Ford, M. M., Eldridge, J. & Samson, H. H. Microanalysis of ethanol self-administration: estrous cycle phase-related changes in consumption patterns. *Alcoholism: Clinical and Experimental Research* **26**, 635-643 (2002).
918 Dazzi, L. *et al.* Estrous cycle-dependent changes in basal and ethanol-induced activity of cortical dopaminergic neurons in the rat. *Neuropsychopharmacology* **32**, 892-901 (2007).
919 Sanchis, R., Esquifino, A. & Guerri, C. Chronic ethanol intake modifies estrous cyclicity and alters prolactin and LH levels. *Pharmacology Biochemistry and Behavior* **23**, 221-224 (1985).
920 LaPaglia, N., Steiner, J., Kirsteins, L., Emanuele, M. & Emanuele, N. The impact of acute ethanol on reproductive hormone synthesis, processing, and secretion in female rats at proestrous. *Alcoholism: Clinical and Experimental Research* **21**, 1567-1572 (1997).
921 LaRese, T. P., Rheaume, B. A., Abraham, R., Eipper, B. A. & Mains, R. E. Sex-specific gene expression in the mouse nucleus accumbens before and after cocaine exposure. *Journal of the Endocrine Society* **3**, 468-487 (2019).
922 Wagner, A. K. *et al.* Evaluation of estrous cycle stage and gender on behavioral outcome after experimental traumatic brain injury. *Brain research* **998**, 113-121 (2004).
923 Behl, C. Oestrogen as a neuroprotective hormone. *Nature Reviews Neuroscience* **3**, 433-442 (2002).
924 Brann, D. W., Dhandapani, K., Wakade, C., Mahesh, V. B. & Khan, M. M. Neurotrophic and neuroprotective actions of estrogen: basic mechanisms and clinical implications. *Steroids* **72**, 381-405 (2007).
925 Spence, R. D. *et al.* Neuroprotection mediated through estrogen receptor-α in astrocytes. *Proceedings of the National Academy of Sciences* **108**, 8867-8872 (2011).
926 Lee, S. J. & McEwen, B. S. Neurotrophic and neuroprotective actions of estrogens and their therapeutic implications. *Annual review of pharmacology and toxicology* **41**, 569-591 (2001).
927 Cao, W. *et al.* Neuroprotective effect of estrogen upon retinal neurons in vitro. *Advances in Experimental Medicine and Biology* **533**, 395-402 (2003).

928 Kim, S., Liva, S., Dalal, M., Verity, M. & Voskuhl, R. Estriol ameliorates autoimmune demyelinating disease: implications for multiple sclerosis. *Neurology* **52**, 1230-1230 (1999).
929 Bird, C. E. Women's representation as subjects in clinical studies: a pilot study of research published in JAMA in 1990 and 1992. *Women and health research: Ethical and legal issues of including women in clinical studies* **2**, 151-173 (1994).
930 Merone, L., Tsey, K., Russell, D. & Nagle, C. Sex inequalities in medical research: A systematic scoping review of the literature. *Women's Health Reports* **3**, 49-59 (2022).
931 Holdcroft, A. Vol. 100 2-3 (SAGE Publications Sage UK: London, England, 2007).
932 Beery, A. K. & Zucker, I. Sex bias in neuroscience and biomedical research. *Neuroscience & Biobehavioral Reviews* **35**, 565-572 (2011).
933 Rossi, A. *et al.* Genetic compensation induced by deleterious mutations but not gene knockdowns. *Nature* **524**, 230-233 (2015).
934 Hudry, E. & Vandenberghe, L. H. Therapeutic AAV gene transfer to the nervous system: a clinical reality. *Neuron* **101**, 839-862 (2019).
935 Bartus, R. T. *et al.* Advancing neurotrophic factors as treatments for age-related neurodegenerative diseases: developing and demonstrating "clinical proof-of-concept" for AAV-neurturin (CERE-120) in Parkinson's disease. *Neurobiology of aging* **34**, 35-61 (2013).
936 Weinberg, M. S., Samulski, R. J. & McCown, T. J. Adeno-associated virus (AAV) gene therapy for neurological disease. *Neuropharmacology* **69**, 82-88 (2013).
937 Kaplitt, M. G. *et al.* Safety and tolerability of gene therapy with an adeno-associated virus (AAV) borne GAD gene for Parkinson's disease: an open label, phase I trial. *The Lancet* **369**, 2097-2105 (2007).
938 Gessler, D. J., Tai, P. W., Li, J. & Gao, G. Intravenous infusion of AAV for widespread gene delivery to the nervous system. *Adeno-Associated Virus Vectors: Design and Delivery*, 143-163 (2019).
939 Zhang, X. *et al.* Customized blood-brain barrier shuttle peptide to increase AAV9 vector crossing the BBB and augment transduction in the brain. *Biomaterials* **281**, 121340 (2022).
940 Zhang, H. *et al.* Several rAAV vectors efficiently cross the blood–brain barrier and transduce neurons and astrocytes in the neonatal mouse central nervous system. *Molecular Therapy* **19**, 1440-1448 (2011).
941 Foust, K. D. *et al.* Intravascular AAV9 preferentially targets neonatal neurons and adult astrocytes. *Nature biotechnology* **27**, 59-65 (2009).
942 Xie, H. *et al.* SaCas9 requires 5′-NNGRRT-3′ PAM for sufficient cleavage and possesses higher cleavage activity than SpCas9 or FnCpf1 in human cells. *Biotechnology journal* **13**, 1700561 (2018).
943 Yin, C. *et al.* In vivo excision of HIV-1 provirus by saCas9 and multiplex single-guide RNAs in animal models. *Molecular Therapy* **25**, 1168-1186 (2017).
944 Broughton, J. P. *et al.* CRISPR–Cas12-based detection of SARS-CoV-2. *Nature biotechnology* **38**, 870-874 (2020).
945 Freije, C. A. *et al.* Programmable inhibition and detection of RNA viruses using Cas13. *Molecular cell* **76**, 826-837. e811 (2019).
946 Liang, X. *et al.* A CRISPR/Cas9 and Cre/Lox system-based express vaccine development strategy against re-emerging Pseudorabies virus. *Scientific reports* **6**, 19176 (2016).

947 Fu, Y., Sander, J. D., Reyon, D., Cascio, V. M. & Joung, J. K. Improving CRISPR-Cas nuclease specificity using truncated guide RNAs. *Nature biotechnology* **32**, 279-284 (2014).